

**PHYSICAL LAYER IMPROVEMENT TECHNIQUES IN
4G/5G WIRELESS COMMUNICATION NETWORKS**

Thesis submitted to
UNIVERSITY OF CALICUT

in fulfillment for the award of the degree of

DOCTOR OF PHILOSOPHY

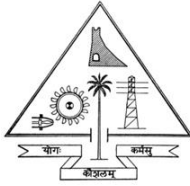


By

Ali M A

Under the Guidance of
Dr. Jasmin E A

**DEPARTMENT OF ELECTRICAL ENGINEERING
GOVERNMENT ENGINEERING COLLEGE, THRISSUR
UNIVERSITY OF CALICUT
2018**



**DEPARTMENT OF ELECTRICAL ENGINEERING
GOVERNMENT ENGINEERING COLLEGE
THRISSUR-680009**

Certificate

This is to certify that the thesis entitled "**Physical Layer Improvement Techniques in 4G/5G Wireless Communication Networks**" is the record of bonafide research work done by Mr. Ali M. A under my supervision and guidance at Department of Electrical Engineering, Government Engineering College, Thrissur in partial fulfillment of the requirements for the Degree of Doctor of Philosophy under the Faculty of Engineering, University of Calicut. All the suggestions/corrections pointed out by the adjudicators are incorporated in the thesis.

Thrissur-9
16/10/2018

Dr. JASMIN E A

DECLARATION

I, Ali M A, hereby declare that the thesis entitled "Physical Layer Improvement Techniques in 4G/5G Wireless Communication Networks" is based on the original work done by myself under the guidance of Dr. Jasmin E A, Associate Professor, Department of Electrical Engineering, Government Engineering College, Thrissur for the award of Ph.D. programme under University of Calicut.

I further declare that this work has not been included in any other thesis submitted previously for the award of any Degree, Diploma, Associateship or Fellowship or any other title for recognition.

Thrissur-9
16/10/2018

Ali M A

ACKNOWLEDGMENT

First and foremost, praises and thanks to Almighty God with a humble heart for His showers of blessings throughout my research work and providing me the determination and courage in pursuing the research study, despite all difficulties.

My deepest gratitude goes first to my supervisor Dr. Jasmin E. A, Associate Professor, Department of Electrical Engineering, Government Engineering College, Thrissur, for her sincere and timely support and guidance throughout the research.

Also, I greatly thank the members of my doctoral committee, Prof. Reguraj, Principal, Government Engineering College, Sreekrishnapuram. Prof. Nandakumar, Professor of the Department of Electrical Engineering and Prof. Jayanand, Principal, Government Engineering College, Thrissur for their time and effort in evaluating my work and providing valuable feedback and suggestions. I express my sincere gratitude to Dr. Amardutt, former Head, Department of Electrical Engineering, Government Engineering College Thrissur for her sincere support and timely encouragements.

I extend my wholehearted gratitude to Dr. Vijayakumar and Dr. K P Indiradevi former Principals of GEC, Thrissur, for their encouragement, suggestions and friendly approach during my research work.

I wish to thank my wife, Shemi P Mohammed and my daughters Nihala Jebin and Nahla Jasmin who have given me courage and unconditional support during my Ph.D. research. Without them, research life could never be so colorful and comfortable.

Last but not the least, I am thankful to all my friends and colleagues at Govt. Engineering College, Thrissur, for their help and motivation throughout the research period.

Ali M A

ABSTRACT

Wireless communication technology has essentially transformed the way we communicate. The era of voice and data communications bound to be wired and can be used only in pre-located places has passed. Now all communication services are wirelessly available in all parts of the Globe, and wireless connectivity has become an essential part of the society as vital as water and electricity.

Future wireless communication systems need to feature multi cellular heterogeneous architectures consisting of improved macro cells and very dense small cell, to support the exponentially rising demand for physical layer throughput. Performance of such structures is always restricted by the unprecedented levels of inter and intra cell interferences. In order to exploit the full benefits of such networks, techniques like massive Multiple Input Multiple Output (massive MIMO), Self-Organizing Networks (SON), cooperation, cognitive radio, etc., are introduced. This will increase the size of the already large heterogeneous architectures to truly enormous networks and necessitates a lot of research, analysis, and developments to get the optimum performance out of it.

Recent studies carried out by many research organizations have predicted that the global mobile data traffic is expected to reach 49 exabytes per month by the year 2021. This is more than four-fold increase compared to the mobile data traffic registered in 2017. All the emerging smart infrastructures that are coming up today like

smart city, smart health, smart transportation, smart grid, etc. need mobile and wireless connectivity for its optimum performance. However, the requirements of these smart infrastructures cannot be met with the existing wireless technology and framework. It forces the industry, researchers, and academia to come up with new innovations and technologies to meet the exploding future demands. Improvement in the Physical layer techniques is found as one of the demanding technology requirement of future wireless communication system.

Accordingly, in this thesis, we apply and improve the already known physical layer techniques and propose solutions for the limitations centered around the physical layer of the wireless networking system.

Multiple Input Multiple Output with Orthogonal Frequency Division Multiplexing (MIMO-OFDM) is one of the most wanted wireless broadband technology and transmission system that has been accepted as the basic building blocks of long-term evolution (LTE) and 4th Generation wireless communication system.

The first stage of the research work is concerned with the study of various modulation schemes used in MIMO-OFDM and to come up with a comprehensive algorithm for adaptive modulation to determine the best modulation scheme for a value of transmit SNR. This is achieved by developing a mapping from the SNR value to the best possible modulation rate keeping the BER constraints. Results obtained proved that adaptive modulation which dynamically acts in response to the channel quality performs at its best and can provide

improvements in the data rate of the transceiver system without compromising much on the bit error rate.

Interference in wireless communications is considered as one of the main causes of performance degradation. Performance of OFDM is highly sensitive to the frequency offset between the transmit and receive signals, which is produced due to the Doppler shift caused by the relative motion between the receiver and transmitter or by the difference in local oscillator frequencies of the transmitter and receiver. This causes loss of orthogonality between the sub carriers which results in inter-carrier interference. To overcome the effect of interferences in MIMO-OFDM wireless networks, an interference cancellation technique combined with adaptive modulation is proposed. Along with interference cancellation technique, adaptive modulation is used to meet the required BER performance by selecting suitable modulation modes based on the channel condition. Doppler assisted channel estimation method is used to estimate the channel. Also, inter-channel/carrier interference (ICI) cancellation scheme is used to integrate the Parallel Interference Cancellation together with the Decision Statistical Combining (PIC-DSC) module to detect the data and transmit it to the estimator to iteratively refine the channel and give interference free channel.

Massive MIMO antenna systems with hundreds or thousands of antennas at the base station and a number of simultaneous active users in each cell, is a promising technology for the future to meet the ever-growing needs of wireless data traffic. Since wireless spectrum is a limited resource, maximizing the spectral efficiency (SE) of the

available spectrum is identified as the best option to satisfy the exponential growth of wireless data traffic. In this work, we analyze the different ways to optimize the spectral efficiency (SE) of a massive MIMO system. The SE performance under various practical constraints and conditions such as limited coherence block length, number of base station (BS) antennas, and number of active users are evaluated through simulation. The SE performance is also evaluated under different linear precoding techniques Minimum Mean Square Error (MMSE), Zero Forcing (ZF) and Maximum Ratio Combining (MRC). Impact of the channel SNR variations on SE and system performance under different duplexing schemes (TDD and FDD) are also evaluated through simulations.

Pilot contamination is identified as the most significant impairment that limits the exploitation of the optimum capacity of massive MIMO. It is caused by the re-use of the same, or at least non-orthogonal pilot sequences, among different cells that degrade the performance of channel estimation. In order to mitigate this issue, we propose a novel partial pilot re-use strategy among users in the adjacent cells, which are close to the base station (BS) and also possesses minimum movement velocity. The social spider optimization algorithm (SSOA), which imitates the cooperative behavior of social spiders, is used for selecting the eligible users for this pilot reuse in the neighboring cells. The algorithm tries to maximize the lowest SINR value for every user in the cell. The performance of the proposed method and algorithm is evaluated through simulations using MATLAB and showed that the new strategy outperforms the conventional pilot assignment methods.

TABLE OF CONTENTS

<i>List of Figures</i>	<i>vi</i>
<i>List of Tables</i>	<i>ix</i>
<i>List of Abbreviations</i>	<i>x</i>
1. Introduction	1
1.1 Motivation	1
1.2 Background: Current State of cellular Communications	5
1.2.1 What are we doing about it?	6
1.2.2 Increased Spectrum	6
1.2.3 Increased network density	8
1.2.4 Increased spectral efficiency	9
1.3 Objectives	9
1.4 Thesis organization	10
1.5 Chapter Summary	12
2. Long Term Evolution (LTE)	13
2.1 Introduction	13
2.2 Key enabling technologies of LTE	15
2.3 Orthogonal Frequency Division Multiplexing(OFDM)	16
2.4 Advantages and disadvantages of OFDM	20
2.5 Multiple input multiple output (MIMO) systems.	22
2.6 Single User and multi-user MIMO	25
2.7 MIMO Channel model	26
2.8 Advantages and disadvantages of MIMO	27
2.9 Chapter Summary	29
3. Adaptive Modulation in MIMO-OFDM Networks	30
3.1 Introduction	30
3.2 Adaptive Modulation	32
3.3 Review of techniques	35

3.4	System model	39
3.4.1	Simulation Parameters	44
3.5	Results and discussions	45
3.6	Chapter Summary	48
4.	Interference and Interference Cancellation in MIMO-OFDM Networks	50
4.1	Introduction	50
4.2	Interference in wireless communication	51
4.2.1	Theoretical background	53
4.2.2	Phase noise	54
4.2.3	Compensation of Phase noise	55
4.2.4	I/Q Mismatch	55
4.2.5	Narrow Band Interference (NBI)	56
4.2.6	NBI compensation	57
4.2.7	Doppler Shift	58
4.3	Inter-Carrier Interference	60
4.3.1	Effect of frequency offset in MIMO-OFDM	64
4.3.2	Successive Interference Cancellation	67
4.3.3	Parallel Interference Cancellation	69
4.4	Review of techniques	71
4.5	System Model	75
4.5.1	Overview	75
4.5.2	Designing of Adaptive Modulation in OFDM	76
4.5.3	Doppler-Assisted Channel Estimation Scheme	78
4.5.4	Overall algorithm	80
4.6	Results and Discussions	82
4.7	Chapter Summary	86
5.	Massive MIMO	88
5.1	Introduction	88
5.1.1	Advantages of massive MIMO	90

5.1.2	Challenges and limitations	93
5.1.3	Analysis of the benefits of massive MIMO	94
5.2	Literature Survey	105
5.2.1	General Overview and tutorials	105
5.2.2	Capacity and fundamental features of Massive MIMO	115
5.2.3	CSI acquisition and related aspects	119
5.2.4	Receiver detection algorithms	125
5.2.5	Precoding algorithms for Downlink	128
5.2.6	Channel modelling and measurements	132
5.2.7	Resource allocation	134
5.2.8	Hardware impairments	137
5.2.9	Antenna aspects	138
5.2.10	Implementation demos and Performance Analysis	141
5.3	Chapter Summary	146
6.	Optimization of Spectral Efficiency in Massive MIMO	148
6.1	Introduction	148
6.2	Throughput in cellular networks	148
6.3	Massive MIMO system and assumptions	151
6.4	Uplink signal transmission	152
6.5	Downlink signal transmission	153
6.6	Spectral efficiency and its importance	154
6.7	Frequency Division Duplexing Vs. TDD	156
6.8	Fundamental Property of Massive MIMO	158
6.9	Channel coherence in wireless communication	159
6.9.1	Coherence Time	159
6.9.2	Coherence Band width	162
6.9.3	Coherence Interval	164
6.9.4	Coherence interval for Ma-MIMO with TDD	165
6.10	Pilot based channel estimation in massive MIMO	166
6.10.1	Pilot orthogonality	167
6.11	Linear Vs Non-linear signal processing	167

6.12	Massive MIMO Precoding and signal detection	168
6.12.1	Dirty Paper Coding(DPC)	169
6.12.2	Linear precoding methods	170
6.12.3	Zero-Forcing	171
6.12.4	Maximum ratio combining(MRC)	172
6.12.5	Minimum Mean-Squared Error	173
6.13	Capacity limits in massive MIMO	174
6.14	Inter-user interference in linear precoding schemes	177
6.15	Channel hardening in massive MIMO	179
6.16	Digital Beamforming	180
6.17	Optimizing number of users for maximum capacity	181
6.18	Related works	182
6.19	System Model	186
6.19.1	Model Characteristics	190
6.20	Results and Discussions	192
6.21	Practical Discussion	204
6.22	Key findings	205
6.23	Chapter Summary	207

7. Pilot Decontamination for Massive MIMO using Social Spider Optimization Algorithm 209

7.1	Introduction	209
7.2	Pilot contamination	209
7.3	Pilot based CSI acquisition	213
7.4	Sources of Pilot Contamination and its effects	215
7.4.1	Contamination due to Non-orthogonal pilot sequences	215
7.4.2	Contamination due to hardware impairments	217
7.4.3	Contamination due to Non-Reciprocal Transceivers	217
7.5	Effect of Pilot Contamination on massive MIMO performance	218
7.6	Pilot contamination: Mitigation methods	221
7.6.1	Time-Shifted Pilot slot allocation	222
7.6.2	Covariance aided method	223
7.6.3	Spatial domain-based scheme	223

7.6.4	Multi-cell cooperation	224
7.6.5	EVD-based Method	224
7.6.6	Data-aided approach	225
7.7	Related works	226
7.8	Problem identification	230
7.9	The system model	231
7.10	Social spider optimization algorithm	236
7.10.1	Fitness calculation using multi-factors	243
7.10.2	Mobility with Received Signal Strength	244
7.11	Normalized Mean Square ERROR	247
7.12	Sum-rate	248
7.13	Results and discussions	248
7.14	Key findings	254
7.15	Chapter Summary	255
8.	Conclusion and Future works	257
8.1	Introduction	257
8.2	Summary and major findings	257
8.3	Limitations of the research	261
8.4	Future works	262
9.	References	263

LIST OF FIGURES

Fig. No.	Title	Page
No.		
1.1	Growth in the no. of connected devices to the Internet	2
1.2	Growth in Global Mobile Data traffic	2
1.3	Growth in the number of wireless devices	4
1.4	Number of Mobile connections worldwide in billions	4
2.1	Basic multi-carrier modulator	17
2.2	Basic multi carrier demodulator	17
2.3	Carrier allocation in Conventional Multicarrier Technique	18
2.4	Carrier allocation Orthogonal MCM Technique	18
2.5	Block diagram of OFDM transmitter	19
2.6	Block diagram of OFDM Receiver	19
2.7	Various MIMO techniques	24
2.8	Single user and multi-user MIMO	25
2.9	MIMO system, with N_t tx antennas and N_r rxv antennas	26
3.1	Chain of operations associated with link adaptation in LTE	33
3.2	Communication system model	39
3.3	Capacity limits under various modulation schemes	40
3.4	Constellation selection to maximize the throughput	41
3.5	Shannon limit and capacity limit	42
3.6	Block diagram of an adaptive modulation system	43
3.7	Comparison between Adaptive and fixed modulation schemes	48
4.1	Broadband interference	51
4.2	Co-channel and adjacent channel interference	52
4.3	Ratio of noise power to carrier power plotted against frequency	56
4.4	Spectrum of received signal with and without transmit I/Q imbalance	57
4.5	Calculation of Doppler Shift due to mobility of User terminal	59
4.6	Effect of Doppler shift on BER in a BPSK system	61
4.7	Effect of Doppler shift on BER in a QPSK system	61
4.8	OFDM subcarrier creates “nulls” and canceling out ICI	62

4.9	SNR loss due to frequency offset in OFDM modulation	67
4.10	Successive Interference Cancellation	69
4.11	Parallel Interference Cancellation	70
4.12	Block diagram of the proposed AM with ICI cancellation	76
4.13	Block Diagram of OFDM with Adaptive Modulation	78
4.14	Constellation selection to maximize the throughput	80
4.15	Overall algorithm	80
4.16	Integrated PIC-DSC interference cancellation scheme	81
4.17	Comparison of the BER vs. SNR performances	83
4.18	Comparison of BER vs. SNR of the proposed PIC-DSC AM scheme	84
4.19	BER vs. Doppler Spread of the proposed PIC-DSC AM scheme	85
4.20	BER vs. SNR of the proposed scheme with ZF and MMSE	86
5.1	SISO communication link	95
5.2	Signal attenuation in wireless medium	96
5.3 (a)	Multiple antennas at the transmitter	96
5.3 (b)	Multiple antennas at the transmitter with channel coefficients	97
5.4	Use of matched filter for beam forming	98
5.5 (a)	Multi-user MIMO	100
5.5 (b)	Multi-user MIMO with channel coefficients	100
5.6	Graph showing the SNR increase with M (Array Gain)	102
5.7	Uplink training with no pilot contamination	104
5.8	Uplink training with pilot contamination	105
6.1	Massive MIMO system with M antennas and K users	152
6.2	FDD and TDD operation showing the link overheads	157
6.3	Average correlation between two i.i.d. Rayleigh channels Vs M	159
6.4	Two path model for the wireless channel	161
6.5	Coherence time T_c	162
6.6	Coherence bandwidth B_c	164
6.7	Allocation of samples in a coherence interval- No downlink Pilots	165
6.8	TDD with time-frequency plane divided into coherence blocks	166
6.9	A multi-user MIMO in the downlink and uplink	175
6.10	Downlink data transmission	187
6.11	Uplink data transmission	188

6.12	Frame structure	192
6.13	SE per cell versus M for different values of K	193
6.14	Impact of coherence length(S) on SE	194
6.15	Impact of coherence block length(S) on SE	195
6.16	SE vs. Coherence block length for different M	196
6.17	Linear Vs. Non-linear signal processing	197
6.18	Linear Vs. Non-linear signal processing (expanded)	198
6.19	Impact of precoding techniques ZF and MRC on SE	199
6.20	Optimum value of K versus M for different values of S	200
6.21	SE Vs. No. of UEs per cell with different M/K ratios	201
6.22	Effect of CSI and pilot sequence length under FDD and TDD mode	202
6.23	Effect of SNR variation on Spectral Efficiency	203
6.24	Effect of SNR variation and different precoding schemes on SE	204
6.25	Massive MIMO operating regions	204
7.1	Contamination of uplink pilot signal	216
7.2	Point to point reciprocity model	218
7.3	Cluster pattern that is repeated for pilot reuse factors of 1,2,3 and 4	220
7.4	Effect of pilot contamination on area throughput	221
7.5	Effect of pilot contamination on energy efficiency	221
7.6	Pilot scheme based on time-shifted pilot slots.	222
7.7	Data-aided approach for pilot decontamination	226
7.8	System Model	231
7.9	Downlink Communication	232
7.10	Uplink Communication	232
7.11	Pilot reuse	234
7.12	Partial pilot reuse	235
7.13	Interference from adjacent cells	236
7.14	Mobile nodes movement computation	245

7.15	NMSE Vs. No. of BS antennas (linear scale)	249
7.16	NMSE Vs. No. of BS antennas for BPSK (linear scale)	250
7.17	NMSE Vs. No. of BS antennas (log scale)	250
7.18	Sum-rate Vs. no. of BS antennas	251
7.19	BER Vs. No. of BS antennas (linear scale)	252
7.20	BER Vs. No. of BS antennas (linear scale-BPSK)	253
7.21	BER Vs. No. of BS antennas (log scale)	253
7.22	NMSE Vs. Number of receiving nodes	254

LIST OF TABLES

Table No.	Title	Page No.
1.1	Expected mobile and wireless scenario by the year 2021	5
3.1	Methods and performance gains of different modulation schemes	37
3.2	BER and Capacity limits of different modulation schemes	41
3.3	MIMO-OFDM Transceiver design parameters	44
3.4	Algorithm for adaptive modulation in 2x2 MIMO_OFDM system	44
3.5	The BER and data rates with SNR 20 dB	46
3.6	The BER and data rates with SNR 15 dB	47
3.7	The BER and data rates with SNR 10 dB	47
4.1	Parameters used in the proposed system	82
4.2	Switching threshold for adaptive modulation	82
6.1	Achieving 1000-fold increase in throughput	150
6.2	Values of T_c , B_c , and τ_c computed at $f_c = 2\text{GHz}$	164
7.1	Comparison of different Pilot based training and feedback Schemes	214
7.2	Comparison between social spider colony and cellular network	241
7.3	Social spider optimization algorithm for pilot assignment	247

LIST OF ABBREVIATIONS

3GPP	3rd generation partnership project
5G	Fifth Generation
AWGN	Additive White Gaussian Noise
BER	Bit Error Rate
CP	Cyclic Prefix
CSI	Channel State Information
DL	Down Link
FDD	Frequency Division Duplex
FDD	Frequency-division duplexing
FFT	Fast Fourier Transform
i.i.d.	Independent and identically distributed
ICI	Inter-Carrier Interference
IFFT	Inverse Fast Fourier Transform
ISI	Inter-Symbol Interference
ITU	International Telecommunication Union
LoS	Line of Sight
LTE	Long-Term Evolution
MIMO	Multiple Input Multiple Output
MMSE	minimum Mean Square Error
MRC	Maximal Ratio Combining
MRT	Maximum ratio transmission
MU	MIMO Multi-User Multiple-Input Multiple-Output
NMSE	Normalized Mean Square Error
OFDM	Orthogonal Frequency Division Multiplexing
QAM	Quadrature Amplitude Modulation
QPSK	Quadrature Phase Shift Keying
RF	Radio frequency
Rx	Receiver
SINR	Signal-to-Interference-Noise Ratio
SNR	Signal-to-Noise Ratio
SSO	Social Spider Algorithm
TDD	Time Division Duplex
Tx	Transmitter
UE	User Equipment
UL	Uplink
UT	User Terminal
ZF	Zero-Forcing

CHAPTER-1

INTRODUCTION

1.1 Motivation

In recent years, there has been an exponential growth in both mobile and fixed internet data traffic. This is due to the excessive increase in the number and usage of mobile phones, laptops, tablets and many other mobile devices which use internet over the wireless network. It is also obvious from the current trend and the upcoming wide usage of the Internet of Things (IoT) that this demand for wireless data will be more severe in the coming future [1].

The Internet of Things is a network of objects and devices that are seemingly interconnected to exchange data, sense the environment and make our life easier. The things around us will start to talk each other electronically. In a recent study conducted by Intel it is expected that by 2020, 50 billion devices will be connected to the Internet. The number of devices which is slightly more than three devices per person now will be increased to more than six per person by 2020. Fig. 1.1 shows the growth in the number of connected devices to the internet from 2012 to 2020 [2].

According to Cisco's latest study and forecast, with the rapid growth in the usage of smart devices, demand for mobile video, the continuing growth of 4G communication networks and an ever-increasing number of wireless users there will be around 800 percentage growth in the wireless data traffic in the coming years. The 4G connections are expected to produce almost six times more traffic

per month than the non-4G connections. Wi-Fi has become a very robust access technology for mobile.

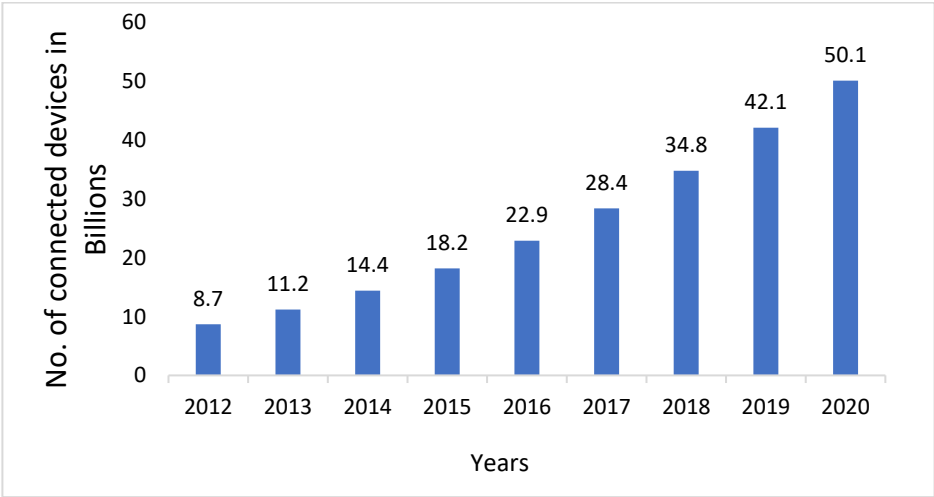


Figure 1.1 Growth in the no. of connected devices to the Internet

data exchange. Mobile phone network operators, neutral host providers, enterprise venue and building owners, commercial segments, sports venues, transportation and healthcare institutions can all support this evolution in Wi-Fi and 4G data traffic.

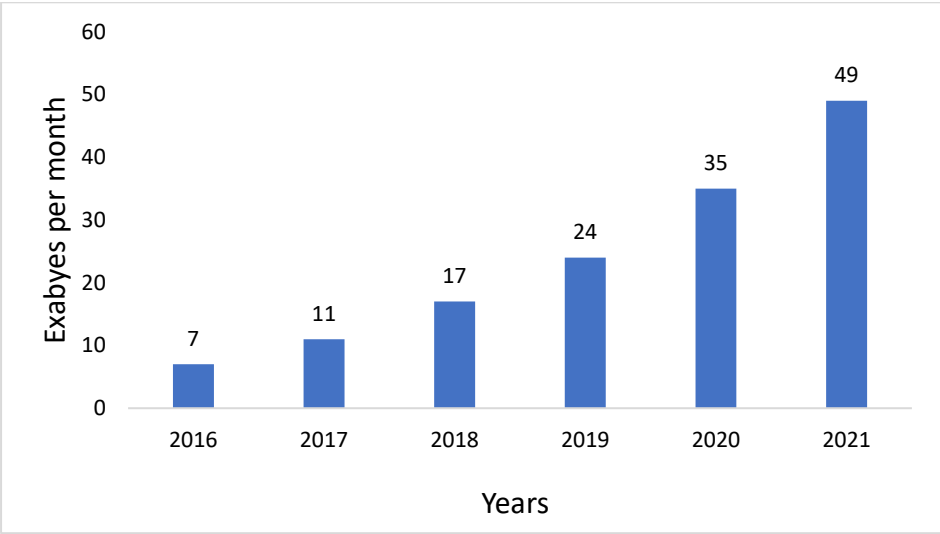


Figure 1.2 Growth in Global Mobile Data traffic

Fig. 1.2 shows a graphical representation of the exponentially growing demand for mobile data traffic and Fig. 1.3 shows the growth in the number of wireless devices. According to the recent studies conducted by CISCO global mobile data traffic will experience a seven-fold increase from 2016 to 2021. Study report also says that Africa and the Gulf countries are expected to have twelve-fold growth in mobile data traffic, but an average of seven-fold growth is predicted in Asia-Pacific region. Central and Eastern Europe, Western Europe and Latin America are expected to have an increase of six-fold growth in mobile data traffic where as it predicts a 5-fold growth in North America [3].

It also predicts that by 2021 more than twenty percentage of the total traffic over the internet would be mobile data. The global mobile data traffic is expected to reach 49 Exabyte per month by the year 2021. As shown in Fig. 1.3 the number of mobile devices will also grow

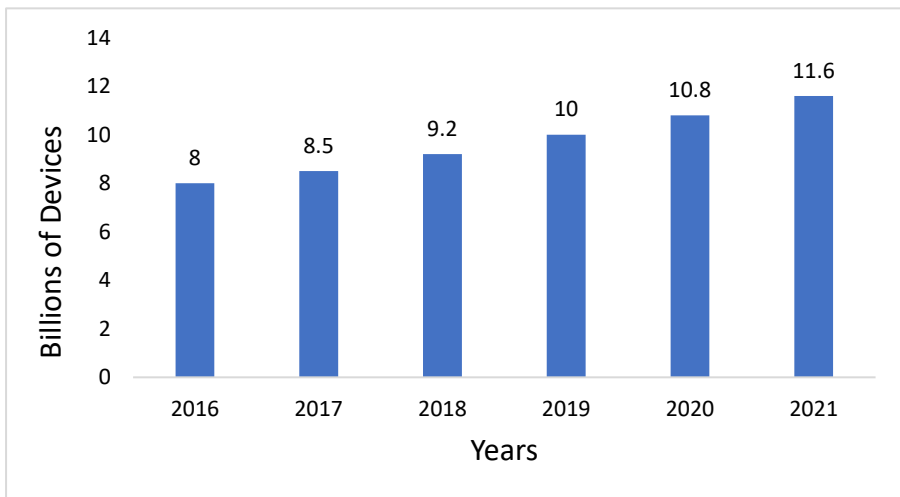


Figure 1.3 Growth in the number of wireless devices

drastically to reach 11.6 billion by 2021 and Fig. 1.4 shows the growth in the cellular mobile connection worldwide from 2010 to 2021

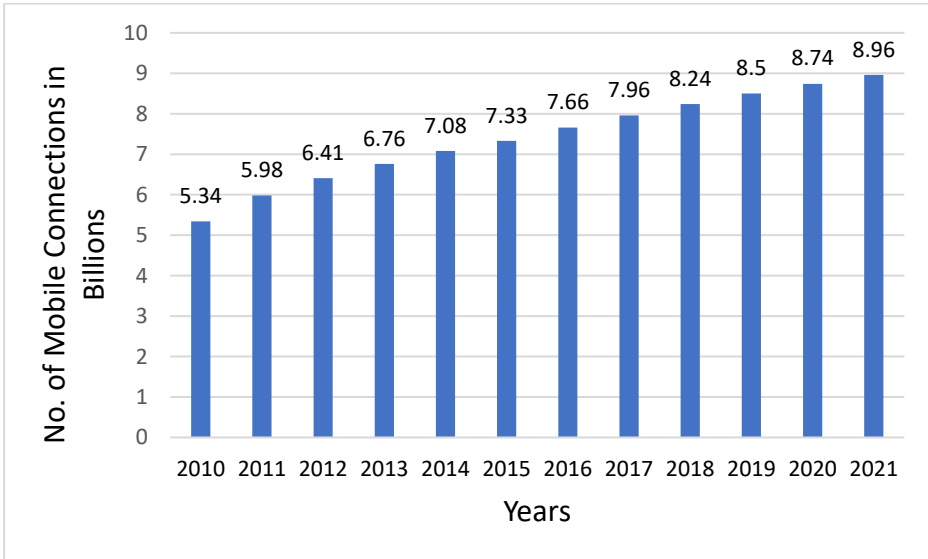







Figure 1.4 Number of Mobile connections worldwide in billions

The following table is a quick reckoner to give an idea about the expected mobile and wireless scenario by the year 2021 and the contributions made by different categories of devices.

Table 1.1 expected mobile and wireless scenario by the year 2021

Device type		Traffic in MBs/Month	
		2016	2021
	Ordinary phone	33	175
	Smart phones	1614	6825
	Virtual reality head sets	840	2790
	Tablet and laptops	3392	7951
	Machine to machine communication (IoT)	203	670

All the studies and predictions detailed above show the inevitability of the development of new technologies and practices to meet the ever-growing demand for wireless data traffic.

1.2 Background: Current State of Cellular Communications

At present, the industry of wireless and mobile communication is undergoing consistent exponential growth in the demand for data traffic (61% growth in annual traffic), with no indications of slow down [4], and exactly the same condition is expected in the case of the number of devices connected to the internet. The reason for this is mainly due to the change in the expectations of customers. They all want to have continuous wireless/mobile connectivity and need streaming audio and video services via their mobile phones, tablets or laptops. The new generation devices manufactured in this category are also more geared to wireless data communications rather than voice communication alone. Moreover, the market for the machine to machine communication is getting more and more important [5]. Taking everything into consideration, the industry is expecting a 1000-fold increase in the capacity of cellular mobile networks over the coming 15 years [6]. The present communication systems are reaching its capacity limits with respect to the physical layer (the so-called "spectrum deficit" [7] or "data tsunami"), particularly in heavily populated city areas with an increased number of connected communication gadgets. Considering the busy transmissions from higher transmission layers and peak hours of communication [8] into account, this is already becoming a problem today.

1.2.1 What are we doing about it?

The question that the communication industry facing today is methods to meet the exponentially growing demand for the data traffic. In a wireless communication network, the total capacity is straight away related to the area throughput (measured as bits/second/ area) of the network. This, in turn, is the combination of three components [9] as given below,

$$\begin{aligned} \text{Area-throughput} &= \text{Cells density (cells/area)} \times \text{Total spectrum (Hertz)} \\ &\times \text{Spectral efficiency (bits/seconds/Hertz/cell)} \end{aligned} \quad (1.1)$$

Traditionally more area throughputs are achieved by increasing the cell density (more number of cells in given area) and/or by providing better spectral efficiency through diversity/modulation/coding methods. Improvements through these techniques will not be sufficient to meet the heavy future demands. So, we have to study and analyze the recent research approaches, in industry and academia, in each of the three components to improve the area throughput for cellular mobile communication [10,11].

1.2.2 Increased Spectrum

The easiest and most obvious method to provide increased throughput is by the use of additional frequency spectrum. Doubling of the frequency spectrum between 300Mhz to 3Ghz range instantly gives us the double of the existing throughput without having much technical difficulties or research but needs to have a doubling in the overall transmitted power⁽¹⁾.

¹ Shannon Hartley Theorem [12], $C = B \log_2(1 + S/N) = B \log_2\left(1 + \frac{P_{sum}/B}{N_0/B}\right) = B \log_2\left(1 + \frac{P_{sum}/B}{N_0}\right)$

Since it is a very straight forward solution, all operators will prefer to have more spectrum and hence the frequency spectrum in the sub 10Ghz band is heavily regulated. It is very much a demand limited possibility and also very costly. In most of the areas, depending upon the geographic area in consideration, a band width of about 1000MHz might already be wireless data services and thus limits the actual gain through this approach to a maximum of about three times improvement. Moreover, this restriction also exaggerates the observation that most of the time a good percentage of the available spectrum is not used. This is the main reason for considering the concept of cognitive radio [13] where the transceiver can intelligently detect the free unused channels available in the spectrum (so-called spectrum holes) and instantaneously jump into this un occupied slot which is allotted to different services. This must be performed without causing any interrupt or interference to the actually allotted service, and that is the area where the cognitive or intelligent part of this approach is coming into picture [14].

Another straight forward solution is to go for high-frequency spectrum where at present, no services are assigned, and the bandwidth is also abundant. The cellular communication in millimeter (mm) wave band (30 to 300GHz) has thus become the hot research topic today [15, 16]. It has got many advantageous like huge bandwidth, small component size, greater beam resolution, low interference and increased security. But shorter transmission range, line of sight (LOS)

requirements, susceptibility to obstructions and weather and costly components are the main challenges [17] in using mm waves.

1.2.3 Increased Network Density

Historically, decrease the cell size (which is to increase the density of cells) was the most advanced technology to meet the demand for increased network capacity [18]. This is a simple approach, and the transmitters and receivers will become spatially closer and give a reduction in path loss, fewer reflections, and fading. In addition, more density means that more cells may be in the same surface area, which influences directly on the equation of the above throughput. Interestingly, this simple densification of cells increases the power and signals interference. This is most intuitively understood in a simple and consistent propagation environment (e.g., line of sight). Right here, the interference power and the signal power increase in proportion as the distance decreases. [18]. Also, the spectral efficiency remains the same in the first approximation. However, increased spatial reuse improves throughput per area [19]. In all cases, the interference induced by adjacent cells increases, if the dense cells serve more user terminals (UT). The classical way to fight against the interference between cells is to use different frequencies in cells that are close to each other (frequency reuse factor greater than one) [20]. However, this reduces the spectral efficiency, thus limiting the overall gain achievable. The modern version of the densification of the cells is often described in the context of small cells [21]. Here, a heterogeneous architecture is considered, in which the great classical cells (called macro) are used for certain tasks (e.g., mobility management), but discharge traffic by existing small cells in the same environment is used. This means that

an arbitrary number of small cells, capable of self-organization, is deployed inside/outside either by the operator or by the consumer. The mixture of macro cells and small cells will affect the spectral efficiency in each cell, in particular, if the small cells are deployed by unorganized users.

1.2.4 Increased Spectral Efficiency

The subject of the most active research on throughput improvement is the increase of spectral efficiency. Spectral efficiency or bandwidth efficiency is defined as the rate of information that can be transmitted in a specific communication system over a given bandwidth. It is a measure of how efficiently a limited frequency spectrum is utilized by the physical layer protocol and sometimes by the media access control. Today cellular networks are, above all, limited by the intra cell interference and inter-cell interference [22]. This situation will also worsen, as modern cellular networks will serve a multitude of users using the same resources (time/frequency) to get improved spectral efficiency.

1.3 Objectives

This research is aimed at investigations into the existing Physical layer network technology of wireless communications, its inadequacies, limitations, challenges and possible improvements in the required network conditions through analytical investigations and simulations using MATLAB simulation tool. Based on this study necessary modifications are suggested, and all these modifications are evaluated.

The following objectives are identified to achieve the aim outlined above;

- To undertake an exhaustive literature collection on Cellular Wireless Networks, its scope, limitations and future impact on communications.

- In depth analysis of the present physical layer technologies, its limitations and modifications suggested in recent publications.

- Validate the technologies under required network conditions through analytical modelling and/or simulations and come up with solutions to the bottlenecks identified.

- Develop modified/novel techniques and algorithms to meet the requirements and validate its performance through analytical modelling and/or simulations.

1.4 Thesis Organization

Remaining chapters of the thesis are organized in the following way:

Chapter 2 provides an overview of Long Term Evolution (LTE), its key features and capabilities. It also explains the two basic enabling technologies used in LTE, Multiple Input Multiple Output (MIMO) systems and Orthogonal Frequency Division Multiplexing(OFDM). The main advantageous and disadvantages, modes of operation of both MIMO and OFDM are discussed in this chapter.

Chapter 3 introduces the concept of adaptive modulation applied to MIMO-OFDM networks and the link adaptation standards used in

LTE. The existing works in this area are reviewed. Developed and tested a simple algorithm to implement adaptive modulation in MIMO-OFDM networks.

Chapter 4 gives a detailed discussion on the various interferences that limits the performance of MIMO-OFDM networks. Different methods available to combat with interferences are also studied. Design, implementation, and testing of inter-channel interference cancellation scheme combined with adaptive modulation are explained in this chapter.

Chapter 5 introduces the concept of massive MIMO and its importance in the present mobile technology to alleviate many of the existing bottlenecks and meet the exponentially growing needs of wireless communication. The available studies and research works in this area are categorized and analysed in this chapter.

Chapter 6 discusses the importance of spectral efficiency in cellular mobile communications. Improvement in spectral efficiency while using massive MIMO technology are analyzed. The important factors that influence the spectral efficiency of massive MIMO are identified, and optimum values of these factors for different operating conditions are found out using algorithms implemented in MATLAB.

Chapter 7 identified the main limiting factor of massive MIMO, i.e., pilot contamination. The causes of pilot contamination, existing studies and research works in mitigating the effect of pilot contamination are analyzed in depth. The novel pilot assignment strategy, its implementation using social spider optimization algorithm and its performance evaluation are given in this chapter.

1.5 Chapter Summary

This chapter summarizes the status, future needs, and expectations of the society in the field of wireless and mobile communications. The developments in this area excite us and form a motivation to study existing works, identify the bottlenecks and design new techniques to improve the performance of wireless and cellular communication. Engineers, Scientists, and Researchers have to take emerging challenges in the design and development of wireless and mobile-based communication systems that can efficiently be integrated with the 4G/5G wireless communications. This chapter also throws light to the structure of the remaining part of this thesis.

CHAPTER-2

LONG TERM EVOLUTION

2.1 Introduction

Long-Term Evolution (LTE) is the technology behind today's 4G cellular networks, the cell phone we have today almost certainly uses LTE to connect to the cellular network. LTE provides high-speed mobile broadband data and digital cellular telephone service supports. All major smartphones and cellular devices manufactured since 2011 support LTE and use LTE for data access and all major commercial communication carriers in India support LTE including BSNL, Reliance, Tata DoCoMo and MTNL. They all use the same technology to provide high-speed mobile data to their customers. LTE is a global open interoperable standard for wireless high-speed cellular data. It is used by virtually all carriers in the entire world for the current generation of cellular communications. LTE standards are developed by the organization called the third-generation partnership project or 3GPP [23]. Approximately every two years 3GPP releases a new version of their standards. This means that by adopting LTE for nationwide broadband network, it is already prepared for 4G and 5G in the future. So 5G technology might have a different name and won't be called as LTE. It will essentially be a new version of the same technology [24].

An LTE network has four major components or subsystems. First is the core network which is the brains of the network. It consists of servers and gateways that control access, quality of service, billing

and network policies. The core provides access to the Internet and multimedia services like telephone calls. Second is the Radio Access Network(RAN), which are the sites of the cell towers. These towers have transceiver equipment and antennas and provide wireless coverage for all devices. The third is the backhaul network which is made up of fibre and microwave connections. The backhaul network connects the radio access network to the core network. The backhaul network represents the roadways, where the data gets from the mobile device back to the core network. So, one can access the network, make telephone calls and access other network services. Last but not the least is the user equipment which consists of cell phones mobile routers and other devices used by individuals to get connected to the RAN [25].

LTE has many features and capabilities, but there are four aspects to the LTE based nationwide broadband network that will really be very beneficial for effective communication. These four features are exclusive spectrum, high-speed data, priority and pre-emption and the self-organizing network (SON) [26].

Regarding the exclusive spectrum, the LTE technology itself also comes in two flavours, A Frequency Division Duplex (FDD) variant and Time Division Duplex (TDD) variant. The FDD variant uses separate frequencies for uplink and downlink in the form of a band pair. These two bands also have sufficient separation to avoid any sort of receiver performance impairment due to transmitted signal interference. In FDD mode there are 32 different frequency bands defined for LTE with different band widths as well as uplink and downlink spacings, all within the range of 700 to 3600MHz.

The LTE TDD mode is operating in unpaired mode because both the uplink (UL) and downlink (DL) share the same frequency band with time division multiplexing. The LTE bands defined from 33 to 44 are reserved for TDD and this also spread within a range of 700 to 3600MHz [27].

The speed of data transmission in LTE starts with a minimum standard of 100Mbps and extend up to a maximum of 1Gbps. In routine situations or major events, too many users trying to access the LTE system at the same time overwhelms the capacity. At the same time, users already on the network are competing for bandwidth. Both situations combine to prevent information from getting through when it is needed most. LTE Priority Manager and Pre-emption solutions deliver the quality of service(QoS) that users expect to ensure so that critical information gets to the right person at the right time.

The ability of the network to repair itself during outages are part of SON. LTE networks can be set up to accommodate for those outages dynamically and on the fly. Networks can automatically go back to its original state. It means that the broadband networks have a much higher degree of resiliency and survivability [28].

2.2 Key Enabling Technologies of LTE

To meet the performance and service requirements of LTE, its design incorporates several enabling and core network technologies. It defines the air interface technology and the access network architecture. The air interface of LTE is based on OFDM and Multiple antenna systems (MIMO) will apparently play a role in increasing the capacity of the wireless link [29].

2.3 Orthogonal Frequency Division Multiplexing (OFDM)

OFDM is a type of Multi Carrier Modulation (MCM) which essentially converts a wideband channel of band width B into parallel narrow band channels of bandwidth B/N . Hence MCM transmits N symbols using N subcarriers in a time period of N/B . Hence the total symbol rate will be $N/(N/B)$, which is equal to B itself as in single carrier system. The advantage of MCM is that by dividing the wideband channel into multiple subcarrier channels of narrow band, the chances of inter symbol interference is eliminated. This is because the band width of each subcarrier is much less than the coherence bandwidth. This in turn greatly simplifies the receiver design essentially in broadband wireless communication. But the main bottle neck of MCM is that it requires a bank of N modulators at the transmitter side and N demodulators at the receiver side and the practical implementation of the same is challenging when N is large [30].

Fig. 2.1 shows the schematic diagram of an MCM. The first stage is a serial to parallel converter(S/P), where the received data for transmission at the rate of R bits/s are converted to N parallel bit streams of R/N bits/s. of all the modulators are combined and transmitted. This is required because in MCM, N parallel symbols are generated and transmitted simultaneously. Next stage is a bank of N parallel modulators with separate carrier frequency to each modulator, and finally, the output is obtained by adding all the modulator outputs.

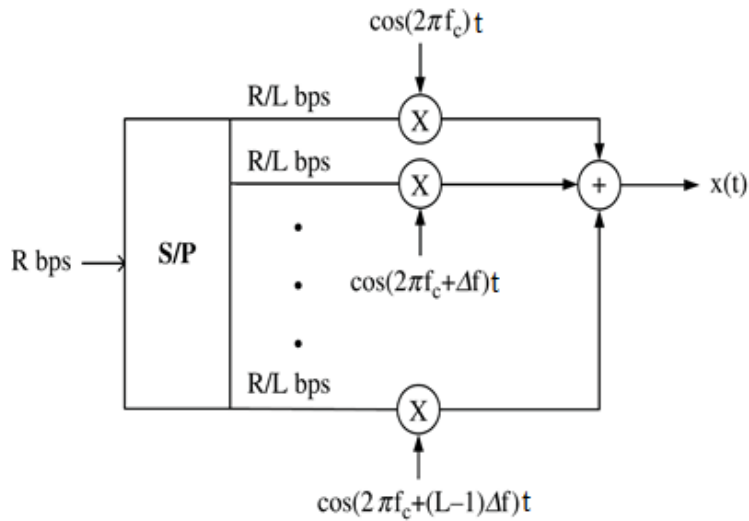


Figure 2.1 Basic multi-carrier modulator where each data stream is modulated separately with different carriers

Fig. 2.2 shows the details of an MCM demodulator where each data stream on the subcarrier is demodulated separately by separate receivers and then converted to a single high rate data stream by a Parallel to Serial(P/S) converter.

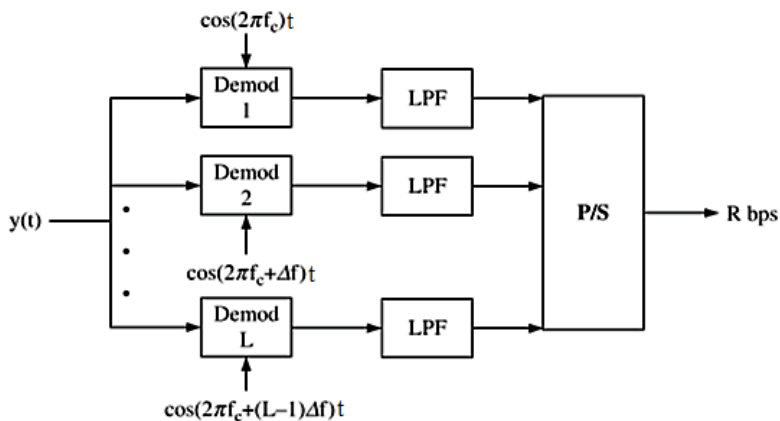


Figure 2.2 Basic multi carrier demodulator with N separate demodulators.

The advancement made by two engineers Weinstein and Ebert, the “Data transmission by frequency division multiplexing using

discrete Fourier transform” [31] known as OFDM, where the composite MCM transmit signal can simply be generated by using IFFT operation, greatly simplified the need for large bank of modulators and demodulators at the transmitter and receiver sides.

In MCM, guard bands are provided in between sub carriers to avoid inter-carrier interference (Fig. 2.3) at the expense of bandwidth efficiency. In OFDM, the centre of one subcarrier is positioned such that it lands into the null of the neighbouring subcarrier as shown in Fig. 2.4 saving bandwidth of more than 50%.

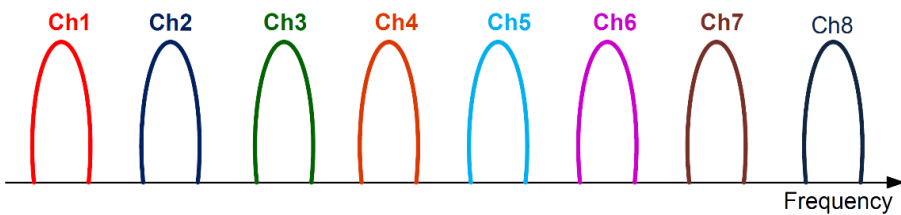


Figure 2.3 Carrier allocation in Conventional Multicarrier Technique

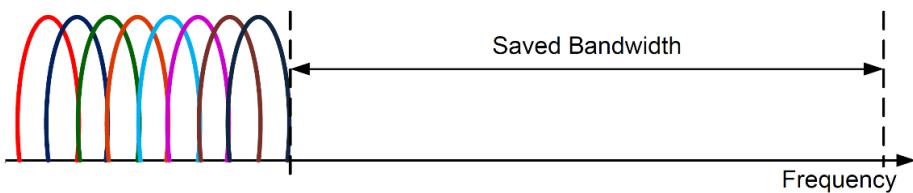


Figure 2.4 Carrier allocation Orthogonal Multicarrier Modulation Technique

Implementing an IFFT at the transmitter and corresponding FFT at the receiver is much simpler than implementing a bank of modulators/demodulators corresponding to each subcarrier. It greatly enhances the practical realizability of the system.

The OFDM explained above needs a slight modification to

completely avoid the Inter Symbol Interference (ISI), which is called as cyclic prefix insertion. It is a guard band made between the OFDM symbols in order to cope with the intra symbol interference. This is done by extending the duration of the symbol and inserting the so-called cyclic prefix into it. It has got two elements, a guard band whose magnitude is equal to the delay spread and duplicate copy of the initial part of the symbol to end of the symbol. So OFDM greatly reduces the implementation complexity of parallel modulator blocks as well as it converts a flat fading channel into a number of parallel flat fading channels and completely eliminates the ISI, paving the way to broadband wireless communication for 4G and 5G standards.

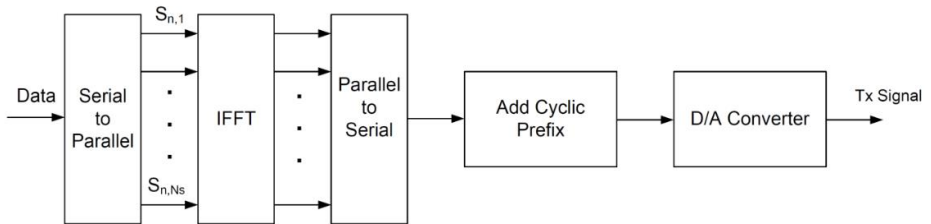


Figure 2.5 Block diagram of OFDM transmitter

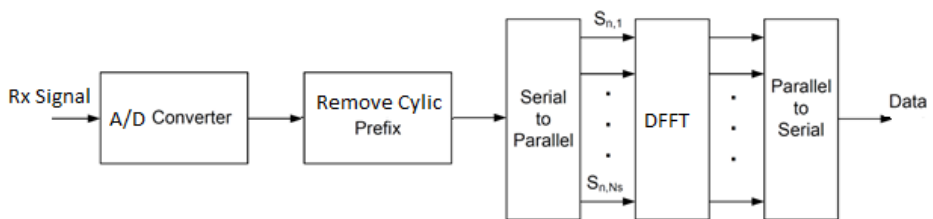


Figure 2.6 Block diagram of OFDM Receiver

The block diagram of an OFDM transmitter is shown in Fig. 2.5 where a single IFFT module replaces the bank of N modulators used in MCM. Fig. 2.6 shows the OFDM receiver with the DFFT which replaces the bank of demodulators in MCM receiver [32].

2.4 Advantages and Disadvantages of OFDM System

OFDM has been used in many high data rate wireless systems because of the numerous advantages. Some of them include:

Resistance to selective fading: OFDM is more resistant to frequency selective fading than single carrier systems because it divides the overall channel into multiple narrow-band channels. These channels being narrowband, suffer from flat fading and appear robust than the wide-band channel.

High Spectrum efficiency: Use of closely-spaced overlapping orthogonal sub-carriers enables data transmission with low bandwidth channels, and hence it makes efficient use of the available spectrum.

Resilience to interference: Interference appearing on a channel may be bandwidth limited, and in this way it does not affect all the sub-channels. This reduces the channel fluctuations.

Resilient to narrow-band effects: Use of adequate channel coding and interleaving make it possible to recover symbols lost due to the frequency selectivity of the channel and narrow band interference.

Resilient to ISI: OFDM is very resilient to inter-symbol and inter-frame interference. This is since each of the sub-channel carries low data rate data stream.

Simpler channel equalization: In conventional digital communication and spread spectrum communication, channel equalization must be applied across the whole channel bandwidth. So channel equalization complexity increases. In contrast, only a one-tap

equalizer is required for OFDM channel equalization as it uses multiple sub-channels. This reduces equalization complexity in OFDM.

Though OFDM has been in wide spread use, there are many challenges and drawbacks to be addressed while considering its use and the main drawbacks are listed below.

Sensitive to carrier offset and drift: OFDM is sensitive to carrier frequency offset and drift compared to the single carrier system

High peak to average power ratio: OFDM signals are characterized by the noise like amplitude variation in the time domain and have relatively large dynamic range leading to high peak to average power ratio (PAPR). This influences the RF amplifier efficiency as the amplifiers need to be linear and accommodate the large amplitude swings and these factors mean that the amplifier cannot operate with a higher efficiency level.

Receiver complexity: Complexity of the OFDM receiver increases with the higher number of sub-channels.

Increased Computational complexity: Computational complexity associated with OFDM system increases both at transmitter and receiver by increasing the number of sub-carriers [33].

LTE uses OFDM technology for its downlink communication, i.e., from the base station to user terminal. OFDM meets the LTE requirement for spectrum flexibility and enables cost-efficient solutions for very wide carriers with high peak rates. It is a well-established technology and used, for example in standards such as IEEE 802.11a/b/g, 802.16, HIPERLAN2, DVB, and DAB.

2.5 Multiple Input Multiple Output Systems

The traditional structure of a wireless communication link consists of a single antenna at the transmitter as well as at the receiver side. This, known as single input single output systems(SISO), was widely used for the past few decades for both mobiles as well as fixed communications. However, due to the huge increase in the data rates and capacity requirements within the restricted spectrum, the necessity of increased spectral efficiencies was originated.

Multiple Input Multiple Output (MIMO) system uses multiple antennas both at the transmitter and receiver side. It offers highly improved performance because it uses multiple paths for propagation of signals from the transmitter to receiver. This is achieved without the use of any additional bandwidth or power. MIMO technology uses antenna arrays for transmission and / or reception to improve the quality of the SNR and / or the transmission rate. This not only makes it possible to reduce the emission level of the radio signals in order to reduce the surrounding electromagnetic pollution but also extend the battery life of mobile devices.

Conventionally, communication engineers considered natural multi-path propagation as a deficiency to be eliminated, but MIMO is the first communication technology that considers multi-path propagation as a phenomenon to be exploited in a useful way. MIMO technology improves the performance of wireless networks by multiplying signals in an efficient and effective way.

MIMO techniques can be categorized into three:

i. *Spatial diversity*: Spatial diversity consists of sending the same data stream simultaneously from different antennas. At the reception, several replicas of the signal are received on each of the antennas and are combined coherently. This combination helps to reduce signal attenuation and compensate for fading introduced by the transmission channel. The spatial diversity presents a good efficiency when the MIMO sub channels are de-correlated from each other. Furthermore, when the number of antennas on the broadcast increases, the signal strength received at a given instant increases, thus improving signal detection.

ii. *Spatial multiplexing*: Spatial multiplexing transmits different data streams on the different transmit antennas through spatially separated beams to different receive antennas. The signals received on the receiving antennas are reassembled to reconstitute the original message. This increases the transmission rate of the MIMO system and called as the multiplexing gain. The channel capacity of a MIMO system is defined by the equation below [34].

$$C = \log_2[\det(I_{N_r} + \frac{\rho}{N_t} HH^\dagger)] \text{ bps/Hz} \quad (2.1)$$

where N_t is the number of transmit antennas, N_r is number of receive antennas, I_{N_r} identity matrix $N_r \times N_r$, \dagger is the trans-conjugate operation. H is the MIMO channel matrix $N_t \times N_r$, $\rho = P/N_oB$ is the SNR at the receiver. P is the total power transmitted, and N_o is the power spectral density of the white Gaussian noise.

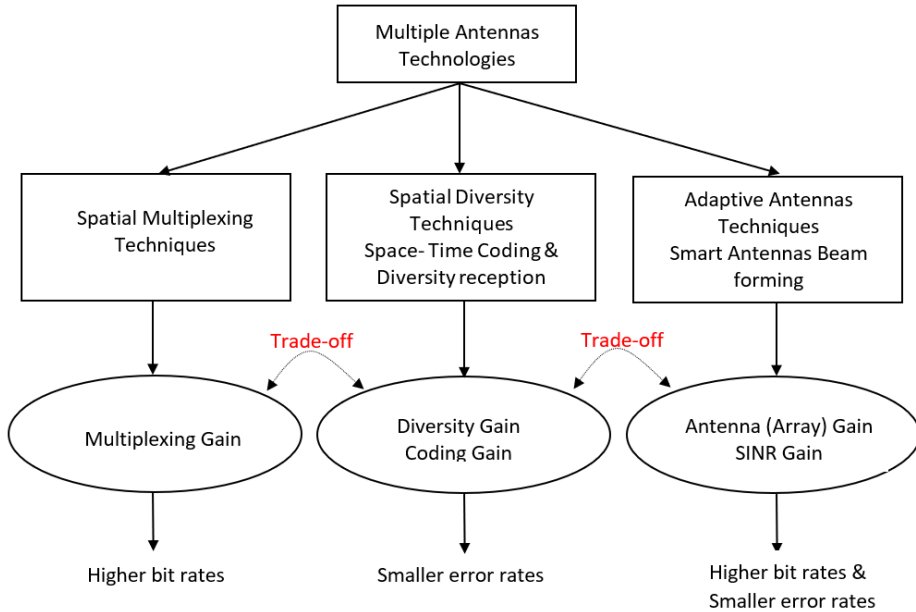


Figure 2.7 Various MIMO techniques

The received signals are decoded and combined to reform the transmitted message. As for MIMO spatial diversity, propagation sub channels must be de-correlated. Diversity gain provides an improvement in the signal to interference ratio and there by transmit power can be reduced without loss of performance. MIMO diversity and multiplexing techniques can be applied together to make use of both the diversity gain and multiplexing gain.

iii. *Adaptive antenna (Beamforming)*: This technique is used to create a certain antenna directive pattern to get the required performance. These antennas can be controlled automatically according to the required conditions. It is thus possible to create constructive / destructive lobes and to optimize transmission between the transmitter and the target. Beam-forming techniques can both extend radio coverage and limit interference between users and surrounding electromagnetic pollution [35].

2.6 Single User and Multi-User MIMO

There are two more variants of MIMO depending on the number of users simultaneously receiving data on the same carriers.

In the Single User MIMO (SU-MIMO), the full system bandwidth is allotted to a single high-speed device during each time slot. i.e., it sends multiple data streams using multiple number of antennas, but all the data streams are focused to single receiver as shown in Fig. 2.8(a).

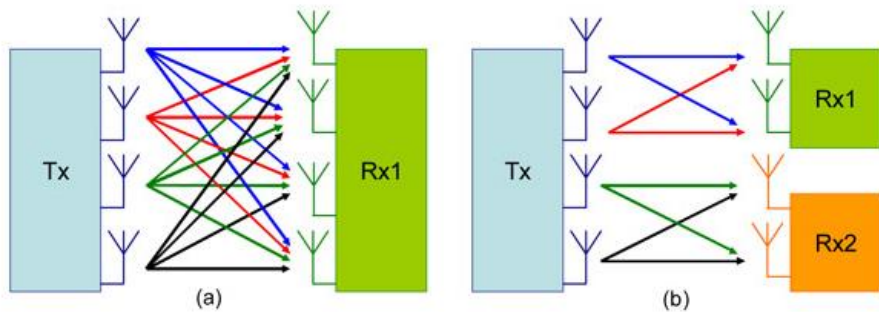


Figure 2.8

(a). SU-MIMO with four streams (b). M-U MIMO with two users and two streams

The Multi-User MIMO (MU-MIMO) allows to share the radio throughput and send data streams to 2 or more users, for example, four transmitting antennas and two antennas in each receiver. It uses the "spatial multiplexing" mode and allows to increase the spectral efficiency of the radio cell (the overall rate) without imposing a high number of antennas in each terminal. This is shown in Fig. 2.8(b)

The combination of MIMO along with OFDM permit to take the advantages of both the techniques but Inter-Carrier Interference(ICI) will occur due to the loss of orthogonality among the subcarriers. This drastically deteriorates the performance of the conventional channel

estimation techniques in MIMO-OFDM systems. This is caused by the frequency shift between the oscillators at the transmitter and receiver side due to Doppler effect, frequency offset and phase noise. MIMO-OFDM is the most prominent air interface technology for 4G and 5G broadband wireless communications.

2.7 MIMO Channel Model

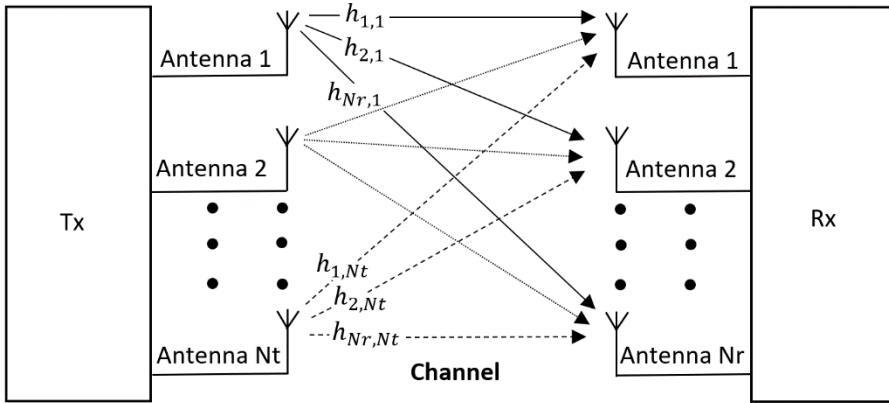


Figure 2.9 MIMO system with N_t transmit antennas and N_r receive antennas

Fig. 2.9 depicts an $N_t \times N_r$ MIMO system with N_t transmit antennas and N_r receive antennas. The input to output relationship for this channel can be expressed as

$$y(t) = H(t) * x(t) + n(t) \quad (2.2)$$

where $H(t)$ is an $N_r \times N_t$ channel response matrix. $x(t)$ is the transmitted signal, $y(t)$ is the received signal, $n(t)$ is additive white Gaussian noise(AWGN), and ‘*’ denotes convolution. If a sufficiently narrow signal bandwidth is assumed then the channel can be considered as a frequency flat channel and then the input-output relationship of the channel will simplify to

$$y = Hx + n \quad (2.3)$$

or

$$\begin{bmatrix} y_1 \\ y_2 \\ \cdot \\ y_i \\ \cdot \\ y_{N_R} \end{bmatrix} = \begin{bmatrix} h_{11} & h_{12} & \dots & h_{1N_T} \\ h_{21} & h_{22} & \dots & h_{2N_T} \\ \cdot & \cdot & \dots & \cdot \\ h_{i1} & h_{i2} & \dots & h_{iN_T} \\ \cdot & \cdot & \dots & \cdot \\ h_{N_R1} & h_{N_R2} & \dots & h_{N_RN_T} \end{bmatrix} \begin{bmatrix} x_1 \\ x_2 \\ \cdot \\ x_i \\ \cdot \\ x_{N_R} \end{bmatrix} + \begin{bmatrix} n_1 \\ n_2 \\ \cdot \\ n_i \\ \cdot \\ n_{N_R} \end{bmatrix} = Hx+n \quad (2.4)$$

where H is the narrowband MIMO channel matrix. This is the channel that is mostly used in the literature and accepted as a good enough approximation [36].

2.8 Advantages and Disadvantages of MIMO

The main advantages and disadvantages of a MIMO system can be summarized as

Advantages:

- The higher data rates with the help of multiple antennas and spatial multiplexing technique. This helps in achieving higher downlink and uplink throughput.
- Reduced bit error rate by using of advanced signal processing algorithms on the received data symbols by multiple antennas.
- Use of beamforming helps in attaining extended cell coverage.
- Minimizes the fading effects due to various diversity techniques.
- High Quality of Service with increased data rate and spectral efficiency.

- Better security because the use of multiple antennas and algorithms brings down the chances of tapping by unauthorized persons.
- Supports a large number of active users per cell.
- Widely accepted in state-of-the-art wireless standards viz. WLAN (802.11n, 802.11ac etc.), WiMAX (IEEE 802.16e), LTE, LTE-Advanced etc.

Disadvantages:

- The higher hardware complexity and resource requirements. Individual RF units for RF signal processing and advanced DSP chip is needed to perform the signal processing.
- Increased power requirements due to increased hardware requirements.
- Higher cost due to increased hardware and advanced software requirements.

Multiple-input, multiple-output antenna technology along with orthogonal frequency-division multiplexing (MIMO-OFDM) is the dominant air interface for 4G and 5G broadband wireless communications. It combines multiple-input, multiple-output (MIMO) technology, which multiplies capacity and signal quality by transmitting different signals over multiple antennas, and orthogonal frequency-division multiplexing (OFDM), which divides a radio channel into a large number of closely spaced subchannels to provide more reliable communications at high speeds.

2.9 Chapter Summary

Long Term Evolution (LTE) offers superior user experience and simplified technology for the present and next-generation mobile broadband communication. In this chapter, we have reviewed the LTE technology, its various features, and capabilities. The basic building blocks of LTE which are OFDM and MIMO are also discussed. Further, the advantages and limiting factors of both OFDM and MIMO have been listed out. In the following chapters, some of these problems are discussed in detail.

CHAPTER-2

LONG TERM EVOLUTION

2.1 Introduction

Long-Term Evolution (LTE) is the technology behind today's 4G cellular networks, the cell phone we have today almost certainly uses LTE to connect to the cellular network. LTE provides high-speed mobile broadband data and digital cellular telephone service supports. All major smartphones and cellular devices manufactured since 2011 support LTE and use LTE for data access and all major commercial communication carriers in India support LTE including BSNL, Reliance, Tata DoCoMo and MTNL. They all use the same technology to provide high-speed mobile data to their customers. LTE is a global open interoperable standard for wireless high-speed cellular data. It is used by virtually all carriers in the entire world for the current generation of cellular communications. LTE standards are developed by the organization called the third-generation partnership project or 3GPP [23]. Approximately every two years 3GPP releases a new version of their standards. This means that by adopting LTE for nationwide broadband network, it is already prepared for 4G and 5G in the future. So 5G technology might have a different name and won't be called as LTE. It will essentially be a new version of the same technology [24].

An LTE network has four major components or subsystems. First is the core network which is the brains of the network. It consists of servers and gateways that control access, quality of service, billing

and network policies. The core provides access to the Internet and multimedia services like telephone calls. Second is the Radio Access Network(RAN), which are the sites of the cell towers. These towers have transceiver equipment and antennas and provide wireless coverage for all devices. The third is the backhaul network which is made up of fibre and microwave connections. The backhaul network connects the radio access network to the core network. The backhaul network represents the roadways, where the data gets from the mobile device back to the core network. So, one can access the network, make telephone calls and access other network services. Last but not the least is the user equipment which consists of cell phones mobile routers and other devices used by individuals to get connected to the RAN [25].

LTE has many features and capabilities, but there are four aspects to the LTE based nationwide broadband network that will really be very beneficial for effective communication. These four features are exclusive spectrum, high-speed data, priority and pre-emption and the self-organizing network (SON) [26].

Regarding the exclusive spectrum, the LTE technology itself also comes in two flavours, A Frequency Division Duplex (FDD) variant and Time Division Duplex (TDD) variant. The FDD variant uses separate frequencies for uplink and downlink in the form of a band pair. These two bands also have sufficient separation to avoid any sort of receiver performance impairment due to transmitted signal interference. In FDD mode there are 32 different frequency bands defined for LTE with different band widths as well as uplink and downlink spacings, all within the range of 700 to 3600MHz.

The LTE TDD mode is operating in unpaired mode because both the uplink (UL) and downlink (DL) share the same frequency band with time division multiplexing. The LTE bands defined from 33 to 44 are reserved for TDD and this also spread within a range of 700 to 3600MHz [27].

The speed of data transmission in LTE starts with a minimum standard of 100Mbps and extend up to a maximum of 1Gbps. In routine situations or major events, too many users trying to access the LTE system at the same time overwhelms the capacity. At the same time, users already on the network are competing for bandwidth. Both situations combine to prevent information from getting through when it is needed most. LTE Priority Manager and Pre-emption solutions deliver the quality of service(QoS) that users expect to ensure so that critical information gets to the right person at the right time.

The ability of the network to repair itself during outages are part of SON. LTE networks can be set up to accommodate for those outages dynamically and on the fly. Networks can automatically go back to its original state. It means that the broadband networks have a much higher degree of resiliency and survivability [28].

2.2 Key Enabling Technologies of LTE

To meet the performance and service requirements of LTE, its design incorporates several enabling and core network technologies. It defines the air interface technology and the access network architecture. The air interface of LTE is based on OFDM and Multiple antenna systems (MIMO) will apparently play a role in increasing the capacity of the wireless link [29].

2.3 Orthogonal Frequency Division Multiplexing (OFDM)

OFDM is a type of Multi Carrier Modulation (MCM) which essentially converts a wideband channel of band width B into parallel narrow band channels of bandwidth B/N . Hence MCM transmits N symbols using N subcarriers in a time period of N/B . Hence the total symbol rate will be $N/(N/B)$, which is equal to B itself as in single carrier system. The advantage of MCM is that by dividing the wideband channel into multiple subcarrier channels of narrow band, the chances of inter symbol interference is eliminated. This is because the band width of each subcarrier is much less than the coherence bandwidth. This in turn greatly simplifies the receiver design essentially in broadband wireless communication. But the main bottle neck of MCM is that it requires a bank of N modulators at the transmitter side and N demodulators at the receiver side and the practical implementation of the same is challenging when N is large [30].

Fig. 2.1 shows the schematic diagram of an MCM. The first stage is a serial to parallel converter(S/P), where the received data for transmission at the rate of R bits/s are converted to N parallel bit streams of R/N bits/s. of all the modulators are combined and transmitted. This is required because in MCM, N parallel symbols are generated and transmitted simultaneously. Next stage is a bank of N parallel modulators with separate carrier frequency to each modulator, and finally, the output is obtained by adding all the modulator outputs.

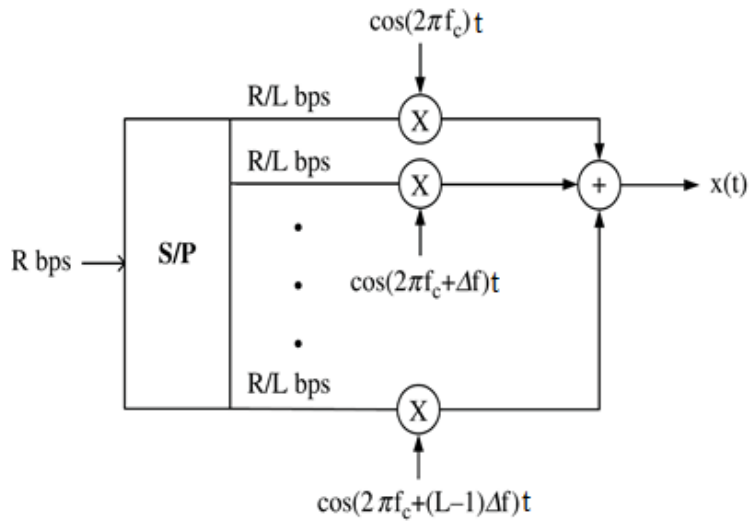


Figure 2.1 Basic multi-carrier modulator where each data stream is modulated separately with different carriers

Fig. 2.2 shows the details of an MCM demodulator where each data stream on the subcarrier is demodulated separately by separate receivers and then converted to a single high rate data stream by a Parallel to Serial(P/S) converter.

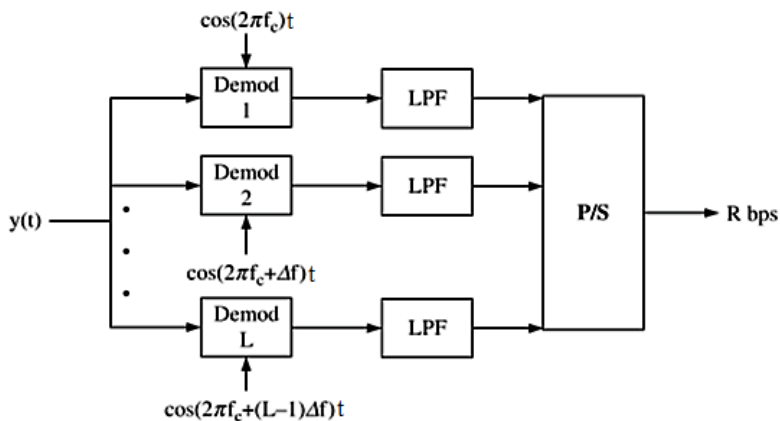


Figure 2.2 Basic multi carrier demodulator with N separate demodulators.

The advancement made by two engineers Weinstein and Ebert, the “Data transmission by frequency division multiplexing using

discrete Fourier transform” [31] known as OFDM, where the composite MCM transmit signal can simply be generated by using IFFT operation, greatly simplified the need for large bank of modulators and demodulators at the transmitter and receiver sides.

In MCM, guard bands are provided in between sub carriers to avoid inter-carrier interference (Fig. 2.3) at the expense of bandwidth efficiency. In OFDM, the centre of one subcarrier is positioned such that it lands into the null of the neighbouring subcarrier as shown in Fig. 2.4 saving bandwidth of more than 50%.

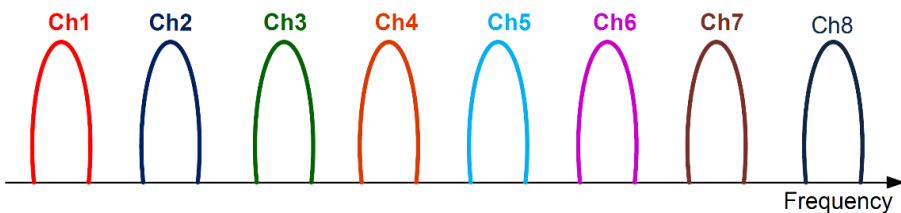


Figure 2.3 Carrier allocation in Conventional Multicarrier Technique

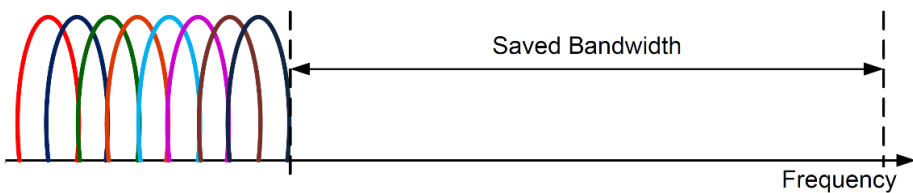


Figure 2.4 Carrier allocation Orthogonal Multicarrier Modulation Technique

Implementing an IFFT at the transmitter and corresponding FFT at the receiver is much simpler than implementing a bank of modulators/demodulators corresponding to each subcarrier. It greatly enhances the practical realizability of the system.

The OFDM explained above needs a slight modification to

completely avoid the Inter Symbol Interference (ISI), which is called as cyclic prefix insertion. It is a guard band made between the OFDM symbols in order to cope with the intra symbol interference. This is done by extending the duration of the symbol and inserting the so-called cyclic prefix into it. It has got two elements, a guard band whose magnitude is equal to the delay spread and duplicate copy of the initial part of the symbol to end of the symbol. So OFDM greatly reduces the implementation complexity of parallel modulator blocks as well as it converts a flat fading channel into a number of parallel flat fading channels and completely eliminates the ISI, paving the way to broadband wireless communication for 4G and 5G standards.

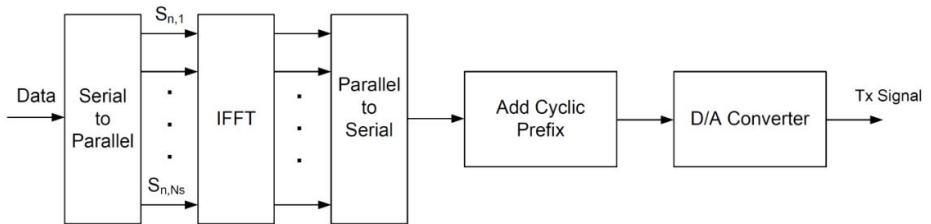


Figure 2.5 Block diagram of OFDM transmitter

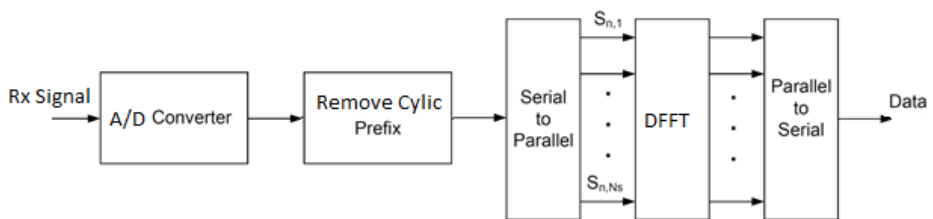


Figure 2.6 Block diagram of OFDM Receiver

The block diagram of an OFDM transmitter is shown in Fig. 2.5 where a single IFFT module replaces the bank of N modulators used in MCM. Fig. 2.6 shows the OFDM receiver with the DFFT which replaces the bank of demodulators in MCM receiver [32].

2.4 Advantages and Disadvantages of OFDM System

OFDM has been used in many high data rate wireless systems because of the numerous advantages. Some of them include:

Resistance to selective fading: OFDM is more resistant to frequency selective fading than single carrier systems because it divides the overall channel into multiple narrow-band channels. These channels being narrowband, suffer from flat fading and appear robust than the wide-band channel.

High Spectrum efficiency: Use of closely-spaced overlapping orthogonal sub-carriers enables data transmission with low bandwidth channels, and hence it makes efficient use of the available spectrum.

Resilience to interference: Interference appearing on a channel may be bandwidth limited, and in this way it does not affect all the sub-channels. This reduces the channel fluctuations.

Resilient to narrow-band effects: Use of adequate channel coding and interleaving make it possible to recover symbols lost due to the frequency selectivity of the channel and narrow band interference.

Resilient to ISI: OFDM is very resilient to inter-symbol and inter-frame interference. This is since each of the sub-channel carries low data rate data stream.

Simpler channel equalization: In conventional digital communication and spread spectrum communication, channel equalization must be applied across the whole channel bandwidth. So channel equalization complexity increases. In contrast, only a one-tap

equalizer is required for OFDM channel equalization as it uses multiple sub-channels. This reduces equalization complexity in OFDM.

Though OFDM has been in wide spread use, there are many challenges and drawbacks to be addressed while considering its use and the main drawbacks are listed below.

Sensitive to carrier offset and drift: OFDM is sensitive to carrier frequency offset and drift compared to the single carrier system

High peak to average power ratio: OFDM signals are characterized by the noise like amplitude variation in the time domain and have relatively large dynamic range leading to high peak to average power ratio (PAPR). This influences the RF amplifier efficiency as the amplifiers need to be linear and accommodate the large amplitude swings and these factors mean that the amplifier cannot operate with a higher efficiency level.

Receiver complexity: Complexity of the OFDM receiver increases with the higher number of sub-channels.

Increased Computational complexity: Computational complexity associated with OFDM system increases both at transmitter and receiver by increasing the number of sub-carriers [33].

LTE uses OFDM technology for its downlink communication, i.e., from the base station to user terminal. OFDM meets the LTE requirement for spectrum flexibility and enables cost-efficient solutions for very wide carriers with high peak rates. It is a well-established technology and used, for example in standards such as IEEE 802.11a/b/g, 802.16, HIPERLAN2, DVB, and DAB.

2.5 Multiple Input Multiple Output Systems

The traditional structure of a wireless communication link consists of a single antenna at the transmitter as well as at the receiver side. This, known as single input single output systems(SISO), was widely used for the past few decades for both mobiles as well as fixed communications. However, due to the huge increase in the data rates and capacity requirements within the restricted spectrum, the necessity of increased spectral efficiencies was originated.

Multiple Input Multiple Output (MIMO) system uses multiple antennas both at the transmitter and receiver side. It offers highly improved performance because it uses multiple paths for propagation of signals from the transmitter to receiver. This is achieved without the use of any additional bandwidth or power. MIMO technology uses antenna arrays for transmission and / or reception to improve the quality of the SNR and / or the transmission rate. This not only makes it possible to reduce the emission level of the radio signals in order to reduce the surrounding electromagnetic pollution but also extend the battery life of mobile devices.

Conventionally, communication engineers considered natural multi-path propagation as a deficiency to be eliminated, but MIMO is the first communication technology that considers multi-path propagation as a phenomenon to be exploited in a useful way. MIMO technology improves the performance of wireless networks by multiplying signals in an efficient and effective way.

MIMO techniques can be categorized into three:

i. *Spatial diversity*: Spatial diversity consists of sending the same data stream simultaneously from different antennas. At the reception, several replicas of the signal are received on each of the antennas and are combined coherently. This combination helps to reduce signal attenuation and compensate for fading introduced by the transmission channel. The spatial diversity presents a good efficiency when the MIMO sub channels are de-correlated from each other. Furthermore, when the number of antennas on the broadcast increases, the signal strength received at a given instant increases, thus improving signal detection.

ii. *Spatial multiplexing*: Spatial multiplexing transmits different data streams on the different transmit antennas through spatially separated beams to different receive antennas. The signals received on the receiving antennas are reassembled to reconstitute the original message. This increases the transmission rate of the MIMO system and called as the multiplexing gain. The channel capacity of a MIMO system is defined by the equation below [34].

$$C = \log_2[\det(I_{N_r} + \frac{\rho}{N_t} HH^\dagger)] \text{ bps/Hz} \quad (2.1)$$

where N_t is the number of transmit antennas, N_r is number of receive antennas, I_{N_r} identity matrix $N_r \times N_r$, \dagger is the trans-conjugate operation. H is the MIMO channel matrix $N_t \times N_r$, $\rho = P/N_oB$ is the SNR at the receiver. P is the total power transmitted, and N_o is the power spectral density of the white Gaussian noise.

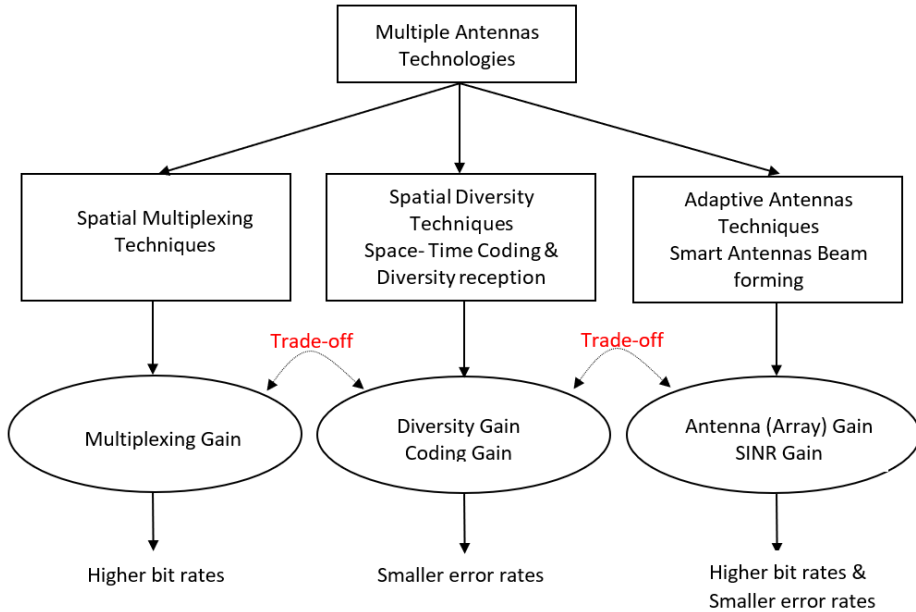


Figure 2.7 Various MIMO techniques

The received signals are decoded and combined to reform the transmitted message. As for MIMO spatial diversity, propagation sub channels must be de-correlated. Diversity gain provides an improvement in the signal to interference ratio and there by transmit power can be reduced without loss of performance. MIMO diversity and multiplexing techniques can be applied together to make use of both the diversity gain and multiplexing gain.

iii. *Adaptive antenna (Beamforming)*: This technique is used to create a certain antenna directive pattern to get the required performance. These antennas can be controlled automatically according to the required conditions. It is thus possible to create constructive / destructive lobes and to optimize transmission between the transmitter and the target. Beam-forming techniques can both extend radio coverage and limit interference between users and surrounding electromagnetic pollution [35].

2.6 Single User and Multi-User MIMO

There are two more variants of MIMO depending on the number of users simultaneously receiving data on the same carriers.

In the Single User MIMO (SU-MIMO), the full system bandwidth is allotted to a single high-speed device during each time slot. i.e., it sends multiple data streams using multiple number of antennas, but all the data streams are focused to single receiver as shown in Fig. 2.8(a).

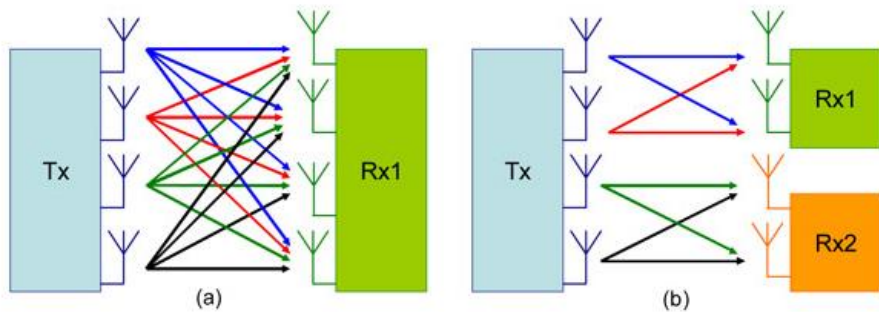


Figure 2.8

(a). SU-MIMO with four streams (b). M-U MIMO with two users and two streams

The Multi-User MIMO (MU-MIMO) allows to share the radio throughput and send data streams to 2 or more users, for example, four transmitting antennas and two antennas in each receiver. It uses the "spatial multiplexing" mode and allows to increase the spectral efficiency of the radio cell (the overall rate) without imposing a high number of antennas in each terminal. This is shown in Fig. 2.8(b)

The combination of MIMO along with OFDM permit to take the advantages of both the techniques but Inter-Carrier Interference(ICI) will occur due to the loss of orthogonality among the subcarriers. This drastically deteriorates the performance of the conventional channel

estimation techniques in MIMO-OFDM systems. This is caused by the frequency shift between the oscillators at the transmitter and receiver side due to Doppler effect, frequency offset and phase noise. MIMO-OFDM is the most prominent air interface technology for 4G and 5G broadband wireless communications.

2.7 MIMO Channel Model

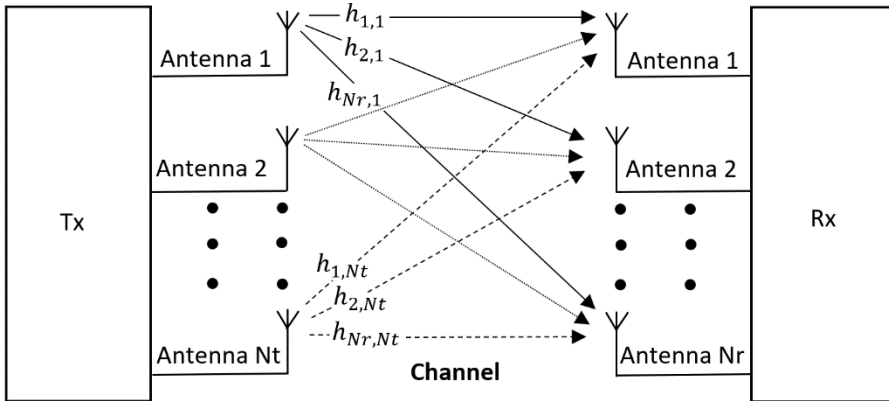


Figure 2.9 MIMO system with N_t transmit antennas and N_r receive antennas

Fig. 2.9 depicts an $N_t \times N_r$ MIMO system with N_t transmit antennas and N_r receive antennas. The input to output relationship for this channel can be expressed as

$$y(t) = H(t) * x(t) + n(t) \quad (2.2)$$

where $H(t)$ is an $N_r \times N_t$ channel response matrix. $x(t)$ is the transmitted signal, $y(t)$ is the received signal, $n(t)$ is additive white Gaussian noise(AWGN), and ‘*’ denotes convolution. If a sufficiently narrow signal bandwidth is assumed then the channel can be considered as a frequency flat channel and then the input-output relationship of the channel will simplify to

$$y = Hx + n \quad (2.3)$$

or

$$\begin{bmatrix} y_1 \\ y_2 \\ \cdot \\ y_i \\ \cdot \\ y_{N_R} \end{bmatrix} = \begin{bmatrix} h_{11} & h_{12} & \dots & h_{1N_T} \\ h_{21} & h_{22} & \dots & h_{2N_T} \\ \cdot & \cdot & \dots & \cdot \\ h_{i1} & h_{i2} & \dots & h_{iN_T} \\ \cdot & \cdot & \dots & \cdot \\ h_{N_R1} & h_{N_R2} & \dots & h_{N_RN_T} \end{bmatrix} \begin{bmatrix} x_1 \\ x_2 \\ \cdot \\ x_i \\ \cdot \\ x_{N_R} \end{bmatrix} + \begin{bmatrix} n_1 \\ n_2 \\ \cdot \\ n_i \\ \cdot \\ n_{N_R} \end{bmatrix} = Hx+n \quad (2.4)$$

where H is the narrowband MIMO channel matrix. This is the channel that is mostly used in the literature and accepted as a good enough approximation [36].

2.8 Advantages and Disadvantages of MIMO

The main advantages and disadvantages of a MIMO system can be summarized as

Advantages:

- The higher data rates with the help of multiple antennas and spatial multiplexing technique. This helps in achieving higher downlink and uplink throughput.
- Reduced bit error rate by using of advanced signal processing algorithms on the received data symbols by multiple antennas.
- Use of beamforming helps in attaining extended cell coverage.
- Minimizes the fading effects due to various diversity techniques.
- High Quality of Service with increased data rate and spectral efficiency.

- Better security because the use of multiple antennas and algorithms brings down the chances of tapping by unauthorized persons.
- Supports a large number of active users per cell.
- Widely accepted in state-of-the-art wireless standards viz. WLAN (802.11n, 802.11ac etc.), WiMAX (IEEE 802.16e), LTE, LTE-Advanced etc.

Disadvantages:

- The higher hardware complexity and resource requirements. Individual RF units for RF signal processing and advanced DSP chip is needed to perform the signal processing.
- Increased power requirements due to increased hardware requirements.
- Higher cost due to increased hardware and advanced software requirements.

Multiple-input, multiple-output antenna technology along with orthogonal frequency-division multiplexing (MIMO-OFDM) is the dominant air interface for 4G and 5G broadband wireless communications. It combines multiple-input, multiple-output (MIMO) technology, which multiplies capacity and signal quality by transmitting different signals over multiple antennas, and orthogonal frequency-division multiplexing (OFDM), which divides a radio channel into a large number of closely spaced subchannels to provide more reliable communications at high speeds.

2.9 Chapter Summary

Long Term Evolution (LTE) offers superior user experience and simplified technology for the present and next-generation mobile broadband communication. In this chapter, we have reviewed the LTE technology, its various features, and capabilities. The basic building blocks of LTE which are OFDM and MIMO are also discussed. Further, the advantages and limiting factors of both OFDM and MIMO have been listed out. In the following chapters, some of these problems are discussed in detail.

CHAPTER-3

ADAPTIVE MODULATION IN MIMO-OFDM NETWORKS

3.1 Introduction

Wireless data communications technology has accepted Long Term Evolution (LTE) as its standard. Its main goal is to maximize the speed and capacity of wireless data networks by exploiting the different modulation and signal processing techniques. Fixed type of modulation techniques cannot make use of the maximum data transfer rate of the changing wireless channel conditions within the allotted bandwidth. This is because the quality of a wireless channel in a practical scenario is continuously being modified and the highest throughput cannot be achieved if the modulation scheme is tailored for a particular value of the channel gain [37].

This work aims to study the various modulation schemes and their performances under various channel conditions and comes up with a comprehensive algorithm to determine the best modulation scheme for a value of transmit SNR. This is achieved by developing a mapping from the SNR value to the best possible modulation rate keeping the BER constraints.

There has been a lot of advancements in digital signal processing and large-scale integrated circuits over many years, and this has led to the development of faster low cost and power efficient modes of communication. Other reasons including high data rates, better error detection and correction techniques, the robustness of the transmitted

signal under varying channel conditions, easier multiplexing techniques, better multiple channel access techniques etc. [38] have led to the success of digital communication over analog communication. Improvements to error detection and correction techniques, encoding and decoding mechanisms, signal conditioning, multi-carrier techniques and equalization along with the advent of digital modulation schemes have made it possible to achieve very high-quality low-cost solutions in the fields of digital communication system. All these factors have made digital communication to be the most suitable choice for wireless applications [39].

Two major types of digital modulation techniques are linear (amplitude shift keying and phase shift keying) and non-linear modulation (frequency shift keying). Although the linear modulation technique is susceptible to more fading, it has higher spectral efficiency when compared to non-linear modulation which is naturally more robust to corruption and fading. The corruption of data could be attributed to many possible factors including the modelling of the channel which might change with time, the attenuation of the signal that may be caused due to the properties of the antenna, thermal noise, inter modulation noise and channel fading which may be caused due to the destructive interference [40]. These factors of noise will reduce the quality of the signal at the receiver making it very difficult to comprehend the received signal which will lead to erroneous decoding of the data. The signal-to-noise ratio (SNR) also depends on the power of the transmitted signal and the channel power gained along with the noise power that gets added.

The types of modulation schemes under consideration are BPSK, QPSK, 16-QAM, and 64-QAM. There are multiple problems that can be listed for a wireless communication system. A typical wireless communication channel causes delays in the signal components and reflection of signals. This results in multipath signal components at the receiver that tend to affect each other randomly. The outcome of this is fading and attenuation of the signal which leads the receiver to decode the signal with a high error probability resulting a lower throughput. Channel fading has always been a problem and has been a highlight in research for many decades. However, the throughput can be increased by increasing the transmitter power high enough to bring down the probability of error to acceptable levels. But, there are a lot of insufficiencies and inefficiencies associated with this approach. Another method is diversity transmission, where the signal is transmitted over multiple channels with statistically independent fading. It provides considerable improvement in the performance but, it has not proved to be cost-effective due to the high equipment costs and high bandwidth requirements. Therefore to achieve high data rates robust and spectrally efficient methods of modulation and coding are required to combat the effects of flat fading channels [41].

3.2 Adaptive Modulation

In wireless communication systems with reciprocal channels, where the channel from the transmitter to the receiver is assumed as approximately the same as the channel from the receiver to the transmitter, the channel characteristics can be estimated by the receiver and the receiver can feedback this information to the transmitter. Then the transmitter can be aware of the channel

conditions in advance and can adapt to appropriate transmission methods suitable for the estimated channel. Such a transmission scheme, which is tailored to the channel conditions present at that time, can always provide better data rates and low bit error rates compared to fixed modulation schemes. Therefore adaptive modulation methods have to be employed in wireless communication networks to maximize the channel utilization and provide high throughput with low bit error rate.

The main focus of adaptive modulation techniques is to maintain a constant E_b/N_o value and correspondingly varying the constellation size, modulation and coding schemes, transmitted power or a combination of these factors. Although techniques have been found to be very effective and efficient, there are practical constraints on its implementation. If the communication channel is modified at a rate faster than it can be estimated, then transmitter fails to adapt to the instantaneous channel conditions [42].

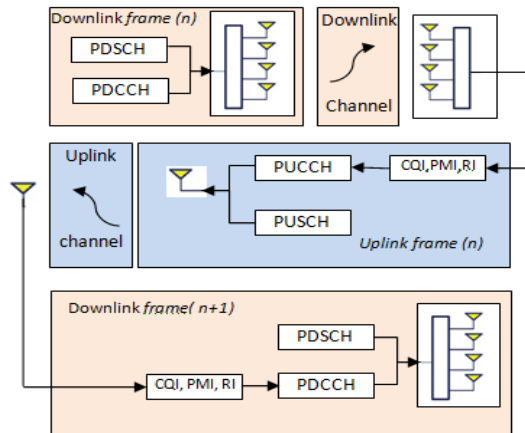


Figure 3.1 Chain of operations associated with link adaptation in LTE

Fig. 3.1 explains the chain of operations associated with link adaptation in an LTE network. The network is divided into downlink and uplink processes. The downlink transmitter forms information resource from Physical Downlink Shared Channel (PDSCH) and Downlink Control Information (DCI). DCI carries information about scheduling assignments whereas PDSCH contains information about used MIMO mode, Modulation and Coding Schemes (MCS), rank information and pre-coder matrix. The mobile receiver then performs channel condition measurement which includes the Channel Quality Indicator (CQI), Rank Indicator (RI) and Pre-coder Matrix Indicator (PMI). Operations for the next sub-frame ($n+1$) are written into PDCCH and sent to the mobile unit. This complete feedback chain is repeated for every sub-frame [43].

The channel quality indicator is a measure of the radio channel quality in the downlink which can specify the modulation scheme to be used for best performance in the downlink data transmission. Precoding matrix indicator gives information about the best precoding matrix to be used for downlink. The rank indicator gives information about the best spatial multiplexing mode that can be used for downlink transmission [44, 45]. In this work, only the CQI is used for feedback and for changing the modulation scheme for the successive sub-frames according to the channel conditions. In the implemented scheme, for a given sub-frame all resource blocks will have the same modulation method and the changes occur in between the sub-frames only.

3.3 Review of Techniques used for Adaptive Modulation

From an extensive review of existing works available in literature, it is observed that adaptive modulation is one of the interesting areas of research in wireless communications networks particularly in the broadband wireless access technologies like Wi-Fi (802.11), WiMAX (802.16e), etc. Adaptive modulation techniques are used for maximizing the throughput and minimize the BER in an OFDM environment.

This section summarizes some of the existing research works in adaptive modulation for wireless communication environment.

Theoretical analysis has been made for the spectral efficiency of MIMO OFDM system with adaptive modulation by Z. Zhendong in [46]. The results are evaluated using simulation along with different modulation schemes. The study shows that the quality of channel state information (CSI) plays an important role in the performance of adaptive modulation schemes.

A MIMO with Space-Time Block Coding (STBC) was analyzed by H. Jinliang *et al.* in [47]. They simulated its performance under four different modulation schemes as well as adaptive modulation. They found performance improvement in the average transmitted power and instantaneous and average BERs under adaptive modulation scheme.

In [48] Z. Zhou *et al.* have shown that a good tradeoff between BER and channel capacity can be achieved by using adaptive MIMO systems using imperfect CSI and D. M. Jimenez *et al.* in [49] analyzed an adaptive MIMO with OFDMA with the lower three-square

constellation QAM schemes. They used rank adaptation method, where the number of active antenna elements was changed according to the transmit channel SNR values. A substantial improvement in the spectral efficiency performance is achieved compared to the standalone transmission schemes.

Variable power adaptive modulation and constant power adaptive modulation were tested using MATLAB simulations on 2x2 MIMO and SISO systems with STBC coding by Y. Xiangbin et al. in [50]. Rayleigh fading channel in both quasi-static and flat fading are considered for optimizing the spectral efficiency performance under the given BER constraints. They have proved that variable power adaptation method gives better average spectral efficiency compared to fixed power scheme and better improvement is achieved in MIMO systems compared to SISO.

A 2x2 MIMO systems with imperfect CSI as well as perfect CSI were analyzed in [51] by X. B. Yu et al. The adaptive modulation with variable power and also with variable antenna configurations are used in their analysis. They considered a Rayleigh fading channel and optimized its capacity with the BER and transmitted power constraints. Their study showed that the variable power adaptive modulation provides better spectral efficiency compared to the constant power counterpart.

A summary of the type, methods and performance gains of the major works are given in the table 3.1. All these works concentrate on optimization on maximizing the throughput or minimizing the BER or minimizing the transmit power.

Table 3.1 Methods and performance gains of different modulation schemes

Method Used	Modulation schemes	Type of Adaptation used	Achievements	Communication channel in use	Channel capacity (bit/sec /Hz)	SNR gain at $BER_T = 10^{-5}$
2x2 MIMO with adaptive modulation Both perfect and imperfect Channel state information[46]	64QAM, 16QAM,4QAM (All square constellation modulations)	Continuous data rate change & Discrete data rate change	Variable rate, variable power and variable power and rate models attained full multiplexing gain. CSI Adaptation process is very sensitive to CSI deficiency.	Flat fading MIMO channel	At lesser SNR values the VRVP method has large SNR penalty. At high SNR region variable rate and variable power and rate methods good capacity improvements.	10dB, 15dB, 20dB for 4QAM,16QAM and 64 QAM respectively
STBC-MIMO with Adaptive Modulation[47]	64QAM, 16QAM,QPSK,BPSK	Switching among different M-QAM schemes	Good improvements in Capacity and average and instantaneous BER and average transmitted power	i.i.d Rayleigh fading channel	Medium and high SNR range gives improved channel capacity.	64QAM= 22.59, 16QAM= 16.61,QPSK= 9.86, , and BPSK= 6.85
Adaptive MIMO- with imperfect CSI [48]	1024-QAM, 256-QAM, 16-QAM, 64QAM, 4-QAM	Variable power Adaptive modulation scheme	Highly robust against imperfections in CSI and provides a very good tradeoff between average capacity and BER	Rayleigh fading-Flat uncorrelated	very good trade off between average capacity and BER	$SNR =$ = 10dB, 15dB, 20dB

Adaptive MIMO-OFDMA system [49]	64QAM 16QAM, QPSK	Adapt no. of active antennas(Rank)	High improvement in channel capacity especially in low SNR region.	Rayleigh fading with spatial correlation.	Substantial improvement in average channel capacity compared to standalone systems with fixed antennas	64QAM= 22.6, 16QAM= 16.75, QPSK=10.35,
STBC-MIMO with Adaptive Modulation[50]	256QAM, 64QAM, 16QAM, 4QAM,	Variable power Adaptive modulation and constant power adaptive modulation	Variable power adaptation method is very effective in improving the channel capacity.	Rayleigh fading channel in both quasi-static and flat fading	Variable power adaptation method gives better average spectral efficiency compared to the fixed power scheme.	3T2R-VP with G3=6dB, 2T2R-VP with G2=7dB, 2T2R-VP with G2=9dB, 2T2RVP with G2=8dB
Adaptive MIMO-system [51]	256QAM 64QAM,16QAM, 4QAM, BPSK	Variable power Adaptive modulation and constant power adaptive modulation with antenna selection	Variable power Adaptive modulation provides better spectral efficiency compared to the constant power counter part.	Quasi-static flat Rayleigh fading channel	Effect of adaptive modulation is more predominant when the number of antennas are more both at the transmitter side and at the receiver side.	SNR= 9.5dB 16QAM with variable power option.

3.4 System model

The communication system under consideration is shown in Fig. 3.2. The channel is a discrete-time varying system which has a time-varying gain and an additive white Gaussian noise. The channel is assumed to be a really flat fading channel with coherent detection. Since the channel is assumed to be flat fading, the bandwidth of the signal is much lesser than that of the channel.

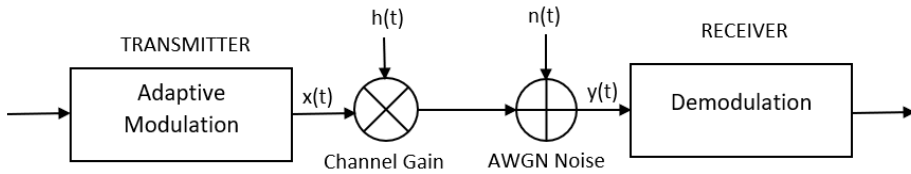


Figure 3.2 Communication system model

This gives an advantage of the spectral characteristics of the channel being preserved over time. Although the amplitude of the signal may vary with time, the probability density function of the flat fading channel is given by the expression

$$p(r) = \begin{cases} \frac{r}{\sigma^2} \exp\left(-\frac{r^2}{2\sigma^2}\right) & (0 \leq r \leq \infty) \\ 0 & (r < 0) \end{cases} \quad (3.1)$$

where r is the range, and σ^2 is the noise variance which is equal to 1. The exponential distribution of the channel is considered due to the multipath effect of the channel. Also, the rate of variation of the channel determines how frequent the transmitter should adapt to the changing channel condition and to choose the best modulation scheme. In order to account for the randomness of noise in the channel, which could corrupt the transmitted signal, it is modeled as additive white Gaussian noise and is flat for all frequencies. Thus the actual

communication channel shown in Fig. 3.2 can be described by the equation

$$y(t) = x(t) * h(t) + n(t) \quad (3.2)$$

where $y(t)$ is the received signal, $x(t)$ is the transmitted signal, $h(t)$ channel response and $n(t)$ is the AWGN.

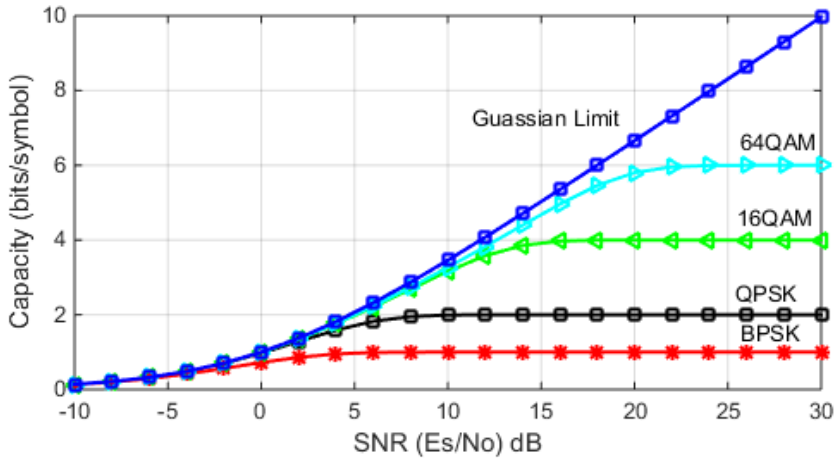


Figure 3.3 Capacity limits under various modulation schemes plotted against SNR

The plot given in Fig. 3.3 shows the capacity limits of various modulation schemes against SNR variations. The blue graph represents the Gaussian limit of the system capacity, and in adaptive modulation, the system will always try to follow this maximum limit for any SNR value. Its values are always much higher than the other schemes, and they keep on increasing with the SNR, whereas for the constant bit rate schemes (fixed modulation), system capacity saturates after a particular transmit SNR and is shown Fig. 3.3. Therefore the benefits of having higher channel SNR is not utilized by fixed modulation systems.

Fig. 3.4 gives the BER plotted against SNR for the different modulation techniques. Table 3.2 is obtained by extracting the values of E_b/N_0 to achieve a BER= 10^{-5} from Fig. 3.4. Since each symbol carries k bits, the symbol to noise ratio is k times the bit to noise ratio, i.e., $E_s/N_0=kE_b/N_0$.

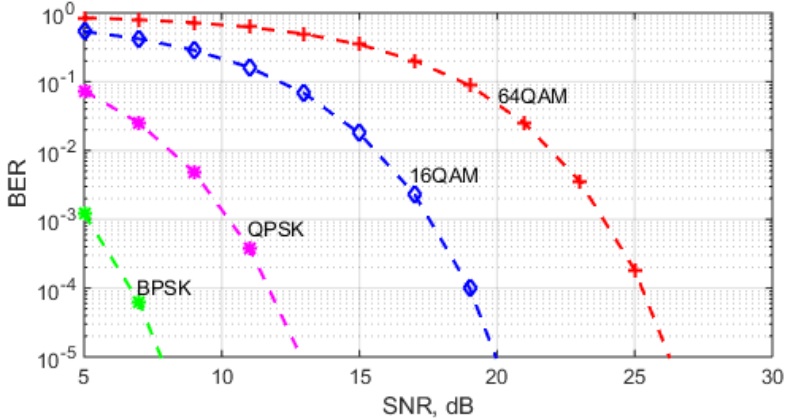


Figure 3.4 Constellation selection to maximize the throughput

The capacity corresponding to each modulation scheme is calculated in Table 3.2 along with the corresponding bit rate and bandwidth. The capacity limit so obtained is plotted in the curve shown in Fig. 3.5 along with the maximum Shannon limit for an AWGN channel.

Table 3.2 BER and Capacity limits of different modulation schemes

Modulation Scheme	Symbol Time	Bit rate Bits/sec	Bandwidth (Hz)	Capacity Bits/sec/Hz	E_b/N_0 required for BER= 10^{-5}
BPSK	T	1/T	1/T	1	9.5
QPSK	T	1/2T	1/T	2	9.8
16QAM	T	1/4T	1/T	4	14
64QAM	T	1/6T	1/T	6	18.5

Now looking at Fig. 3.4 again, the modulation scheme is mapped to SNR values and symbol error rates for 64 QAM, 16QAM, and QPSK, BPSK are shown against the SNR. From this SNR range, the constellation has to selected is determined. Assuming a BER constraint of 10^{-3} when the SNR value is less than 5 dB, the system does not transmit because the system would be receiving erroneous data. In between 5 dB and 10dB QPSK is selected to meet the BER constraint. Between 10dB to 17.5 dB, 16QAM and above 17.5dB 64QAM are selected in order to achieve maximum system throughput keeping the BER constraint.

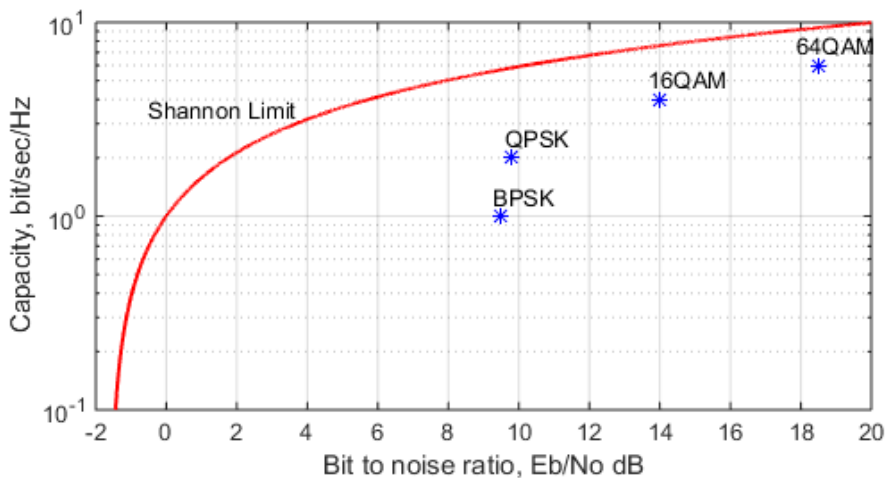


Figure 3.5 Shannon limit and capacity limit by various modulation schemes

Here a simple algorithm has been used to determine the best modulation scheme which can be used for a flat fading channel where the channel characteristics change for every timeslot. This result is utilized to turn the channel to a high level of efficiency and also achieving high data throughput rates while satisfying the BER

constraints. There are multiple modulation schemes that could be used by the transmitter module but, here specifically we analyze the BPSK, QPSK, 16QAM and 64QAM modulation schemes.

The block diagram of an adaptive modulation system is shown in Fig. 3.6. From the received packets the receiver estimates the channel quality indicator (CQI) module and feedback this information to the transmitter to reconfigure the transmitter modulator for the next packet transmission. It can enable up to four times more capacity on the same channel bandwidth depending on the base modulation rate. Adaptive modulation is provided at any given time depending on path conditions. Adaptive

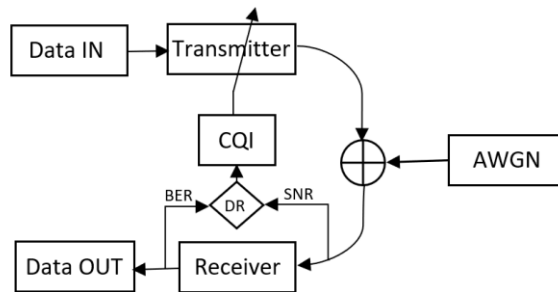


Figure 3.6 Block diagram of an adaptive modulation system

modulation is represented over four modulation rates BPSK, QPSK, 16QAM, and 64QAM. The higher the rate, the higher the data carrying capacity of the system. When path conditions are good, which is typically true for most of the time, the highest 64QAM rate is used to provide four times more capacity than with BPSK. As path conditions deteriorate, the more robust lower capacity lower modulation rates are automatically brought into service. The most robust BPSK rate is typically engineered to support a guaranteed availability to ensure continued operation under worst path conditions. A properly designed

adaptive modulation system can support an Ethernet grade quality of service. Thus, adaptive modulation maximizes the potential of existing channel bandwidths and frequency allocations. It allows end-users to leverage existing investments to achieve a lower cost per megabit data throughput.

3.4.1 Simulation Parameters

Table 3.3 MIMO-OFDM Transceiver design parameters

1	No. of transmit antennas	2
2	No. of Receive antennas	2
3	No. of Sub carriers	128
4	CP length	32
5	Channel bandwidth	20MHz
6	Modulation type	BPSK, QPSK, 16QAM, 64QAM and AM
7	Doppler shift	70
8	SNR in dB	0 to 25
9	No. of bits transmitted	10^8

Table 3.4 Algorithm to implement adaptive modulation for 2x2 MIMO_OFDM system

1	Set the simulation parameters like No. of antennas, No of subcarriers, No. of frames, etc.
2	Energy and bits are allotted in the range of each subcarrier
3	Calculate the number of bits to be transmitted

4	Generate the Rayleigh fading channels and set channel gains for each channel
5	Initialize the antennas
6	Select Modulation type (AM, BPSK, QPSK, 16QAM, 64QAM)
7	Transmit randomly generated data
8	Receive signal and perform equalization (ZF)
9	Calculate the number of errors
10	Calculate BER
11	Calculate CQI and determine the type of modulation
12	Plot BER against SNR
13	Repeat for different modulation schemes

3.5 Results and Discussions

In the simulation with no adaptation, when higher order modulations such as 64QAM is used, we get high data rates with a high probability of error and on the other hand when using lower order modulation such as BPSK or QPSK we get a low probability of errors at the expense of data rates. If modulation scheme is selected randomly without looking into the channel quality an average data rate and BER will be obtained. In adaptive modulation, feedback is applied, and for each sub-frame, the modulation scheme is selected on the basis of channel quality. When the channel is found clean probability of error will be low, and we employ higher modulation rates and obtain high data rate with low BER. When the channel quality is low, modulation with lower rates is used so as to maintain acceptable BER at the expense of data rate. However, as we select a modulation scheme based on channel quality, we obtain the best compromise in

conditions of both low and high channel qualities. As a result, by observing the Tables 3.5 to 3.7 and the plot on Fig. 3.7 we can see that the best tradeoff in terms of high data rate and reasonable BER is achieved by using adaptive modulation.

Without using adaptive modulation, the transceiver system is simulated first with three different types of modulation kept fixed irrespective of the channel condition. Simulation is repeated for the same values of SNR and with Adaptive Modulation (AM). The BER and average data rate for different simulations are listed in Table 3.5. The process is repeated for SNR values of 15dB, and 10dB and results are listed in Table 3.6 and Table 3.7 respectively.

Analyzing the simulation results reveals that the given combinations of physical layer parameters with adaptive modulation give a good increase in the spectral efficiency of the transceiver system. Table 3.4 shows the results with 20dB SNR. By examining the shaded columns (16QAM and AM), we can see that our set up is

Table 3.5 The BER and data rates for different types of modulation schemes with SNR value of 20 dB

SNR in dB	20	20	20	20
Modulation	QPSK	16QAM	64QAM	AM
Data rate(Mbps)	28.34	57	88	73.27
Modulation rate(bits/symbol)	2	4	6	4.98
BER	0	1×10^{-6}	1×10^{-4}	6.5×10^{-5}

Table 3.6 The BER and data rates for different types of modulation schemes with SNR value of 15 dB

SNR in dB	15	15	15	15
Modulation	QPSK	16QAM	64QAM	AM
Data rate(Mbps)	28.34	57	88	61.5
Modulation rate(bits/symbol)	2	4	6	4.2
BER	0	3×10^{-5}	2.5×10^{-3}	6×10^{-4}

Table 3.7 The BER and data rates for different types of modulation schemes with SNR value of 10 dB

SNR in dB	10	10	10	10
Modulation	QPSK	16QAM	64QAM	AM
Data rate(Mbps)	28.34	57	88	60
Modulation rate(bits/symbol)	2	4	6	4.14
BER	1×10^{-5}	1.2×10^{-2}	2.5×10^{-2}	1.6×10^{-2}

giving 16Mbps improvement in data rate at the expense of reasonably small hike in BER. If the same comparison is made between 64QAM and AM, we can see that the BER of AM has been improved by 54% with a slight reduction in data rate. The performance improvement by using adaptive modulation for SNR values of 15dB and 10dB are also shown Table 3.6 and 3.7.

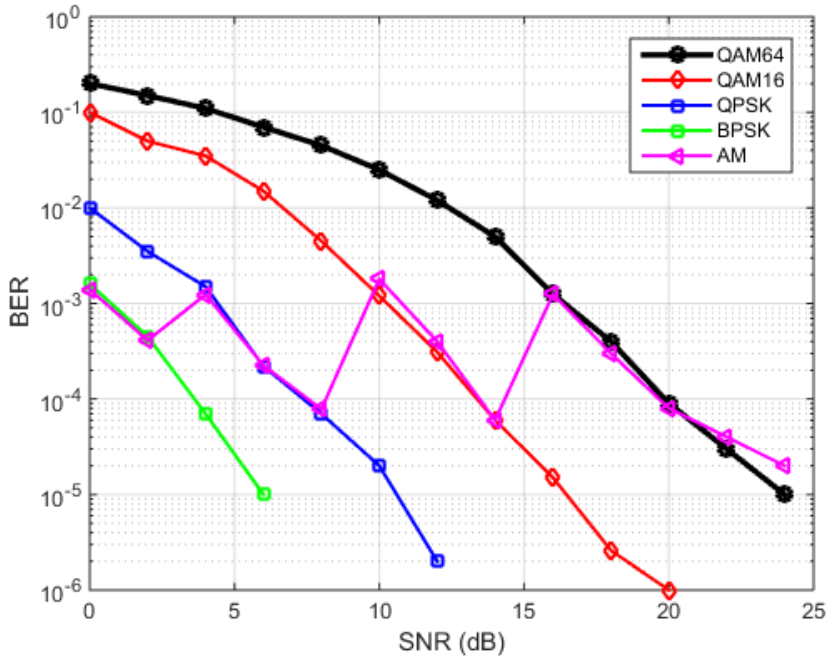


Figure 3.7 Comparison between Adaptive modulation and various fixed modulation schemes

Fig. 3.7 shows the comparison of BER in four fixed modulation methods 64QAM, 16QAM, QPSK and BPSK and Adaptive modulation for a wide range of SNR values from 0dB to 25 dB. Adaptive modulation always gives the best performance in terms of BER compared to the other three types of modulation schemes. Combining all these results, we can conclude that the best trade-off in terms of high data rate and reasonable BER is achieved by using adaptive modulation.

3.6 Chapter Summary

We analyzed the LTE specification standards for link adaptation and operations associated with link adaptations that are carried out at the

receiver for providing feedback of different system parameters to use at the transmitter for selecting an appropriate modulation scheme for the subsequent sub-frames. It is the most reactive way designed in communication systems to combat with the unpredictable channel environments. The attractive use of adaptive communications will bring more robustness and flexibility compared to fixed modulation schemes. In other words, the objective of the adaptive system is to stay opportunistic in favorable circumstances while achieving acceptable quality margin in a time-varying communication link. In this study adaptive modulation is represented over four modulation rates, BPSK, QPSK, 16-QAM and 64-QAM. In adaptive modulation, feedback is applied, and for each sub-frame, the modulation scheme is selected based on the channel quality. For adaptive modulation to work correctly, it requires an accurate estimation of the channel condition at the receivers' end to make decisions and act accordingly. When the channel is found clean probability of error will be low, and a higher modulation rate is used to obtain high data rate with low BER. When the channel quality is low the more robust modulation schemes with lower constellation is used so as to maintain acceptable BER at the expense of data rate. However, when a modulation scheme based on channel quality is selected, the best compromise in conditions of both low and high channel qualities are obtained. As demonstrated through simulations, the adaptive modulation which dynamically acts in response to the channel quality performs at its best. Our results proved that adaptive modulation with proper physical layer parameter selections could give considerable improvements in the data rate of the transceiver system without compromising much on the bit error rate.

CHAPTER-4

INTERFERENCE AND INTERFERENCE CANCELLATION IN MIMO-OFDM NETWORKS

4.1 Introduction

MIMO-OFDM is one of the most wanted wireless broadband technology and transmission system which has been accepted as the basis of fourth generation (4G) wireless communication system. It is so flexible and adaptable to stay in power even in the coming up 5G technologies. Performance of OFDM is highly sensitive to the frequency offset between transmit and receive signals. This is due to the Doppler shift caused by the relative motion between receiver and transmitter or by the difference in their local oscillator frequencies. This causes loss of orthogonality between the sub carriers which results in inter-carrier interference [52]. To overcome the effect of interferences, an Adaptive Modulation and Interference Cancellation technique for a MIMO-OFDM wireless network is proposed. Along with interference cancellation technique, Adaptive Modulation is used to meet the required BER performance by selecting suitable modulation modes based on the channel condition. Doppler assisted channel estimation method is used to estimate the channel. Also, inter-channel/carrier interference (ICI) cancellation scheme is used to integrate the Parallel Interference Cancellation together with the Decision Statistical Combining (PIC-DSC) module to detect the data and transmit it to the estimator to iteratively refine the channel estimation. Simulation studies have been carried out to analyze the BER performance of the system.

4.2 Interference in Wireless Communication

Interference can be defined as the phenomenon that occurs when two waves meet/overlap as they travel over a same channel/media. As a result of this, the shape, amplitude phase and frequency of the interfering waves may change according to the way they interfere each other.

In wireless communication scenario, if we consider any one communication channel, there are basically three types of interferences. One is broad band interference, where interference forms a broad source, like microwave signals interfere with the signal uniformly in the entire channel bandwidth as shown in Fig. 4.1. Depending on the strength of the interfering signal we might be having troubles in identifying the information in the channel. The second type is the co-channel interference, which is originated from two different radio transmitters using the same frequency.

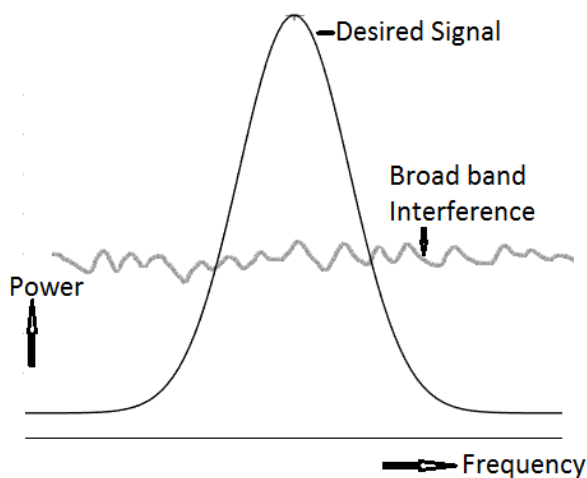


Figure 4.1 Broadband interference

There can be several causes for co-channel radio interference. In cellular mobile communication, the frequency spectrum is a precious resource which is divided into non-overlapping frequency bands and assigned to different cells. However, after certain geographical distance, the frequency bands are reused. i.e., same spectrum bands are reassigned to other distant cells. Fig. 4.2 describes these two types of interferences. Co-channel interference in cellular mobile networks is caused by frequency reuse in different cells. Besides the intended signal from within the cell, signals at the same frequencies (co-channel signals) arrive at the receiver from the undesired transmitters located in some other cell and lead to deterioration in the receiver performance [53].

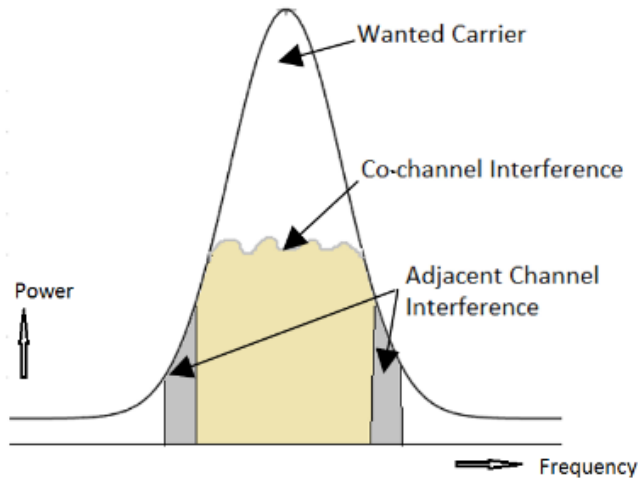


Figure 4.2 Co-channel and adjacent channel interference

Signal to co-channel interference ratio(S/I) at the desired receiver can be defined as $\frac{S}{I} = \frac{S}{\sum_{i=1}^{N_i} I_i}$ where S is the desired signal power from the desired source, I_i is the interfering power caused from the i^{th}

interfering channel. N is the number of interfering sources. Co-channel interference can be minimized by carefully designing the frequency reuse strategy [54].

The last type is adjacent channel interference resulting from signals which are adjacent to the desired signal. This is mainly caused by the imperfect receiver filters which allows nearby frequencies to leak into the pass band of the desired channel. Adjacent channel interference can be minimized by careful filter designing, channel assignment and by keeping a guard band in between adjacent channels [55].

In addition to the general category of noises explained above, because of the special nature of MIMO OFDM signals, its performance is highly degraded by the presence of inter-carrier interference (ICI), phase noise, narrow band interference (NBI) and I/Q imbalance [56].

4.2.1 Theoretical Background

When two radio signals S_1 and S_2 interfere in free space, and if that are combinedly received by a radio receiver then the total received signal will be the vector sum of these two interfering signals.

$$S(t) = S_1(t) + S_2(t) + n(t). \quad (4.1)$$

where $n(t)$ is the noise present in the channel. Now consider the signal S_i , received by a radio receiver and converted to the baseband

$$S_i(t) = H * h * A(t) \cos[2\pi t(\gamma + f(t)) + \psi(t)] \quad (4.2)$$

where $*$ is the convolution operation, $A(t)$ is the amplitude, $f(t)$ is the frequency and $\psi(t)$ is the phase shift for the signal that is being sent by the transmitter. Due to the non-ideal conditions of the receiver and

transmitter hardware and due to the Doppler shift in a mobile communication environment, the carrier frequency used both at the transmitter and receiver may not be properly replicated causing a frequency offset of γ . h is the response of the filter used at the receiver side for proper pulse shaping and unwanted signal rejection. Finally, H is the wireless channel gain which represents the effects of attenuations, multipath propagation, etc.

Now using Euler's function, we can rewrite the Eqn. 4.2 for the signal $S_i(t)$ as

$$S_i(t) = A(t)\cos(\varphi(t)) - jA(t)\sin(\varphi(t)) \quad (4.3)$$

where $\varphi(t) = 2\pi(\gamma + f(t))t + \psi(t)$, which represents the instantaneous value of phase of the converted baseband signal.

The real part of the signal represented in Eqn.4.3 can be expressed as I . For simplicity of analysis we assume the carrier frequency f_c and filter response h are fixed and known at the receiver. The channel gain H is also assumed as it produces only a channel attenuation and phase shift related to the distance traveled which remains constant for the entire duration of packet transmission. Now it is quite easy to reconstruct the original transmitted signal S_i from the received signal R_i [57].

4.2.2 Phase Noise

Phase noise is produced due to the non-linearities and instabilities of the local oscillator at the transmitter and receiver side. It can be considered as a parasitic phase modulation in the oscillator's signal, which otherwise should be ideally a unique carrier with constant frequency and amplitude. Phase noise in a system can be shown as

proportional to the square of the instantaneous frequency variations [58]. The effects of phase noise on OFDM signal are mainly the constant phase error and inter carrier interference. Constant phase error indicates the fixed phase rotation common to all the subcarriers in an OFDM symbol [59], and ICI is due to the adjacent subcarriers which are interfering with each other. If the ratio between the bandwidth of phase noise and intercarrier spacing in OFDM is close to unity, ICI will be the dominating component where as if the ratio is small constant, phase error will be the main noise contributor [60].

4.2.3 Compensation of Phase Noise

MIMO-OFDM receivers are very sensitive to the phase noise generated due to frequency offset among the local oscillator and carrier frequencies. Phase noise is the main limiting factor in the performance of high data rate OFDM systems. The most commonly used method for phase noise cancellation is by estimating the frequency offset with pilot symbols and compensating the same on the data subcarriers. Compared to ICI, constant phase error correction is relatively easier [61]. Fig. 4.3 shows the graph plotted for the ratio of noise power to carrier power against frequency when the carrier frequency is taken as 500 Hz.

4.2.4 I/Q Mismatch

I/Q Mismatch or imbalance occurs when the in-phase and quadrature phase components in the RF front end of the receiver are precisely not the same. In MIMO-OFDM networks a separate down converting circuit is used for each RF channel, and the value of I/Q mismatch for one channel will be independent of the values for the

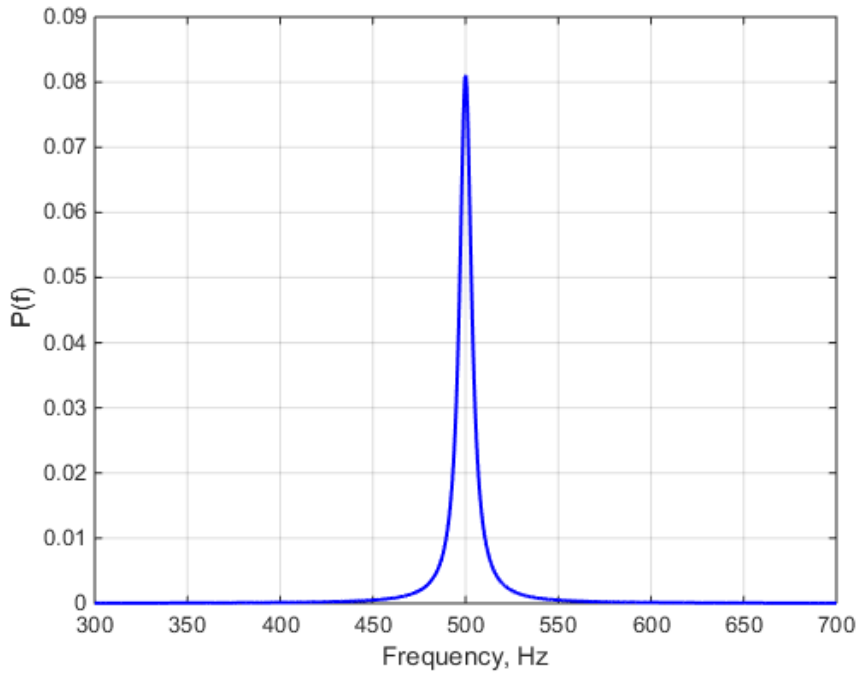


Figure 4.3 Ratio of noise power to carrier power plotted against frequency

channels. In OFDM networks, I/Q imbalance introduces inter-carrier interference from the mirror subcarrier. Because of the ICI component, MIMO-OFDM systems are highly reactive to the I/Q imbalance [62].

To mitigate this effect, a strict condition for matching of the two streams are to be followed in the front-end RF circuits or compensation can be done in the baseband receiver for the imbalance caused [63]. The graph in Fig. 4.4 shows the amplitude of the received spectrum against frequency for a phase imbalance of 5° .

4.2.5 Narrow Band Interference (NBI)

Signal interference, which is within the device's bandwidth and much smaller than the system bandwidth, can be considered as Narrow-Band Interference (NBI). NBI is produced when two or more

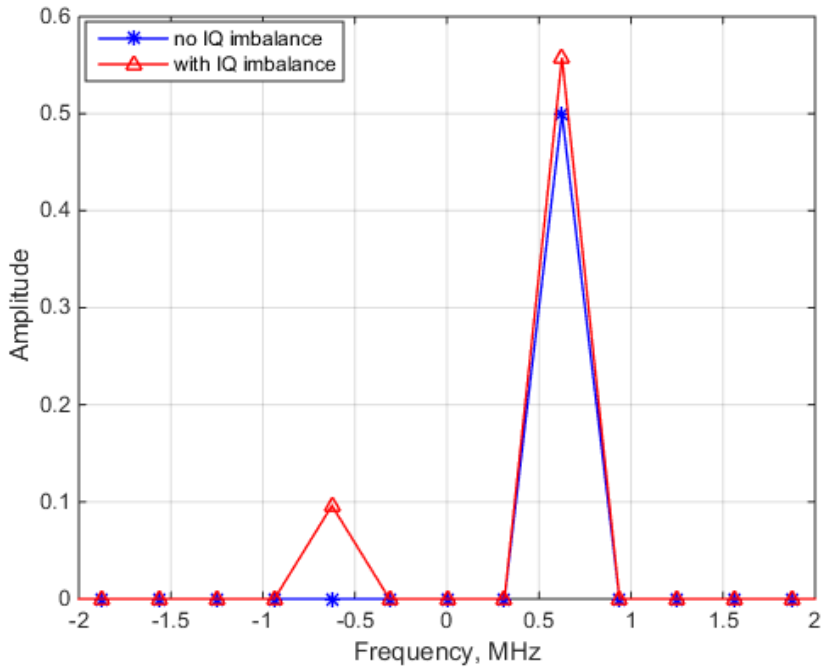


Figure 4.4 Spectrum of received signal – with and without transmit I/Q imbalance

nearby systems operate on the same frequency band. It is more predominant in the license-free frequency band (ISM band), where interference is received from devices such as Wi-Fi access points, Bluetooth operating equipment, microwave ovens, cordless phones, etc. In OFDM systems, if the frequency of the NBI doesn't exactly match with one of the subcarrier frequency then the whole spectrum of NBI will spread to the entire bandwidth of the OFDM communication system [64].

4.2.6 NBI Compensation

To compensate the effect of NBI in OFDM systems, the main techniques used are frequency identification and canceling, frequency

excision, prediction error filtering and adaptive narrow band filtering [65]. In frequency identification and canceling method, the Phase and amplitude of NBI are assessed from the peak magnitude of the received spectra by using maximum likelihood detection. In frequency excision method, the NBI, which comes as a maximum peak in the received signal spectra is removed by equating it with the threshold value. In the adaptive narrowband bandpass filter method, the center frequency of this filter is made equal to that of the NBI frequency and the filter weights are modified by using LMS algorithm [66].

4.2.7 Doppler Shift

Doppler spread is a parameter that describes the time-varying nature of the channel in a small-scale region. When a mobile receiver or a transmitter station move in a certain direction at a constant rate, a change in phase and frequency will be caused due to the difference in the propagation path and this effect is known as the Doppler shift.

When a pure sinusoidal tone of frequency f_c is transmitted, the received signal spectrum, called the Doppler spectrum, will have components in the range $f_c - f_d$ to $f_c + f_d$, where f_d is the Doppler shift. The amount of spectral broadening depends on f_d which is a function of the relative velocity of the mobile and the angle θ between the direction of motion of the mobile and direction of arrival of the scattered waves. If the baseband signal bandwidth is much greater than f_d the effects of Doppler spread are negligible at the receiver [67]. This is a slow fading channel.

When the mobile station moves at a constant rate v_m over a path of length d and endpoints A and B , it receives a signal from the far-end

source T_x as shown in the Fig. 4.5.

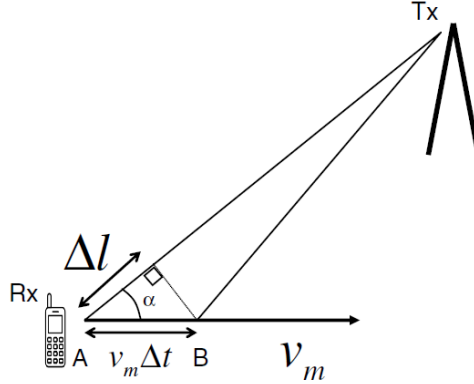


Figure 4.5 Calculation of Doppler Shift due to a mobility of User terminal

Radio waves starting from the source T_x , points is received by the mobile station at the points A and B . Then the path difference is:

$$\Delta l = d \cos \alpha = v_m \Delta t \cos \alpha \quad (4.4)$$

where d is the distance between A and B . Now this path difference Δl will produce a phase difference given by

$$\Delta \phi = \frac{2\pi \Delta l}{\lambda} = \frac{2\pi v_m \Delta t}{\lambda} \cos \alpha \quad (4.5)$$

Then the Doppler spread f_d can be calculated as

$$f_d = \frac{1}{2\pi} \frac{\Delta \phi}{\Delta t} = \frac{v_m}{\lambda} \cos \alpha \quad (4.6)$$

The maximum Doppler shift is achieved when $\cos(\alpha) = 1$, or equivalently when $\alpha = 0$ and the receiver is moving towards the signal source and is given by:

$$f_{d,max} = \frac{v_m}{c} \quad (4.7)$$

Hence the mobile equipment sees the incoming signal as a wave of

frequency:

$$f = \frac{\Delta\phi}{2\pi\Delta t} = \frac{1}{2\pi} \frac{2\pi f_c \Delta t + \frac{2\pi}{\lambda} v_m \Delta t \cos(\alpha)}{\Delta t} = f_c + f_c \frac{v_m}{c} \cos(\alpha) \quad (4.8)$$

Therefore, the incoming signal appears to have undergone a frequency shift by $f_c \frac{v_m}{c} \cos(\alpha)$. This phenomenon is called the Doppler effect, and the frequency shift $f_c \frac{v_m}{c} \cos(\alpha)$ is called the Doppler shift (f_d). f_d will be maximum when $\cos(\alpha) = 1$, or equivalently when $\alpha = 0$ and the mobile terminal is moving towards the transmitter and is given by:

$$f_{d,max} = \frac{v_m}{c} \quad [68].$$

The effect of Doppler shift in BER is plotted in Fig. 4.6 for BPSK and in Fig. 4.7 for QPSK modulations, for three different values of normalized Doppler shift 0, 0.001 and .09. It is clear from the graphs that the Doppler shift considerably increases the BER, and when comparing the QPSK and BPSK, we can see that the effect is more predominant in QPSK.

4.3 Inter-Carrier Interference

The subcarriers used in OFDM are very closely packed, and due to orthogonality among these subcarriers, the null of one subcarrier will be exactly at the peak of the other subcarrier. This orthogonality has to be properly maintained throughout the communication to ensure efficient modulation performance of OFDM. ICI is produced when sub-carriers lose this perfect orthogonality. This is shown in Fig 4.8 where OFDM with four subcarriers at an equal spacing of Δf is shown.

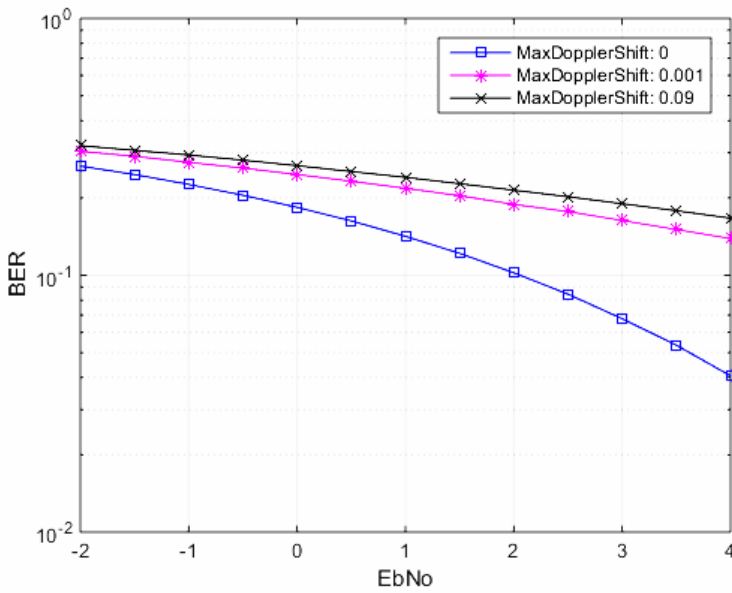


Figure 4.6 Effect of Doppler shift on BER in a BPSK system

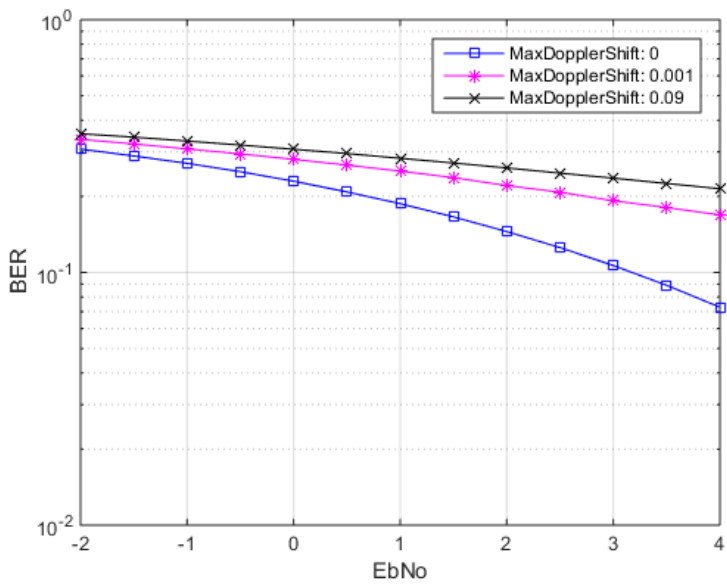


Figure 4.7 Effect of Doppler shift on BER in a QPSK system

Corresponding to the peak of any one sub carrier, all the other subcarriers are having a zero value (nulls) canceling the ICI without the use of any complex filtering or guard band. This condition is lost when there is a frequency offset and corresponding to the sampling of any subcarrier we get a non-zero value of other subcarriers creating ICI.

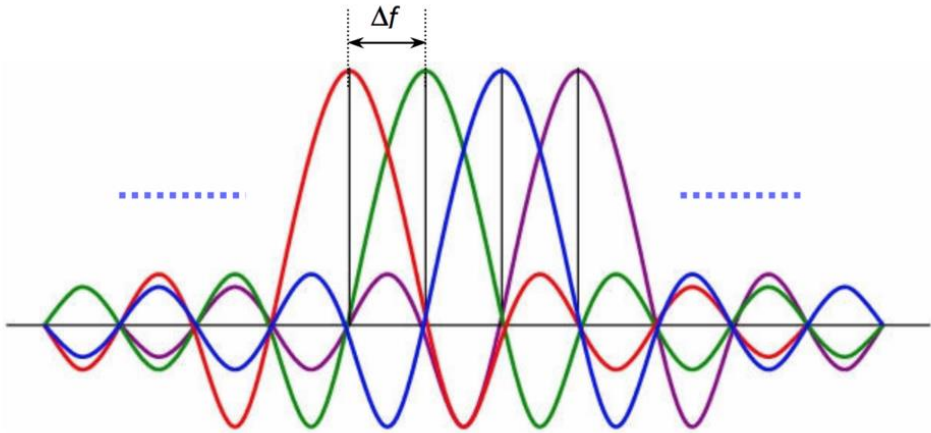


Figure 4.8 OFDM subcarrier creates “nulls” and canceling out ICI

ICI is caused by two reasons:

- i. The frequency offset at the receiver compared to that of the transmitter. This could be caused by the Doppler shift in frequency due to the mobility of the user or by the frequency shift between the transmitter and receiver frequencies. This may also be caused by the time domain synchronization error.
- ii. Delay spread of radio channel exceeds the cyclic prefix introduced. MIMO-OFDM converts a MIMO frequency selective channel into a set of parallel MIMO flat fading channels, such that across each sub-carrier, the net wireless communication systems looks like a MIMO flat-fading system.

Mathematically the output across each subcarrier can be written as

$$Y_{(0)} = H_{(0)}X_{(0)} \quad (4.9)$$

$$Y_{(1)} = H_{(1)}X_{(1)} \quad (4.10)$$

$$Y_{(N-1)} = H_{(N-1)}X_{(N-1)} \quad (4.11)$$

i.e., the vector $\bar{Y}_{(0)}$ is now $\bar{H}_{(0)}$ times $\bar{X}_{(0)}$, where $\bar{X}_{(0)}$ is the transmit vector across the 0th sub carrier, $\bar{H}_{(0)}$ is the flat fading channel matrix, and $\bar{Y}_{(0)}$ is the received vector across the 0th sub carrier. Similarly, all the N sub carriers are shown. It is similar to OFDM except that the Y and X are vectors. In general it can be written as

$$\bar{Y}_{(k)} = \bar{H}_{(k)}\bar{X}_{(k)} \quad (4.12)$$

where $\bar{Y}_{(k)}$ is the $r \times 1$ receive vector, $\bar{X}_{(k)}$ is the $t \times 1$ transmit vector and $\bar{H}_{(k)}$ is the flat fading channel matrix corresponding to subcarrier k .

Each $\bar{Y}_{(0)}, \bar{Y}_{(1)}, \dots, \bar{Y}_{(n-1)}$ can be processed by a simple MIMO ZF receiver for detection of transmit vectors $\hat{X}_{(0)}, \hat{X}_{(1)}, \dots, \hat{X}_{(n-1)}$ as seen in Eqn. (4.13) [69].

$$\hat{X}_{(k)} = (\bar{H}_{(k)})^\dagger \bar{Y}_{(k)} \quad (4.13)$$

$(\bar{H}_{(k)})^\dagger$ is the pseudo-inverse of the channel matrix $\bar{H}_{(k)}$

MIMO equalization for a MIMO frequency selective channel poses a much more challenge for communication compared to SISO frequency selective systems.

4.3.1 Effect of Frequency Offset in MIMO-OFDM

OFDM is a delicately balanced system, and the presence of carrier frequency offset can introduce severe distortions in an OFDM system as it results in the loss of orthogonality. If Δf_0 is the frequency offset and B/N is the subcarrier bandwidth, the normalized frequency offset ϵ can be written as

$$\epsilon = \frac{\Delta f_0}{B/N} \quad (4.14)$$

The larger the frequency offset, the greater is this inter carrier interferences and dealing with frequency offset is, in fact, a very important aspect of any OFDM system.

To model this, consider a system with frequency offset ϵ normalized with respect to the subcarrier bandwidth. Then the baseband received samples can be written as

$$y_n = \frac{1}{N} \sum_{k=-\frac{N}{2}}^{\frac{N}{2}} X_k H_k e^{j2\pi n \frac{(k+\epsilon)}{N}} + W_n \quad (4.15)$$

The received signal sample $Y_{(n)}$ is given as summation of $X_k H_k e^{j2\pi n (k+\epsilon)/N}$ plus the noise component w_n , where X_k is the data transmitted on the k^{th} subcarrier, H_k is the channel coefficient across the k^{th} subcarrier, N is the number of sub carriers. This equation can be very easily verified by putting $\epsilon = 0$,

$$y_n = \frac{1}{N} \sum_{k=-\frac{N}{2}}^{\frac{N}{2}} X_k H_k e^{-j2\pi n \frac{k}{N}} + W_n \quad (4.16)$$

Performing the FFT of this received symbols $y_{(0)}, y_{(1)} \dots y_{(N-1)}$ at the receiver, the l^{th} FFT coefficient corresponds to the symbol received on

the l^{th} subcarrier can be written as

$$y_l = \frac{1}{N} \sum_n \sum_{k=-\frac{N}{2}}^{\frac{N}{2}} X_k H_k e^{J2\pi n \frac{k}{N}} e^{-J2\pi n \frac{l}{N}} + W_l \quad (4.17)$$

$$= \frac{1}{N} \sum_k \sum_n X_k H_k e^{J2\pi (k-l) \frac{n}{N}} + W_l \quad (4.18)$$

$$= X_l H_l + \sum_n \sum_{k=-\frac{N}{2}}^{k/2} X_k H_k e^{J2\pi \frac{(k-l)n}{N}} + W_l \quad (4.19)$$

In the absence of carrier frequency offset, for $k \neq l$, the second term in the Eqn. 19 becomes zero because the $\sum_n e^{j2\pi n(k-l)/N}$ becomes equal to zero. Hence, we have

$$Y_l = H_l X_l + W_l \quad (4.20)$$

where the first term is the original OFDM relation for the l^{th} subcarrier. Now let us see what happens to the signal when there is carrier frequency offset, for that consider the Eqn. (4.17), received symbol across the l^{th} subcarrier is given by

$$Y_l = \frac{1}{N} \sum_n X_l H_l e^{j2\pi n \epsilon / N} + \frac{1}{N} \sum_{k=-\frac{N}{2}, k \neq l}^{n/2} X_k H_k e^{j2\pi (k-l+\epsilon)n/N} + W_l \quad (4.21)$$

This can be further simplified by using the following result

$$\sum_{n=0}^{N-1} e^{j\theta n} = \frac{\sin N\theta/2}{\sin \theta/2} e^{j\phi} \quad (4.22)$$

where $e^{j\phi}$ is the phase factor, which does not affect the power and need not to be taken care of.

Applying this in Eqn. (4.19)

$$Y_l = H_l X_l \frac{\sin \pi \epsilon}{\sin \frac{\pi \epsilon}{N}} \frac{1}{N} e^{j\phi_l} + \underbrace{\sum_{k=-\frac{N}{2}, k \neq l}^{n/2} H_k X_k \left(\frac{\sin \pi \epsilon}{N \sin \left(\pi \frac{l-k+\epsilon}{n} \right)} \right)}_{\text{(Interference)}} e^{j\phi_{kl}} + W_l \quad (4.23)$$

In the above equation also when ϵ tends to 0, the \sin term tends to 1, and the second term which corresponds to the inter-carrier interference also tends to zero giving us the result for perfect condition. The third term W_l is the Gaussian noise part [70].

In this condition, since we have noise along with interference signal to evaluate the performance we calculate the SINR and is given by

$$SINR = \frac{\text{Signal Power}}{\text{Interference+Noise Power}} \quad (4.24)$$

$$SINR = \frac{\text{Signal Power}}{E\{|I_l|^2\} + \sigma_n^2} \quad (4.25)$$

$$\text{Signal Power} = E\{|H_l|^2\}E\{|X_l|^2\} \left(\frac{\sin \pi \epsilon}{N \sin \pi \epsilon / N} \right)^2 \quad (4.26)$$

For large number of subcarriers, i.e large N

$$\lim_{n \rightarrow \infty} \sin \frac{\pi \epsilon}{N} = \frac{\pi \epsilon}{N} \quad (4.27)$$

$$N \sin \frac{\pi \epsilon}{N} \gg N \frac{\pi \epsilon}{N} = \pi \epsilon \quad (4.28)$$

On simplification and assuming N= number of subcarriers as very large, we get the SINR in the presence of carrier frequency offset ϵ as equal to

$$SINR = \frac{P|H|^2 \left(\frac{\sin \pi \epsilon}{\pi \epsilon} \right)^2}{0.822 P|H|^2 (\sin \pi \epsilon)^2 + \sigma_n^2} \quad (4.29)$$

The numerator represents the signal power, the first term in the denominator is the interference power from the intercarrier interference and σ_n^2 is the noise power.

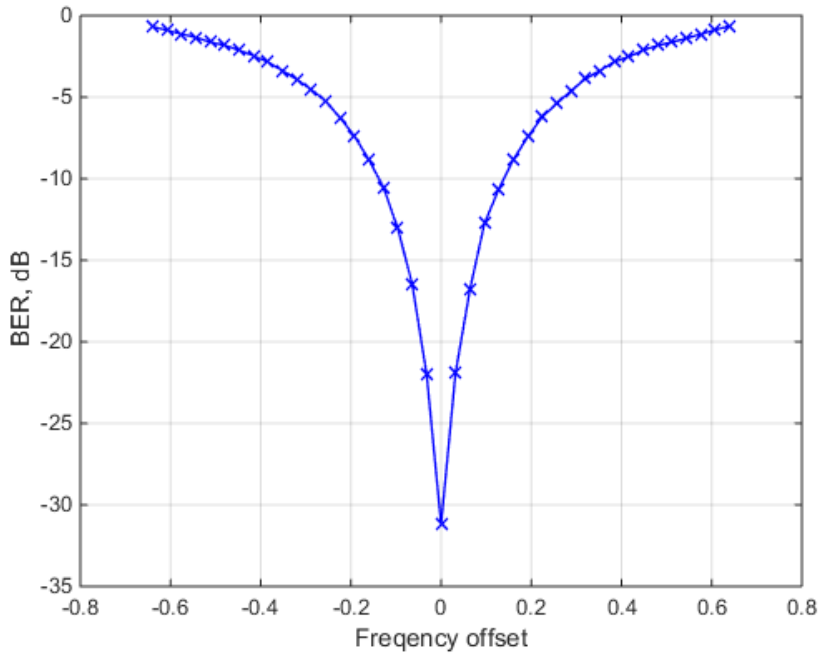


Figure 4.9 SNR loss due to frequency offset in OFDM modulation

Fig. 4.9 shows the variations in BER plotted against frequency offset in a BPSK system in OFDM with FFT size of 64 and number of subcarriers equal to 52. ICI due to frequency offset can be completely removed or can be reduced by estimating the offset frequency and dynamically correcting the sub-carrier spacing accordingly.

In the following section, we discuss the different interference cancellation techniques that are widely used in wireless communication systems.

4.3.2 Successive Interference Cancellation (SIC)

In interference limited communication system the performance can be highly improved by Successive Interference Cancellation (SIC), where the projected effect of interference on the detected data is canceled in

a serial manner. In SIC receivers [71,72], received signals are ranked in descending order of signal power. The signal with the strongest power (say for User 1) is sent through the conventional (e.g.: MMSE receiver) detector and the message sent is decoded. The decoded message is regenerated and subtracted from the original received signal, $y_{(t)}$, which is delayed to allow time for processes required before subtraction. The residual signal, $y'_{(t)}$ does not contain the signal for User 1, and consequently, it does not contain media access interference due to User 1. The receiver selects the next strong signal and repeats the process as for User 1. This is shown in Fig. 4.10. The process continues until all the users have been detected. Alternatively, the process could continue until sufficient number of powerful signals have been detected and canceled. The residual signals can then be detected using conventional detector as usual. SIC introduces lengthy delays in detection. The user with least received signal power can only be detected after all stronger users have been detected. In addition, this system relies on the normal imbalance in received signal power. The first signal detected (for User-1) is done using the conventional detector in the presence of media access interference. If this detection is wrong then the subtracted signal is also wrong. Rather than canceling interference, it would be increased. This problem is known as error propagation which is one of the main factors that limits the performance of SIC. SIC performs worse than the conventional receiver when the received signal power is balanced.

The application of SIC in communication was first analyzed by Kohno et al. in [73], for spread spectrum communication. Subsequently, it has been widely discussed in many literatures for multi-user application in

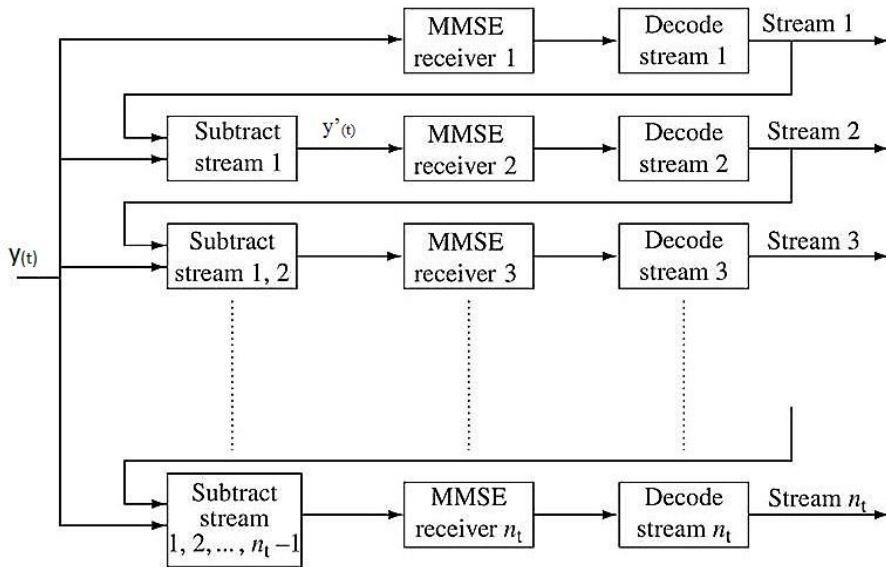


Figure 4.10 Successive Interference Cancellation

spread spectrum. Application of SIC for MIMO communication was first developed by Foschini et al. in [74]. The performance improvement of MIMO on the application of SIC is two-fold i) the post-processing gain of the successive layers are greatly enhanced by the reduction of interference ii) For every successive layer that is assessed, will have a higher diversity order which also supplements to higher gain. However, SIC do not take the spatial distribution of the users in to consideration.

4.3.3 Parallel Interference Cancellation

Parallel Interference Cancellation (PIC) is similar to SIC in principle [75]. It subtracts (cancels out) interference from the received signal before detecting the desired users. The difference in PIC as compared to SIC is that cancellation of interference is done at once. (in parallel).

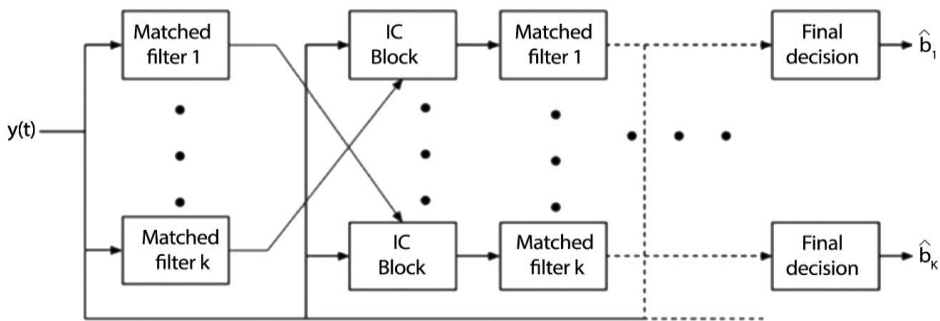


Figure 4.11 Parallel Interference Cancellation

Fig. 4.11 shows the PIC detector. The received signal $y(t)$ is sent through the first stage of detection. This is usually the conventional detector or a linear multiuser detector like the decorrelating detector. The output of this first stage is regenerated to obtain the received signal, $\hat{b}_{(t)}$ for each user. After that, the interference signal is summed up and subtracted from $y(t)$. $y(t)$ is delayed to allow time for processes required before subtraction of interference. The remaining signal is assumed to be free of multiple access interference. Final detection can, therefore, be done with the conventional detector. The ordering of signals in received signal power is no longer required. Delay in detection is also greatly reduced. However, knowledge of channel attenuation and delay is required to enable the system correctly estimate the signals to be subtracted.

The Parallel Interference Cancellation receiver can be cascaded into multiple iterative stages [76]. This iteration results in convergence ultimately to a decorrelating detector if the system load is not greater than 17% [77]. Convergence can be improved by using graduated weights to limit the interference. PIC works better than SIC when all

the users in the communication system under consideration receive signals with equal power strength [78,79].

Neda Aboutorab et al. in [80] have proposed an Iterative Channel Estimation with Parallel ICI for High-Mobility MIMO-OFDM networks. An easy parallel interference cancellation method linked with a decision statistical combining scheme is used to remove the ICI and improve data signal detection. It mainly focuses on the process of estimating the channel state information for high mobility user by considering Doppler effect due to the variant wireless channel to improve the performance of ICI cancellation. But this work does not take any consideration about any modulation technique in terms of improving the throughput and BER performance based on the feedback of channel state condition.

In this work, we propose to design a parallel ICI cancellation scheme along with adaptive modulation for MIMO-OFDM networks. This is achieved by using the feedback from channel state condition to properly select the modulation and thereby improving throughput and BER performance.

4.4 Review of Techniques Used for Interference Cancellation

Right from the beginning of wireless communication, interference and its mitigation are hot topics of research. This section will review the state of the art research contributions and practical implementations that effectively manage interference in wireless communication networks.

In [81], Shaverdian *et al.* have proposed robust distributed beamforming with interference coordination in downlink cellular

networks for addressing the robustness against the uncertainties in the channel parameters. The distributiveness of beamforming, spatial multiplexing and power allocation in multi-antenna BSs of a multicell network under the frequency reuse is considered as an optimization problem and minimized the overall transmission power of BSs subjected to SINR constraints at each mobile station under channel uncertainties. They used semi definite relaxation and the S-Lemma with a limited information exchange among BSs to achieve distributiveness. The optimization problem is first recast into a numerically tractable one, where each BS obtains a local version of its coupling variables. Then an iterative algorithm is used to coordinate inter-cell interference across multiple BSs. Septimus et al. in [82] proposed an approach for alleviating inter-carrier interference in OFDM systems by considering the signal reconstruction problem at the receiver end as an Integer Least Squares (ILS) problem. They developed a spectral approach called as sequential probabilistic ILS to decode the OFDM signals by extending probabilistic ILS to reduce inter-carrier interference.

A blind interference alignment (BIA) scheme using reconfigurable antenna technology to attain a high degree of freedom (DoF) or diversity gain in K-user interference channels has been proposed by Lu et al. in [83]. For that, two DoF-oriented BIA schemes are proposed that included full and partial interference alignment among all the users then compared the achievable DoF of the two schemes with each other. Then, three diversity-oriented BIA schemes with space-time coding are proposed by assuming a constant transmission rate to achieve both spatial diversity gain and

reconfigurable antenna pattern diversity gain. With different trade-offs among the diversity gain, the rate and the decoding complexity, the BIA is employed with threaded algebraic space-time (TAST) codes, orthogonal space-time block codes (OSTBCs) and multiplexing Alamouti codes respectively. After that, they compared the BIA with those codes regarding code rate and cost of decoding complexity.

End-to-end average symbol error probability (ASEP) of dual-hop relaying networks with pilot-symbol assisted M-array phase-shift keying (M-PSK) modulation which uses the selective Decode and Forward (DF) protocol while relays are equipped with multiple receive antennas is analyzed by Sagias et al. in [84]. The channels' state information is obtained per antenna branch based on the Least-Squares Estimation (LSE) technique using pilot symbols. Also, coherent detection based on maximal-ratio combining and ICI cancellation scheme are performed on the receiving end. Exact end to end analytical ASEP expressions are derived for binary and quadrature phase-shift keying, while approximate high signal-to-noise ratio (SNR) expressions are obtained for any order M-PSK modulation formats to extract the cooperation-gain and diversity-order.

The degrees of freedom for the constant MIMO interference channel with coordinated multipoint (CoMP) transmission in which each message is jointly transmitted by multiple successive transmitters were developed and tested by Wilson et al. in [85]. The transmission scheme of the proposed approach used two-stage scheme that involved both zero forcing and Interference Alignment to develop a constant MIMO interference channel with CoMP transmission. The combined effect is called derived channel which is proceeded in two stages by

first applying ZF and then IA sequentially at the transmitters.

In [86] Phan-Huy et al. have proposed Make-It-Real (MIR) precoders for MIMO OFDM/QAM without inter-carrier interference in which new precoders called MIR MRT and MIR MMSE precoders. These are based on traditional maximum ratio transmission (MRT) minimum mean square error (MMSE) precoders and are used to perform data multiplexing in the spatial domain for OFDM/QAM. These precoders are designed so that the equivalent channel including precoding and propagation is "made real" without breaking the orthogonality of OFDM/QAM in the frequency domain. At the receiver side, demodulation is done to extract the original signal. Then the performance of OFDM/QAM with MIR MMSE and MIR MRT precoder is compared with traditional MIMO OFDM with ZF, MRT, and MMSE precoders.

The BER performance of OFDM system with adaptive modulation that divides the whole subcarriers into blocks of adjacent subcarriers is analyzed by Borkarin et al. in [87] using MATLAB simulation. Based on the calculated average instantaneous SNR at the receiver side, the same modulation scheme is applied to all subcarriers of the same block. The modulation that has to be used by the transmitter for its next OFDM symbol will be determined by the channel-quality estimate of the receiver based on the current OFDM symbol.

In [80], Aboutorab et al. have proposed channel estimation and inter carrier interference cancellation scheme for a MIMO-OFDM system. They estimated the wireless channel simultaneously by using pilot symbols, data symbols, and Doppler spread information at the

receiver. Then the interpolation weights for the weighted time-domain channel are designed using Doppler spread and time-domain channel correlations. The channel estimates are obtained using the least-square method. When all the channel coefficients are obtained, simplified parallel interference cancellation (PIC) scheme is used along with decision statistical combining (DSC) module to cancel the ICI and improve data symbol detection and the SINR. These data symbols are estimated by the detector and used to further refine the channel estimation iteratively.

An adaptive algorithm which perfectly adapts the transmission rate according to the radio channel and interference combined with any interference cancellation schemes has not been analyzed in any of the works discussed in literature. Accordingly in this work a parallel interference cancellation (PIC) is developed along with adaptive modulation scheme and its BER performance is evaluated.

4.5 System Model

4.5.1 Overview

Fig. 4.12 represents the block diagram of the proposed system where Doppler-assisted channel estimation technique is used with the adaptive modulation scheme. Inter-Carrier Interference (ICI) degrades the overall performance of the system, so it is highly important to incorporate some ICI cancellation techniques. In the ICI cancellation scheme used here, a combination of data detection and PIC-DSC is used for each iteration of the channel estimation, and then the PIC-DSC output is delivered to the detector. Next, the channel estimator is again

fed with the detected data elements, thereby refining the channel estimation through each iteration.

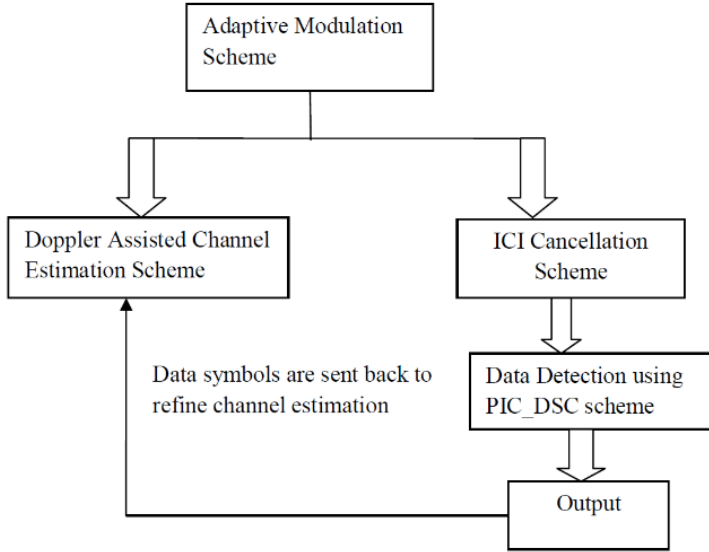


Figure 4.12 Block diagram of the proposed Adaptive modulation with ICI cancellation

4.5.2 Designing of Adaptive Modulation in OFDM

This section describes the designing of Adaptive Modulation in OFDM along with the ICI cancellation scheme. Orthogonality of subcarriers is the main part of OFDM. It has been observed that OFDM can easily be carried out by FFT and IFFT.

Let $I = [I_0, I_1, I_2, \dots, I_{N-1}]^T$ be the inputs after converting serial input data to parallel. then

$$z(t) = \frac{1}{U} \sum_{u=0}^{U-1} I_n e^{j2\pi\Delta f t}, 0 \leq t \leq UT \quad (4.30)$$

This is the complex baseband OFDM signal, where T represents the

data period, UT represents symbol interval in OFDM and $\Delta f = \frac{1}{UT}$ denotes spacing of the subcarrier.

For transmission of OFDM, the whole subcarriers are divided into a number of subcarriers. The same modulation method is used for every subcarrier of the same block. The modulation technique for the following symbol will be determined by the channel quality estimation of the receiver based on the present OFDM symbol. For our work, the channel estimation is done by the use of a Doppler assisted channel estimation scheme which will be explained in the subsequent section. The subcarrier SNR for this method will be calculated at the point of receiver end. The received signal at any subcarrier is given as

$$P_u = J_u I_u + G_u \quad (4.31)$$

where J_u is any subcarriers channel coefficient, I_u - the transmitted symbol

G_u - Gaussian noise sample

The SNR(instantaneous) can be computed as

$$SNR = \frac{J_u^2}{U_0} \quad (4.32)$$

U_0 - noise variance

For the real signal, $BW = \frac{1}{2}$ of the sampling rate.

$$\text{The average power } -U_0 = \frac{u_0 f_r}{2} \quad (4.33)$$

u_0 - One sided-power spectral density of noise in W / Hz .

In the proposed method given in Fig. 4.13, modulation method is identified after channel estimation at the receiver side, and this

information is sent to the transmitter through the feedback channel. Frame by frame adaptation is done for the modulation. The instantaneous value of SNR for the signal received is calculated using the channel estimator. Based on this SNR, the best modulation method to be used for the next transmission frame is determined. Modulation selector block at the transmitter performs this task, and an adaptive modulator block produces the required modulation on the basis of the instantaneous SNR. After modulation, the output is converted into parallel signal and then IFFT is used to transform the signal from discrete frequency domain to discrete time domain i.e. the OFDM. After that stage cyclic prefix is inserted to avoid any possibility of inter symbol interference. The signal is then converted to serial and transmitted to channel. An additive white Gaussian channel is assumed here, and at the receiver side, an exact reverse operation is performed to recover the data.

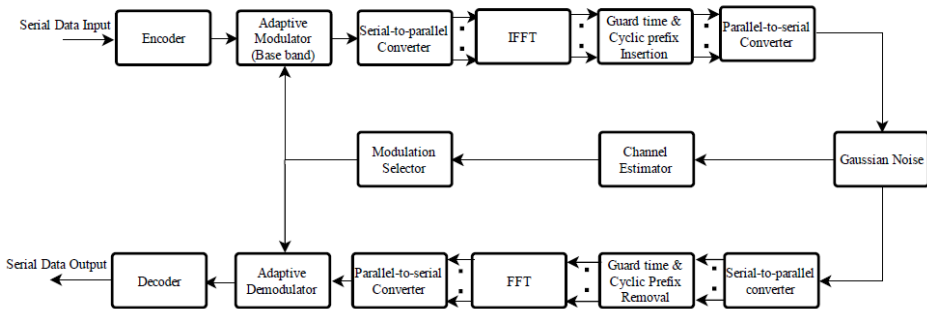


Figure 4.13 Block Diagram of OFDM with Adaptive Modulation

4.5.3 Doppler-Assisted Channel Estimation Scheme

In this section, the iterative Doppler-assisted channel estimation [80] that uses Doppler spread, time domain channel correlations and computation of data symbols is briefly described. In this scheme the

channel estimation is carried out by simultaneous use of the iterative estimates of the data symbols and Doppler spread information, The Doppler spread s_d is computed by using the speed of the receiver v (in meters per second), which is given as below

$$s_d = \frac{v s_c}{C} \quad (4.34)$$

Where s_c denotes the carriers frequency, and C is the velocity of light in m/s. Moreover, the normalized Doppler spread is given as

$$S_d = \left(\frac{s_d}{\Delta s} \right) \quad (4.34)$$

where Δs denotes the spacing between subcarriers.

In the channel estimation technique with Doppler assistance, time domain markers are used. These are nothing but the time-domain channel coefficients denoted as a weighted representation of the selected channel coefficients. These weights are estimated in such a fashion that channel estimation errors are reduced. At the receiver end, the required time domain channel correlation is estimated by the iterative process with the help of the available Doppler spread information. The least square method is used for estimating the time domain markers. The estimates of the ICI produced by the Doppler spread is subtracted from the input signal received using the PIC module. The output of this section is then fed to the DSC unit where the decision statistics signal is obtained through the successive combining of the values of iterations carried out in the current and previous stages. The iterative receiver along with the PIC-DSC module is given in Fig. 4.14. In each channel estimation cycle, the ICI produced due to Doppler-spread is generally removed by the PIC-DSC section. Here, the PIC-DSC procedures are merged into one iterative process.

Moreover, the data detection and PIC_DSC are carried out only once, and the detected data symbols are transmitted back to the channel estimator which gives lower computational complexity.

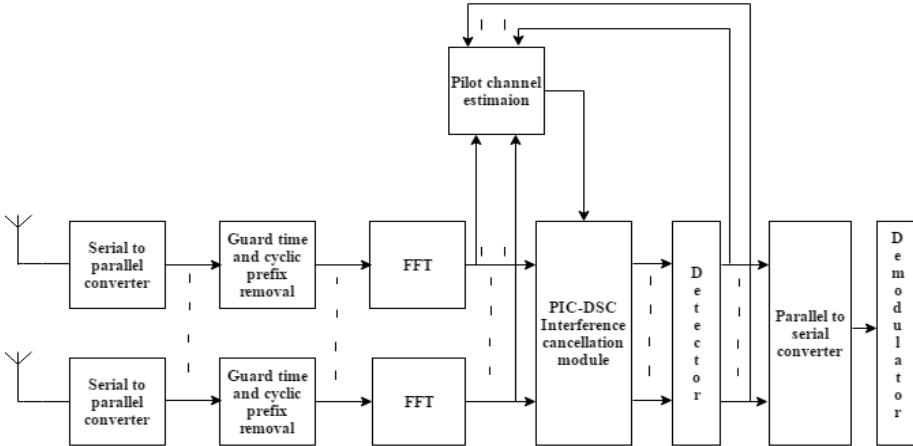


Figure 4.14 Integrated PIC-DSC interference cancellation scheme

4.5.4. Over all Algorithm

Fig. 4.15 gives the BER plotted against SNR for different modulation techniques ranging from BPSK to 64QAM. From this plot considering an BER value of 10^{-3} , the modulation scheme to be used is selected and send to the transmitter. The flow chart shown in Fig. 4.16 gives the steps involved in the interference cancellation scheme along with adaptive modulation.

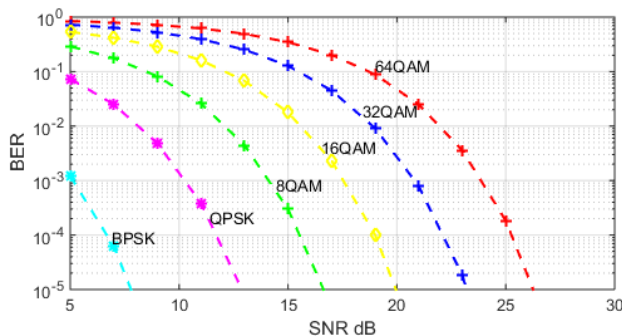


Figure 4.15 Constellation selection to maximize the throughput

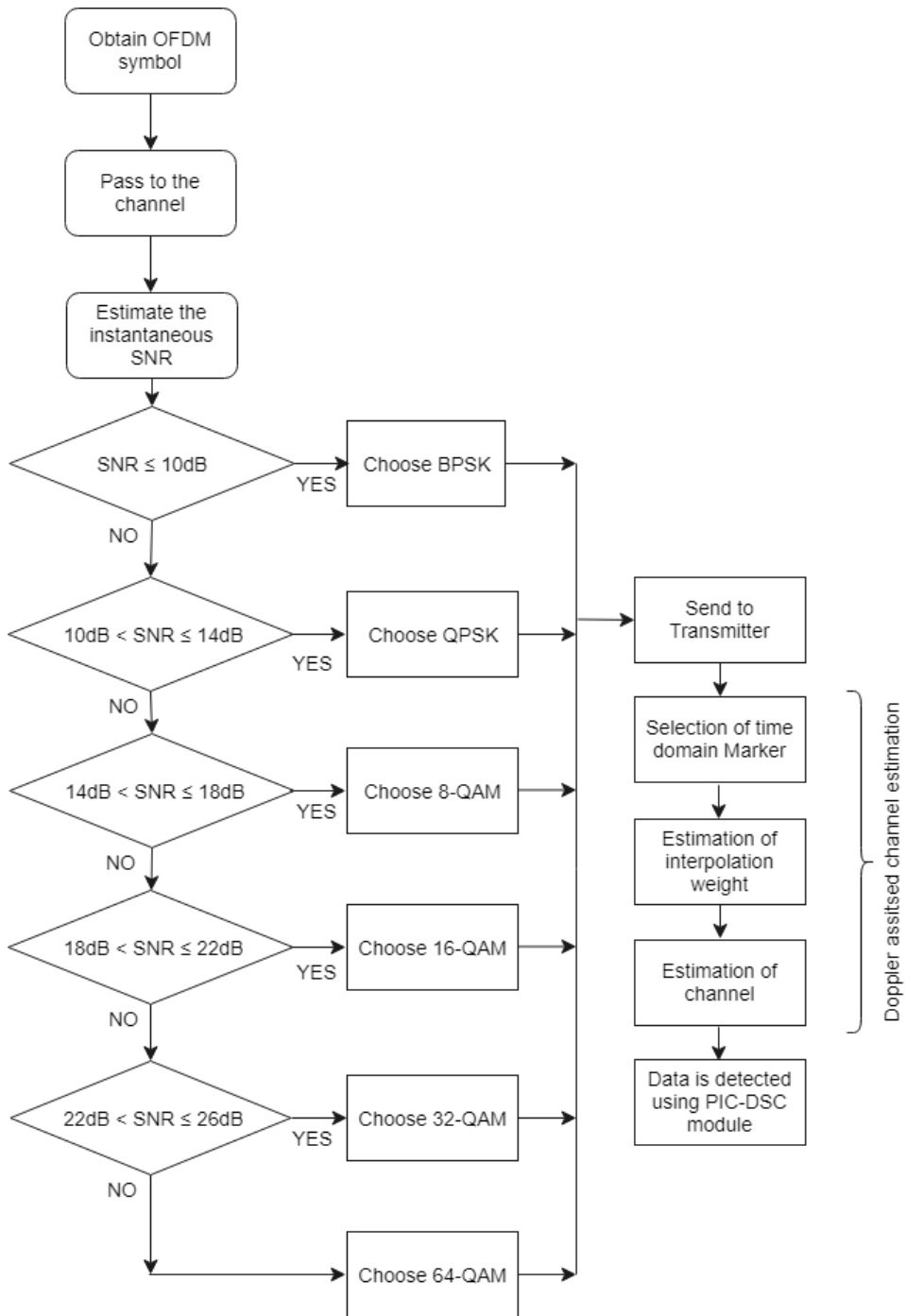


Figure 4.16 Overall algorithm

4.6 Results and Discussions

The parameters used for the proposed scheme is given below in the Table 4.1, and the Table 4.2 shows the switching thresholds used by the modulation selector of the adaptive modulator based on the instantaneous value of SNR. The modulation method has been changed between BPSK to 64-QAM for different ranges of SNR.

Table 4.1 Parameters used in the proposed system

No.	Parameters	values
1	Modulation	QAM
2	No. of transmitting antenna(N_t)	2
3	No. of receiving antenna(N_r)	2
4	Signal to Noise Ratio	0:4:34
5	Doppler Spread	0.025,0.1,0.2

Table 4.2 Switching threshold for adaptive modulation

Threshold	Modulation
$SNR \leq 10\text{dB}$	BPSK
$10\text{dB} < SNR \leq 14\text{dB}$	QPSK
$14\text{dB} < SNR \leq 18\text{dB}$	8 QAM
$18\text{dB} < SNR \leq 22\text{dB}$	16 QAM
$22 \text{ dB} < SNR \leq 16\text{dB}$	32QAM
$SNR > 26\text{dB}$	64QAM

Fig. 4.17 gives the comparison of the BER performance of the system for different Doppler spreads. It is evident from the plot that the BER performance degrades with the increase in Doppler spread for the same value of SNR. This is because when the Doppler spread is higher the received signal experience more frequency dispersion leading to

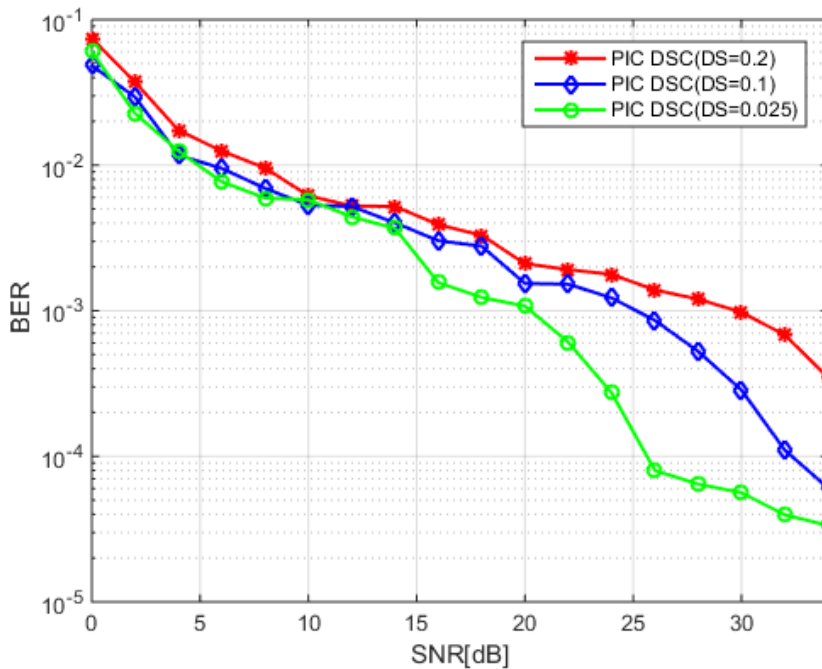


Figure 4.17 Comparison of the BER vs. SNR performance of the PIC-DSC interference cancellation technique for the Doppler spreads of 0.025, 0.1 and 0.2.

signal distortion and increased BER. Wireless channels with high Doppler spread will have signal components in which each are varying independently in phase over time, and therefore such channels experience more fading and signal degradation.

Fig. 4.18 demonstrates the BER performance of the suggested strategy for canceling interference, i.e., PIC DSC AM scheme is more

effective than the existing PIC DSC scheme for the entire range of SNR. The simulation has been repeated for different values of Doppler spread, and the results stand true for all the values. This improvement in the performance has been achieved by the adaptive modulation used along with PIC-DSC interference cancellation which switches the modulation between BPSK to 64-QAM according to the calculated value of the SNR to give better performance according to the channel quality variation.

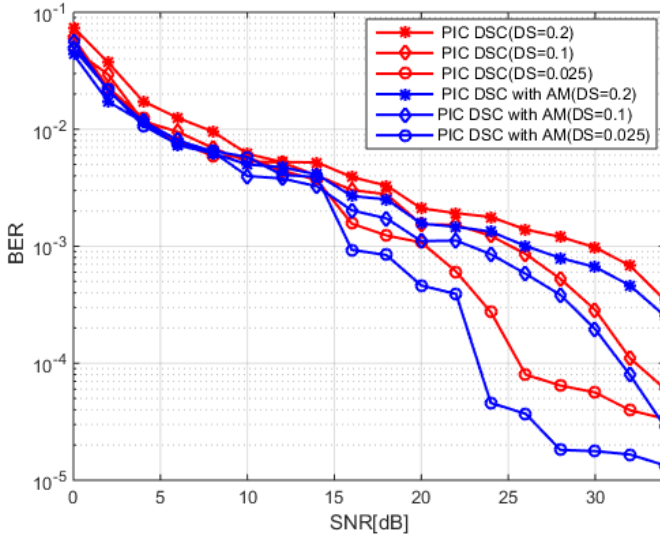


Figure 4.18 Comparison of the BER vs. SNR performances of the proposed PIC DSC AM interference cancellation scheme with existing PIC DSC scheme for Doppler spread of 0.025, 0.1 and 0.2.

In Fig. 4.19, the simulation result shows that the BER of the proposed method of interference cancellation is less than that of the existing method of PIC-DSC for all the normalized Doppler spreads of 0.025, 0.1 and 0.2. The multi path propagation also causes some difference in the Doppler shifts of the two different signals coming in different directions. In a very similar way the phase shifted radio

signals that nulls out each other by destructive interference, the frequency shifted signals interfere and create fading. The wide range of adaptation from BPSK to 64-QAM makes it possible to keep performance always better irrespective of the Doppler spreads.

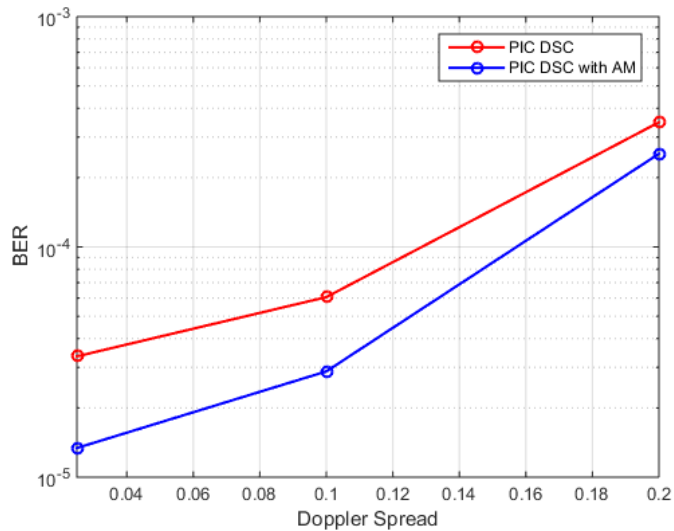


Figure 4.19 BER vs. Doppler Spread of the proposed PIC DSC AM and existing PIC DSC scheme.

In the Fig. 4.20, the BER performance of the proposed method is compared with the Zero-forcing (ZF) and Minimum Mean Square Error detection (MMSE) methods. It is clear from the graphs that the proposed method outperforms all other schemes.

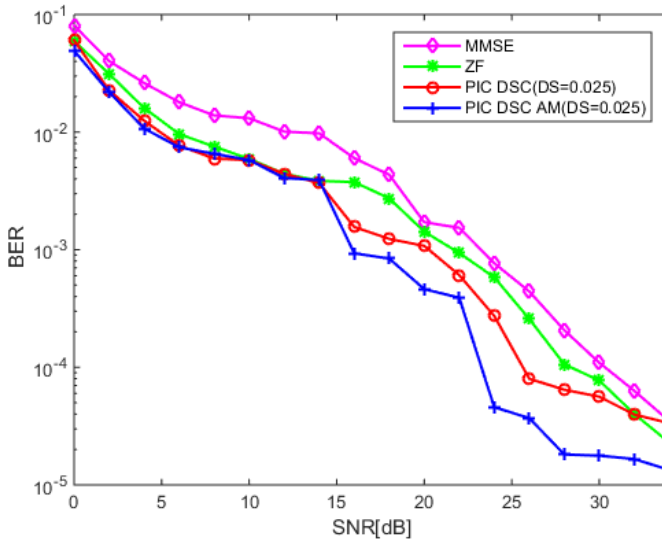


Figure 4.20 Comparison of the BER vs. SNR performances of the proposed PIC DSC AM, existing PIC DSC, zero-forcing (ZF) and Minimum mean square error (MMSE) methods

4.7 Chapter Summary

An adaptive modulation scheme along with interference cancellation techniques for the MIMO-OFDM wireless network is developed and implemented using MATLAB. Together with PIC, adaptive modulation is used to meet the required BER performance by selecting suitable modulation modes based on the channel condition. In addition, the ICI cancellation scheme used integrates the parallel interference cancellation together with the decision statistical combining module to detect the data. These data symbols are estimated by the detector and used to further refine the channel estimation iteratively.

Simulation results showed that adding adaptive modulation based on the calculated value of the SNR along with ICI cancellation

improves the BER performance of the MIMO-OFDM system for the entire range of SNR as well as for all values of Doppler spreads. It also proved that the proposed method stands better compared to the ZF and MMSE based channel equalizers.

CHAPTER-4

INTERFERENCE AND INTERFERENCE CANCELLATION IN MIMO-OFDM NETWORKS

4.1 Introduction

MIMO-OFDM is one of the most wanted wireless broadband technology and transmission system which has been accepted as the basis of fourth generation (4G) wireless communication system. It is so flexible and adaptable to stay in power even in the coming up 5G technologies. Performance of OFDM is highly sensitive to the frequency offset between transmit and receive signals. This is due to the Doppler shift caused by the relative motion between receiver and transmitter or by the difference in their local oscillator frequencies. This causes loss of orthogonality between the sub carriers which results in inter-carrier interference [52]. To overcome the effect of interferences, an Adaptive Modulation and Interference Cancellation technique for a MIMO-OFDM wireless network is proposed. Along with interference cancellation technique, Adaptive Modulation is used to meet the required BER performance by selecting suitable modulation modes based on the channel condition. Doppler assisted channel estimation method is used to estimate the channel. Also, inter-channel/carrier interference (ICI) cancellation scheme is used to integrate the Parallel Interference Cancellation together with the Decision Statistical Combining (PIC-DSC) module to detect the data and transmit it to the estimator to iteratively refine the channel estimation. Simulation studies have been carried out to analyze the BER performance of the system.

4.2 Interference in Wireless Communication

Interference can be defined as the phenomenon that occurs when two waves meet/overlap as they travel over a same channel/media. As a result of this, the shape, amplitude phase and frequency of the interfering waves may change according to the way they interfere each other.

In wireless communication scenario, if we consider any one communication channel, there are basically three types of interferences. One is broad band interference, where interference forms a broad source, like microwave signals interfere with the signal uniformly in the entire channel bandwidth as shown in Fig. 4.1. Depending on the strength of the interfering signal we might be having troubles in identifying the information in the channel. The second type is the co-channel interference, which is originated from two different radio transmitters using the same frequency.

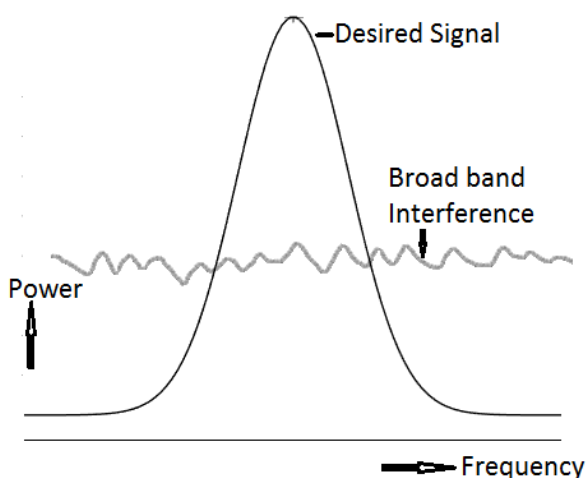


Figure 4.1 Broadband interference

There can be several causes for co-channel radio interference. In cellular mobile communication, the frequency spectrum is a precious resource which is divided into non-overlapping frequency bands and assigned to different cells. However, after certain geographical distance, the frequency bands are reused. i.e., same spectrum bands are reassigned to other distant cells. Fig. 4.2 describes these two types of interferences. Co-channel interference in cellular mobile networks is caused by frequency reuse in different cells. Besides the intended signal from within the cell, signals at the same frequencies (co-channel signals) arrive at the receiver from the undesired transmitters located in some other cell and lead to deterioration in the receiver performance [53].

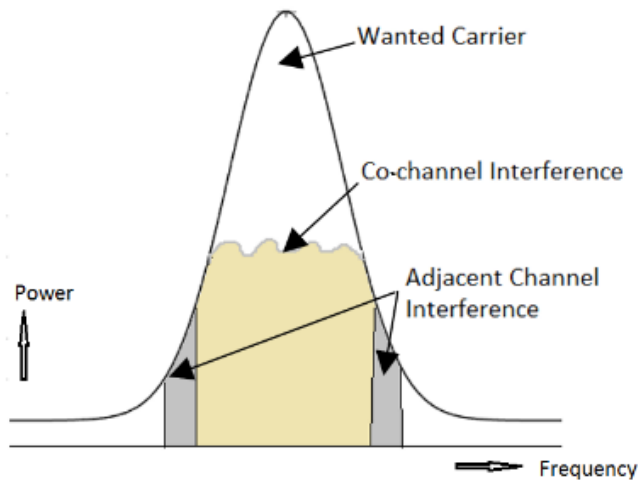


Figure 4.2 Co-channel and adjacent channel interference

Signal to co-channel interference ratio(S/I) at the desired receiver can be defined as $\frac{S}{I} = \frac{S}{\sum_{i=1}^{N_i} I_i}$ where S is the desired signal power from the desired source, I_i is the interfering power caused from the i^{th}

interfering channel. N is the number of interfering sources. Co-channel interference can be minimized by carefully designing the frequency reuse strategy [54].

The last type is adjacent channel interference resulting from signals which are adjacent to the desired signal. This is mainly caused by the imperfect receiver filters which allows nearby frequencies to leak into the pass band of the desired channel. Adjacent channel interference can be minimized by careful filter designing, channel assignment and by keeping a guard band in between adjacent channels [55].

In addition to the general category of noises explained above, because of the special nature of MIMO OFDM signals, its performance is highly degraded by the presence of inter-carrier interference (ICI), phase noise, narrow band interference (NBI) and I/Q imbalance [56].

4.2.1 Theoretical Background

When two radio signals S_1 and S_2 interfere in free space, and if that are combinedly received by a radio receiver then the total received signal will be the vector sum of these two interfering signals.

$$S(t) = S_1(t) + S_2(t) + n(t). \quad (4.1)$$

where $n(t)$ is the noise present in the channel. Now consider the signal S_i , received by a radio receiver and converted to the baseband

$$S_i(t) = H * h * A(t) \cos[2\pi t(\gamma + f(t)) + \psi(t)] \quad (4.2)$$

where $*$ is the convolution operation, $A(t)$ is the amplitude, $f(t)$ is the frequency and $\psi(t)$ is the phase shift for the signal that is being sent by the transmitter. Due to the non-ideal conditions of the receiver and

transmitter hardware and due to the Doppler shift in a mobile communication environment, the carrier frequency used both at the transmitter and receiver may not be properly replicated causing a frequency offset of γ . h is the response of the filter used at the receiver side for proper pulse shaping and unwanted signal rejection. Finally, H is the wireless channel gain which represents the effects of attenuations, multipath propagation, etc.

Now using Euler's function, we can rewrite the Eqn. 4.2 for the signal $S_i(t)$ as

$$S_i(t) = A(t)\cos(\varphi(t)) - jA(t)\sin(\varphi(t)) \quad (4.3)$$

where $\varphi(t) = 2\pi(\gamma + f(t))t + \psi(t)$, which represents the instantaneous value of phase of the converted baseband signal.

The real part of the signal represented in Eqn.4.3 can be expressed as I . For simplicity of analysis we assume the carrier frequency f_c and filter response h are fixed and known at the receiver. The channel gain H is also assumed as it produces only a channel attenuation and phase shift related to the distance traveled which remains constant for the entire duration of packet transmission. Now it is quite easy to reconstruct the original transmitted signal S_i from the received signal R_i [57].

4.2.2 Phase Noise

Phase noise is produced due to the non-linearities and instabilities of the local oscillator at the transmitter and receiver side. It can be considered as a parasitic phase modulation in the oscillator's signal, which otherwise should be ideally a unique carrier with constant frequency and amplitude. Phase noise in a system can be shown as

proportional to the square of the instantaneous frequency variations [58]. The effects of phase noise on OFDM signal are mainly the constant phase error and inter carrier interference. Constant phase error indicates the fixed phase rotation common to all the subcarriers in an OFDM symbol [59], and ICI is due to the adjacent subcarriers which are interfering with each other. If the ratio between the bandwidth of phase noise and intercarrier spacing in OFDM is close to unity, ICI will be the dominating component where as if the ratio is small constant, phase error will be the main noise contributor [60].

4.2.3 Compensation of Phase Noise

MIMO-OFDM receivers are very sensitive to the phase noise generated due to frequency offset among the local oscillator and carrier frequencies. Phase noise is the main limiting factor in the performance of high data rate OFDM systems. The most commonly used method for phase noise cancellation is by estimating the frequency offset with pilot symbols and compensating the same on the data subcarriers. Compared to ICI, constant phase error correction is relatively easier [61]. Fig. 4.3 shows the graph plotted for the ratio of noise power to carrier power against frequency when the carrier frequency is taken as 500 Hz.

4.2.4 I/Q Mismatch

I/Q Mismatch or imbalance occurs when the in-phase and quadrature phase components in the RF front end of the receiver are precisely not the same. In MIMO-OFDM networks a separate down converting circuit is used for each RF channel, and the value of I/Q mismatch for one channel will be independent of the values for the

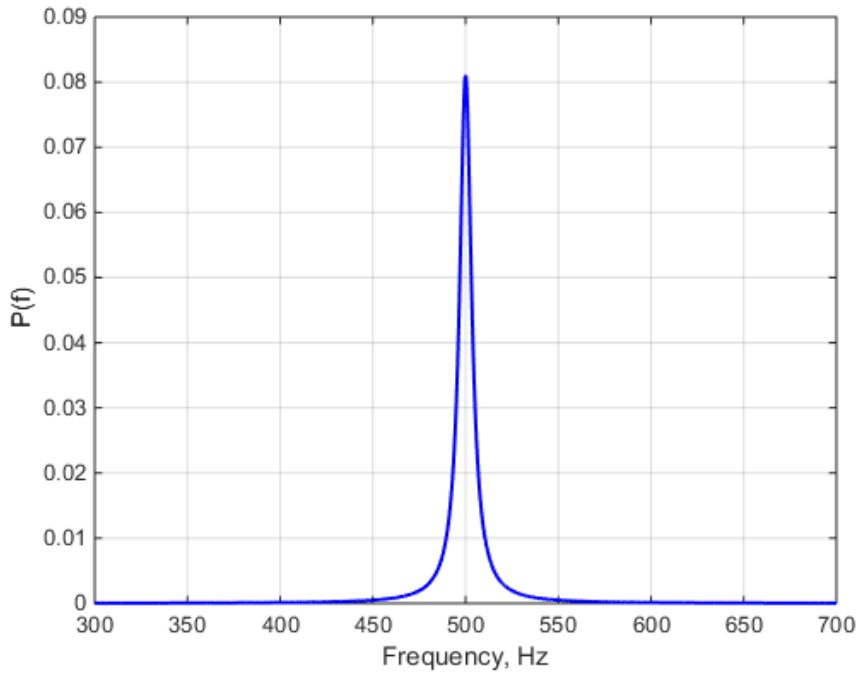


Figure 4.3 Ratio of noise power to carrier power plotted against frequency

channels. In OFDM networks, I/Q imbalance introduces inter-carrier interference from the mirror subcarrier. Because of the ICI component, MIMO-OFDM systems are highly reactive to the I/Q imbalance [62].

To mitigate this effect, a strict condition for matching of the two streams are to be followed in the front-end RF circuits or compensation can be done in the baseband receiver for the imbalance caused [63]. The graph in Fig. 4.4 shows the amplitude of the received spectrum against frequency for a phase imbalance of 5° .

4.2.5 Narrow Band Interference (NBI)

Signal interference, which is within the device's bandwidth and much smaller than the system bandwidth, can be considered as Narrow-Band Interference (NBI). NBI is produced when two or more

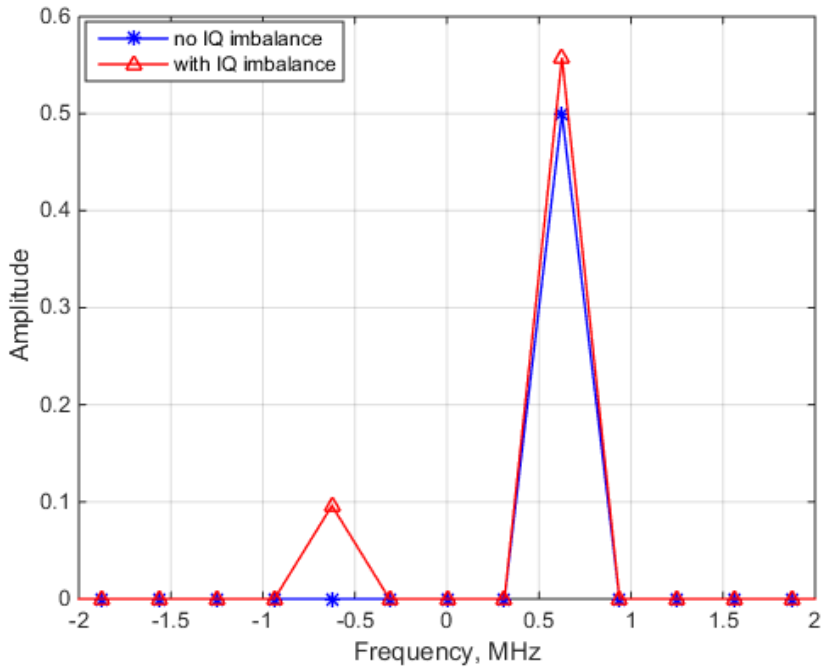


Figure 4.4 Spectrum of received signal – with and without transmit I/Q imbalance

nearby systems operate on the same frequency band. It is more predominant in the license-free frequency band (ISM band), where interference is received from devices such as Wi-Fi access points, Bluetooth operating equipment, microwave ovens, cordless phones, etc. In OFDM systems, if the frequency of the NBI doesn't exactly match with one of the subcarrier frequency then the whole spectrum of NBI will spread to the entire bandwidth of the OFDM communication system [64].

4.2.6 NBI Compensation

To compensate the effect of NBI in OFDM systems, the main techniques used are frequency identification and canceling, frequency

excision, prediction error filtering and adaptive narrow band filtering [65]. In frequency identification and canceling method, the Phase and amplitude of NBI are assessed from the peak magnitude of the received spectra by using maximum likelihood detection. In frequency excision method, the NBI, which comes as a maximum peak in the received signal spectra is removed by equating it with the threshold value. In the adaptive narrowband bandpass filter method, the center frequency of this filter is made equal to that of the NBI frequency and the filter weights are modified by using LMS algorithm [66].

4.2.7 Doppler Shift

Doppler spread is a parameter that describes the time-varying nature of the channel in a small-scale region. When a mobile receiver or a transmitter station move in a certain direction at a constant rate, a change in phase and frequency will be caused due to the difference in the propagation path and this effect is known as the Doppler shift.

When a pure sinusoidal tone of frequency f_c is transmitted, the received signal spectrum, called the Doppler spectrum, will have components in the range $f_c - f_d$ to $f_c + f_d$, where f_d is the Doppler shift. The amount of spectral broadening depends on f_d which is a function of the relative velocity of the mobile and the angle θ between the direction of motion of the mobile and direction of arrival of the scattered waves. If the baseband signal bandwidth is much greater than f_d the effects of Doppler spread are negligible at the receiver [67]. This is a slow fading channel.

When the mobile station moves at a constant rate v_m over a path of length d and endpoints A and B , it receives a signal from the far-end

source T_x as shown in the Fig. 4.5.

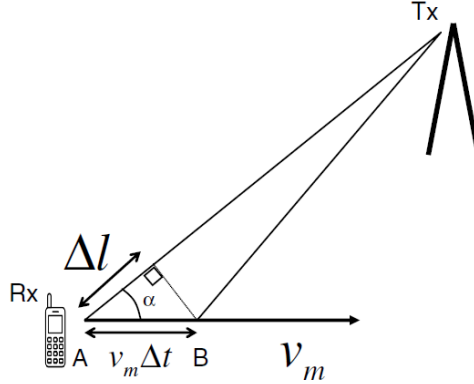


Figure 4.5 Calculation of Doppler Shift due to a mobility of User terminal

Radio waves starting from the source T_x , points is received by the mobile station at the points A and B . Then the path difference is:

$$\Delta l = d \cos \alpha = v_m \Delta t \cos \alpha \quad (4.4)$$

where d is the distance between A and B . Now this path difference Δl will produce a phase difference given by

$$\Delta \phi = \frac{2\pi \Delta l}{\lambda} = \frac{2\pi v_m \Delta t}{\lambda} \cos \alpha \quad (4.5)$$

Then the Doppler spread f_d can be calculated as

$$f_d = \frac{1}{2\pi} \frac{\Delta \phi}{\Delta t} = \frac{v_m}{\lambda} \cos \alpha \quad (4.6)$$

The maximum Doppler shift is achieved when $\cos(\alpha) = 1$, or equivalently when $\alpha = 0$ and the receiver is moving towards the signal source and is given by:

$$f_{d,max} = \frac{v_m}{c} \quad (4.7)$$

Hence the mobile equipment sees the incoming signal as a wave of

frequency:

$$f = \frac{\Delta\phi}{2\pi\Delta t} = \frac{1}{2\pi} \frac{2\pi f_c \Delta t + \frac{2\pi}{\lambda} v_m \Delta t \cos(\alpha)}{\Delta t} = f_c + f_c \frac{v_m}{c} \cos(\alpha) \quad (4.8)$$

Therefore, the incoming signal appears to have undergone a frequency shift by $f_c \frac{v_m}{c} \cos(\alpha)$. This phenomenon is called the Doppler effect, and the frequency shift $f_c \frac{v_m}{c} \cos(\alpha)$ is called the Doppler shift (f_d). f_d will be maximum when $\cos(\alpha) = 1$, or equivalently when $\alpha = 0$ and the mobile terminal is moving towards the transmitter and is given by:

$$f_{d,max} = \frac{v_m}{c} \quad [68].$$

The effect of Doppler shift in BER is plotted in Fig. 4.6 for BPSK and in Fig. 4.7 for QPSK modulations, for three different values of normalized Doppler shift 0, 0.001 and .09. It is clear from the graphs that the Doppler shift considerably increases the BER, and when comparing the QPSK and BPSK, we can see that the effect is more predominant in QPSK.

4.3 Inter-Carrier Interference

The subcarriers used in OFDM are very closely packed, and due to orthogonality among these subcarriers, the null of one subcarrier will be exactly at the peak of the other subcarrier. This orthogonality has to be properly maintained throughout the communication to ensure efficient modulation performance of OFDM. ICI is produced when sub-carriers lose this perfect orthogonality. This is shown in Fig 4.8 where OFDM with four subcarriers at an equal spacing of Δf is shown.

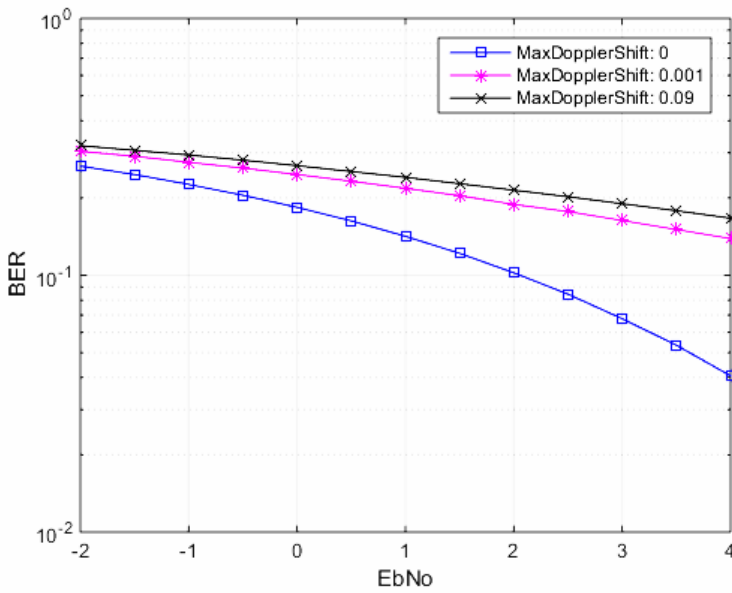


Figure 4.6 Effect of Doppler shift on BER in a BPSK system

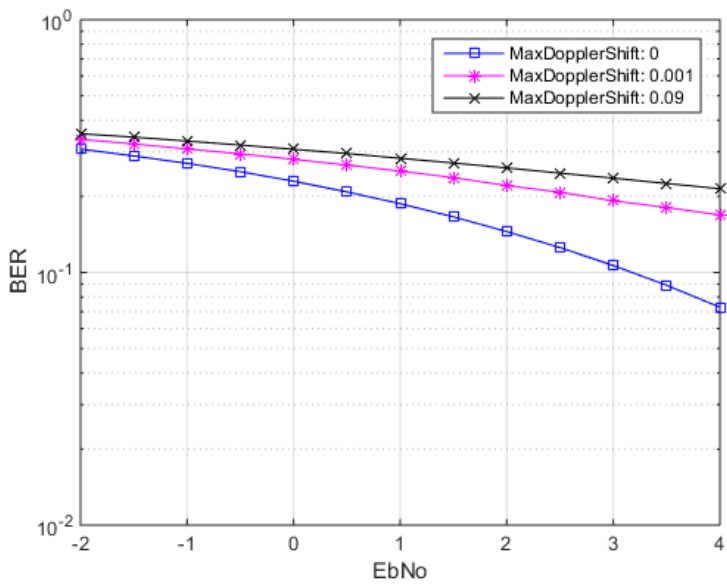


Figure 4.7 Effect of Doppler shift on BER in a QPSK system

Corresponding to the peak of any one sub carrier, all the other subcarriers are having a zero value (nulls) canceling the ICI without the use of any complex filtering or guard band. This condition is lost when there is a frequency offset and corresponding to the sampling of any subcarrier we get a non-zero value of other subcarriers creating ICI.

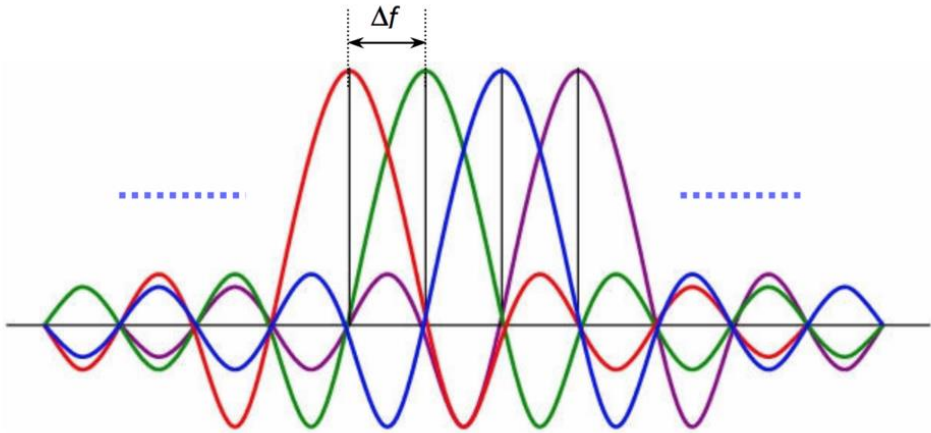


Figure 4.8 OFDM subcarrier creates “nulls” and canceling out ICI

ICI is caused by two reasons:

- i. The frequency offset at the receiver compared to that of the transmitter. This could be caused by the Doppler shift in frequency due to the mobility of the user or by the frequency shift between the transmitter and receiver frequencies. This may also be caused by the time domain synchronization error.
- ii. Delay spread of radio channel exceeds the cyclic prefix introduced. MIMO-OFDM converts a MIMO frequency selective channel into a set of parallel MIMO flat fading channels, such that across each sub-carrier, the net wireless communication systems looks like a MIMO flat-fading system.

Mathematically the output across each subcarrier can be written as

$$Y_{(0)} = H_{(0)}X_{(0)} \quad (4.9)$$

$$Y_{(1)} = H_{(1)}X_{(1)} \quad (4.10)$$

$$Y_{(N-1)} = H_{(N-1)}X_{(N-1)} \quad (4.11)$$

i.e., the vector $\bar{Y}_{(0)}$ is now $\bar{H}_{(0)}$ times $\bar{X}_{(0)}$, where $\bar{X}_{(0)}$ is the transmit vector across the 0th sub carrier, $\bar{H}_{(0)}$ is the flat fading channel matrix, and $\bar{Y}_{(0)}$ is the received vector across the 0th sub carrier. Similarly, all the N sub carriers are shown. It is similar to OFDM except that the Y and X are vectors. In general it can be written as

$$\bar{Y}_{(k)} = \bar{H}_{(k)}\bar{X}_{(k)} \quad (4.12)$$

where $\bar{Y}_{(k)}$ is the $r \times 1$ receive vector, $\bar{X}_{(k)}$ is the $t \times 1$ transmit vector and $\bar{H}_{(k)}$ is the flat fading channel matrix corresponding to subcarrier k .

Each $\bar{Y}_{(0)}, \bar{Y}_{(1)}, \dots, \bar{Y}_{(n-1)}$ can be processed by a simple MIMO ZF receiver for detection of transmit vectors $\hat{X}_{(0)}, \hat{X}_{(1)}, \dots, \hat{X}_{(n-1)}$ as seen in Eqn. (4.13) [69].

$$\hat{X}_{(k)} = (\bar{H}_{(k)})^\dagger \bar{Y}_{(k)} \quad (4.13)$$

$(\bar{H}_{(k)})^\dagger$ is the pseudo-inverse of the channel matrix $\bar{H}_{(k)}$

MIMO equalization for a MIMO frequency selective channel poses a much more challenge for communication compared to SISO frequency selective systems.

4.3.1 Effect of Frequency Offset in MIMO-OFDM

OFDM is a delicately balanced system, and the presence of carrier frequency offset can introduce severe distortions in an OFDM system as it results in the loss of orthogonality. If Δf_0 is the frequency offset and B/N is the subcarrier bandwidth, the normalized frequency offset ϵ can be written as

$$\epsilon = \frac{\Delta f_0}{B/N} \quad (4.14)$$

The larger the frequency offset, the greater is this inter carrier interferences and dealing with frequency offset is, in fact, a very important aspect of any OFDM system.

To model this, consider a system with frequency offset ϵ normalized with respect to the subcarrier bandwidth. Then the baseband received samples can be written as

$$y_n = \frac{1}{N} \sum_{k=-\frac{N}{2}}^{\frac{N}{2}} X_k H_k e^{j2\pi n \frac{(k+\epsilon)}{N}} + W_n \quad (4.15)$$

The received signal sample $Y_{(n)}$ is given as summation of $X_k H_k e^{j2\pi n (k+\epsilon)/N}$ plus the noise component w_n , where X_k is the data transmitted on the k^{th} subcarrier, H_k is the channel coefficient across the k^{th} subcarrier, N is the number of sub carriers. This equation can be very easily verified by putting $\epsilon = 0$,

$$y_n = \frac{1}{N} \sum_{k=-\frac{N}{2}}^{\frac{N}{2}} X_k H_k e^{-j2\pi n \frac{k}{N}} + W_n \quad (4.16)$$

Performing the FFT of this received symbols $y_{(0)}, y_{(1)} \dots y_{(N-1)}$ at the receiver, the l^{th} FFT coefficient corresponds to the symbol received on

the l^{th} subcarrier can be written as

$$y_l = \frac{1}{N} \sum_n \sum_{k=-\frac{N}{2}}^{\frac{N}{2}} X_k H_k e^{J2\pi n \frac{k}{N}} e^{-J2\pi n \frac{l}{N}} + W_l \quad (4.17)$$

$$= \frac{1}{N} \sum_k \sum_n X_k H_k e^{J2\pi (k-l) \frac{n}{N}} + W_l \quad (4.18)$$

$$= X_l H_l + \sum_n \sum_{k=-\frac{N}{2}}^{k/2} X_k H_k e^{J2\pi \frac{(k-l)}{N} n} + W_l \quad (4.19)$$

In the absence of carrier frequency offset, for $k \neq l$, the second term in the Eqn. 19 becomes zero because the $\sum_n e^{j2\pi n(k-l)/N}$ becomes equal to zero. Hence, we have

$$Y_l = H_l X_l + W_l \quad (4.20)$$

where the first term is the original OFDM relation for the l^{th} subcarrier. Now let us see what happens to the signal when there is carrier frequency offset, for that consider the Eqn. (4.17), received symbol across the l^{th} subcarrier is given by

$$Y_l = \frac{1}{N} \sum_n X_l H_l e^{j2\pi n \epsilon / N} + \frac{1}{N} \sum_{k=-\frac{N}{2}, k \neq l}^{n/2} X_k H_k e^{j2\pi (k-l+\epsilon) n / N} + W_l \quad (4.21)$$

This can be further simplified by using the following result

$$\sum_{n=0}^{N-1} e^{j\theta n} = \frac{\sin N\theta/2}{\sin \theta/2} e^{j\phi} \quad (4.22)$$

where $e^{j\phi}$ is the phase factor, which does not affect the power and need not to be taken care of.

Applying this in Eqn. (4.19)

$$Y_l = H_l X_l \frac{\sin \pi \epsilon}{\sin \frac{\pi \epsilon}{N}} \frac{1}{N} e^{j\phi_l} + \underbrace{\sum_{k=-\frac{N}{2}, k \neq l}^{n/2} H_k X_k \left(\frac{\sin \pi \epsilon}{N \sin \left(\pi \frac{l-k+\epsilon}{n} \right)} \right)}_{\text{(Interference)}} e^{j\phi_{kl}} + W_l \quad (4.23)$$

In the above equation also when ϵ tends to 0, the \sin term tends to 1, and the second term which corresponds to the inter-carrier interference also tends to zero giving us the result for perfect condition. The third term W_l is the Gaussian noise part [70].

In this condition, since we have noise along with interference signal to evaluate the performance we calculate the SINR and is given by

$$SINR = \frac{\text{Signal Power}}{\text{Interference+Noise Power}} \quad (4.24)$$

$$SINR = \frac{\text{Signal Power}}{E\{|I_l|^2\} + \sigma_n^2} \quad (4.25)$$

$$\text{Signal Power} = E\{|H_l|^2\}E\{|X_l|^2\} \left(\frac{\sin \pi \epsilon}{N \sin \pi \epsilon / N} \right)^2 \quad (4.26)$$

For large number of subcarriers, i.e large N

$$\lim_{n \rightarrow \infty} \sin \frac{\pi \epsilon}{N} = \frac{\pi \epsilon}{N} \quad (4.27)$$

$$N \sin \frac{\pi \epsilon}{N} \gg N \frac{\pi \epsilon}{N} = \pi \epsilon \quad (4.28)$$

On simplification and assuming N= number of subcarriers as very large, we get the SINR in the presence of carrier frequency offset ϵ as equal to

$$SINR = \frac{P|H|^2 \left(\frac{\sin \pi \epsilon}{\pi \epsilon} \right)^2}{0.822 P|H|^2 (\sin \pi \epsilon)^2 + \sigma_n^2} \quad (4.29)$$

The numerator represents the signal power, the first term in the denominator is the interference power from the intercarrier interference and σ_n^2 is the noise power.

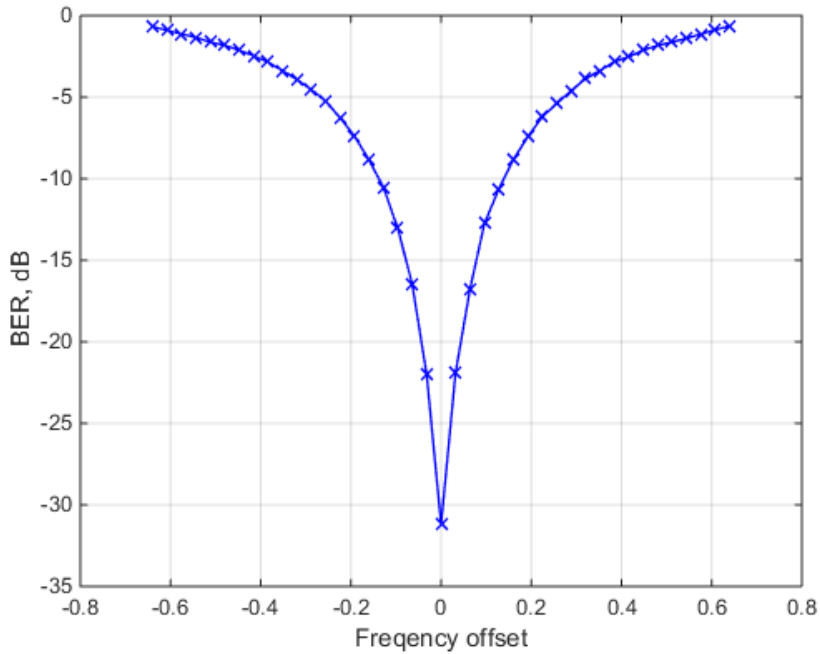


Figure 4.9 SNR loss due to frequency offset in OFDM modulation

Fig. 4.9 shows the variations in BER plotted against frequency offset in a BPSK system in OFDM with FFT size of 64 and number of subcarriers equal to 52. ICI due to frequency offset can be completely removed or can be reduced by estimating the offset frequency and dynamically correcting the sub-carrier spacing accordingly.

In the following section, we discuss the different interference cancellation techniques that are widely used in wireless communication systems.

4.3.2 Successive Interference Cancellation (SIC)

In interference limited communication system the performance can be highly improved by Successive Interference Cancellation (SIC), where the projected effect of interference on the detected data is canceled in

a serial manner. In SIC receivers [71,72], received signals are ranked in descending order of signal power. The signal with the strongest power (say for User 1) is sent through the conventional (e.g.: MMSE receiver) detector and the message sent is decoded. The decoded message is regenerated and subtracted from the original received signal, $y_{(t)}$, which is delayed to allow time for processes required before subtraction. The residual signal, $y'_{(t)}$ does not contain the signal for User 1, and consequently, it does not contain media access interference due to User 1. The receiver selects the next strong signal and repeats the process as for User 1. This is shown in Fig. 4.10. The process continues until all the users have been detected. Alternatively, the process could continue until sufficient number of powerful signals have been detected and canceled. The residual signals can then be detected using conventional detector as usual. SIC introduces lengthy delays in detection. The user with least received signal power can only be detected after all stronger users have been detected. In addition, this system relies on the normal imbalance in received signal power. The first signal detected (for User-1) is done using the conventional detector in the presence of media access interference. If this detection is wrong then the subtracted signal is also wrong. Rather than canceling interference, it would be increased. This problem is known as error propagation which is one of the main factors that limits the performance of SIC. SIC performs worse than the conventional receiver when the received signal power is balanced.

The application of SIC in communication was first analyzed by Kohno et al. in [73], for spread spectrum communication. Subsequently, it has been widely discussed in many literatures for multi-user application in

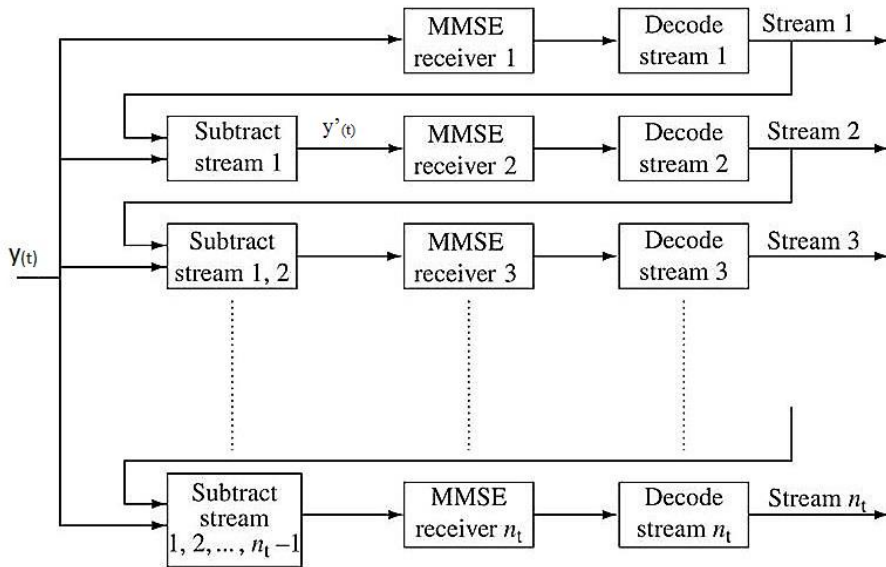


Figure 4.10 Successive Interference Cancellation

spread spectrum. Application of SIC for MIMO communication was first developed by Foschini et al. in [74]. The performance improvement of MIMO on the application of SIC is two-fold i) the post-processing gain of the successive layers are greatly enhanced by the reduction of interference ii) For every successive layer that is assessed, will have a higher diversity order which also supplements to higher gain. However, SIC do not take the spatial distribution of the users in to consideration.

4.3.3 Parallel Interference Cancellation

Parallel Interference Cancellation (PIC) is similar to SIC in principle [75]. It subtracts (cancels out) interference from the received signal before detecting the desired users. The difference in PIC as compared to SIC is that cancellation of interference is done at once. (in parallel).

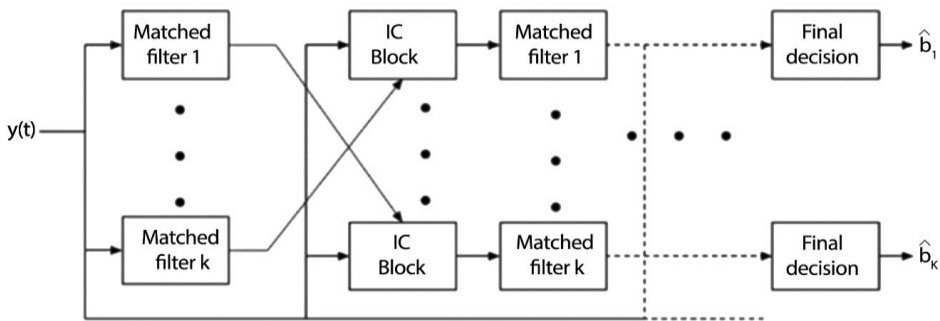


Figure 4.11 Parallel Interference Cancellation

Fig. 4.11 shows the PIC detector. The received signal $y(t)$ is sent through the first stage of detection. This is usually the conventional detector or a linear multiuser detector like the decorrelating detector. The output of this first stage is regenerated to obtain the received signal, $\hat{b}_{(t)}$ for each user. After that, the interference signal is summed up and subtracted from $y(t)$. $y(t)$ is delayed to allow time for processes required before subtraction of interference. The remaining signal is assumed to be free of multiple access interference. Final detection can, therefore, be done with the conventional detector. The ordering of signals in received signal power is no longer required. Delay in detection is also greatly reduced. However, knowledge of channel attenuation and delay is required to enable the system correctly estimate the signals to be subtracted.

The Parallel Interference Cancellation receiver can be cascaded into multiple iterative stages [76]. This iteration results in convergence ultimately to a decorrelating detector if the system load is not greater than 17% [77]. Convergence can be improved by using graduated weights to limit the interference. PIC works better than SIC when all

the users in the communication system under consideration receive signals with equal power strength [78,79].

Neda Aboutorab et al. in [80] have proposed an Iterative Channel Estimation with Parallel ICI for High-Mobility MIMO-OFDM networks. An easy parallel interference cancellation method linked with a decision statistical combining scheme is used to remove the ICI and improve data signal detection. It mainly focuses on the process of estimating the channel state information for high mobility user by considering Doppler effect due to the variant wireless channel to improve the performance of ICI cancellation. But this work does not take any consideration about any modulation technique in terms of improving the throughput and BER performance based on the feedback of channel state condition.

In this work, we propose to design a parallel ICI cancellation scheme along with adaptive modulation for MIMO-OFDM networks. This is achieved by using the feedback from channel state condition to properly select the modulation and thereby improving throughput and BER performance.

4.4 Review of Techniques Used for Interference Cancellation

Right from the beginning of wireless communication, interference and its mitigation are hot topics of research. This section will review the state of the art research contributions and practical implementations that effectively manage interference in wireless communication networks.

In [81], Shaverdian *et al.* have proposed robust distributed beamforming with interference coordination in downlink cellular

networks for addressing the robustness against the uncertainties in the channel parameters. The distributiveness of beamforming, spatial multiplexing and power allocation in multi-antenna BSs of a multicell network under the frequency reuse is considered as an optimization problem and minimized the overall transmission power of BSs subjected to SINR constraints at each mobile station under channel uncertainties. They used semi definite relaxation and the S-Lemma with a limited information exchange among BSs to achieve distributiveness. The optimization problem is first recast into a numerically tractable one, where each BS obtains a local version of its coupling variables. Then an iterative algorithm is used to coordinate inter-cell interference across multiple BSs. Septimus et al. in [82] proposed an approach for alleviating inter-carrier interference in OFDM systems by considering the signal reconstruction problem at the receiver end as an Integer Least Squares (ILS) problem. They developed a spectral approach called as sequential probabilistic ILS to decode the OFDM signals by extending probabilistic ILS to reduce inter-carrier interference.

A blind interference alignment (BIA) scheme using reconfigurable antenna technology to attain a high degree of freedom (DoF) or diversity gain in K-user interference channels has been proposed by Lu et al. in [83]. For that, two DoF-oriented BIA schemes are proposed that included full and partial interference alignment among all the users then compared the achievable DoF of the two schemes with each other. Then, three diversity-oriented BIA schemes with space-time coding are proposed by assuming a constant transmission rate to achieve both spatial diversity gain and

reconfigurable antenna pattern diversity gain. With different trade-offs among the diversity gain, the rate and the decoding complexity, the BIA is employed with threaded algebraic space-time (TAST) codes, orthogonal space-time block codes (OSTBCs) and multiplexing Alamouti codes respectively. After that, they compared the BIA with those codes regarding code rate and cost of decoding complexity.

End-to-end average symbol error probability (ASEP) of dual-hop relaying networks with pilot-symbol assisted M-array phase-shift keying (M-PSK) modulation which uses the selective Decode and Forward (DF) protocol while relays are equipped with multiple receive antennas is analyzed by Sagias et al. in [84]. The channels' state information is obtained per antenna branch based on the Least-Squares Estimation (LSE) technique using pilot symbols. Also, coherent detection based on maximal-ratio combining and ICI cancellation scheme are performed on the receiving end. Exact end to end analytical ASEP expressions are derived for binary and quadrature phase-shift keying, while approximate high signal-to-noise ratio (SNR) expressions are obtained for any order M-PSK modulation formats to extract the cooperation-gain and diversity-order.

The degrees of freedom for the constant MIMO interference channel with coordinated multipoint (CoMP) transmission in which each message is jointly transmitted by multiple successive transmitters were developed and tested by Wilson et al. in [85]. The transmission scheme of the proposed approach used two-stage scheme that involved both zero forcing and Interference Alignment to develop a constant MIMO interference channel with CoMP transmission. The combined effect is called derived channel which is proceeded in two stages by

first applying ZF and then IA sequentially at the transmitters.

In [86] Phan-Huy et al. have proposed Make-It-Real (MIR) precoders for MIMO OFDM/QAM without inter-carrier interference in which new precoders called MIR MRT and MIR MMSE precoders. These are based on traditional maximum ratio transmission (MRT) minimum mean square error (MMSE) precoders and are used to perform data multiplexing in the spatial domain for OFDM/QAM. These precoders are designed so that the equivalent channel including precoding and propagation is "made real" without breaking the orthogonality of OFDM/QAM in the frequency domain. At the receiver side, demodulation is done to extract the original signal. Then the performance of OFDM/QAM with MIR MMSE and MIR MRT precoder is compared with traditional MIMO OFDM with ZF, MRT, and MMSE precoders.

The BER performance of OFDM system with adaptive modulation that divides the whole subcarriers into blocks of adjacent subcarriers is analyzed by Borkarin et al. in [87] using MATLAB simulation. Based on the calculated average instantaneous SNR at the receiver side, the same modulation scheme is applied to all subcarriers of the same block. The modulation that has to be used by the transmitter for its next OFDM symbol will be determined by the channel-quality estimate of the receiver based on the current OFDM symbol.

In [80], Aboutorab et al. have proposed channel estimation and inter carrier interference cancellation scheme for a MIMO-OFDM system. They estimated the wireless channel simultaneously by using pilot symbols, data symbols, and Doppler spread information at the

receiver. Then the interpolation weights for the weighted time-domain channel are designed using Doppler spread and time-domain channel correlations. The channel estimates are obtained using the least-square method. When all the channel coefficients are obtained, simplified parallel interference cancellation (PIC) scheme is used along with decision statistical combining (DSC) module to cancel the ICI and improve data symbol detection and the SINR. These data symbols are estimated by the detector and used to further refine the channel estimation iteratively.

An adaptive algorithm which perfectly adapts the transmission rate according to the radio channel and interference combined with any interference cancellation schemes has not been analyzed in any of the works discussed in literature. Accordingly in this work a parallel interference cancellation (PIC) is developed along with adaptive modulation scheme and its BER performance is evaluated.

4.5 System Model

4.5.1 Overview

Fig. 4.12 represents the block diagram of the proposed system where Doppler-assisted channel estimation technique is used with the adaptive modulation scheme. Inter-Carrier Interference (ICI) degrades the overall performance of the system, so it is highly important to incorporate some ICI cancellation techniques. In the ICI cancellation scheme used here, a combination of data detection and PIC-DSC is used for each iteration of the channel estimation, and then the PIC-DSC output is delivered to the detector. Next, the channel estimator is again

fed with the detected data elements, thereby refining the channel estimation through each iteration.

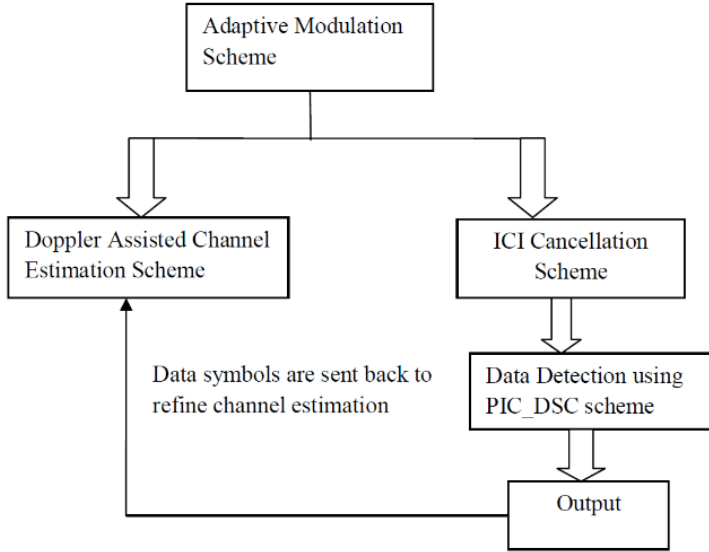


Figure 4.12 Block diagram of the proposed Adaptive modulation with ICI cancellation

4.5.2 Designing of Adaptive Modulation in OFDM

This section describes the designing of Adaptive Modulation in OFDM along with the ICI cancellation scheme. Orthogonality of subcarriers is the main part of OFDM. It has been observed that OFDM can easily be carried out by FFT and IFFT.

Let $I = [I_0, I_1, I_2, \dots, I_{N-1}]^T$ be the inputs after converting serial input data to parallel. then

$$z(t) = \frac{1}{U} \sum_{u=0}^{U-1} I_n e^{j2\pi\Delta f t}, 0 \leq t \leq UT \quad (4.30)$$

This is the complex baseband OFDM signal, where T represents the

data period, UT represents symbol interval in OFDM and $\Delta f = \frac{1}{UT}$ denotes spacing of the subcarrier.

For transmission of OFDM, the whole subcarriers are divided into a number of subcarriers. The same modulation method is used for every subcarrier of the same block. The modulation technique for the following symbol will be determined by the channel quality estimation of the receiver based on the present OFDM symbol. For our work, the channel estimation is done by the use of a Doppler assisted channel estimation scheme which will be explained in the subsequent section. The subcarrier SNR for this method will be calculated at the point of receiver end. The received signal at any subcarrier is given as

$$P_u = J_u I_u + G_u \quad (4.31)$$

where J_u is any subcarriers channel coefficient, I_u - the transmitted symbol

G_u - Gaussian noise sample

The SNR(instantaneous) can be computed as

$$SNR = \frac{J_u^2}{U_0} \quad (4.32)$$

U_0 - noise variance

For the real signal, $BW = \frac{1}{2}$ of the sampling rate.

$$\text{The average power } -U_0 = \frac{u_0 f_r}{2} \quad (4.33)$$

u_0 - One sided-power spectral density of noise in W / Hz .

In the proposed method given in Fig. 4.13, modulation method is identified after channel estimation at the receiver side, and this

information is sent to the transmitter through the feedback channel. Frame by frame adaptation is done for the modulation. The instantaneous value of SNR for the signal received is calculated using the channel estimator. Based on this SNR, the best modulation method to be used for the next transmission frame is determined. Modulation selector block at the transmitter performs this task, and an adaptive modulator block produces the required modulation on the basis of the instantaneous SNR. After modulation, the output is converted into parallel signal and then IFFT is used to transform the signal from discrete frequency domain to discrete time domain i.e. the OFDM. After that stage cyclic prefix is inserted to avoid any possibility of inter symbol interference. The signal is then converted to serial and transmitted to channel. An additive white Gaussian channel is assumed here, and at the receiver side, an exact reverse operation is performed to recover the data.

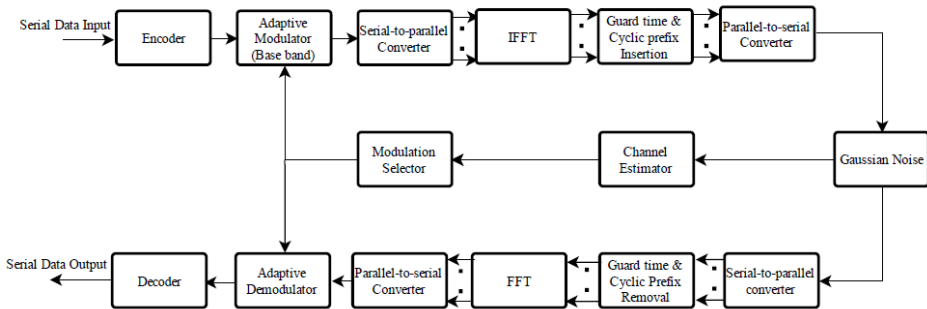


Figure 4.13 Block Diagram of OFDM with Adaptive Modulation

4.5.3 Doppler-Assisted Channel Estimation Scheme

In this section, the iterative Doppler-assisted channel estimation [80] that uses Doppler spread, time domain channel correlations and computation of data symbols is briefly described. In this scheme the

channel estimation is carried out by simultaneous use of the iterative estimates of the data symbols and Doppler spread information, The Doppler spread s_d is computed by using the speed of the receiver v (in meters per second), which is given as below

$$s_d = \frac{v s_c}{C} \quad (4.34)$$

Where s_c denotes the carriers frequency, and C is the velocity of light in m/s. Moreover, the normalized Doppler spread is given as

$$S_d = \left(\frac{s_d}{\Delta s} \right) \quad (4.34)$$

where Δs denotes the spacing between subcarriers.

In the channel estimation technique with Doppler assistance, time domain markers are used. These are nothing but the time-domain channel coefficients denoted as a weighted representation of the selected channel coefficients. These weights are estimated in such a fashion that channel estimation errors are reduced. At the receiver end, the required time domain channel correlation is estimated by the iterative process with the help of the available Doppler spread information. The least square method is used for estimating the time domain markers. The estimates of the ICI produced by the Doppler spread is subtracted from the input signal received using the PIC module. The output of this section is then fed to the DSC unit where the decision statistics signal is obtained through the successive combining of the values of iterations carried out in the current and previous stages. The iterative receiver along with the PIC-DSC module is given in Fig. 4.14. In each channel estimation cycle, the ICI produced due to Doppler-spread is generally removed by the PIC-DSC section. Here, the PIC-DSC procedures are merged into one iterative process.

Moreover, the data detection and PIC_DSC are carried out only once, and the detected data symbols are transmitted back to the channel estimator which gives lower computational complexity.

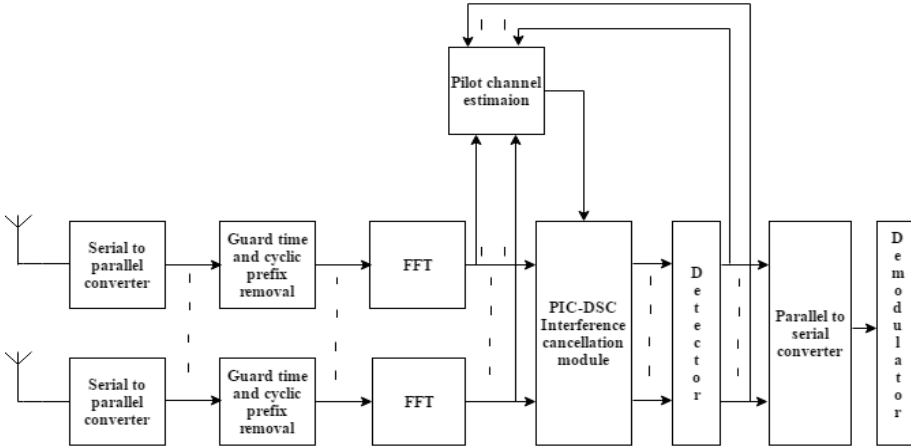


Figure 4.14 Integrated PIC-DSC interference cancellation scheme

4.5.4. Over all Algorithm

Fig. 4.15 gives the BER plotted against SNR for different modulation techniques ranging from BPSK to 64QAM. From this plot considering an BER value of 10^{-3} , the modulation scheme to be used is selected and send to the transmitter. The flow chart shown in Fig. 4.16 gives the steps involved in the interference cancellation scheme along with adaptive modulation.

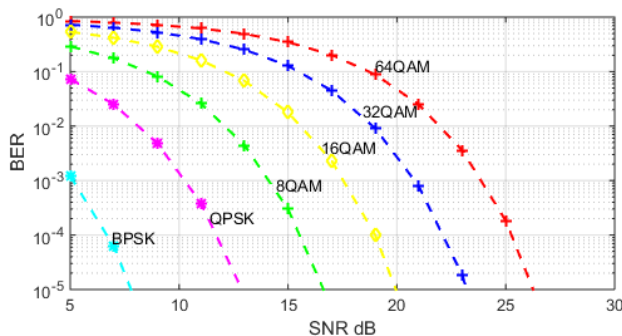


Figure 4.15 Constellation selection to maximize the throughput

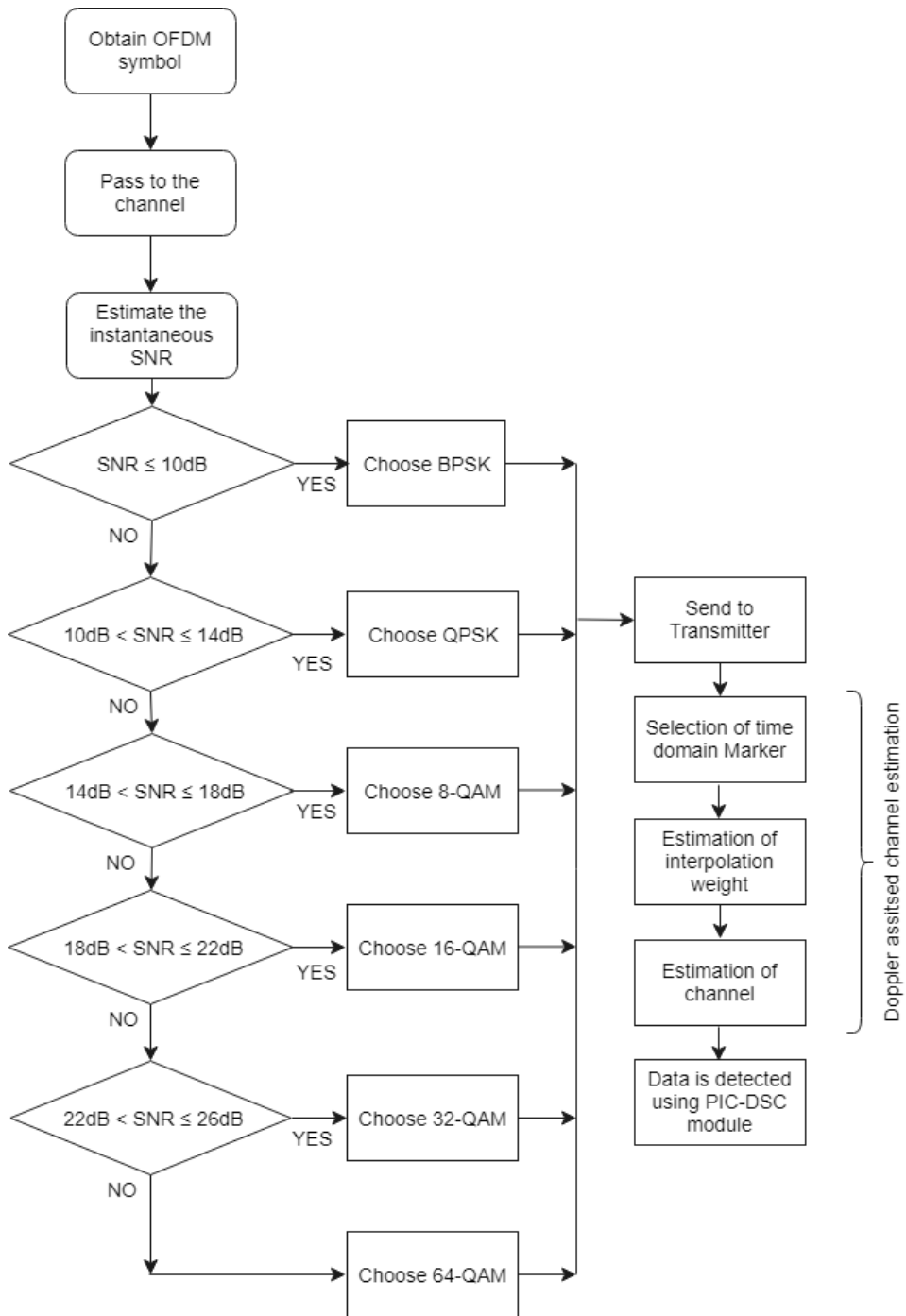


Figure 4.16 Overall algorithm

4.6 Results and Discussions

The parameters used for the proposed scheme is given below in the Table 4.1, and the Table 4.2 shows the switching thresholds used by the modulation selector of the adaptive modulator based on the instantaneous value of SNR. The modulation method has been changed between BPSK to 64-QAM for different ranges of SNR.

Table 4.1 Parameters used in the proposed system

No.	Parameters	values
1	Modulation	QAM
2	No. of transmitting antenna(N_t)	2
3	No. of receiving antenna(N_r)	2
4	Signal to Noise Ratio	0:4:34
5	Doppler Spread	0.025,0.1,0.2

Table 4.2 Switching threshold for adaptive modulation

Threshold	Modulation
$SNR \leq 10dB$	BPSK
$10dB < SNR \leq 14dB$	QPSK
$14dB < SNR \leq 18dB$	8 QAM
$18dB < SNR \leq 22dB$	16 QAM
$22 dB < SNR \leq 16dB$	32QAM
$SNR > 26dB$	64QAM

Fig. 4.17 gives the comparison of the BER performance of the system for different Doppler spreads. It is evident from the plot that the BER performance degrades with the increase in Doppler spread for the same value of SNR. This is because when the Doppler spread is higher the received signal experience more frequency dispersion leading to

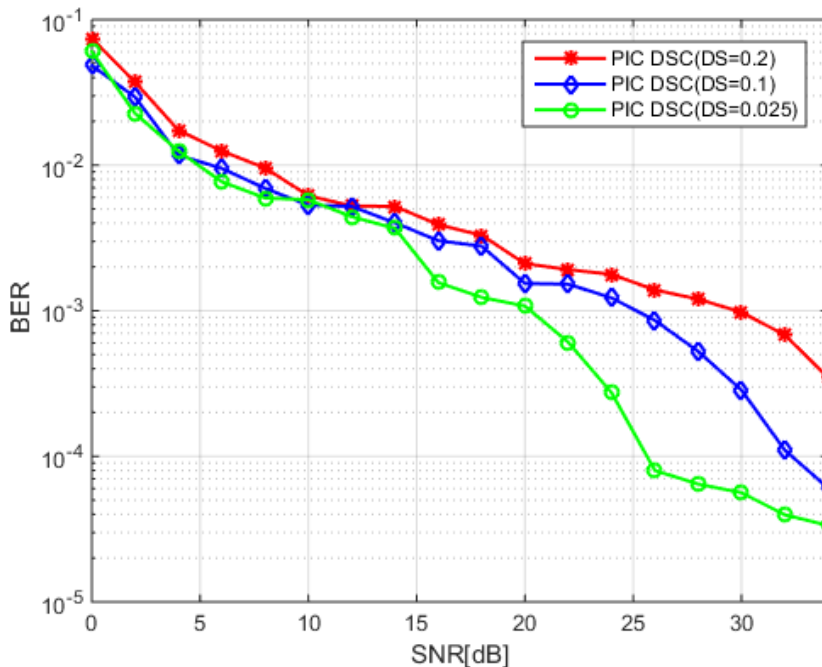


Figure 4.17 Comparison of the BER vs. SNR performance of the PIC-DSC interference cancellation technique for the Doppler spreads of 0.025, 0.1 and 0.2.

signal distortion and increased BER. Wireless channels with high Doppler spread will have signal components in which each are varying independently in phase over time, and therefore such channels experience more fading and signal degradation.

Fig. 4.18 demonstrates the BER performance of the suggested strategy for canceling interference, i.e., PIC DSC AM scheme is more

effective than the existing PIC DSC scheme for the entire range of SNR. The simulation has been repeated for different values of Doppler spread, and the results stand true for all the values. This improvement in the performance has been achieved by the adaptive modulation used along with PIC-DSC interference cancellation which switches the modulation between BPSK to 64-QAM according to the calculated value of the SNR to give better performance according to the channel quality variation.

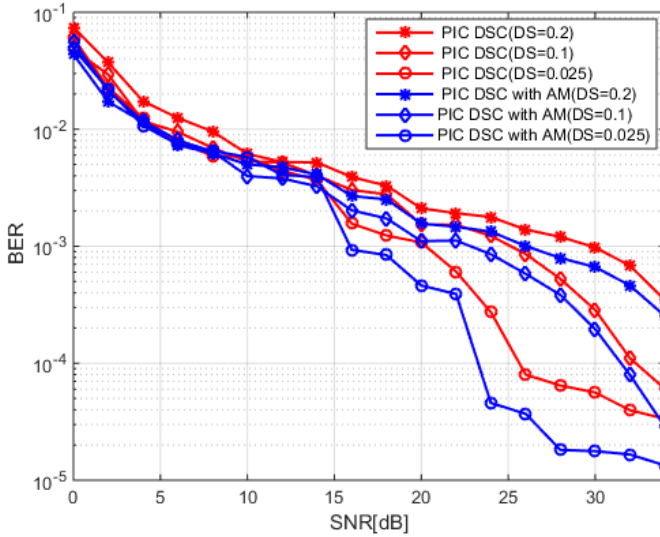


Figure 4.18 Comparison of the BER vs. SNR performances of the proposed PIC DSC AM interference cancellation scheme with existing PIC DSC scheme for Doppler spread of 0.025, 0.1 and 0.2.

In Fig. 4.19, the simulation result shows that the BER of the proposed method of interference cancellation is less than that of the existing method of PIC-DSC for all the normalized Doppler spreads of 0.025, 0.1 and 0.2. The multi path propagation also causes some difference in the Doppler shifts of the two different signals coming in different directions. In a very similar way the phase shifted radio

signals that nulls out each other by destructive interference, the frequency shifted signals interfere and create fading. The wide range of adaptation from BPSK to 64-QAM makes it possible to keep performance always better irrespective of the Doppler spreads.

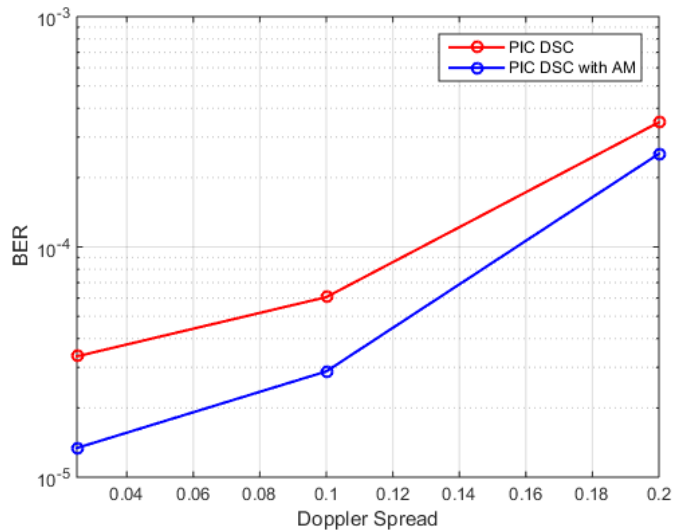


Figure 4.19 BER vs. Doppler Spread of the proposed PIC DSC AM and existing PIC DSC scheme.

In the Fig. 4.20, the BER performance of the proposed method is compared with the Zero-forcing (ZF) and Minimum Mean Square Error detection (MMSE) methods. It is clear from the graphs that the proposed method outperforms all other schemes.

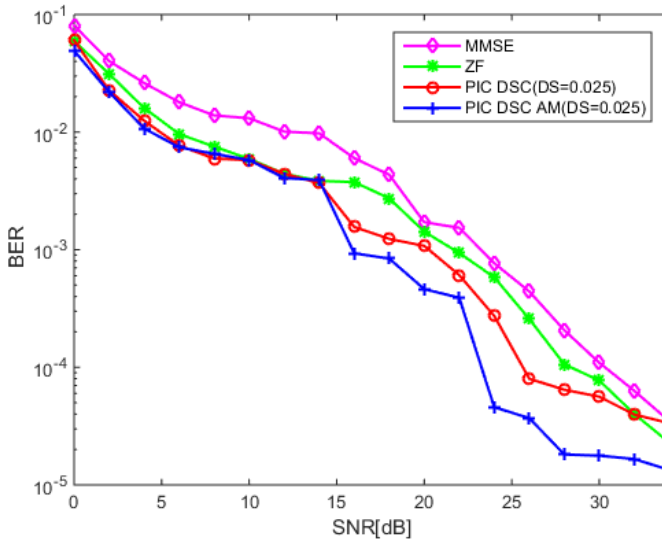


Figure 4.20 Comparison of the BER vs. SNR performances of the proposed PIC DSC AM, existing PIC DSC, zero-forcing (ZF) and Minimum mean square error (MMSE) methods

4.7 Chapter Summary

An adaptive modulation scheme along with interference cancellation techniques for the MIMO-OFDM wireless network is developed and implemented using MATLAB. Together with PIC, adaptive modulation is used to meet the required BER performance by selecting suitable modulation modes based on the channel condition. In addition, the ICI cancellation scheme used integrates the parallel interference cancellation together with the decision statistical combining module to detect the data. These data symbols are estimated by the detector and used to further refine the channel estimation iteratively.

Simulation results showed that adding adaptive modulation based on the calculated value of the SNR along with ICI cancellation

improves the BER performance of the MIMO-OFDM system for the entire range of SNR as well as for all values of Doppler spreads. It also proved that the proposed method stands better compared to the ZF and MMSE based channel equalizers.

CHAPTER-5

MASSIVE MIMO

5.1 Introduction

Massive multiple-input multiple-output also known as large-scale antenna systems/very large MIMO/hyper MIMO or full dimensional MIMO proposed in [88], is identified as the best way to optimize the performance of a wireless communication system. In massive MIMO large number of extra antennas are added to help focusing the energy into smaller regions of space to bring huge improvements in throughput and radiated energy efficiency [89].

Owing to its potential to focus energy to a narrow beam, such system is very often studied for multi-user transmissions because a very large number of antennas are necessary for the implementation of such transmissions and it should allow all the users to benefit from the entire frequency band in use at any time[90].

Massive MIMO systems have attracted great interest since the 5G objectives have been introduced in the year 2011[91]. The convergence towards a dense and heterogeneous network [92] and the numerous systems that make it up, a system operating at millimeter wavelengths [93] becomes essential to address the need for very high data rates on small targeted areas. In addition, very high energy focusing capacity allows more transmissions with low energy consumption. Such energy-efficient networks [94,95] are significant point of interest for the future communications systems.

Massive MIMO, in which the base stations are equipped with very large number of coherently operating antennas, provides both diversity gain and multiplexing gain [96]. This means that a network antenna can simultaneously receive data from multiple devices, and also send to different recipients at the same time. With all these antennas and complex signal processing, relay towers can use various propagation modes to send more data with greater reliability.

In wireless communication networks the signals transmitted from the antenna are attenuated by fading because of multi path propagation and shadowing by large obstacles in between the source and destination which raises a significant challenge on the reliability of wireless communication. Communication with multiple antenna at the transmitter and/or receiver is a popular technology available to improve the reliability of communications through diversity [11]. The deployment of several antenna elements at the transmitter and/or receiver of a communication link enhances wireless communication to an extra dimension in space. This means that the advantages that come with MIMO are very similar to the benefits we have with two ears instead of a single ear, which allow us to distinguish sounds from different directions. It means that the technique allows exploiting the directivity of the signal as an extra dimension of resource on top of bandwidth in wireless communications systems. This exactly is the reason for considering MIMO as the most prominent technology for the present cellular mobile communication standards, known as Long Term Evolution (LTE) and LTE advanced [91]. For future 5th generation mobile communications, we are still seeking solutions for keeping pace with the ever-increasing demand and for higher and

higher data rates in a more and more connected world of already today and even more on tomorrow. Here lies the relevance of massive MIMO, which is MIMO with very large number of antennas, 100s to 1000s, at the BS transmitters. Obviously, this will change the shape of future antennas dramatically [97].

When the number of antennas M in a massive MIMO system increases, several interesting and useful things began to happen in the communication system. In the following section the key advantages of massive MIMO system are analyzed one after another.

5.1.1 Advantageous of Massive MIMO

Huge increase in the data capacity: Massive MIMO increases the data rate to a large extent because of the large number of antennas. Each antenna can send out independent data streams and more number of terminals can be served simultaneously giving full band width to each terminal. It can increase the capacity to 10 times or more because of the spatial multiplexing used. If an independent and identically distributed Gaussian signal is considered at the transmitter, then assuming perfect channel state information at the receiver we can write the expression for capacity as

$$C = \log_2 \det(I + \frac{p_t}{N_o} HH^H) \text{ bits/sec/Hz} \quad (5.1)$$

where I is the identity covariance matrix of the Gaussian noise, P_t is the transmitted power, N_o is the noise power, and the propagation coefficients in the channel matrix are normalized as $Tr[HH^H] \approx MK$. where M is the number of BS antennas and K is the number of users [98]. Theoretically, the capacity of a MU-MIMO system increases

with the $\min(M, K)$. When both M and K in a system becomes very large the rank of HH^H grows and provides a large increase in the sum rate capacity [99].

High energy efficiency: The huge increase in the energy efficiency of massive MIMO is made possible by the fact that with the use of very large number of antennas energy can be focused with extreme sharpness into very narrow regions in space. The underpinning theory is the coherent superposition of different wavefronts by proper spacing of antennas and shaping of signals sent out by the antennas [100]. The BS can make sure that the all such wavefronts collectively sent out from the antennas sum up constructively at the exact places of the intended mobile users, and randomly (destructively) at almost all other places. Interferences among such narrow-focused beams will be at minimum and it can further suppressed by using proper precoding techniques. Studies have proved that a properly designed massive MIMO can provide energy efficiency up to 100 times better than normal MIMO.

High reliability: The receivers of the massive MIMO system are provided with multiple copies of the transmitted signal by multiple antennas. As a result, the probability of deep fade in any of the transmitted information signal is drastically reduced. This improvement in the quality and reliability of wireless link is achieved through the spatial diversity gain [101].

Enhanced physical security: The large array gain and the nearly orthogonal channels from BS to UEs provides a dramatic increase in the physical layer security against passive eaves dropping in massive

MIMO systems without the use of any formal crypto systems [102].

Needs only low power inexpensive components: Massive MIMO can be built with inexpensive, low power components because the expensive ultra linear 50W amplifiers used with conventional systems are replaced by hundreds of low power amplifiers of mW range [103]. Massive MIMO decreases the restrictions on linearity and accuracy of individual amplifier and radio frequency chain. It needs only very low complexity linear signal processing methods. Another key property of Massive MIMO is channel hardening. Under some conditions, when the number of BS antennas is large, the channel becomes (nearly) deterministic and hence, the effect of small-scale fading is averaged out. The system scheduling, power control, etc., can be done over the large-scale fading time scale instead of over the small-scale fading time scale. This simplifies the signal processing significantly [104].

Reduced inter-user interference: When the number of antennas in the array increases, the corresponding channel vectors of the terminals asymptotically become mutually orthogonal [89]. This ensures concurrent reception and coherent combining of the signals to the area where UEs are located, also gives reduced inter-user interference and thereby an increase in the received SNR.

Simplified multiple access: Massive MIMO simplifies the multiple access layer because the channel hardens, so that frequency domain scheduling no longer pays off and also each terminal can be given with the full bandwidth, which renders most of the physical layer control signaling redundant [105].

Other advantages: In addition to the advantages listed above, massive MIMO also offers significant reduction of latency on the air interface, increases the robustness to intentional jamming because it offers many excess degrees of freedom that can be used to cancel signals from intentional jammers. The same advantage which makes the massive MIMO dominant over fading also makes it robust against the failure of one or few antennas [89].

5.1.2 Challenges and Limitations of Massive MIMO

There are many issues and challenges associated with massive MIMO discussed in literature which needs more research and refinement. The important ones are listed below.

Pilot contamination: TDD mode of operation is assumed in massive MIMO for facilitating channel estimation by using pilots transmitted by users during the uplink time slots. The pilot sequences sent by the UEs in the cell and adjacent cells must be orthogonal for BSs to correctly estimate channel vectors of their users [98]. The possible number of available orthogonal pilots is always limited by the channel coherence time and delay spread [89]. Therefore, in order to accommodate large number of users, non-orthogonal pilot sequences are used in the adjacent cells and as a result the estimated channel vector in a given cell will become correlated with the non-orthogonal pilot sequences of the adjacent cells. The negative effects of the above-mentioned pilot reuse are called as pilot contamination [97]

High signal processing complexity: Massive MIMO uses a very large number of antennas and it requires complex signal processing for proper shaping of the signals and multiplexing of UEs.

It is also sensitive to beam alignment because exceptionally narrower beam is used which is highly sensitive to mobility of UEs [106].

Channel reciprocity: Generally, in massive MIMO channel reciprocity is assumed between downlink and uplink for obtaining CSI at the BSs. This holds good only in narrow band TDD systems but not valid for broad band TDD and FDD systems [107].

Channel estimation: There are two problems associated with the Massive MIMO channel estimation process using pilot signals. First the optimal downlink pilots should be mutually orthogonal between antennas which means that the amount of time-frequency resources needed for downlink pilots scales as the number of antennas. So a massive MIMO system would require up to 100 times more such resources than a conventional system [108]. The second problem is that the number of channel responses that each terminal must estimate is also proportional to the number of base station antennas.

Propagation Models: In massive MIMO models, as the number of BS antennas increases, the distinct user channels are assumed as spatially uncorrelated, but studies conducted using real antennas showed that this assumed orthogonality is not valid with increasing BS antennas [97].

5.1.3 Analysis of the Benefits of Massive MIMO

This section will start with elaborate description of the techniques, step by step, from SISO to massive MIMO which will explore all the foresaid advantages of massive MIMO.

In wireless communication environment, the basic point of interest is on signals and how they must be designed such that they travel most efficiently from the transmitter in a mobile cellular infrastructure to our smartphones and tablet PCs in our hands. For that, we analyze a special feature of the air interface namely MIMO, which refers to the deployment of multiple antenna elements at the transmitters and the receivers of communication links.

The wireless communication link which suffers mainly from the attenuation of the signal strengths and the interference between users. Multiple antenna systems referred to as MIMO are the well-known solutions to these problems and Massive MIMO promises additional advantages over the standard solutions.

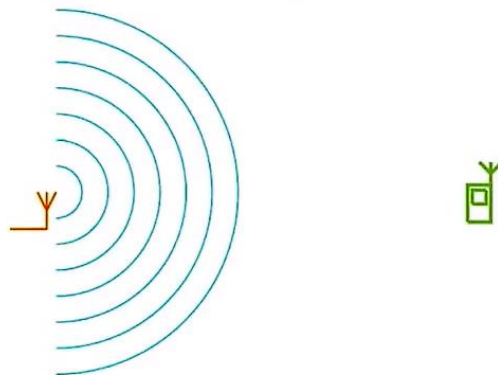


Figure 5.1 SISO communication link

Consider the simple physical wireless channel shown in Fig.5.1 with single transmitter antenna element which is transmitting a signal to a single receiver antenna element. The main issue is the attenuation of the signal in the wireless medium. As shown in Fig. 5.2, if the signal has to travel a couple of kilometers distance from the transmitter to the receiver, the signal experiences a huge attenuation

of about a factor of 100 million which refers to an attenuation of 80 dB. It means that the signal at the receiver is very weak.

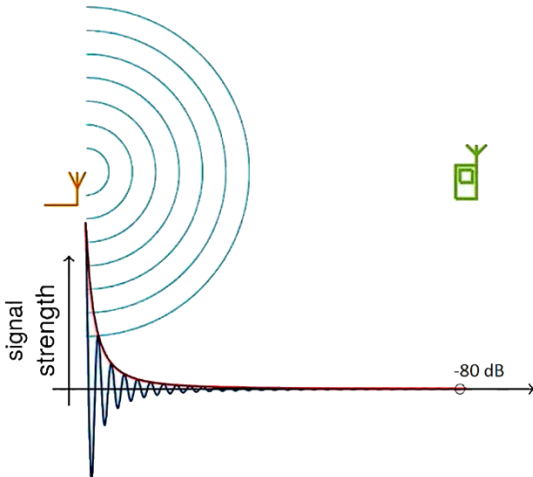


Figure 5.2 *Signal attenuation in wireless medium*

One of the solutions to this high attenuation problem is the deployment of multiple antennas at the transmitter which is multiple input single output antenna system as shown in Fig.5.3(a).

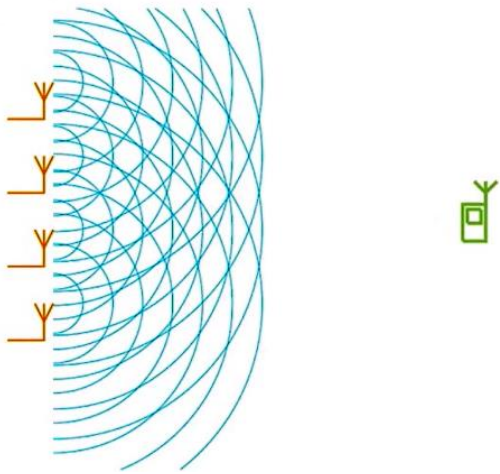


Figure 5.3(a) *Multiple antennas at the transmitter*

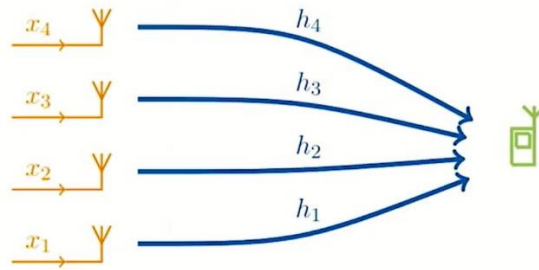


Figure 5.3(b) Multiple antennas at the transmitter with channel coefficients

To analytically analyze this, we will replace this with more abstract illustration shown in Fig.5.3(b). Here each antenna at the transmitter is linked to the antenna at a receiver and characterized by a complex number h_1 h_2 h_3 and h_4 which relates to a so-called baseband representation model. Then the signal at the receiver y can be represented as a linear combination of the transmitted signals x_1 , x_2 , x_3 , and x_4 at the transmitter which arrives at the receiver with linear weights h_1 h_2 h_3 and h_4 which equals the respective channel coefficients.

Then the signal received at the mobile receiver can be expressed as

$$y = \sum_{m=1}^4 h_m x_m + n, \quad \text{where } h_m \in \mathbb{C} \quad (5.2)$$

$$\text{i. e. } y = \sum_{m=1}^4 h_m x_m + n \quad (5.3)$$

$$y = h^T x + n \quad (5.4)$$

In all these models explained above, there is an additional noise term n that refers to any kind of temporal or another kind of noise at the receivers.

Now the question is how to design these transmit signals x_1 , x_2 , x_3 , and x_4 . If we want to transmit a dedicated signal x to the receiver, it can be done by one of the most prominent solutions, called as a matched filter. In a matched filter the coefficients or weight factors w_1 , w_2 , w_3 , and w_4 are made equal to the complex conjugate of the channel coefficients as shown in the equation below

$$w = \frac{h^*}{\|h\|} \quad (5.5)$$

where h^* is the complex conjugate of the channel vector and $\|h\|$ is the length of the channel vector. Then this w is known as the beam forming factor.

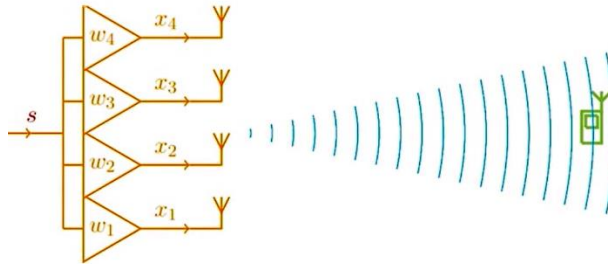


Figure 5.4 Use of matched filter for beam forming

The signals are multiplied before transmission with this weight vectors as shown in Fig. 5.4. Then the received signal in Eqn. 5.3 will become

$$y = \frac{h^T h^*}{\|h\|} s + n = \|h\| s + n \quad (5.6)$$

The matched filter makes the coefficients of the weight factors w_1 , w_2 , w_3 and w_4 equal to the conjugate complex of the channel coefficients. This has the effect that it will be able to concentrate or focus the radiated waveforms in the direction of the receiver and there

is no energy wasted in the direction where no receiver is placed. The respective received signal y is equal to an inner product of the channel vector h^T multiplied with its complex conjugate normalized by the length of the channel vector. This basically means that the received signal is the dedicated signal s with a scaling factor $\|h\|$ which is equal to the length of the channel vector or the norm of the channel vector plus the respective noise component n . Then the SNR which is the ratio between the power of the desired signal over the power of the noise and under certain desired conditions and assumptions this will become proportional to the number of antenna elements M as given in equation below and is called as array gain [109].

$$SNR = \frac{\|h\|^2 \sigma_s^2}{\sigma_n^2} \propto M \quad (5.7)$$

Now we will proceed to the next stage of MIMO which is called as multiuser MIMO. This is called as multi-user communication because communication in a cellular network is not a single show between one base station and one user. All the users want to have communication services by the providers, so to cope with the huge demands of communications in a network, it has been found that it is useful to have multiple receivers served in the same bandwidth and during the same time slot. The problem associated with this technique is that, as shown in Fig. 5.5(a), each receiver not only gets the waveforms which are dedicated to him but also will overhear the signals which are actually meant for the other users and this phenomenon is called interference, which is the second major problem in wireless communications.

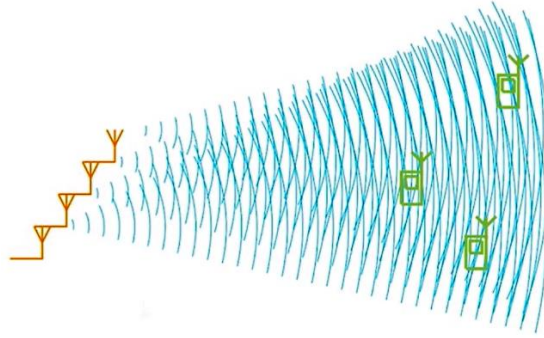


Figure 5.5(a) Multi user MIMO

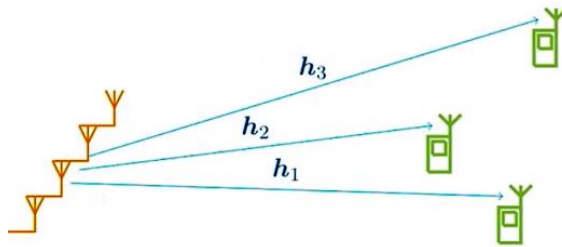


Figure 5.5(b) Multi-user MIMO with channel coefficients

In order to study this in more detail, we consider the detailed illustration by a more mathematical notation for each link (Fig.5.5(b)) from the base station to receivers. The channel vectors are represented as h_1 h_2 h_3 for the receivers 1, 2 and 3, and each channel vector consists of so many channel coefficients as we have n transmit antennas. For the signal model of the above system, the signal received at the receiver i is the inner product of the respective channel vector h_i^T with the compound signal vector x plus an individual noise term at this receiver i . The compound channel vector x is the linear combination of all dedicated signals to all users, because in the shared medium all users share the same bandwidth and the same time slot, multiplied with a beam former which is a matched filter in this case. The signal received by the i^{th} receiver can be expressed as in Eqn.5.8

$$y_i = h_i^T x + n_i, \quad x = \sum_{i=1}^K \frac{h_i}{\|h_i\|} S_i \quad (5.8)$$

In addition to the two terms described above the transmission model shown will have one more term as seen in Eqn.5.9. The first term ($\|h_i\|s_i$) has already been introduced in the single user model, it is the dedicated signal to the user i , which is equal to the signal S_i multiplied by the norm of its the channel vector. The third term is the additive white noise corresponding to each channel n_i . The additional term (second term) is due to the signals which come by the overhearing from the other users. This depends on the inner product of the general channel vector of the user i with the channel vectors of all the other users. If this term does not vanish then the interference in the worst case might even be larger than the useful signal and this obviously will corrupt the signal transmission and may even cause break down of the communication link.

$$y_i = \|h_i\|s_i + \sum_{\substack{j=1 \\ j \neq i}}^K \frac{h_i^T h_j^*}{\|h_j\|} S_j + n_i \quad (5.9)$$

So considering the interference term in the expression for SNR given in Eqn. 5.7 will be modified into signal to interference plus noise ratio and is given by

$$SINR_i = \frac{\|h_i\|^2 \sigma_{s_i}^2}{\sum_{\substack{j=1 \\ j \neq i}}^K \frac{h_i^T h_j^*}{\|h_j\|} \sigma_{s_j}^2 + \sigma_{n_i}^2} \quad (5.10)$$

The additional term appeared in the denominator corresponds to the interference from the signals of other users. This is the major problem to be addressed and solved in multiuser communication. One of the typical solutions is either equalization at the receivers or pre-

equalization at the transmitters. It means that in addition to the use of the simple version of a matched filter at the receiver precoding or pre-equalization at the transmitter end is also used and that makes the process very complicated.

Instead of going through the complicated equalization process at the receiver or pre-equalization process at the transmitter, there exists another solution for interference cancelation, which is nothing but the massive MIMO. In this case, the number of antennas used is huge, about hundreds to thousands at the transmitter and the typical advantage of using multiple transmitter elements is the array gain. It is already learned from Eqn. 5.7 that, under certain conditions the SNR is proportional to the number of antenna elements and by using a huge number of antenna elements a very large SNR can be achieved as shown in Fig. 5.6.

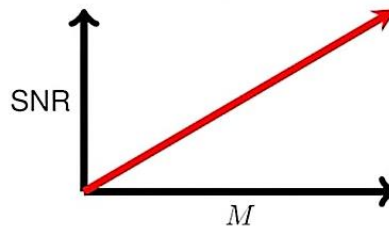


Figure 5.6 Graph showing the SNR increase with M (Array Gain)

But in practice, we get much more than what we explained above as the array gain, which is nothing but the asymptotic orthogonality. i.e. Under certain conditions, when the number of antenna elements is very large, the inner product of two different channel vectors become equal to zero (Eqn. 5.11). To explain that consider the SINR Eqn. 5.10, where the term in the denominator,

$h_i^T h_j^*$ is the major term that accounts the interference from other channels. For massive MIMO this term tends to zero and that in turn reduces the SINR in Eqn. 5.10 to that of SNR in Eqn. 5.7 which has only the normal noise component but no interference component. It also means that by employing massive MIMO, simple beam forming technique can be used, the matched filter, at the receiver side by not taking into account the interference noise. Thus massive MIMO system can afford robust and simple signal processing method at the receiver highly improving the cost and power efficiency of mobile equipment, which is very important in mobile cellular networks.

$$\frac{h_i^H h_j}{M} \rightarrow 0 \quad (5.11)$$

In order to get the full benefits of using a matched filter, the channel weight factors used at the transmitter must be equal to the complex conjugate of the channel coefficients(Eqn. 5.5). In order to do that, before transmission, the transmitter must know the channel coefficients and for that, an uplink training has been proposed as the solution for massive MIMO communication[110]. That means, before the transmitter can send data information to the receiver, the receiver sends some information to the base station on agreement with both the sides and is called as training symbols or pilots (Fig. 5.7). Based on the properties of this received pilot signal, the transmitter can estimate the unknown channel vector h , but like in any other communication, there might be some noise added to the pilot signal which may lead to a corrupted version (\hat{h}) of the original channel vector (h).

$$\hat{h} = h + n \quad (5.12)$$

This noise addition is manageable, but the real problem is while one UE transmits a pilot to the BS, there might be a second user which also wants to have access and get the service from the BS, sends training data to the base station (Fig. 5.8). If the BS is not aware of this, it may take this data as part of the training information sent by the original user and may lead to dramatic effects on the downlink communication.

$$\hat{h} = h + h_I + n \quad (5.13)$$

This effect of corrupting the pilot by interference from other pilots is called as pilot contamination where the interfering part of the channel vector (h_I) contaminates the channel vector (h) of the original user.

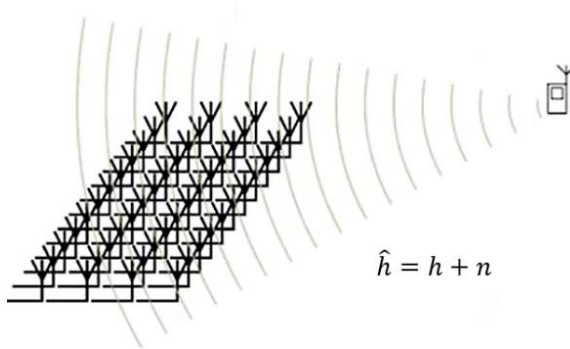


Figure 5.7 Uplink training with no pilot contamination

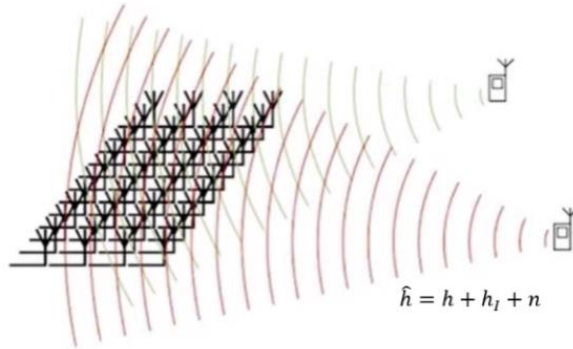


Figure 5.8 Uplink training with pilot contamination

5.2 Literature Survey

In order to understand the heights of the merits provided by the massive MIMO, limiting factors and challenges involved in its implementation, a detailed literature review on all aspects of massive MIMO has been conducted and is inscribed in this section.

5.2.1 General Overview and Tutorials

Massive MIMO was identified as the key technology for the future wireless technology which needs to handle 100s or 1000s of orders of magnitude of more data traffic. This overview section considers the publications that discuss the general aspects and features of massive MIMO.

In Paper [111] E. Björnson et al. throw light into the very common features of massive MIMO and clears all myths that spread around about massive MIMO especially about its data carrying capacity, a number of antennas to be used at the base station, its suitability for millimeter waves frequency bands, beam forming techniques used, etc. It clearly explains with the aid of experimental results why all these myths are not true. It also considers the two

modes, FDD and TDD modes of operation of massive MIMO and analyzed its possible benefits and drawbacks. The linear processing method that must be used at the base station of massive MIMO is also analyzed by the authors. Over all this highlights all the aspects of massive MIMO a new researcher has to look into before starting research and will help a lot to identify the hot areas of research in this field.

E. G. Larsson et al. in Paper [97] clearly highlights all the potentials of massive MIMO which makes it suitable as the backbone transmission technology for the 4G wireless system and the upcoming 5G. Authors explain all the advantages of using massive MIMO for high data rates and at the same time clearly examines many challenges it faces now in order to achieve the full benefits of the envisaged technology. Synchronization of the massive antenna system, achieving a practical distributed processing algorithm, computational complexity are some of them identified by the author to look into by any new researcher.

S. Yang et al. [112] presented an extensive survey of MIMO explaining the MIMO detection fundamentals considering a history of 50 years and then came up with the strategies that used for different large-scale MIMO detectors. They have identified many low complexity linear mimo detectors for obtaining the finest performance in large-scale MIMO receivers. All the analysis has been done by dividing the MIMO into two groups, type-1: where the number of active users is much less than the number of base station antennas and type-2: where the number of active users is comparable with the number of base station antennas.

The efficiency and scalability of decentralized beam forming in massive MIMO system with several hundreds of BS antennas are demonstrated in a general processing unit (GPU) cluster R. Sharan et al. in [113]. Each antenna group achieves the beam forming locally with associated radio frequency elements. The algorithm used here requires only minimum interchange of consensus data among clusters and local channel state information.

S. Chaudhari et al. [114] discuss an entirely new topic of massive MIMO cognitive radio networks with an objective to support a maximum number of secondary users in the downlink transmission. The system model is designed with secondary base stations where several simultaneous secondary users exist along with primary users. Optimization for maximizing the number of secondary users in downlink data transmission from the secondary base station in the cognitive radio network is carried out by using a three-step algorithm. Results have shown that equal power and equal rate schemes perform on a comparable scale if the number of secondary user equipment is less.

The security aspects of massive MIMO communication link has been analyzed by B. Chen et al. in [115]. Physical layer security feature called as original symbol phase rotation (OSPR) is employed in massive MIMO system to protect legitimate transmitters from eavesdropping. They have proposed a secure massive MIMO system with sufficiently large but finite number of base station antennas, tested its security performance and showed that it could achieve a considerable level of security against eavesdropping even with an unlimited number of base station antennas. The authors suggested the

proposed scheme as a good candidate for secure and green communications.

A novel data transmission and signal detection approach for single input multiple output (SIMO) communication system was proposed by T. Bogale et al. in [116]. The proposed method uses a bandwidth of B and a wireless channel with L multipath channels and thereby an improved data rate has been achieved compared to the existing OFDM systems. The performance has been evaluated through theoretical approach as well as through simulation.

Secure communication in massive MIMO Rician channels using artificial noise assisted jamming in a transmitter deployed with very large antenna array was designed and analyzed by J. Wang et al. in [117]. They proved that uniform jamming is more useful, compared to directional jamming, in reducing the security outage probability when the distance from the eavesdropper to the user is less than a threshold. Secure transmission in Multi-user and multi-cell scenarios of massive MIMO are also discussed in this paper.

The uplink transmission of a massive MIMO multi-user system is studied extensively under the presence of a smart jammer by H. Pirzadeh et al. in [118]. The jammer was aimed at degrading the total spectral efficiency of the genuine system by confronting the transmissions both in the training phase as well as in the data transmission phase. The work demonstrated that the jammer causes pilot contamination and thereby enforce severe damage to the total spectral efficiency of the genuine system.

H. Q. Ngo et al. [119] designed a communication relay system in multi-pair full duplex mode. The relay system is deployed with massive antenna arrays whereas each of the transmitting and receiving nodes is having a single antenna. They were successful in proving that the use of massive antenna arrays at the relay station can multiply the spectral efficiency even up to two times the number of active communicating pairs in the system. Paper also suggested a power allocation pattern for the system which selects optimum power for the individual nodes as well as for the relay station in order to maximize the energy efficiency for given value of spectral efficiency and peak power. With this method, the energy efficiency has been significantly improved for the above system.

Kien T. Truong et al. in [120] analyzed the distributed antenna structure for improving the sum rate compared with true centralized architecture. It also demonstrated the difference in performance between the precoding schemes of MRC and MMSE. User clustering was also experimented and showed that great performance improvement could be achieved through this method.

Two efficient methods to improve the energy efficiency of a cellular communication system without compromising the quality of service parameters are deeply investigated by Emil Bjornson et al. in [93]. The first method is by employing large antenna arrays on the existing base stations of the cellular system and thereby providing accurate focusing of the full transmitted energy to the actual users. The second method is by employing small cell access points to send the data traffic from base stations thereby ensuring most of the data traffic localized. They experimentally showed that the total energy

efficiency could be significantly improved by combining small cells and massive MIMO.

Time division duplex based massive MIMO network architecture is over laid with small cells and two duplexing schemes, TDD and reverse TDD, are experimented by Kianoush Hosseini in [121]. The BS "sacrifices" some of its antennas for interference cancellation while the TDD protocol allows for implicit coordination across both tiers. Simulation results show that, given a sufficiently large number of BS antennas, the proposed scheme can significantly improve the sum-rate of the SC tier at the price of a small macro performance loss.

Zhengzheng Xiang et al. in [122] investigated cellular network with massive MIMO system under a multicast transmission environment. A multicast beam former is first designed with perfect CSI. Second, an imperfect CSI scenario using conventional channel state estimation method considering the effect of pilot contamination is considered. Third, they proposed a new pilot allocation scheme for this multi-cell multi casting system to mitigate the pilot contamination effects. Numerical results were obtained for all the three configurations and verified with simulation. Results proved the effectiveness of the proposed scheme for completely removing the effect of pilot contamination and improve the sum rate.

The possibility of making the downlink communication channel in a multicell cell massive MIMO system secure under the presence of an eavesdropper was investigated by Jun Zhu et al. in [123]. They used artificial noise generation with matched filter precoding at the

base station of the cells to block the eavesdropper who tries to intercept a genuine user through a passive multi-antenna system. They evaluated the ergodic secrecy rate and the probability of secrecy outage for different cases of training and pilot contamination. It has been identified that secure communication is not possible if the number of BS antennas used by the eavesdropper is too large and in the presence of pilot contamination the secrecy rate cannot be increased directly with the increase in the number of BS antennas.

The concept of clustering user terminals in a single cell mobile network environment with uniform linear antenna array at the base station was studied by Qiang He et al. [124]. An entirely different method is adopted here to combine the multi-user MIMO with sectorization. Each of the sectors is covered by several RF beams of similar directional characteristics. The proposed method of sectorization was giving a greatly improved sum rate in comparison with a normal massive MIMO system.

Callum T. Neil et al. in [125] examined some practical deployment problems faced by massive MIMO systems. This paper explored the impact of various antenna topologies in spatial correlation and MIMO performance. They also demonstrated that an antenna array distributed into different clusters could reduce the spatial correlation and improve system performance to a great extent.

Italo Atzeni in [126] discussed the effect of pilot contamination and proposed a novel method to mitigate the effect of the same in massive MIMO systems. User terminals close to their respective base stations are allotted with the same pilots and the improvement

regarding the spectral efficiency is evaluated analytically as well as through simulations.

In [127] Feng Jiang et al. were tried to use the massive MIMO technology in a wireless sensor network considering the fusion center as equivalent to the BS with a large number of antennas and wireless channels between the fusion center and sensor nodes. Results are validated through simulations, and significant performance improvements are observed compared to the single antenna at the fusion center.

Peter J. Smith et al. [128] analyzed a distributed massive MIMO specifically for the per-user signal-to-interference-plus-noise-ratio (SINR) as the number of antenna elements becomes large. They developed a system model for the above with distributed transmit antennas and analyzed the impact of the number of antenna clusters on spatial correlation and the per-user SINR.

Practical restrictions in user association of a massive MIMO TDD system, both in a centralized scheme as well as in distributed scheme, was analyzed by Yi Xu. Eta al [129]. Optimal algorithms were developed, and the efficiency of proposed system was verified through simulation.

In [130] João S. Lemos et al. designed a communication relay system with large antenna arrays on both at the receiver side and at the transmitter side. These arrays are used for suppressing the loop back interference in the system. It was assumed to have an imperfect channel state information available at the relay center and used MMSE filters to suppress the interference. Performance evaluation

was done through simulation by calculating the bit error rate and energy efficiency both at the relay station and at the receiver.

A massive MIMO system with a goal of minimizing the total transmitted power across all the base stations was designed by Subhash Lakshmi Narayana et al. in [131]. They framed a multicell beam forming scheme which needs only less amount of data exchange among the different base stations. The transmitted power is minimized keeping the constraint in user terminals signal to interference noise ratio. Results are evaluated through simulations and showed that designed scheme satisfies the users SINR constraints achieving minimum transmit power in the massive MIMO system.

Distributed beam forming for a common group of user terminals in a massive MIMO base station deployed with large antenna arrays was studied by Jinho Choi in [132] and investigated the effect of spatial correlation on the system performance. The approach used here is that each base station forms a radio beam without any cooperation with other base stations. The performance was evaluated through simulations and found that the distributed power allocation performs better than that of joint power allocation scheme when the signal to interference noise ratio is not too large.

Physical layer security for ensuring safe data transmission in a massive MIMO downlink communication system was designed in [133] by Y. Ozan Basciftci. They introduced a new beam forming strategy which can provide information security without the use of special encoding techniques for transmission. Counter methods to

stop jamming of pilot signals at the base station by the eavesdropper were also developed and tested through simulations.

In [134] Dževdan K et al. discussed the opportunities and challenges of integrating physical layer security with Massive MIMO systems. They first demonstrated that the Massive MIMO which in itself is robust against passive Eavesdropping attacks. Then they reviewed the pilot contamination that actively attacks the channel estimation process. This contamination of pilot attack not only drastically reduces the achievable secret capacity, but also its detection is very difficult. It is then proceeded by examining some methods from the literature that detect active attacks in massive MIMO. Finally, this article surveyed research problems that are open and most important to address in the future and also some promising research directions are given to solve them.

Jesper H. Sørensen et al. in [135] presented the pilot contamination problem in crowded scenarios of massive MIMO where users within a single cell must share a small set of pilot sequences. Intracellular pilot contamination is considered as a random-access problem and explained the recent developments in this area of research. Settings in massive MIMO provides two essential properties; almost orthogonality between user channels and highly stable channel powers. The proposed solution is highly efficient, easily surpassing the conventional approach of ALOHA random access, but the main drawback was higher error rate due to the accumulation of errors in the algorithm. However, this disadvantage is shown to be significantly reduced when the number of antennas at the base station is considerably increased.

MIMO performance in a Cell-free Massive MIMO was analyzed by considering the effects of the channel estimation by Hien Quoc Ngo et al. in [136]. They also compared the performance of cell-free massive MIMO systems to the small cell systems in massive MIMO. The results showed that the cell-free systems could give greatly improved throughput compared to that of small cell systems in terms of performance. Furthermore, the cell-free massive MIMO systems are found more robust under fading channel environment compared to small cell systems.

Researches carried out about the general aspects of massive MIMO system are studied here. The myths and misconceptions about massive MIMO has been cleared. The advantageous, disadvantageous, the fundamental challenges faced on implementing the massive MIMO, scalability and security features etc. are also covered.

5.2.2 Capacity and Fundamental Features of Massive MIMO

Everyone needs higher speeds on their mobile phones and other gadgets, to get that we need networks with more data capacity. But with limited spectrum how come operators can increase the capacity. MIMO and beam forming can deliver high throughput and increase network capacity. Here in this section we will see the studies carried out in increasing the capacity limits of massive MIMO and associated changes in the fundamental features of the network.

A massive MIMO system with spatial common sparsity both in phase domain and time domain was studied by Zhen Gao, et al. in [137] and investigated the capacity and propagation conditions of the

system over genuine sparse channels. The relationship between sparse massive MIMO channel and massive MIMO OFDM systems are well illustrated in their study and proved that spatial common sparsity could provide highly positive propagation conditions in massive MIMO systems.

In [138] Thomas L. Marzetta theoretically analyzed and studied all the favorable and unfavorable effects of increasing the number of antennas at the base station of a cellular mobile system. He found that even when the channel estimate is very noisy, the system can give a satisfactory performance by adding more and more antennas to the base station. All the adverse effects of uncorrelated noise and fast fading channels disappeared completely when the limit of transmitting base station antennas is increased to infinity. The only problem that remained was the inter-cell interference caused due to the reuse of the same pilot sequences in adjacent cells.

Hien Quoc Ngo et al. [94] theoretically derived the expressions for energy efficiency and spectral efficiency of very large multi-user massive MIMO systems and experimentally verified that through simulations. They demonstrated that all the advantages of massive MIMO system could be achieved by using very simple linear processing schemes such as maximum ratio combining and zero forcing at the base stations. The only issue that adversely affected the performance and remains unsolved was the pilot contamination.

A multiple input single output (MISO) system with a base station having a large number of antennas compared to the active mobile nodes was studied by Antonios Pitarokoilis et al. in [139].

Frequency selective Gaussian broadcast channel was assumed, and single carrier modulation scheme was used instead of OFDM. This eliminated the problems of large peak to average ratio and improved the power efficiency to a great extent.

Right from the beginning of massive MIMO concept for cellular mobile communication to till date researchers are working hard to trace out the adverse effects of pilot contamination. Ralf R. M^uller et al. in [140] suggested a highly practical algorithm with the complexity of polynomials for mitigating the effects of pilot contamination. It was analyzed by using random matrix theory, and probability theory and results are verified through simulations.

Enhanced network architecture with TDD was suggested for massive MIMO systems by H. Huh et al. in [141]. The design was aimed at reducing the number of base station antennas to 10 times less than its normal numbers in massive MIMO and at the same time provide comparable spectral efficiency with the normal system. The key concept used for achieving the same was clustering the user nodes to different equivalence classes and develop a scheduler to handle the channel frequency and time to different classes.

Performance of the two very widely used precoders for massive MIMO cellular system. Conjugate beam forming, and zero forcing was compared in terms of its spectral efficiency and energy efficiency by Hong Yang et al. in [142]. Conjugate beam forming was suggested compared to zero-forcing because of its superior robustness and decentralized architecture, but looking at the spectral-efficiency

performance zero-forcing works considerably better compared to conjugate beam forming.

In [143] Ayfer Ozgur et al. evaluated how the data transmission capacity of a distributed MIMO transmission system varies with the number of active cooperating user terminals, the area of each group and the distance among them. All these are considered in a line of sight environment, and these results are used to find out whether distributed MIMO can give considerable data capacity improvement compared with old ad-hoc network system with a large number of individual randomly distributed sender-receiver pairs.

A multi-cell time division duplex massive MIMO system was analyzed for pilot contamination and its adverse effects on deteriorating the channel state information by Jubin Jose et al. in [144]. They were also developed a multi-cell MMSE based precoding scheme that greatly alleviates the effects of pilot contamination. Their approach was not requiring any coordination among the base stations, and it was giving significant improvement over many of the other popular precoding schemes.

The use of filter bank multi carrier communication in massive MIMO systems was introduced by Arman Farhang et al. in [145]. Cosine modulated multi-tone communication was selected as the most suitable choice for the multicarrier system. High flexibility, improved bandwidth efficiency, large spacing over subcarriers, use of blind channel equalization, low peak to average power ratio and low carrier frequency offset were the advantages identified for the proposed system.

A practical Massive MIMO system with space-constrained antenna topology was designed and evaluated by Christos Masouros et al. in [146]. Here when the number of antenna elements is increased within the limited space, it enforces an inversely proportional reduction in the distance between the antennas which indicates that the interference between users does not disappear in the massive MIMO system. They demonstrated that inter-user interference converges smoothly to zero for physically unconstrained antenna arrays.

Works carried out in the areas of the data carrying capacity, energy efficiency, beam forming, antenna spacing constraints etc. of the massive MIMO systems are analyzed. In all these areas massive MIMO performs better but there exist a lot of challenges and limitations to be addressed for getting the optimum performance envisioned for massive MIMO.

5.2.3 CSI Acquisition and Related Aspects

Availability of high precision channel state information is very critical in achieving the promising capacity and other performance gains of massive MIMO, and that too must be done without having many additional overheads. Different ways to achieve this are analyzed here in this section.

A blind channel state estimation algorithm to determine the effective channel gain at each active user terminal without using any pilots in the downlink was proposed by Hien Quoc Ngo in [147]. Massive MIMO system with TDD architecture was considered, and each base station obtains the CSI through uplink pilot signals sent by

the user terminals. The proposed method considerably overperformed most of the conventional methods that approximate the channel gains by their schemes.

Pilot contaminations that are resulted from the reuse of pilots are found as one of the major performance bottle necks for massive MIMO systems. A novel algorithm mitigating this pilot contamination problem was designed by Yonghee Han et al. in [148]. The new pilot design with arbitrary length based on alternating minimization approach was used and tested using simulations. The main attraction of the approach was the flexibility in designing the pilot sequences for maximizing the spectral efficiency.

Channel state information used at the transmitter side takes the main role in accomplishing the important benefits of massive MIMO systems. In [149] a projection based differential feedback protocol was proposed for frequency division duplex based systems by Yonghee Han et al. for estimating the required CSI. Proposed design significantly reduced the complexity and amount of encoding at the transmitter side and achieved greater throughput improvement with less amount of channel feedback.

A distributed channel estimation algorithm for the channel state estimation of correlated Rayleigh fading channels was developed by Alam Zaib et al. in [150]. It was using a novel distributed Linear Minimum Mean Square Error(LMMSE) algorithm. They also analyzed the effects of pilot contamination on the performance variation of mean square error (MSE) under different CSI acquiring techniques. The results were validated through simulations.

A massive MIMO communication system with intermittent terminal activity was considered in [151] by Elisabeth de Carvalho et al. Here the main problem in consideration was the intra-cell pilot contamination rather than inter-cell pilot contamination in normal massive MIMO systems. Authors proposed a random access method for pilot allocation which can easily reduce the effect of intra-cell pilot contamination to a great extent.

In [152] X. Zhu et al. proposed a novel scheme for pilot allocation based on graph coloring. An interference graph is first created, then the algorithm efficiently allocates pilots among user terminals in the graph. The improvement in the spectral efficiency has been verified through simulations.

Spatial correlation among antennas in the base station are exploited for reducing the feedback overhead in the FDD based massive MIMO system explained by L. Byungju in [153]. Well organized antenna grouping methods are utilized to map different correlated antennas to one representative unit and a little portion of the feedback resources is used to represent the grouping pattern. The number of bits required for CSI feedback is considerably reduced. The proposed method is found very suitable for integration into the dual code book structure of LTE advanced.

In massive MIMO pilot contamination attacks can happen during the training phase when an attacker sends correlated pilot (training) signal as that of the genuine user. This spoils the channel estimation process and successful precoder/beam former design aiding the eavesdropper. J K. Tugnait in [154] proposed a solution for

the above problem by random sequence super imposing on the pilot sequence of the genuine user which permits the use source enumeration schemes to identify the pilot contamination attacks. Proposed method was analyzed and its contamination attack identification performance was demonstrated through simulations.

A novel scheme to acquire channel state information at each user terminal beam forming training was designed and analyzed by Ngo et al. in [103]. Unlike the conventional method of sending long pilot sequences, whose length is related to the number of base station antennas, here a short pilot sequence is beamformed to each user for estimating the real channel gain. The advantage of this method is that the estimation overhead only depends on the number of active user terminals. Numerical results are derived assuming Maximum ratio combining and zero forcing methods of precoding and are verified using simulations. Results showed that the proposed method performs well when the user node mobility is moderate or minimum.

An extremely efficient channel quantization method for massive MIMO systems using minimum feedback for beam forming was proposed by Junil Choi in [155]. The proposed method uses noncoherent sequence detection duality with source encoding. The encoding techniques used were non-coherent trellis coded quantization where the complexity of coding increases with the number of base station antennas. Monte Carlo simulations were carried out to demonstrate the validity of the proposed method.

Successive channel estimation frame work at the user terminals using the open loop and closed loop training methods for FDD

massive MIMO systems was proposed by Junil Choi et al. in [156]. Closed loop training requires only low amount of feedback by the user terminal, and under low SNR condition, it gives better performance in terms of the spectral efficiency of the system.

Pilot contamination occurs when user terminals concurrently transmit nonorthogonal pilot sequences to the base station, Fabio Fernandes et al. in [157] proposed a practical scheme to eliminate such concurrent transmissions from user terminals of adjacent cells. They also analyzed the effects of power allocation in the interference limited environment and proved that combining these two methods would give a performance improvement in rate gains by a factor 18 compared to the normal system.

The practical impairment happening to massive MIMO uplink and downlink system due to Channel aging was addressed by Kien T. Truong et al. in [158]. They numerically evaluated the aging effects using accurate parameters, and by using simulation, they demonstrated how aging degrades the performance in terms of spectral efficiency. They showed that this degradation could be overcome to a great extent by the use of temporal correlation of the channel.

Particle swarm optimization (PSO) is a computational method that optimizes a problem by iteratively trying to improve a candidate solution with regard to a given measure of quality. Christopher Knievel et al. in [159] and Christopher Knievel in [160] used an extension of this PSO algorithm called as corporative PSO for estimation of MIMO channel. The paper discussed the overall

complexity of the algorithm and compared the obtained results with the normal method of minimum mean square error estimator using Monte Carlo simulations.

A coordinated approach for massive MIMO channel estimation was discussed by Haifan Yin et al. in [161]. They first established a channel estimation method using the Bayesian approximation which explicitly uses the covariance statistics in the inter-cell interference environment. Then a new pilot assignment plan which carefully selects a group of user terminals for assigning correlated pilot sequences is also tested. Results showed that the proposed method was almost completely removing the deteriorating effects of pilot contamination.

A novel channel estimation and pilot optimization algorithm for massive MIMO downlink system was proposed by T.E Bogale et al. in [162]. First, the channel estimation problem was converted to a weighted sum mean square error minimization problem carrying new variables and pilot symbols. The newly introduced variables are then optimized using minimum mean square error algorithm, and Rayleigh quotient approaches. Pilot sequences of all mobile stations are optimized by using this simple iterative algorithm. The proposed algorithm was tested through simulation and found that it is superior in term of mean square error to that of normal semi orthogonal pilot symbols and minimum mean square channel estimation.

Channel estimation and associated issues are of very important topic for research in wireless communication area. Studies carried out in this area discussed the effective models for massive mimo system

and channel. The signal processing used for channel estimation on the basis of uplink (UL) pilots are well analyzed. Many new techniques and algorithms for channel estimation are also introduced and evaluated.

5.2.4 Receiver Detection Algorithms

Massive MIMO technology is envisaged mainly to use with mobile devices, and low complexity signal detection algorithms are of prime importance to provide better bit error rate performance at very high data rates and high mobility environments. One of the challenges in the design of large-scale multiuser MIMO-OFDM systems is developing low-complexity detection algorithms. Studies carried out to support the above-mentioned fact are examined under this heading.

Optimal Data detection algorithms for massive MIMO systems with a large number of antennas at the transmit and receive side are normally associated with excessive computational complexity. Most of the methods available in the literature for reducing this computation complexity are sub optimal in nature. A novel and optimal data detection algorithm based on approximate message passing was proposed in [163] by Charles Jeon et al. Here the noisy communication channel of the MIMO system is decoupled into a number of unconstrained additive Gaussian white noise with the same SNR and then the approximate message passing algorithm is used to trace the actual noise variance of all decoupled Gaussian channels in each iteration. Simulations showed that the algorithm performs optimally in all genuine systems with finite dimensions.

A low precision but optimum detector with minimum computation complexity was developed by Ali J. Al-Asker et al. in [164]. They used different disintegration schemes for the design of linear detectors with user-defined precision and fixed-point arithmetic was used for simulating its hardware implementation. Simulation results showed that performance of the disintegration schemes is greatly improved compared to other schemes of detection.

Three low complexity data detection algorithms for massive MIMO communication system using artificial intelligence giving near-optimal performance published in literature were investigated and analyzed by A. Chockalingam in [165]. These three algorithms were belief propagation based message passing algorithm and two local neighborhood search based algorithms, known as likelihood ascent search and reactive tabu search algorithms. A comparison study is made on the basis of their computational complexity and bit error rate performance under different network environments. Results showed that no one could claim any advantage over other as each one has got its own merits and demerits depending on the different network environments,

Lattice reduction algorithms are now commonly used in many applications in computation and mathematics. An element-based lattice reduction algorithm for massive MIMO detection was formulated by Q. Zhou et al. in [166]. The main aim of the proposed algorithm was to minimize the diagonal components of the covariance matrix for noise and thereby minimizing the orthogonality issues of the original channel matrix. Results were analyzed through simulations and showed that the proposed algorithm was giving

significant performance improvement in bit error rate compared to most of the low complexity detectors while maintaining low complexity.

A range of approximate message passing algorithms with very low computational complexity are designed and analyzed in [167] by Sheng Wu et al. Message passing algorithms are represented over the factor graph, and by using of the minimum Kullback-Leibler (KL) divergence criterion, messages of massive multiuser MIMO are approximated with continuous Gaussian messages. After approximation, numerous signal processing methods are used to attain a low complexity near-optimal performance. First, the principle of expectation propagation is employed to compute the approximate Gaussian messages, where the symbol belief is approximated by a Gaussian distribution, and then the approximate message is calculated from the Gaussian approximate belief. Results are verified through simulations and found that the proposed AMP algorithms are superior with many existing complex algorithms.

A high bandwidth data detection algorithm was designed and first developed its VLSI design for a single carrier FDMA based large scale MIMO system by Michael Wu et al. in [168]. A new approximate matrix inversion scheme which minimizes the computational complexity for linear data detection was developed. The detector circuit selection was done on the basis of the ratio between BS antennas and number of user terminals. The VLSI architecture was then developed and implemented using Xilinx FPGA and showed that it could reach up to 600Mbps with 128 BS antennas.

An optimum minimum mean square error detection and matched filter detection algorithms, for a single carrier frequency division equalization multi-user MIMO with very large antennas, were developed and studied by Paulo Torres et al. in [169]. Results were analyzed through simulations and showed that the proposed algorithm was giving significant performance improvement in bit error rate compared to most of the low complexity detectors while maintaining low complexity.

Receiver data detection algorithms used for cellular wireless communication systems must be of low complexity, high energy efficiency and highly economic as it is meant for the user mobile equipment. Precision, computational complexity and simplicity in implementation are the main features analyzed, in the works discussed here, for optimizing the detector performance.

5.2.5 Precoding Algorithms for Downlink.

The practical issues of having uncertain channel knowledge, high propagation losses and implementing optimal nonlinear precoding are solved more-or-less automatically by enlarging system dimensions. The beauty of massive MIMO technology is that it provides numerous advantages with very low complexity linear signal processing methods. It makes use of simple and linear precoding algorithms and a detailed literature study available in this area is described here.

A fully functional massive MIMO communication system that combats inter-cell interference and permits the use of effective hybrid analog/digital network architectures was designed and tested through

simulations by Ahmed Alkhateeb et al. in [170]. An explicit multi-layer precoding that crumbles the precoding matrix of each base station into the product of three separate precoding matrices is designed. These separate matrices are called as layers, which are correctly planned to suppress any inter-cell interference and intra cell multi-user interferences. It also ensures maximum signal power at the receiving node and less channel training overhead. The designed multi-layer precoding model is evaluated by simultaneous, and the results showed considerable data rate and signal coverage improvement compared to the existing single layered architectures.

A low complexity constant envelope precoding algorithm suitable for frequency selective massive MIMO channels was proposed by S. K. Mohammed et al. in [171]. The system was designed for a multi-user environment with base stations equipped with nonlinear power amplifiers. A joint optimization of constant envelop signals was made from samples of consecutive time instances. The total power required per antenna under this constant envelop design was about 1db less compared with that of the conventional systems. Simulations also showed that both in the total transmit power environment and constant envelope environment the required total transmit power from all the antennas of a base station reduces by 3db when the number of antennas at the base station is doubled.

Potential performance of a massive MIMO system with MMSE decoding used at the receiver was evaluated in [172] by Cédric Artigue et al. Here each sequence of symbols is approximated by wiener filters before the actual decoding. The channel state information is made available at the receiver side, and 2nd order

statistics of the channels is made available at the transmitter side of the system. Numerical experiments on the proposed precoder proved that the algorithm is computationally very light and at the same time it maximizes the ergodic mutual information.

A Gaussian MIMO communication system with vector precoding which makes use of "replica method" in statistical physics for its analysis was developed and analyzed by Benjamin M. Zaidel et al. in [173]. Here the transmit station includes a linear front end along with nonlinear precoding system which minimizes the transmitting energy by means of the technique called as "input alphabet relaxation". Performance of the aforementioned precoding method was evaluated through simulations and compared with linear ZF and Tomlinson–Harashima Precoding (THP) methods found significant improvement in spectral efficiency.

A linear Hermitian precoding technique for a distributed massive MIMO system was proposed by Jianwen Zhang et al. in [174]. In a distributed system number of transmitters will be jointly serving a single receiving node and, in such systems,, it is very difficult to get the full channel state information at the transmitters and hence a new strategy of designing systems with partial channel state information at the transmitter(CSIT) was used in the proposed method. The linear Hermitian precoding scheme used here transforms the individual channels into a Hermitian matrix form. They analytically proved that the proposed scheme provides an efficient precoding solution for distributive environment giving maximum capacity in terms of achievable data rates and also it reduces the overhead in obtaining the CSI in distributed MIMO systems.

A linear dual structured multi user precoding scheme for a multi user multi polarized massive MIMO system was proposed by Jaelyn Park et al. in [175]. A MIMO model with large number of multi-polarized antenna elements at the base station was first developed, a dual structured precoding algorithm was then developed for minimizing the feedback overhead for acquiring the CSI. The switching between the dual modes of precoding was done on the basis of the spatial grouping of the mobile stations which are, i) preprocessing based on spatial correlation and ii) the preprocessing based on spatial correlation as well as polarization. The evaluation of the proposed scheme showed a significant reduction in the feedback overhead along with improvement in the sum rate.

A collection of new computationally low complex linear precoding algorithms for a single cell multi user massive MIMO downlink system was proposed by Axel M^uller et al. in [176] and [177]. They used different reduced rank filtering schemes working on the truncated polynomial expansion (TPE) concept. TPE ensures a smooth balancing of the total system through the complexity of precoding. Analytical expressions are derived for the achievable rates and experimentally verified the same. The TPE decoding showed many advantages like the elimination of the need for computing the precoding matrix in advance, reduced delay in transmission of the first symbol, and is more suitable for real-time hardware implementation.

A survey of different precoding algorithms and its performance evaluation under massive MIMO environment is carried out. The main aspect that is considered for the design of precoders is the

ability to minimize and manage different kinds of interferences. Reasons for selecting linear precoding schemes for massive MIMO and its benefits are also well investigated.

5.2.6 Channel Modeling and Measurements

Channel models of any communication system represent the propagation characteristics of RF signals in radio environments and are very important for assessing the performances of wireless communication systems. The state of art concepts in channel models for massive MIMO is investigated in this section.

The channel behavior of a massive MIMO under actual practical situations was thoroughly investigated in the paper [178] by Xiang Gao et al. The studies were made at outdoor to outdoor channel measurements using uniform cylindrical antenna array(UCA) and uniform linear antenna array(ULA). Three representative wireless channel conditions i) closely located to the base station and with line-of-sight (LOS) antennas ii) closely located to the base station and with non-line-of-sight (NLOS) antennas and iii) located far away from the base station. Studies illustrated that massive MIMO gives enhanced orthogonality among the channels assigned to different mobile users and improved channel stability compared to normal MIMO. Out of the three different situations studied, the closely located mobile users with LOS was showing worst user orthogonality of the channels, and NLOS scenario was giving most favorable channel conditions with maximum spatial separations even though the users are closely placed.

Theoretically, in massive MIMO communication system as the number of base station antennas are increased the random behavior of channel properties starts to become more and more deterministic. This was practically investigated by Xiang Gao et al. in [179] by doing channel measurements in a residential area having a base station with 128 antenna ports. The main property analyzed during measurement was the orthogonality among channels which determines the complexity of the precoding schemes that need to be used for the downlink system. They also evaluated the performance of two precoding schemes, zero forcing and minimum mean square error as a function of the number of antenna elements used at the base station. Studies showed that for two single antenna users, linear precoding schemes give 98% of the optimal capacity by having only 20 antennas at the base station.

Most of the works in massive MIMO communication area were theoretically based on many crucial assumptions on the properties of the wireless channels which were not properly validated through measurements. Several important practical aspects of massive MIMO system were studied by J Hyoids et al. in [180] through an outdoor measurement in a cellular system with scalable virtual antenna array at the base station. They mainly analyzed the theoretical assumptions made on independent and identically distributed (i.i.d.) channel vectors, correlation coefficients of channel vectors and the number of channel matrices. Studies proved that despite the differences in the assumed conditions of i.i.d and practical measurements, most of the theoretically proved performance improvements of using massive antenna arrays could be achieved in practice.

Almost a similar type of measurement mentioned in [178] was made by Sohail Payami in [181], and most of the transmission properties like channel gain, small-scale fading, and angular power spectrum were measured and analyzed using very large antenna arrays. They practically demonstrated that large antenna arrays were giving a substantial improvement in the performance characteristics.

A wideband non-stationary two-dimensional multi confocal ellipse model for very large antenna array was designed and practically implemented by Shangbin Wu et al. in [182]. The influences of spherical wave front on the line of sight and non-line of sight propagations were studied. Studies showed that there are dynamic properties and non-stationarities of groups on the antenna array in massive MIMO channels, and comparable conclusions were also made in the practical antenna measurements made by Payami [181] and Hoydis [180].

Channel modelling is very important for assessing the performances of wireless communication systems. One of the important challenges still faced by massive MIMO is how to effectively model and measure the communication channels. Investigations here sorted out the special things to be done while modelling massive MIMO channel compared to the conventional MIMO channels.

5.2.7 Resource Allocation

A well designed massive MIMO system aims at jointly optimizing the number of antennas, power allocation, user scheduling, etc. Most of the conventional resource allocation schemes are

unnecessary in massive MIMO systems because of its channel hardening property and multiplexing capability. The various resource allocation schemes suited for massive MIMO and its performance gains are analyzed here.

A novel resource allocation scheme for a large-scale MIMO system that optimizes the system sum rate was developed and tested by Rami Hamdi in [183]. A sum-rate maximization problem was formed with low complexity linear zero-forcing precoder with an assumption that equal power is received by each user. Results showed that instantaneous sum rate is not maximized when all the radio frequency chains are simultaneously activated, hence an arbitrary antenna selection algorithm was developed for finding the optimal number of RF chains to be activated for maximum sum rate.

Liu et al. [184] studied the performance of channel estimation and achievable uplink rate in multi-cell massive MIMO systems based on the least squares (LS) and minimum mean squared error (MMSE) methods respectively. A modified NMSE metric derived from the MSE metric, called the relative channel estimation error (RCEE) is proposed and closed-form expressions for its expectation E_{RCEE} and the achievable uplink rate for any number of base station antennas M is derived. It is found that when M grows to infinity, the RCEE and the E_{RCEE} converge to some constant value due to the channel hardening effect which further helps to design the pilot power allocation (PPA) algorithm for minimizing the average E_{RCEE} per user in the target cell.

A relay beamformer design based on the minorization maximization technique was devised in [185] by Naghshet al. to maximize the achievable communication sum-rate in massive MIMO AF relay networks. This method provides quality solutions to the design problem for an arbitrary number of operators L . Each iteration of the proposed method consists of solving a strictly convex constrained quadratic program which further shows the performance improvement in terms of solution quality and computational efficiency when compared to other methods.

A joint optimal pilot and data power allocation problem in single-cell uplink massive MIMO systems is considered by H. V. Cheng et al. in [186]. A closed form solution for the optimal length of training interval is first derived. Two commonly used performance parameters namely max-min spectral efficiency (SE) and sum SE optimization are investigated, and efficient optimization algorithms are developed.

A joint pilot assignment and resource allocation for maximization of system energy efficiency (SEE) in multi-user and multi-cell MMIMO network is studied in [187] by Nguyen et al. The authors have developed a novel iterative algorithm that aims to optimize the power allocation, the number of activated antennas and the pilot assignment. The proposed solution approach can also be used to address the sum rate (SR) maximization problem. Numerical results have shown that the proposed algorithm achieves much better performance in terms of total SR and SEE than that due to the conventional pilot assignment scheme.

The conventional resource allocation strategies and standards are not necessarily followed while considering the resource allocation for massive MIMO systems. This is because of the channel hardening and favourable propagation properties of massive MIMO. Here in this section, the most advanced thoughts and ideas for cost-effective resource allocation suitable for massive MIMO systems are discussed.

5.2.8 Hardware Impairments

Massive MIMO uses cheap, low cost and low power transceivers which may cause hardware impairments and that in turn limits the performance of massive MIMO. Amplifier non-linearity, Oscillator phase noise, quantization noise and IQ imbalance are some of the main sources of hardware impairments. The impact of these components on the performance of massive MIMO investigated in published literature is referred here.

A practical massive MIMO communication system is always affected by many hardware impairments that may come at the transmitter side such as non-linearities of the amplifier, quantization processes, phase noise, etc. An optimal data detection scheme under the presence of all these impairments was considered by Ramina Ghods et al. in [188]. They came up with a highly efficient data detection algorithm which works perfectly under the presence of all transmitter hardware impairments. Substantial improvements in performance (symbol error rate) were obtained compared to the detection algorithms that are un aware of hardware impairments without adding any computation overheads to the detection process.

Bei Yin et al. in [189] studied methods to combine massive MIMO with full duplex communications. For that, they suggested two novel self-interference cancellation methods which can increase the additional degrees of freedom available in the massive MIMO systems. They also showed that the performance degradation produced by residual transmitter side RF impairments could be significantly reduced by increasing the number of antennas used at the BS and by using passive antenna isolation methods.

In this section the effects of hardware impairments on the performance of MU massive MIMO system were studied both by theory and simulation. Well established hardware impairment models available in literature were used for simulation. Few of the works are carried out using more realistic and sophisticated models based on actual measurements and antenna array simulations.

5.2.9 Antenna Aspects

In massive MIMO, base stations are provided with a large number of antennas. This profusion of antennas gives many new, exciting aspects of antenna design compared to normal MIMO. Some difficulties present in old technology are non-existent in massive MIMO, whereas new issues in need of solutions come up. Studies carried out in this regard are listed here.

The complexity of a massive MIMO system lies mainly on its requirement for computationally complex data detection algorithms in the uplink where users transmit to the BS and the difficulty of concentrating the transmitted signal (beam forming) to the desired user for the downlink communication. Li, Kaipeng, et al in their

works [190-192] analyzed these facts and came up with a decentralized processing algorithm in the base band signal which can remove the above bottlenecks by segregating the antenna arrays at the BS into groups where each of this group is allotted with completely independent RF chains. Novel decentralized algorithms for beam forming and data decoding were developed and tested by evaluating the error performance of the system. Scalability of such systems towards thousands of base station antennas is also demonstrated through simulations.

Deli Qiao et al. in [193] analyzed broad beam antenna design for massive MIMO based cellular mobile system with uniform rectangular arrays and uniform linear arrays for the base station. In a broad beam design, the same intensity of power is to be radiated in all directions and generating such a perfect system is practically very difficult. The proposed method generated a broad beam which is almost flat in all directions and plotted its radiated power intensity.

A base station antenna array with 64 elements of dual polarized antenna elements with 128 ports was set up by Jose Flordelis et al. in [194]. The set was tested with eight mobile users with single antenna who were restricted to move randomly within a diameter of five meters at pedestrian speed. Simple linear precoders, zero forcing, and matched filters were used. The experiment proved that user positioned even close to each other can also be spatially separated without any interference in massive MIMO systems.

The use of RF absorbers along with very large antenna array with directive antennas for favorable improvements in propagation

characteristics of a radio channel was experimentally investigated by Andres Alayon Glazunov et al. in [195]. For the above experimental set up they placed the antenna array in a reverberation chamber, and a multi-dimensional characterization of the channel was done using 40 different antenna positions at the 1Ghz frequency. The Rician K-factor, the average power, the rms delay spread, the coherence bandwidth, the mean delay, the beamforming power angle spectrum and array antenna correlation were investigated for a number of different arrangements in the reverberation chamber. They showed that the radio frequency absorbers placed in the chamber increased the rate of the power decay of the impulse response and produced a change of the spatial(fading) statistics of the field magnitude distribution. It also significantly increased the frequency selectivity at different positions in the chamber.

Rusek et al. in [89] explained about the LTE standard, multi user MIMO, its multiplexing gain, errors that may happen in channel state information due to interference. Extremely robust design of Massive MIMO antenna system where failures of individual antennas are instantly swapped is discussed. This paper has considered the propagation aspects of very large MIMO as well as analyzed the various linear precoding schemes to reduce the complexity of algorithms used in the transmit and receive schemes. Pilot contamination which is the performance limiting factor of massive mimo is also well explained.

Y. Liu et al. in [196] considered large-scale antenna system based on a new waveform recovery theory assuming that the antenna number is infinity and the channels from different antennas are fully

independent. It has been proved that a combination of a single carrier with large-scale antenna system is a good candidate for the future wireless communication system.

An entirely different massive MIMO system where the base station equipped with a very large number of distributed antennas receiving information from several users all using single antenna was studied by Ang Yang et al. in [197]. The effect of the location and the number of BS antennas, the transmit power, and the path-loss exponent on system performance are well studied analytically and then verified through simulations. Work showed that compared to centralized massive MIMO system the circularly distributed massive MIMO system always performs better in terms of average achievable data transmission rate.

In this section many new and exciting aspects of antenna design compared to normal MIMO are evaluated. Discussed the impact of different types of antenna array patterns on the performance of a massive MIMO system.

5.2.10 Implementation, Demos and Performance Analysis.

Massive MIMO is an entirely new concept introduced very recently. To learn the advantages as well as to identify the limitations and challenges faced by massive MIMO, the system has to be implemented and its performance has to be evaluated. This section provides an insight into the studies conducted in this regard.

Geraci et al. in [198] explained the use of unlicensed spectrum of RF to coexist along with the conventional licensed frequency bands and there by increases the spatial reuse and spectral efficiency

along with considerable reduction in pilot contamination. They designed a massive MIMO system with licensed cellular frequency co existing along with unlicensed Wi-Fi frequency band in the base station for the entire scheduling and transmission operations. Performance of the above system is evaluated through simulations by considering the sum rate as well as the interference levels of this system and comparing it with the conventional licensed spectrum assisted approach. Results showed considerable improvement with the mutual interference level falling below the regulatory threshold. Large cellular data rates are achieved without causing any degradation to the Wi-Fi network performance deployed within the same cellular area.

Ngo et al. in [199] explains an entirely different concept of cell-free massive MIMO where a large number of access points distributed over a wide area simultaneously serves a small number of user terminals with the same frequency and time resources. The main objective of this is providing coherent processing over geographically distributed antennas as it works over a single BS. It requires only relatively simple beam forming as well as signal processing methods. The cell-free massive MIMO and small cell systems are studied under different conditions through simulations and results proved that this cell-free massive MIMO system could significantly outperform small cell systems in terms of data rate and spectral efficiency.

Li Kaipeng et al. in [200] presented a novel decentralized beam forming method for multi user massive MIMO. In this they divided the base station antenna array into a number of clusters and each cluster is linked with fully independent hardware for computing. The

highlight of the method is that it requires only locally collected channel state information and least amount of agreement in information among the different clusters. They experimentally demonstrated the scalability and effectiveness of their design using several hundreds of antennas at the base station transmitter.

Li et al. in [201] analyzed three different approaches of small cell in-band wireless backhaul massive MIMO systems. Complete Time-Division Duplex (CTDD), Zero-Division Duplex (ZDD), and ZDD with Interference Rejection (ZDD-IR). They proved through simulation that the small cell in-band wireless backhaul has the capability to provide much-increased throughput for massive MIMO systems. Particularly, within the three approaches, CTDD is the simplest one and attained reasonably good improvement in throughput.

A time division duplex-based network architecture which combines the advantages of massive MIMO overlaid with small cells was introduced by Hoyds et al. [202]. The channel reciprocity is exploited for every device to reuse its received estimate of interference covariance matrix for the pre-coding used. A simple pre-coding scheme is proposed which requires channel information collected locally and doesn't require any data transfer between devices. Simulation results showed that the proposed scheme could provide data throughput of the order of 10 Gbps per square km which can further improve by deploying more BS antennas or providing more small cells.

Two efficient methods to improve the energy efficiency of a cellular communication system without compromising the quality of service parameters are deeply investigated by Emil Bjornson et al. in [93]. The first method is by employing large antenna arrays on the existing base stations of the cellular system and thereby providing accurate focusing of the full transmitted energy to the actual users. The second method is by employing small cell access points to send the data traffic from base stations thereby ensuring most of the data traffic localized. They experimentally showed that the total energy efficiency could be significantly improved by combining small cells and massive MIMO.

Bogale et al. [203] proposed a hybrid method for beam forming in multi user massive MIMO for its downlink frequency selective channels. They first identified the required number of RF chains and paired phase shifters both are digitally controlled and verified that this set up provides the same performance level of a digital beam forming method which utilizes the same number of transmitter antennas as that of the used RF chain. Experimental results verified the correctness of all theoretical derivations as well as the performance improvement of the proposed system over existing designs in both frequencies selective as well as flat fading channels.

Massive MIMO communication system uses a very large number of antennas at the base station and provides a significant improvement in the system performance, but whether all these antennas are really and equally contributing to this improvement. This was practically investigated by Xiang Gao et al. in [204]. The experiment was conducted in the 2.6GHz band and demonstrated that

in many situations these individual antennas of the large array do not contribute equally to the system performance. A considerable number of RF transceiver chains can be removed without substantial loss in performance. Antenna selection algorithms were developed, and performance analysis showed that it could effectively save energy usage, cost, and hardware implementation complexity.

Network performance improvement through coordinated multipoint transmission was analyzed by Qiaoyang Ye in [205]. A distributed form of MIMO which doesn't require channel state information among their coordinating base stations is considered, and results are verified through simulations. This scheme provided significant improvements in the spectral efficiency and sum-rate compared to the normal transmission system.

Jakob Hoydis et al. in [206] posed a very important question “how many antennas do a massive MIMO system need?” to the readers and tried to find out an answer to same both analytically as well as through simulations. A massive MIMO system in TDD architecture and both the uplink and downlink transmission of the cellular network were considered for analysis and claimed that massive MIMO TDD systems are the most promising cellular network architecture for wireless communication.

A large-scale distributed antenna system under multi user scenario was modeled by Jingon Joung et al. in [207]. Common issues of such distributed systems like the complexity of computation, more energy consumption, high latency, large signaling overhead, etc. are considered for detailed study and analysis. To mitigate the effects

of the above-mentioned problems they proposed an antenna selection based on channel gain and a user terminal clustering based on interference. The performance of the proposed system is validated through simulations and found significant improvement in energy efficiency of the system.

Demonstration models of massive MIMO available in literature are studied and the performance evaluation carried out for different aspects of the system are analyzed. All the works are performed using simulations using MATLAB and actual implementation studies are lacking in the literature because of the large infrastructure, expertise and cost required for the same.

5.3 Chapter Summary

In this chapter the concept of massive MIMO has been introduced, its merits and limitations are discussed in detail. The step by step explanation on how going massive gives out the magical benefits of massive MIMO system is given. A thorough literature survey has been carried out specifically on the various aspects of massive MIMO.

Huge improvement in the data rate is identified as the main advantage of using massive MIMO for cellular mobile communications and because of this property it is considered as the most promising technology available today to address the ever-increasing demand for wireless throughput. Two important aspects that are found lacking in the literature are i) The spectral efficiency that determines the throughput in a massive MIMO system depends on many of the system parameters, standards and methods used.

Optimization of the spectral efficiency by considering all these parameters, standards and methods altogether is not yet carried out in any of the works. ii) Pilot contamination is identified as the most significant drawback of massive MIMO systems that limits the spectral efficiency. Right from the beginning of massive MIMO concept for cellular mobile communication to till date researchers are working hard to trace out the adverse effects and mitigation methods of pilot contamination. Though lots of proposals are available in the existing literature, complete elimination of the same is still a bottleneck to be solved. Coming chapters will discuss some of its advantages, methods to optimize these benefits, main drawbacks and its mitigation methods.

CHAPTER -6

OPTIMIZATION OF SPECTRAL EFFICIENCY IN MASSIVE MIMO

6.1 Introduction

Massive Multiple Input Multiple Output antenna system, with hundreds or thousands of antennas at the base station and number of simultaneous active users in each cell, is a promising technology for the future to meet the ever-growing needs of wireless data traffic. Since wireless spectrum is a limited resource, maximizing the spectral efficiency (SE) of the available spectrum is the best option to meet the ever-growing demand of wireless data traffic. In this chapter we analyse the different ways to optimize the spectral efficiency (SE) of a massive MIMO system in Time Division Duplex (TDD) architecture. The system performance under various practical constraints and conditions such as limited coherence block length, number of base station (BS) antennas, and number of active users are evaluated through simulation. The SE performance is also evaluated under different linear precoding techniques minimum mean square error(MMSE), zero forcing (ZF) and maximum ratio combining (MRC). Impact of the channel SNR variations, the different duplexing schemes (TDD and FDD) on SE is also evaluated through simulations.

6.2 Throughput in Cellular Networks

Massive MIMO is an antenna technology for futuristic networks that is 5G and beyond. The aim of this work is to achieve maximum

spectral efficiency in 5G systems by using massive MIMO. Massive MIMO make use of a large number of antennas at the base stations which are all low costs and low-power. These antennas cumulatively work to provide advantages such as increased spectrum efficiency which facilitates the base station to support a large number of users, reduced latency due to reduced fading reduced power consumption and many more as we discussed in the previous chapter.

Since from the very beginning of wireless communication, the data traffic is being doubled approximately on every two and half years period. This exponential growth in the traffic is currently true for the case of cellular mobile and wireless local area networks. There is no valid reason to think that this trend is going to cease in the near future, in fact, a marginally higher increase rate is foreseen by the recent surveys conducted CISCO and ERICSON [3,4]

To meet this rapid growth in the data rate and rapid spread of internet of things(IoT), the 5-G design goals [208] have suggested an increase in area throughput by a factor of 1000. The simple formula to calculate the network throughput in wireless networks is given by

$$\underbrace{\text{Throughput}}_{\text{bits/s}} = \underbrace{\text{Cell density}}_{\text{Cells/Area}} \times \underbrace{\text{Available spectrum}}_{\text{Hz}} \times \underbrace{\text{Spectral efficiency}}_{\text{bits/s/Hz/cell}}$$

This equation holds three components, and hence three different options are available to improve the throughput of the wireless communication network. First one is to increase the cell density which is the most traditional way to improve throughput in which dividing the cell radius by a factor of n will give us n^2 number of more cells. This method is very expensive in terms of deployment

and operational costs. The second component is the spectrum, and we know that the spectrum is a limited resource which cannot be increased above the available limit. Also when going for higher frequencies (above 5 GHz), the propagation loss also increases restricting its use to short range line of sight environments. Hence the most suitable frequency range for cellular mobile remains below 5GHz offering good network coverage and service qualities [209]. A band width of almost 1GHz has already been allotted for cellular applications, and wireless local area networks and further major increase in this is not expected in future.

Increasing the cell density and available BW were the methods followed so far for increasing the throughput. The third option of increasing spectral efficiency has not been used so far for large improvements in the throughput, but it can be the driving force and may become the primary way to achieve the expected throughput in future 5G networks.

Table 6.1 Achieving a 1000-fold increase in throughput

	More spectrum	Higher cell density	Higher spectral efficiency
Nokia	10×	10×	10×
SK Telecom	3×	56×	6×

└──────────┘

New Regulations,
Cognitive radio &
higher frequencies

└──────────┘

Smaller cells &
heterogeneous
deployments

└──────────┘

Massive MIMO
Techniques

After having many surveys and studies, Nokia and SK Telecom have come up with two different proposals [210] to achieve this 1000

fold increase in the throughput, which are shown in the table 6.1. Hence within the available spectrum the two options to cater the growing demand are by increasing the cell density (more number of cells with a smaller size for a specific area) and by technical improvements in the physical layer to provide more spectral efficiency.

The second possibility, i.e., providing high spectral efficiency, is examined in this work where different methods to maximize the spectral efficiency of a massive MIMO system are studied. The effect of the number of BS antennas, number of active users per cell and coherent block length on the spectral efficiency is thoroughly examined through simulation. Zero-forcing precoding technique is considered for our analysis, and the results are also compared with other precoding techniques, maximum ratio combining (MRC) and Minimum Mean Square Error (MMSE) methods. The impact of channel SNR variation on SE and different precoding techniques are also evaluated.

6.3 Massive MIMO System and Assumptions

At first, to begin our analysis a multi-user MIMO system with one BS and K number of active users shown in Fig 6.1 is considered. The BS consists of M number of symmetrical antennae, and each user terminal is equipped with a single antenna. It is assumed that the same frequency and time band are shared by all K users. It is also assumed that there exist a perfect CSI among the BS and users. During each training phase channels are acquired at the BS and UTs. .

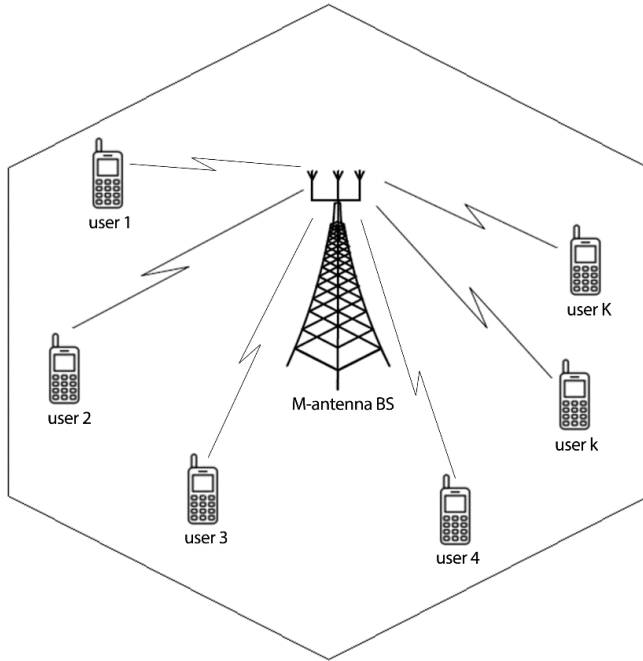


Figure 6.1 Massive MIMO system with M antennas and K users

The training method is selected assuming the use of TDD architecture. In the above. situation, the channel matrix is given by $\mathbf{H} \in \mathbb{C}^{M \times K}$ where M and K are the number of BS antennas and number of active UTs. Then the channel matrix for one of the user (k^{th} user) and BS will be an $M \times 1$ matrix represented as h_k [211].

6.4 Uplink Signal Transmission

Now we will analyse the uplink signal transmission, which refers to the transmission from mobile nodes to the BS. Assume S_k as the information signal transmitted from the k^{th} user. Then $\mathbb{E}\{|s_k|^2\} = 1$, and since all the k users share the same frequency and time frame, we can calculate the $M \times 1$ signal vector at the BS by summing up the signal transmitted from all the K users.

$$y_{ul} = \sqrt{p_u} \sum_{k=1}^K h_k s_k + n \quad (6.1)$$

$$y_{ul} = \sqrt{p_u} Hs + n \quad (6.2)$$

where P_u represents the average SNR and n is the additive noise vector. ul stands for uplink. From this received signal y_{ul} , and CSI the base station can very easily obtain the signals transmitted from all the K users through coherent detection. Then the total uplink sum-rate can be calculated by the following equation [212].

$$C_{ul,sum} = \log_2 \det (I_K + p_u H^H H) \quad (6.3)$$

The above result is achieved by assuming successive interference cancellation (SIC) technique in the uplink channel. In SIC after detecting the first user, the signal of that user is subtracted from the total received signal before detecting the second user and so on.

6.5 Downlink Signal Transmission

Downlink transmission is the situation where the base stations transmit signals to all the K active mobile terminals in the cell. If the signal vector transmitted from the BS array is assumed as x then $x \in \mathbb{C}^{M \times 1}$ and $\{\mathbb{E}\|x\|^2\} = 1$. The total signal received by the k^{th} user can be written as

$$y_{dl,k} = \sqrt{p_d} h_k^T x + z_k \quad (6.4)$$

where z_k is the additive noise component at the k^{th} user and p_d is the average SNR. Assuming the noise as Gaussian with zero mean and unit variance the total signal vector received by all the k users can be obtained as

$$y_{dl} = \sqrt{p_d} H^T x + z \quad (6.5)$$

6.6 Spectral Efficiency and its Importance

When the spectral efficiency of a single antenna input and single antenna out system (SISO) is considered, its maximum limit is determined by the Shannon capacity given as below

$$SE = \log_2(1 + SNR) \text{ bits/s/Hz} \quad (6.6)$$

Here the channel noise is assumed to be as additive white Gaussian noise (AWGN). Thus, the above equation reveals that the channel capacity is a logarithmic function of the SNR and to improve the SE we need to have an exponential increase in the signal power. That means, in order to increase the SE of a SISO channel from 2 to 4 bits/s/Hz, then the SNR or signal power must be increased from 3 to 15, a fivefold increase. Next level of improvement of SE from 4 to 8 bits/s/Hz requires an increase of 17 times more power. In other words, in order achieve a linear increase in the SE, the transmitted signal power must be increased exponentially, which is clearly a highly inefficient and also non-scalable way of improving SE. This approach also fails when the nearby cells, likewise increase power to improve their SE causing high inter-cell interferences. Therefore, a different approach must be identified for improving SE of cellular networks.

In a cellular communication network, several mobile terminals are served by a single base station. In traditional systems, this is made possible by dividing the available time and frequency resources among different users. So, an effective way of improving the spectral efficiency is to provide several parallel communications between BS and mobile users. If there are N number of parallel transmissions,

then total SE become N times the spectral efficiency of a SISO system.

$$SE = N \log_2(1 + SNR) \text{ bits/s/Hz} \quad (6.7)$$

The above situation can be achieved by multiple transmit and/or multiple receive antennas, and we get the following two different scenarios

- i) Point to point MIMO: single BS communicates with a single mobile user both having multiple antennas.
- ii) Multiuser MIMO: A single BS with multiple antennas communicate simultaneously with many mobile users either with single or with multiple antennas.

Among these, the MU-MIMO option is most suitable for scalable cellular networks [212]. As explained in the previous section the frequency used for cellular communication is in 1-5GHz range which makes a signal wavelength of 5-25 cms. In this wavelength deploying more number of antennas on a compact mobile user terminal will be practically difficult for achieving the point to point MIMO where as we can very easily set up a MU-MIMO system with BS equipped with a sufficiently large number of antenna elements of this dimension to communicate parallelly with multiple user terminals with single antenna. Secondly, the parallel communication channels between the BS and mobile users are to be independent, and this condition is very difficult to achieve when multiple antennas are closely placed in a single user terminal for point to point MIMO. In MU-MIMO, if the mobile users are few meters apart, which is true in many practical scenarios, the above channel independency can be

very easily achieved. Finally, when multiple antennas are equipped with mobile terminals, a complex signal processing will be required at the user terminal to separate the different data streams, which increases the complexity and cost of mobile equipment. Where as in MU-MIMO user terminals need to decode only one data stream and hence remains simple and economical [213].

6.7 Frequency Division Duplexing Vs. Time Division Duplexing

In massive MIMO systems, many user terminals are spatially multiplexed over the same frequency-time resources yielding coherent beam forming gain which directly give very less interference and enhanced coverage of cell edge areas. There are two distinct methods to implement the uplink and downlink communication within the same frequency band, namely FDD and TDD. In FDD separate frequency bands are allotted for both uplink and downlink. Since distinct frequencies are used, due to frequency selective fading, pilot sequences and channel estimation processes are required both in the uplink and downlink. This necessitates the use of an average pilot length of $(M+K)/2$ for every sub-channel [214]. In TDD mode of operation the entire frequency spectrum is used for both uplink and downlink, but at separate time intervals as shown in Fig. 6.2. If the communication is switching between uplink and downlink at a speed higher than the channel coherence time (the period over which the channel characteristics remain steady), then channel estimation and pilot sequences are required only in one direction. This, in turn, reduces the pilot length requirement to $\min(M,K)$ for every sub-channel. The details are shown in Fig. 6.2.

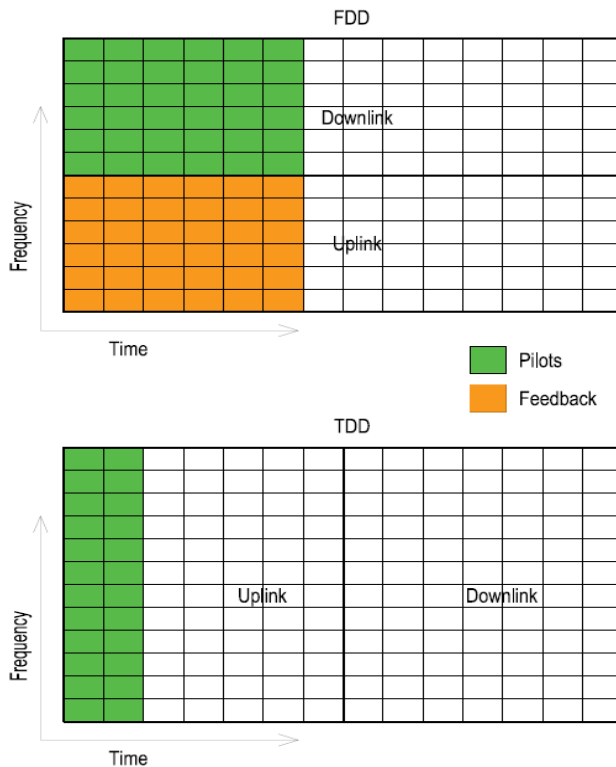


Figure 6.2 FDD and TDD operation showing the link overheads

There are many advantages for TDD system when compared with FDD. In TDD only the BS needs to know about the CSI for coherent processing of the antennas. The channel estimation overhead is proportional only to the number user terminals and independent of the number of BS antennas making it completely scalable to the number of user terminals. The channel estimation time is less, and it gets more time to send data giving more spectral efficiency. The uplink and downlink capacity ratio can be dynamically changed according to the requirement. TDD systems are cheaper than FDD because it doesn't need a diplexer to provide isolation between the transmission and reception.

6.8 Fundamental Property of Massive MIMO

Now let us analyse, how massive MIMO with a large number of BS antennas and simple linear ZF processing, provides a data capacity approaching that of an ideal condition of without interference. The answer is clear from the massive MIMO definition “Massive MIMO is a multi-user MIMO system that serves multiple users through spatial multiplexing over a channel with favourable propagation in time-division duplex and relies on channel reciprocity and uplink pilots to obtain channel state information”. In wireless communication a propagation is said to be favourable when users are mutually orthogonal in some practical sense [111].

It means that, if we assume $\mathbf{h}_1 \in \mathbb{C}^M$ is the channel vector for a user k_1 and $\mathbf{h}_2 \in \mathbb{C}^M$ to another user k_2 then these two users will be orthogonal if $\mathbf{h}_1^H \mathbf{h}_2 = 0$, but this never becomes true in a real communication system. But it can be made practically true if we say that the users are practically orthogonal when $\mathbf{h}_1^H \mathbf{h}_2$ has a mean of zero and variance much less than 1. [215]. Eqn. 6.8 shows that the inner product of two Rayleigh channels h_i and h_j , when normalised with M , tends to become zero as M increases to infinity [216].

$$\frac{h_i^H h_j}{M} \rightarrow 0, \text{ as } M \rightarrow \infty \quad (6.8)$$

The graph shown in Fig. 6.3 demonstrate that as the number of antennas at the BS grows large, the correlation (spatial alignment) between two independent and identically distributed (i.i.d.) channels disappear. The Y axis indicates the average correlation between two i.i.d channels under Rayleigh fading. It shows that the expected value

of the correlation between two i.i.d. Rayleigh channels h_i and h_j as a function of the number of BS antennas. This can be explained with the theory of large numbers [215].

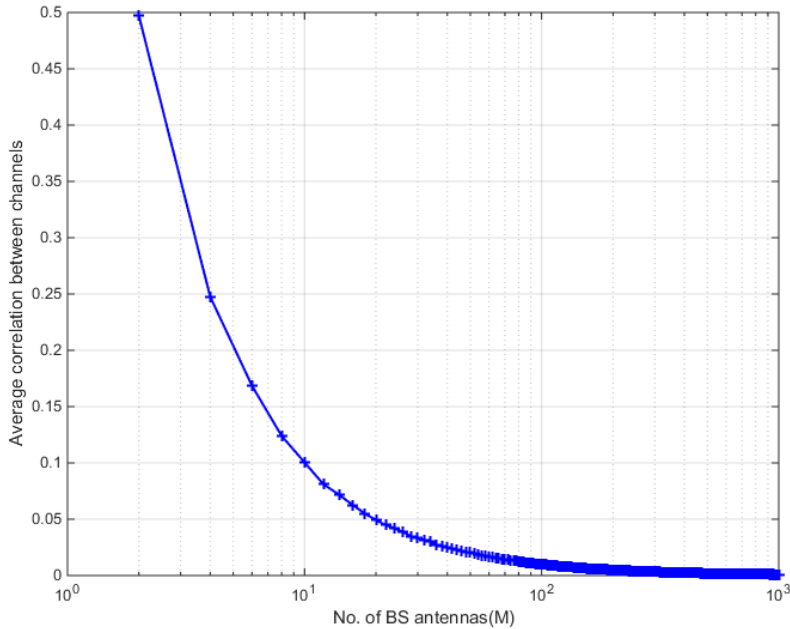


Figure 6.3 Average correlation between two i.i.d. Rayleigh channels as a function of M

6.9 Channel Coherence in Wireless Communication

6.9.1 Coherence Time

In wireless communication networks, channel state information(CSI) is essential in order to have coherent detection of signals at the receiving end. The acquired CSI at any time is valid only for a duration where the channel behaviour can be assumed as constant. Coherence time is defined as the time duration in which the channel is assumed to be constant; it is denoted as T_c and measured in seconds. This parameter depends on the carrier frequency used and

user mobility. Coherence time varies inversely with the velocity of the user terminal. In present communication systems, such as LTE and LTE-A, channels are estimated periodically at regular intervals. This method is inefficient as some of the spectrum resources are wasted by acquiring the CSI more frequently than required as most of the users do have noticeably large coherence time. Pilot aided channel estimation is the most widely used method for CSI acquisition in MIMO communication.

To understand channel coherence quantitatively the two-path model shown in Fig. 6.4 is useful. To analyse the effect of T_c in signal propagation, we consider a simple two-path model with a signal $x(t)$ is transmitted and it reaches the mobile node via two distinct paths, one direct and another by a direct reflection as shown in Fig. 6.4. Then definitely there will be time differences on the two arrived signal, and that can be estimated as phase shifts. Considering the details in Fig. 6.4 and applying superposition theorem to the two components, the total received signal at the mobile can be expressed as

$$y(t) = \left(e^{-i2\pi f c \frac{d_1}{c}} + e^{-i2\pi f c \frac{d_2}{c}} \right) x(t) \quad (6.9)$$

Simplifying the above equation, we get

$$y(t) = \left(e^{-i2\pi \frac{d_1}{\lambda}} + e^{-i2\pi \frac{d_2}{\lambda}} \right) x(t) \quad (6.10)$$

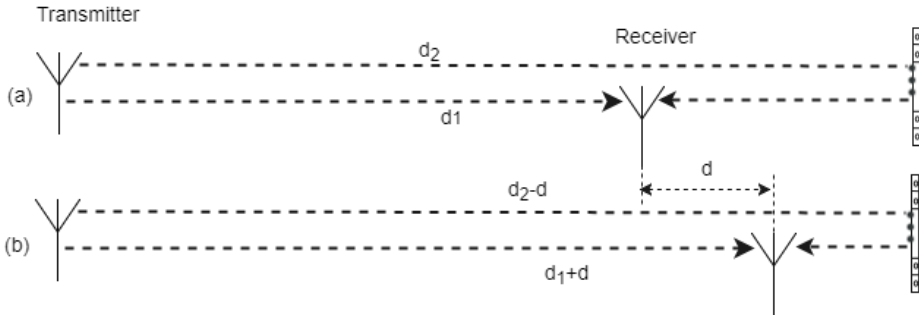


Figure 6.4 Two path model for a wireless channel to explain the channel coherence

When the user equipment is placed at integer multiples of d/λ the two paths add up constructively giving the received signal $y(t) = 2x(t)$. Now if the UE is moved a distance of d towards the right as shown in Fig. 6.4(b), then the two signals will add up destructively, and the received signal becomes equal to

$$y(t) = \left(e^{-i2\pi\frac{d}{\lambda}} + e^{-i2\pi\frac{-d}{\lambda}} \right) x(t) \quad (6.11)$$

Simplifying the above we get

$$y(t) = 2 \cos\left(2\pi\frac{d}{\lambda}\right) x(t) \quad (6.12)$$

The destructive interference happens when the cosine term becomes equal to zero, and this occurs periodically for displacements which are multiples of $\lambda/2$. So if the UE is moving with a velocity of v m/s then the coherence time is given by

$$T_c = \frac{\lambda}{2v} \text{ seconds} \quad (6.13)$$

Hence coherence time can be defined as the time a UE takes to move half a wave length of distance.

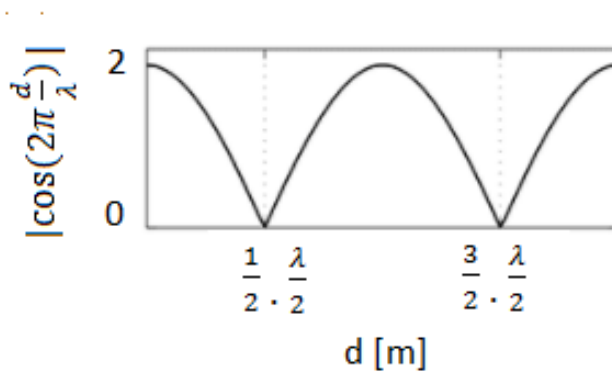


Figure 6.5 Coherence time T_c is the time that UE takes to travel the distance between the two nulls.

In reality, the communication environment is entirely different from the two-path model explained above, as the transmitted signal entails a direct path and number of reflected indirect paths of different amplitudes. It results in a complex-valued response, but the coherence time given in equation 6.13 remains valid as a good approximation [216].

6.9.2 Coherence Bandwidth

Now if the time duration of the transmitted signal is lesser than the coherence time of T_c , then we get a time-invariant relationship between $y(t)$ and $x(t)$, where $y(t)$ can be expressed as

$$y(t) = \int_{-\infty}^{\infty} d\tau g(\tau)x(t - \tau) \quad (6.14)$$

in which $g(\tau)$ is the impulse response of the channel, and the channel frequency response is given by

$$G(f) = \int_{-\infty}^{\infty} dt g(t)e^{-i2\pi ft} \quad (6.15)$$

The magnitude of this channel frequency response $|G(f)|$ changes with the frequency f , and the frequency interval over which the $|G(f)|$ stays constant is known as coherence bandwidth B_c measured in Hz . If the distance d_1 and d_2 shown in Fig. 6.4 are selected in such a way as to get d_1/λ , and d_2/λ are integers, then for a sinusoidal transmitted signal of $x(t) = e^{i\pi ft}$, the received signal will be equal to

$$y(t) = (e^{-i2\pi(f_c+f)\frac{d_1}{c}} + e^{-i2\pi(f_c+f)\frac{d_2}{c}})e^{i2\pi ft} \quad (6.16)$$

where

$$G(f) = e^{-i2\pi(f_c+f)\frac{d_1}{c}} + e^{-i2\pi(f_c+f)\frac{d_2}{c}} \quad (6.17)$$

Simplifying the above we get

$$G(f) = e^{-2i\pi f\frac{d_1}{c}} + e^{-i2\pi f\frac{d_2}{c}} \quad (6.18)$$

and the magnitude $|G(f)|$ is equal to

$$|G(f)| = |e^{-2i\pi f\frac{d_1}{c}} + e^{-i2\pi f\frac{d_2}{c}}| \quad (6.19)$$

$$= 2|\cos(\pi f\frac{d_1-d_2}{c})| \quad (6.20)$$

From the above equation, it is clear that $|G(f)|$ periodically reaches zero at $c/|d_1-d_2|$ Hz apart. This is shown in Fig. 6.6. The coherence bandwidth, in analogues to coherence time, can be defined as the spacing between two nulls(zeros) of $|G(f)|$,

$$B_c = \frac{c}{|d_1-d_2|} \quad (6.21)$$

In other words, $|G(f)|$ should remain substantially constant over the frequency interval defined by equation 6.21. Again, the values $c/|d_1-d_2|$ is called as the delay spread of the channel, and $g(t)$ is time limited to $c/|d_1-d_2|$ seconds.

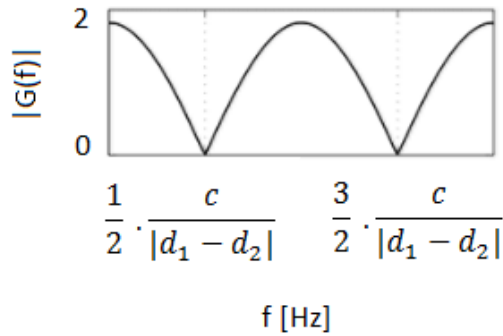


Figure 6.6 Coherence BW B_c is the frequency difference between the two nulls

6.9.3 Coherence Interval

The product of the coherence band width B_c and coherence time T_c is known as the coherence interval τ_c . It can be considered as the time-frequency space of BW B_c and time T_c . It means that $B_c T_c$ samples are required to define a signal that fits into one coherence interval.

Or
$$\tau_c = B_c T_c \text{ samples} \quad (6.22)$$

Table 6.2 illustrates the values of T_c , B_c and τ_c computed as per equations 6.13, 6.21 and 6.22 at a carrier frequency of 2GHz for two different mobility scenarios.

Table 6.2 Values of T_c , B_c , and τ_c computed at $f_c = 2\text{GHz}$

	Indoors $ d_1 - d_2 = 30 \text{ meters}$	Outdoors $ d_1 - d_2 = 1000 \text{ meters}$
Pedestrian $v = 1.5 \text{ m/s}$ (5.4 km/h)	$B_c = 10 \text{ MHz}$ $T_c = 50 \text{ ms}$ $\tau_c = 5000000$	$B_c = 300 \text{ kHz}$ $T_c = 50 \text{ ms}$ $\tau_c = 15000$

Vehicular $v = 30 \text{ m/s}$ (108 km/h)	N/A	$B_c = 300 \text{ MHz}$ $T_c = 2.5 \text{ ms}$ $\tau_c = 750$
---	-----	---

6.9.4 Coherence Interval for a Massive MIMO in TDD Architecture

As discussed in earlier sessions the TDD architecture is most suitable for massive MIMO to make the training overhead independent of the number of BS antennas. It is also assumed as only one end of the system is transmitting at a time, either BS or UE (half-duplex operation) and hence the coherence interval is divided into two as uplink and downlink sub intervals, which need not be equal. Fig. 6.7 describes this situation.

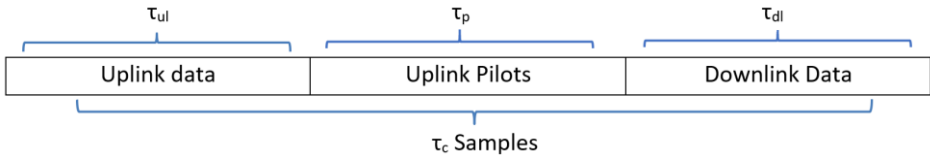


Figure 6.7 Allocation of samples in a coherence interval- No downlink pilots

Here $\tau_{ul} + \tau_p + \tau_{dl} = \tau_c$

(6.23) The size of the coherence interval is significant in many ways, the net channel capacity of the system with K number of active UEs is given by

$$C_{net,k} = \left(1 - \frac{\tau_p}{\tau_c}\right) C_{inst,k} \quad (6.24)$$

It means the net capacity of the system is equal to a penalty factor $\left(1 - \frac{\tau_p}{\tau_c}\right)$ multiplied by the instantaneous capacity. So, if we have longer coherence interval, then there will be more room for

pilots and that in turn allow us to accommodate and multiplex more number of users in the same area. By taking these capacities given in Eqn. 6.24 and summing them up over all terminals, we get the maximum net achievable sum rate as given below.

$$Net\ sumrate = \frac{1}{2} \left(1 - \frac{\tau_p}{\tau_c}\right) \sum_{k=1}^K C_{int,k} \quad (6.25)$$

The term $\frac{1}{2}$ is taken because the total resources are divided between uplink and downlink.

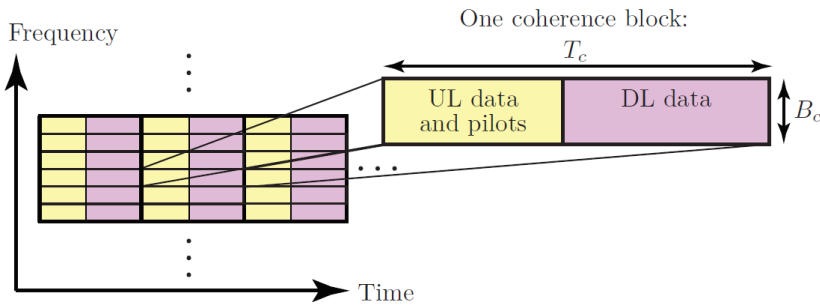


Figure 6.8 TDD architecture with time-frequency plane divided into coherence blocks

Fig. 6.8 gives a clear picture of how the time and frequency planes are divided into coherence blocks where each channel is assumed as frequency flat and time-invariant. The allotted frequency range B_c equally divided into all the subcarriers of OFDM.

6.10 Pilot Based Channel Estimation in Massive MIMO

A wide band radio channel can be divided into coherence intervals of T_c seconds duration and bandwidths of W_c Hz. This will provide $\tau_c = B_c T_c$ independent frequency flat channels. Fig. 6.7 explains the three operations that make use of the above interval, i.e., transmission of uplink data, transmission of uplink pilots and then

transmission of downlink data. τ_p of every interval τ_c is used for the pilot transmission in the Uplink, and from this pilot, the base stations obtain the CSI.

6.10.1 Pilot Orthogonality.

If the number of active users in the cell is K , then each coherence-interval τ_c should occupy K number of pilot sequences and to avoid any sort of interference among these pilots, it should be all orthogonal to each other. The problem that may arise is that usage of orthogonal pilots for a large number of simultaneous active terminals can cause large resource consumption particularly when the coherence interval is short.

Conventional communications systems can make use of more number of pilot sequences than the number of active UEs and avoid the risk of pilot collisions and contamination. In contrast, the massive MIMO systems are supposed to have 20 to 40 times more number of active UEs on the same time-frequency resources compared to conventional systems. In simple words, if 40 times more UEs are active, then the pilot contamination will be 40 times more severe.

6.11 Linear Signal Processing Vs. Non-linear Signal Processing

Signal processing or precoding techniques in MIMO systems can be divided into two categories, linear precoding, and non-linear precoding. The optimal performance is attained by using nonlinear precoding techniques which can effectively eliminate the interference between different users and achieve optimal performance. However, non-linear techniques are highly complex, and that makes it

unrealistic due to hundreds of antennas used in massive MIMO systems.

For most propagation environments, the use of an excessive number of BS antennas over the number of users yields favourable propagation where the channel vectors between the users and the BS are pair wisely (nearly) orthogonal. Under favourable propagation, the effect of inter-user interference and noise can be eliminated with simple linear signal processing (linear precoding in the downlink and linear decoding in the uplink), and these simple linear processing schemes are nearly optimal. In other words, by using the simple maximum ratio transmission (MRT) in the downlink and maximum ratio combining (MRC) technique at the uplink, the adverse effects of intracell interference, fast fading, un correlated noise, etc. are effectively vanished as the number of antennas at the base station increases to very large. Also, massive MIMO decreases the restrictions on linearity and accuracy of individual amplifiers and radio frequency chains used at the transceiver units. It needs only very low complexity linear signal processing methods [217].

6.12 Massive MIMO Precoding and Signal Detection Techniques

In multi-user MIMO the precoding and signal detection techniques are mainly planned for separation of data streams with the lowest possible inter-user interference. In the uplink, the signals coming from all the users are post filtered by the BS, where as in the downlink the signals to the intended users are pre-filtered by the BS. Channel state information is required at the BS to accomplish this

processing and is not so necessary at the receiver where relatively simple processing is required.

From the existing studies, dirty paper coding has been identified as the optimum precoder for downlink communication and successive interference cancellation (SIC) detection for the uplink communication to have the optimum capacity [218]. But these two methods are nonlinear processes and are highly complex for implementation. Linear processes like zero-forcing(ZF), Maximum ratio combining(MRC) and minimum mean square error (MMSE) are simple in practice but give sub-optimal performance in the sum rate. However, for massive MIMO all the linear schemes become virtually optimal as the number of antennas increases to a very large number.

6.12.1 Dirty Paper Coding(DPC)

In a multi-user MIMO downlink channel, optimum sum-rate capacity can be achieved by using DPC [219]. In this method, each BS selects a code word in such a way that the inter user interference is completely eliminated. DPC was originally proposed in [220] to combat additive interferences in a medium.

In DPC instead of fighting with the interference, it adapts to it by properly choosing codewords in the direction of interference. This method was applied to multi-user MIMO since it was described in [221]. But the practical implementation of DPC involves extra complexity, and it remains unsolved. Alternatively, many sub-optimal schemes with highly reduced complexity, such as linear precoding schemes, are used in practice.

6.12.2 Linear Precoding Methods

Maximum ratio combining (MRC), zero forcing(ZF) and minimum mean square error (MMSE) are the most commonly used linear methods in massive MIMO systems. Linear precoding is considered here for the downlink, and in the uplink, the corresponding linear detection scheme is used. This section gives a good comparison and analysis of these three linear precoding and detection schemes.

When linear precoding is used at the BS, the transmit vector can be written as [111]

$$z = W\sqrt{P}x, \quad (6.26)$$

where W represents the precoding matrix, P_i , where $i= 1,2,3 \dots K$, gives the power to different users and x is the transmit symbol vector for all the active users. Purpose of the precoding matrix W is to map the signal $s = \sqrt{P}x$ to for all the intended users appropriately in all the M antennas. To achieve this, W can be designed with various objectives like maximizing SNR and maximum inter-user interference cancellation, both subjected to the maximum total power restriction $\mathbb{E}\{\|z\|^2\} = 1$ This restriction can be written as

$$Tr\{PW^H W\} = 1 \quad (6.27)$$

Where $Tr\{.\}$ is called as the matrix trace and in the DL transmission model the total transmitted power is taken as P_{dt} .

6.12.3 Zero-Forcing

Zero-Forcing (ZF) precoding scheme cancels out the inter-user interference to its maximum. It can be derived from the optimization method given below [222]

$$W_{ZF} = \arg \min \mathbb{E}\{\|Ws\|^2\} \quad \text{s.t. } HW = I. \quad (6.28)$$

here we are optimizing for a W_{ZF} , with minimum transmit energy, which can completely cancel out the inter user interference. To do that the easy method is Moore-Penrose pseudo-inverse of the corresponding channel,

$$\text{i.e., } W_{ZF} = H^\dagger = H^H(HH^H)^{-1} \quad (6.29)$$

and then the equation for the received signal becomes

$$y = \sqrt{p_{d1}}s + n \quad (6.30)$$

In which every user receives its corresponding signal $\sqrt{p_{d1}}s$ without any inter user interference or cross talk. The only extra term is the channel noise component n . Hence by using this simple ZF scheme the inter user interference can be completely canceled, but "it is always impossible to get something for nothing." This method suffers from the power penalty due to the nulling effect. To explain this limitation let us now consider the sum-power restriction given in Eqn. 6.27 which can be re written as

$$\sum_{i=1}^K P_{ZF,i} [(HH^H)^{-1}]_{i,i} = 1 \quad (6.31)$$

where P_{ZF} is the power allocation matrix and $P_{ZF,i}$ is the i^{th} diagonal element in it. The power that can be allotted to each user terminal is determined by the channel condition. The power penalty will become

zero if the matrix H has got the full rank and the Gram matrix HH^H is a diagonal matrix. It means all the channels from the BS to the K user terminals are fully orthogonal to each other, and the the transmitted power P_{dt} will fully available to the individual user signals. However, when some of the user channels are aligned to each other losing its orthogonality and the Gram-matrix becomes ill-conditioned [223]. This makes $[(HH^H)^{-1}]_{i,i}$ to increase and there by (Eqn. 6.31) making $P_{ZF,i}$ smaller, i.e., less energy is allotted to the individual users, and more is spent on the nulling, which results in very less received power for some of the users. An identical effect will occur at the receiver during ZF detection and is known as noise enhancement.

6.12.4 Maximum Ratio Combining

Maximum Ratio Combining (MRC) also known as matched filtering aims at maximizing the received SNR of every user. The process will be clear by solving the following optimization problem [224].

$$W_{MRC} = \arg \max W \frac{E\{s^H y\}}{\sigma_n^2} \quad \text{s.t. } Tr\{P_{MRC} W^H W\} = 1 \quad (6.32)$$

And the solution to the optimization is the Hermitian transpose of the channel matrix

$$W_{MRC} = H^H \quad (6.33)$$

Then for the i^{th} user, with an arbitrary power of P_{MRC} , the effective received signal model is

$$y_i = \sqrt{p_{d1}} [HH^H]_{i,i} s_i + \sqrt{p_{d1}} \sum_{j=1, j \neq i}^K [HH^H]_{i,j} s_j + n_i \quad (6.34)$$

where the first term represents the maximized received signal intended for the user i , the second term represents inter user interference from all other users except i and the last term gives the additive white noise. Owing to the maximization process of the received SNR at every user, MRC will be suitable for noise limited scenarios [225]. In high SNR conditions the performance will be limited by inter user interference, and in that case, ZF is superior to MRC. By adjusting the phase and power of the signals fed to the different transmitter antennas, ZF and MRC make the signals to follow a multipath channel, after diffraction, reflection and scattering, arrive at the users in different ways. With ZF, the multipath signals are destructively added up to zero for the intended user at the location of the other users, resulting in no interference but a decrease in the received signal strength of the intended user. With MRC, the multipath signals are added up constructively at the intended user location but cause interference for the other users.

6.12.5 Minimum Mean-Squared Error

As seen in the previous sessions, ZF is appropriate for high SNR conditions and MRC for low SNR conditions. In MMSE the basic idea is estimating the noise co-variance at the receiving user side and send back the same to the transmitting side to have a better precoder design which stands good for the entire range of SNR.

The optimization steps for getting MMSE are summarized below [226]

$$W_{MMSE} = \arg \min \mathbb{E}\{\|y - \sqrt{p_{a1}}s\|^2\} \quad (6.34)$$

Substituting for y we get

$$W_{MMSE} = \arg \min \mathbb{E}\{\|(HW - I)s - n/\sqrt{p_{d1}}\|^2\} \text{ s.t. } Tr\{P_{MMSE}W^H W\} = 1 \quad (6.35)$$

Here the effort is done to minimize the mean square error between the transmitted and received signals. One likely method to get this is ZF with $HW=I$, which occurs when the transmitted power over the downlink P_{dl} is arbitrarily high, but with limited transmitter power, the noise variance σ_n^2 is also to be considered. That makes the solution to MMSE as

$$W_{MMSE} = H^H(HH^H + \alpha I)^{-1} \quad (6.36)$$

where $\alpha = \frac{K\sigma_n^2}{p_{dl}}$ and K is the number of active users. This general form of MMSE described in Eqn. 6.36 is also known as regularize ZF or RZF with α as the regularization parameter. Corresponding to high SNRs which corresponds to $\alpha = 0$, the MMSE becomes the same as ZF, and corresponding to low SNRs, which corresponds to $\alpha = \infty$ it converges to MRC. In between these two extreme values of zero and infinity MMSE outperforms the MRC and ZF in terms of its sum rate performance because the MSE value is lesser than the other two schemes. The power penalty due to the interference suppression is smaller in MMSE than in ZF.

6.13 Capacity Limits in Massive MIMO

Let us first consider the simple model described in Fig. 6.9, where the BS with M antennas which serves K number of single antenna user terminals in the spatial domain conceived within a single cell (spatial multiplexing). Channel reciprocity is assumed between uplink and downlink, and hence the uplink channel matrix will be the transpose of the downlink channel matrix.

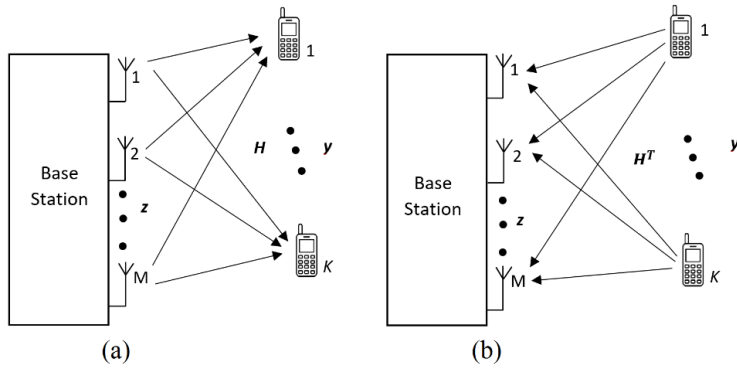


Figure 6.9 A multi-user MIMO in the (a) downlink and (b)uplink

Then for each time-frequency resource available, the downlink signal model can be written as [228]

$$\mathbf{y} = \sqrt{p_{dl}}\mathbf{H}\mathbf{z} + \mathbf{n} \quad (6.37)$$

where \mathbf{y} is the received signal vector at the K users, \mathbf{H} is the propagation channel matrix, \mathbf{z} is the transmitter precoder vector across the M BS antennas, and \mathbf{n} is the white Gaussian noise with independently and identically distributed (i.i.d) circularly symmetric complex Gaussian $CN(0, \sigma_n^2)$ elements. Now assuming $\mathbb{E}\{\|\mathbf{z}\|^2\} = 1$ will make the P_{dl} to carry the total downlink transmit power. We first scaled the transmitted power with K number of users and then scaled it down with M number of BS antennas. i.e., i) $p_{dl}=K\rho$ and ii) $p_{dl}=K\rho/M$, where ρ is the SNR factor. We always assume the noise variance equal to unity $\sigma_n^2=1$,

Throughout our analysis channel reciprocity has been assumed between the uplink and downlink channel and hence the uplink channel matrix is \mathbf{H}^T and the signal model can be written as

$$\mathbf{z} = \sqrt{p_{ul}}\mathbf{H}^T + \mathbf{n} \quad (6.38)$$

P_{ul} is the total transmitted power from all the user terminals.

The downlink sum rate that can be achieved by DPC coding in MU-MIMO network can be expressed as [229]

$$C_{DPC} = \max \log_2 \det \left(I + \frac{p_{dl}}{\sigma_n^2} H^H P_{DPC} H \right) \text{ s.t. } \sum_{i=1}^K P_{DPC,i}. \quad (6.39)$$

For DPC coding inter user interference is practically zero and in linear precoding schemes, we can consider this as additive noises at the receiver. The individual user rate depends upon the receive SINR of the user which in turn decided by the precoder W , and allocation of power P . The receive SINR for the i^{th} user can be given as

$$\gamma_i = \frac{p_{dl} | [HW]_{i,i} |^2 P_i}{p_{dl} \sum_{j=1, j \neq i}^K | [HW]_{i,j} |^2 P_j + \sigma_n^2} \quad (6.40)$$

the denominator of the above equation represents the total of the inter user interferences received by the i^{th} user from all other channels plus the Gaussian noise, whereas the numerator represents the signal power of the i^{th} user.

Considering the sum-power constraint given in Eqn. 6.27, the Eqn. 6.39 becomes

$$C = \max_P \sum_{i=1}^K \log_2 (1 + \gamma_i) \quad \text{s.t. } \sum_{i=1}^K P_i [W^H W]_{i,i} = 1 \quad (6.41)$$

Considering inter user interference as noise is an easy solution but is not optimal.

6.14 Inter-user Interference in Linear Precoding Schemes

As the value of the number of antenna elements in the BS increases the term $[HH^H]_{i,i}$ in Eqn. 6.34 also becomes large, but the off-diagonal elements $[HH^H]_{i,j}$, where $i \neq j$ grow much slower than the

diagonal elements. If we assume H as an i.i.d channel with complex Gaussian coefficients $CN(0, \sigma_h^2)$, $\sigma_h^2 < \infty$, the examining $\frac{1}{M} HH^H$, the diagonal elements can be written as

$$\frac{1}{M} [HH^H]_{i,i} = \frac{1}{M} \sum_{m=1}^M |H_{i,m}|^2 \quad (6.42)$$

and the off-diagonal elements as

$$\frac{1}{M} [HH^H]_{i,j} = \frac{1}{M} \sum_{m=1}^M H_{i,m} H_{j,m}^*, \quad i \neq j \quad (6.43)$$

Then according to the central limit theorem [227], as the value of M goes to infinity, both the distributions of off-diagonal and diagonal elements converge to Gaussian.

$$\frac{1}{M} [HH^H]_{i,i} \rightarrow N(\mu_0, \frac{\sigma_0^2}{M}) \quad (6.44)$$

$$\frac{1}{M} [HH^H]_{i,j} \rightarrow CN(\mu_1, \frac{\sigma_1^2}{M}), \quad i \neq j \quad (6.45)$$

where $\mu_0 = \mathbb{E}\{|H_{i,m}|^2\}$, $\sigma_0^2 = \text{var}\{|H_{i,m}|^2\}$, $\mu_1 = \mathbb{E}\{H_{i,m} H_{j,m}^*\}$ and $\sigma_1^2 = \text{var}\{H_{i,m} H_{j,m}^*\}$. As the value of M goes to infinity, variances of both off-diagonal distributions and diagonal distributions approach to zero, i.e. $M \rightarrow \infty$, $\frac{\sigma_0^2}{M} \rightarrow 0$ and $\frac{\sigma_1^2}{M} \rightarrow 0$.

On the diagonal $|H_{i,m}|^2 = \text{Re}\{H_{i,m}\}^2 + \text{Im}\{H_{i,m}\}^2$ trails the chi-squared distribution with 2 degrees of freedom and $\mu_0 = \sigma_h^2$. At the off-diagonal elements the $\mu_1 = \mathbb{E}\{H_{i,m}\} \mathbb{E}\{H_{j,m}^*\} = 0$ because channel coefficients are independent random variables. Then the final equation will be

$$\frac{1}{M} HH^H \rightarrow \sigma_h^2 I, \quad \text{as } M \rightarrow \infty \quad (6.46)$$

The interesting phenomena is that as the number of BS antennas grow larger and larger individual user channels becomes more and more orthogonal. It removes the inter user interference, and the BS can communicate with multiple users simultaneously with maximum data rate. The significance is that it is achieved by using simple linear precoding and detection schemes.

Now apply Eqn. 6.46 in Eqn. 6.39, then we get the sum-rate capacity of DPC scheme as

$$C_{DPC} = \max \sum_{i=1}^K \log_2 \left(1 + \frac{p_{d1} M \sigma_h^2 P_{DPC,i}}{\sigma_n^2} \right) \text{ s.t. } \sum_{i=1}^K P_{DPC,i} = 1, \quad (6.47)$$

The optimum solution to the above equation will be when the power allocation $P_{DPC,i} = \frac{1}{K}$

Substituting this in Eqn. 6.47

$$C_{DPC} = K \log_2 \left(1 + \frac{p_{d1} M \sigma_h^2}{K \sigma_n^2} \right) \quad (6.48)$$

Here K is the number of users, and it represents the multiplexing gain achieved by the Massive MIMO system, and M is the number of BS antennas represents the array gain.

In the case of linear precoding schemes, applying Eqn. 6.46 in Eqn. 6.40 the term due to interference in the denominator of Eqn. 6.40 vanishes for all W_{MRC} , W_{ZF} , and W_{MMSE} . Then from Eqn. 6.46 the achievable sum rate for all the three linear precoding schemes can be derived as

$$C_{ZF} = C_{MF} = C_{MMSE} = K \log_2 \left(1 + \frac{p_{d1} M \sigma_h^2}{K \sigma_n^2} \right) \quad (6.49)$$

and is the same as the capacity derived for DPC scheme in Eqn. 6.48.

6.15 Channel Hardening in Massive MIMO

In general, channel hardening means that a fading channel behaves as if it was a non-fading channel. The randomness is still there, but its impact on the communication is negligible. Consider the massive MIMO system in Eqn. 6.44 and 6.45 as the number of BS antennas M grow larger and larger, the instabilities in the $\frac{1}{M}HH^H$ elements rapidly decrease to its respective mean values. This is due to the channel hardening effect in massive MIMO. As mentioned before it doesn't mean that the variations in H reduce to zero, but its effects are negligible, and we get stable outputs after processing [230].

The main results of channel hardening are listed below.

- i) Eliminates the effects of small scale fading: The downlink transmitted power is scaled down by the factor of M , ($P_{dt} = \frac{\rho K}{M}$, in Eqn. 6.40), and that stabilizes the receive SINRs for all the users for all the three types of precoding schemes used. In other words, the SINRs do not fluctuate with the small-scale fading of the channel.
- ii) More stable precoders and detectors: For a given value of P in Eqn. 6.26, due to channel hardening and interference reduction, the variations in the power of the precoded signal z becomes less and more stable, i.e., $\|z\|^2 = \|w\sqrt{p_x}\|^2$ will become stable irrespective of the variations in the transmit symbol x .
- iii) Slower time scale for resource allocation: In Eqn. 6.41, $W^H W$ is hardened in all precoder schemes, and hence the

power allocation P that maximizes the sum rate capacity becomes more stable. Therefore, the power allocation needs to be restructured only when there is large scale fading occurs in the channel.

- iv) Steady value of sum rate capacity: Since the effect of small-scale fading is nullified, the sum rate defined in Eqn. 6.41 also becomes stable, and the probability of getting a rate much lesser than the ergodic rate becomes very less.

The effect of channel hardening on different transmission schemes is studied and analysed in detail in [231,232]. The increase in the number of antennas M makes the random behaved channel to a deterministic one. If both the antenna number M and the number of active users K increases to infinity with M/K remaining constant the eigen value distributions of $\frac{1}{M}HH^H$ also converges to Marchenko Pastur distribution [233].

6.16 Digital Beamforming

In a normal transmitter antenna array, by adjusting the phases and amplitudes of the signal components to different antenna elements, we can steer and focus the obtained direction of beams. This is called as analogue beam forming. Varying the number of antenna elements, signal amplitude and phases multiple beams can be formed and steered to serve different user terminals. In analogue beam forming the number of independent RF-chains limits the number of orthogonal beams and that in turn limits the maximum number of users. But in full dimension, MIMO 3-directional beam can be formed with different elevation and azimuth angles to closely

trace different users [234,]. More number of BS antennas make the beam narrower making the users independent without interference.

The linear precoding scheme explained in section 6.12 works differently from its functioning in analogue beam forming. Here instead of steering the beam towards the intended user, the signals are constructively added up at the intended user and destructively added at all other user locations. As the number of BS antennas grows larger both the effects, constructive adding as well as destructive adding becomes more and more predominant and making the signal strength to go high at the intended user as well as very low interfering signal to other users.

Digital beam forming in massive MIMO forms a very aggressive and flexible means of spatial multiplexing. It also provides easy control over the number of users without any hardware limitation. In massive MIMO, since channel reciprocity is employed, digital beam forming doesn't require any array calibration which a typical limitation of analogue beam is forming where the complexity of calibration increases with the increase in antenna array size.

6.17 Optimizing Number of Users for Maximum Capacity

Here we aim to optimize the number of users K to get maximum sum rate capacity out of a given number of BS antennas and Coherence block length. While looking for the above the main issues faced are,

- it is very difficult to find tractable expressions connecting the above parameters.
- Interference is subjected to the positions of all the users.

Now consider a massive mimo system with BS equipped with M number of antennas and K number of user terminals with a single antenna. Here M is large and fixed whereas K is variable. The geometric location of the user $k \in \{1, \dots, K\}$ in the cell $l \in B$ is $Z_{lk} \in \mathbb{R}^2$

The most anticipated situation for massive MIMO for maximizing the data rate is to ensure mutual orthogonality explained in favorable propagation. For a fixed deterministic channel with channel matrix as H , the sum capacity is expressed as

$$C_{sum} = \log_2 |I_M + \rho_{ul} H H^H| \quad (6.50)$$

Where p_{ul} is the uplink SNR for a single terminal, H is a $M \times K$ matrix with M number of BS antennas and K number of active mobile users.

6.18 Related Works

This section summarises the important works related to the study and analysis of the spectral efficiency performance of massive MIMO networks in recent publications.

Spectral efficiency is an important performance measure in wireless cellular networks. The area spectral efficiency and area energy efficiency of a multiuser massive MIMO wireless cellular system is theoretically examined by Y. Xin et al. in [235] and obtained the system parameters for maximum area spectral efficiency. They have considered the pilot contamination effect and derived a general and closed-form approximation for area spectral efficiency in a cellular system with massive MIMO. The impact of pilot contamination on the spectral efficiency has been considered in detail

by Müller et al. in [140], and Wang et al. [236]. It gives a vigorous study on this under various channel conditions. However, there still exist some adverse factors that affect the performance of the TDD systems in practice, such as calibration error in uplink and downlink radio frequency chains and problems due to hardware impairments are studied by Guey et al. in [237] and E. Bjornson et al. in [227]. All these factors are analysed and its impact on the spectral efficiency is analysed in these papers.

The energy efficiency and spectral efficiency of multi-layer full duplex amplify, and forward relay systems are studied in H. Cui al. in [238] and S. Jin et al. in [239] and it shows that massive MIMO antennas can normalize the small-scale fading by using simple signal processing methods and thereby minimize the transmitted power without affecting the performance of the system.

In [240] H. D. Nguyen et al. have compared massive MIMO and small cell networks and showed that the small cell systems perform better in terms of the energy efficiency and massive MIMO outperforms in terms of rate performance and spectral efficiency in all operating conditions. T. Van Chien et al. in [241], a multi-cell massive MIMO downlink system using non-coherent joint transmission is optimized to have minimum transmit power consumption keeping all the QoS fulfilled. Four different power management schemes are designed for various channel estimation. Techniques and its performance are evaluated using simulation models in [242] by Z. Zhang et al. The SE is analytically compared between two channel estimation methods and evaluated the performance of full duplex and half duplex modes of operation. It is

also demonstrated that the energy efficiency is steady as the number of relay antennas increases to infinity. An energy efficient resource allocation scheme for massive MIMO FDD systems for improved spectral efficiency is investigated and numerical results are obtained. Macro cells with massive MIMO base stations on highly concentrated small cells are studied by J. G. Andrews et al. in [91] and by J. Hoydis et al. in [202]. They have shown that the utilization of an excessive number of antennas at the base station for interference management greatly improves the spectral efficiency and gives extended coverage.

Different precoding schemes used for massive MIMO wireless systems are analysed by Selvan et al. in [243] and SE is evaluated by using simulation models. Massive MIMO characteristics under large scale fading with perfect and imperfect CSI are analysed by Lin et al. in [244] and an expression for SE is derived as a function of the number of transmitting antennas, the number of users and the transmit power. These expressions are validated through simulations for different large-scale fading parameters.

Mathematical expressions for SE are derived which are valid for the uplink as well as downlink transmissions and are evaluated using MATLAB simulation models considering maximum ratio combining method for channel estimation by Björnson et al. in [245]. The impact of massive analogue to digital converters on the SE of flat fading channels in massive MIMO systems are thoroughly studied in by Risi et al. in [246] and Liang et al. in [247]. It assumes Rayleigh fading channel and one-bit resolution for the ADC which is often not true in line-of-sight wireless communications.

The SE of massive MIMO systems in Rician fading channels with low-resolution ADCs are investigated under perfect and imperfect Channel State Information by Zhang in [248]. It shows how the Rician K factor and base station antenna numbers and the ADC resolution affect the uplink SE.

In centralized MIMO where receive and transmit antennas are co-located both at the receive and transmit side and in distributed MIMO base station antennas are placed at different physical locations and connected through wide band fibre optic links. C-MIMO is practically easy to install and for theoretical analysis. D-MIMO suffers from various levels of path losses and in turn, its analysis becomes very complex. However, D-MIMO has advantages such as high spectral efficiency, better coverage area, improved multiplexing gain and better network planning. The SE performance of D-MIMO and C-MIMO are studied by Xia et al. in [249] and Schuh et al. in [250]. A generic channel model, meeting the requirements of both massive C-MIMO and D-MIMO with all important physical parameters and environmental parameters, is developed and tested using simulations by G. N. Kamga et al. in [251].

In [252] Ramprashad et al. proved that the simple Linear Single-User Beam-Forming (LSUBF) and random user scheduling, can give a significant increase in the spectral efficiency of TDD cellular systems without any combined processing in the base station antennas with a condition that for each active user a large number of transmitting antennas are used at each base station. The concept of dynamic clustering of cooperating base stations and multi-user MIMO in a mixed mode have been discussed in vast published

literature [253-258]. A wireless communication network with MIMO TDD architecture, which requires a fewer number of antennas per active user, has been studied by H Huh et al. in [259] and shown that it can reach spectral efficiencies that are comparable with the normal Massive MIMO scheme.

Huge improvement in the data rate is identified as the main advantage of using massive MIMO for cellular mobile communications and because of this property it is considered as the most promising technology available today to address the ever-increasing demand for wireless throughput. The spectral efficiency that determines the throughput in a massive MIMO system depends on many of the system parameters, standards and methods used. Optimization of the spectral efficiency by considering all these parameters, standards and methods altogether is not yet carried out in any of the works.

6.19 System Model

Consider a massive multi-user MIMO system represented in Fig. 6.1 with BS carrying M number of antennas K number of active parallel uplink/downlink users. The downlink data transmission system model used for the simulation is shown in Fig. 6.10. Here each antenna is supplied with the sum of information symbols intended for each of the users. Antenna-1 multiplies the signal x_1 intended for user-1 with the conjugate of the estimated channel (h^*_{11}) and each of the antennas does the same thing. Hence all the signals in tailing x_1 arrive in phase at user-1 and hence the amplitude of beam-forming gain goes with antenna M and they tend to arrive at out of

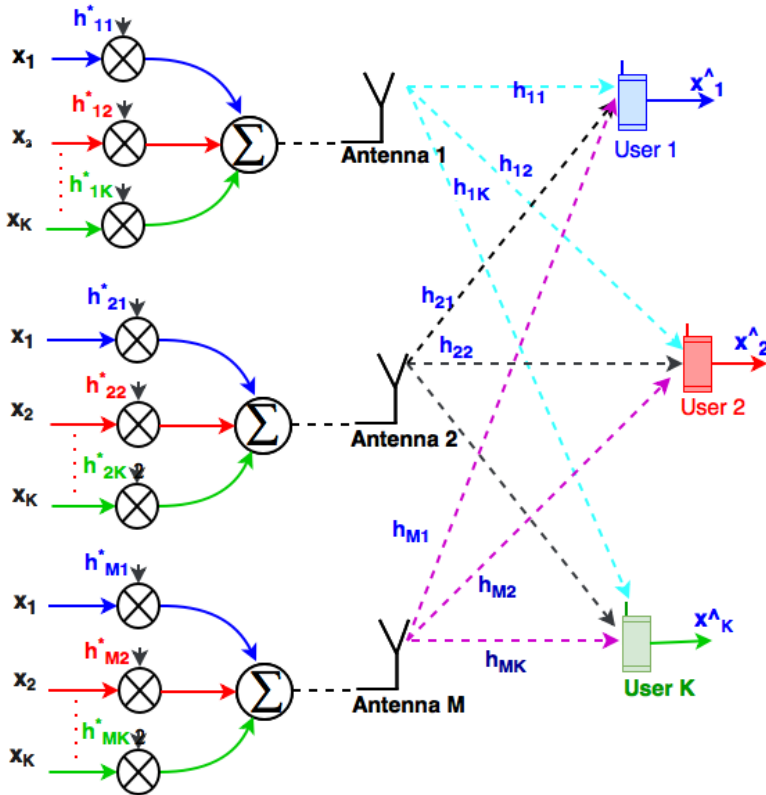


Figure 6.10 Downlink data transmission

phase at the other users and hence their amplitude goes as the square root of them. It uses the simplest possible precoding and beamforming technique, which is zero forcing.

In the uplink data transmission model is shown in Fig. 6.11. Signals from different users are collected by the antenna and then individually multiplied by the conjugate of the channel estimate and then it is added with the corresponding multiplier outputs from the other antennas to get the desired signal. The uplink signal received at the BS_j in a frame is given by

$$y_j = \sum_{l=1}^L \sum_{k=1}^K \sqrt{p_{lk}} h_{jlk} x_{lk} + n_j \quad (6.51)$$

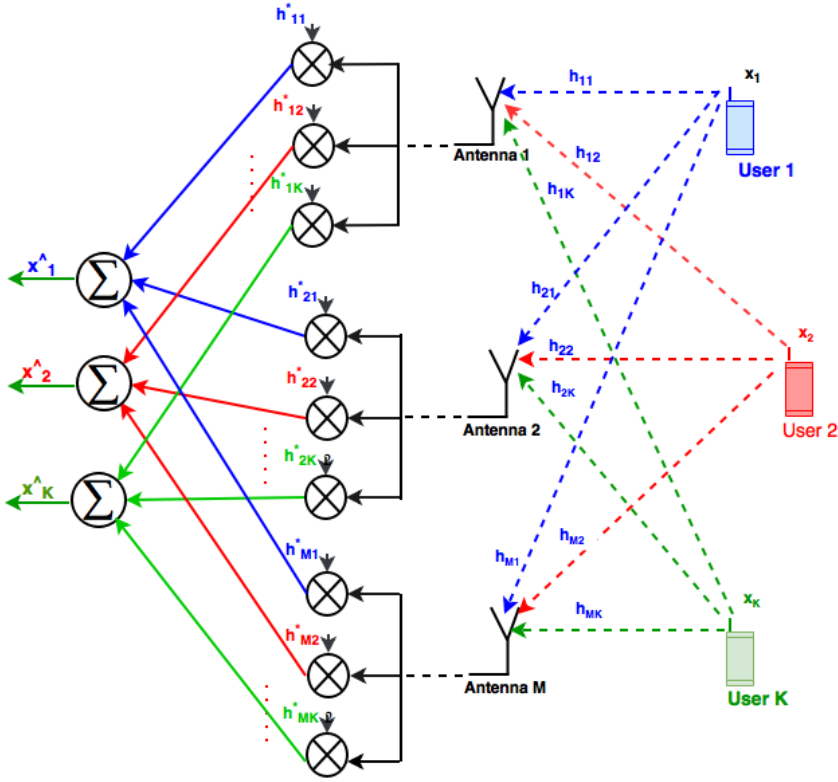


Figure 6.11 Uplink data transmission

where L is the number of cells, K is the number of users, X_{lk} is the symbol transmitted by the k^{th} user in the l^{th} cell and p_{lk} is the transmit power, h_{jlk} denotes the channel response between the j^{th} BS and k^{th} UE in the l^{th} cell in a given frame and n_j is the additive noise component.

The received signal on the downlink by the k^{th} user at the j^{th} cell is given by

$$Z_{jk} = \sum_{l=1}^L \sum_{k=1}^K h_{ljk}^T w_{lm} S_{lm} + n_{jk} \quad (6.52)$$

where h^T is the transpose of the channel response h , S_{lm} is the symbol meant for m^{th} user in l^{th} cell, w_{lm} is the precoding vector and n_{jk} is the additive noise.

The theoretical maximum of the attainable uplink and downlink spectral efficiencies are given by the following equations [111].

$$SE_{UL} = \partial^{UL} \left(1 - \frac{B}{S}\right) \mathbb{E}_{(x)}\{\log_2(1 + SINR_{jk}^{(UL)})\} [bits/s/Hz] \quad (6.53)$$

$$SE_{DL} = \partial^{DL} \left(1 - \frac{B}{S}\right) \mathbb{E}_{(x)}\{\log_2(1 + SINR_{jk}^{(DL)})\} [bits/s/Hz] \quad (6.54)$$

The spectral efficiency expressions for the uplink and downlink are almost identical, only the uplink and downlink fractions differ. $\mathbb{E}_{(x)}$ is the expectation of the UE positions and SINR is the effective signal-to-interference-and-noise ratio. Now when we consider the number users K per cell the SE expressions per cell for uplink and downlink can be expressed as

$$SE_j^{UL} = K \partial^{(UL)} \left(1 - \frac{B}{S}\right) \log_2(1 + 1/I_j) [bits/s/Hz/cell] \quad (6.55)$$

$$SE_j^{DL} = K \partial^{(DL)} \left(1 - \frac{B}{S}\right) \log_2(1 + 1/I_j) [bits/s/Hz/cell] \quad (6.56)$$

where SE_j represents the SE of the j^{th} cell, B is the number of symbols in a data frame, S is the coherence block length and I_j represents the interference. The next consideration that has to be taken is the finite and asymptotic analysis. Here we assume that the uplink fraction and downlink fraction give a sum of 1. i.e. $\partial^{(DL)} + \partial^{(UL)} = 1$, then the SE can be expressed as

$$SE_j = K \left(1 - \frac{B}{S}\right) \log_2(1 + 1/I_j) [bits/s/Hz/cell] \quad (6.57)$$

This makes the analysis much easier because the final spectral efficiency equation that we arrived at is independent of two factors $\partial^{(DL)}$ and $\partial^{(UL)}$, the uplink and downlink fractions. This permits us to analyse and optimize the spectral efficiency of the communication system as a whole without considering the downlink and uplink separately.

6.19.1 Model Characteristics

In this work, we have considered following characteristics for the massive MIMO wireless model

- i) Amplify and forward relaying scheme: Basically, it sends an amplified version of the received signal in the last time slot and compared with the other relaying scheme such as decode and forward. This scheme requires very much less computing power and incurs very less delay.
- ii) Dual hop transmission system: Each of the hops is dependent on each other.
- iii) Full Duplex communication: Wireless full duplex system allows simultaneously transmitting and receiving signals over a single channel. The uplink and downlink channel transmitter and receiver function independently.
- iv) TDD scheme of communication: In time division duplex communication links different time slots in same frequency band are allocated for the uplink and downlink channels as per the network load requirements.

- v) Number of BS antennas and users: Base station has M number of Transceiver antennas and supports K number of active users in each cell.
- vi) Noise variance $\sigma_R^2 = \sigma_D^2$: Noise is purely random and has zero mean, noise power is equal to its variance. Here noise variance at the receiver and the destination is assumed to be the same.
- vii) The signal to noise ratio(SNR): SNR which is the measure of signal power to the background noise power is assumed to be ranging from 0 dB to 5 dB.
- viii) Channel Estimation using pilot signals: Channel estimation is the technique to measure the characteristics of a wireless channel and an easy method to do this is by comparing known transmitted (pilot) signals and the received signals. Since we have only limited number of orthogonal sequences to be used as pilots, they must be reused in adjacent cells and this similar adjacent cell pilot orthogonal signal interfere with each other and cause pilot contamination.
- ix) Frame structure: A total number of 'S' symbols are transmitted in a frame, out of which 'B' is the number of symbols used for pilot transmission. From the remaining (S-B) symbols $\partial^{DL}(S - B)$ symbols are used for downlink and $\partial^{UL}(S - B)$ symbols are used for uplink ∂^{DL} and ∂^{UL} are the fractions for downlink and uplink transmission. Details are shown in Fig. 6.12

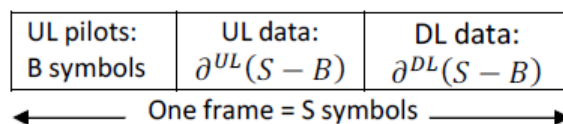


Figure 6.12 Frame structure

- x) Coherence time and bandwidth: Coherence time is, the time duration over which the impulse response of the channel remains constant, taken as T_c seconds. Coherence bandwidth is the range of frequencies in which the channel is assumed as flat, taken as W_c Hz. Then block length $S=W_cT_c$ symbols, we set $S=400$ (e.g.: 200kHz coherence bandwidth and 2ms coherence time).
- xi) Pilot reuse factor: It is the number of cells in a cluster in which the same pilot sequence is used. Pilot reuse factor $\beta = B/K \geq 1$: B is the number of symbols in a frame used for pilot transmission and K is the number of users. Value of β is overall considered as greater than one.
- xii) Precoding algorithm: Precoding is a technique where transmitter sends information coded according to the pre-knowledge of the channel. Here the conventional linear precoding schemes Zero Forcing is used. MRC and MMSE are also considered for comparison.

6.20 Results and Discussions

A simulation model with the above said characteristics has been set up using MATLAB to evaluate the SE performance of the Massive MIMO antenna system. All users are assumed with the same SNR value and independent Rayleigh fading channels with perfect CSI. The effect of various parameters like number of BS antennas, number of active users, coherence block length, and different precoding algorithms on SE is studied and results are analysed.

In Fig. 6.13 variation of the SE is plotted against the number of BS antennas ranging from 10 to 1000 keeping the number of active UEs (K) in each cell as constant. The simulation is repeated for a wide range of active UEs from 2 to 80. The simple linear precoding technique, zero forcing is used for the above simulation. From simulation results, it can be inferred that the SE increases abruptly with the number of BS antennas at

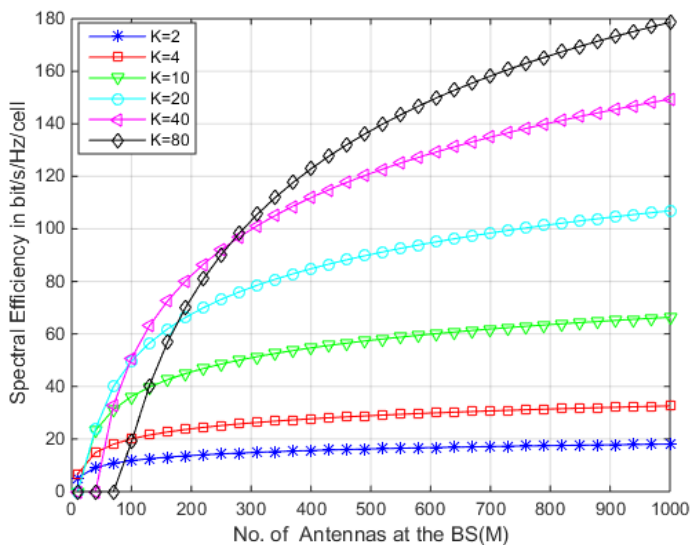


Figure 6.13 SE per cell versus M for different values of K

the beginning and later it becomes almost saturated. With less number of users, SE reaches its maximum with less number of BS antennas because only less number of spatially diverse beams are required to serve all the UEs and also there is no need for very narrow beam shaping. When we compare the SE plot for $K=40$ and $K=80$ at the initial portion where the number of BS antennas are less, $K=40$ gives better spectral efficiency than $K=80$. This is because in this region the number of BS antennas is not sufficient to provide the necessary

beam-forming and spatial diversity required for the large number of users. This situation will create more ICI and reduces the SE.

In Fig. 6.14 variation of the SE is shown against the number of UEs keeping the number of BS antennas as constant. Consider the red coloured plot with $M=100$, where SE increases with an increase in K and reaches the maximum value of 54 when K becomes 30 and then reduces gradually

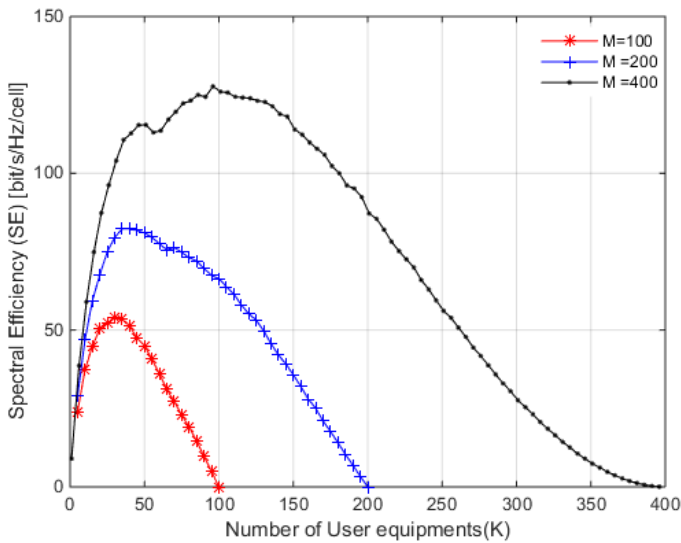


Figure 6.14 SE per cell versus K for different M

and reaches zero for a value of K equal to 100. It shows that 30 is the optimum number of users that can be served with 100 number of BS antennas, trying to serve more number users will make the available number of BS antennas insufficient to form the necessary spatial diversity and beam-forming. Increasing the value of M from 100 to 400 rises and optimum K from 30 to 100. So, it is preferable to have M/K ratio of more than 4 to get the best out of the massive MIMO

system. This is again verified in Fig. 6.21 by plotting SE performance for various M/K ratio.

Fig. 6.15 shows the effect of coherence block length (S) on the per cell SE. Massive MIMO can schedule more number of UEs when the value of coherence block length is high and that will give a good improvement in SE when both the coherence block length and number of UEs are large. When $K=20$, the system has to schedule only less number of UEs and most of that will be successful even when the coherence length is 400 and an increase to 800 will not give considerable improvement in SE, whereas the SE improvement is very high in $K=40$, for the same increase of S from 400 to 800.

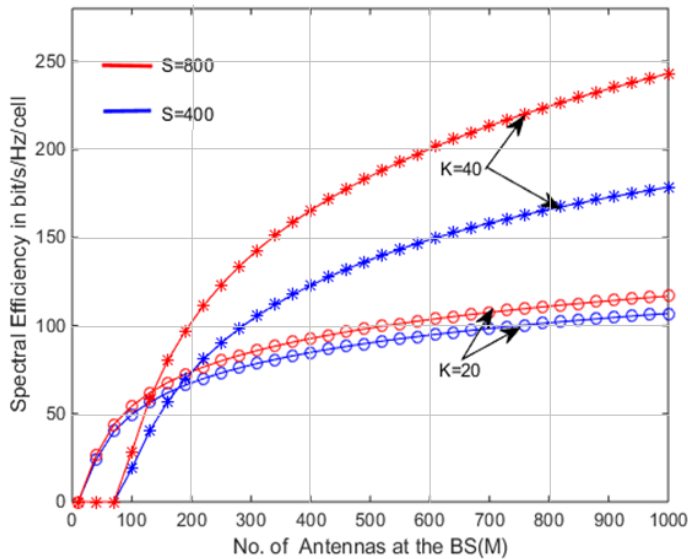


Figure 6.15 Impact of coherence block length(S) on SE

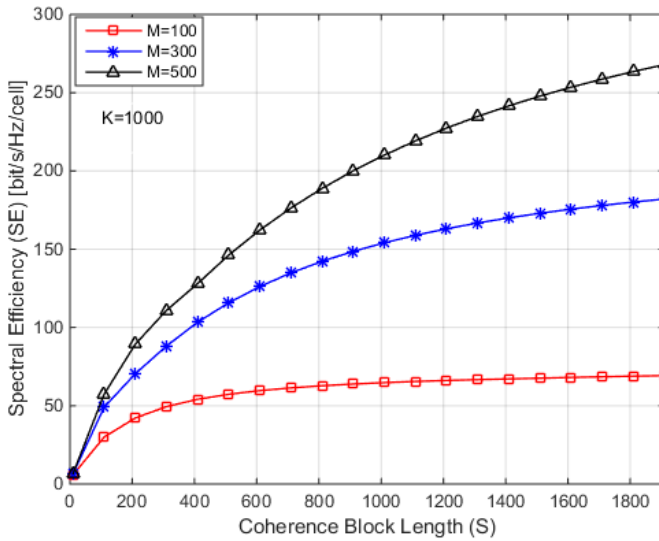


Figure 6.16 SE vs. Coherence block length for different M

Fig. 6.16 shows the SE variation against the coherence block length. The SE saturates faster when $M=100$, because here the SE is limited by the number of BS antennas and not by the coherence block length. For $M=500$ the SE increases with increase in coherence block length because the number of UE is kept as high at 1000 and the system needs to schedule all these UEs and that needs longer coherence block lengths.

Fig. 6.17 shows the comparison between simple linear signal processing scheme (ZF) that used at the receiver in place of complex non-linear processing. It shows that a simple linear signal processing scheme like ZF would give almost the same spectral efficiency achievable with nonlinear processing schemes if the number of antennas at the BS(M) is larger than twice the number of active mobile terminals($K=10$). It is also important to note that both schemes are reaching the SE of ideal condition with no interference

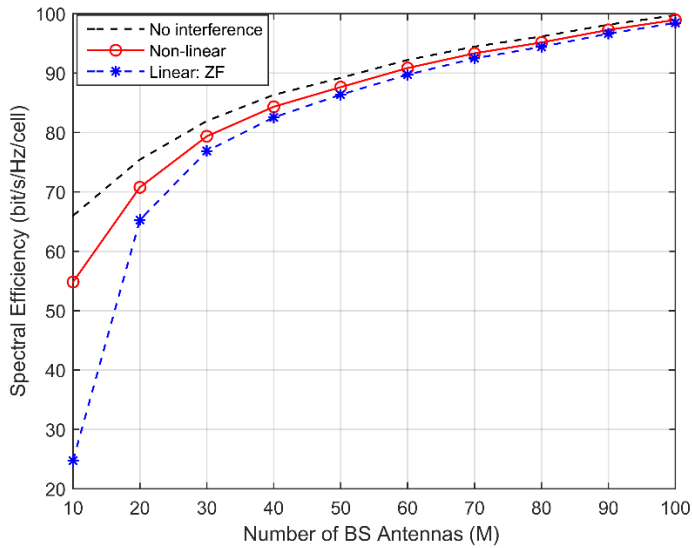


Figure 6.17 Linear Vs. Non-linear signal processing

when the number of M is to about five times the number of active users.

To understand the SE performance when $M < 2K$, the simulation plot in Fig. 6.17 is expanded between $M = 2$ to 20 and is given in Fig. 6.18. It is clear that when $M = K$, the SE of non-linear processing scheme is double than that of linear processing scheme but as the number of $M \geq 2K$ the difference between the values of SE for the two schemes become negligible. It also shows the drastic deterioration of the SE value when M is made less than K . The SE decreases from 50 to 5 when M is reduced from 12 to 8. So, in order to have the benefits of massive MIMO system along with the simplicity of linear signal processing at the receiver, we must ensure a minimum antenna size of $M=2K$.

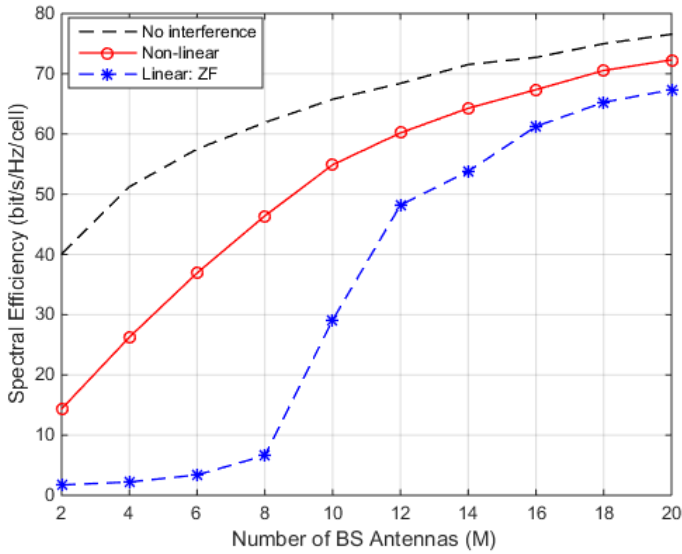


Figure 6.18 Linear Vs. Non-linear signal processing (expanded)

In Fig. 6.19 we analyse the potential of SE under three different linear precoding techniques Minimum Mean Square Error, Zero-Forcing and Maximum Ratio Combining. An excessive number of base station antennas compared with the number of users makes the simple linear signal processing techniques work to nearly optimal in massive MIMO systems [214]. Hence in this plot, we can find for all the three schemes the SE increases in the same manner with an increase in the number of BS antennas. With MRC precoding the BS tries to maximize the received SNR of each data stream neglecting the effect of multi-user interference whereas ZF receivers take the inter user interference into consideration and neglect the effect of noise and MMSE receiver always try to maximize the received SINR. Hence ZF always outperforms MRC and gives better SE for all values of K as well as M. MMSE outperforms both MRC and ZF in terms of its SE performance because the MSE value is lesser than the other

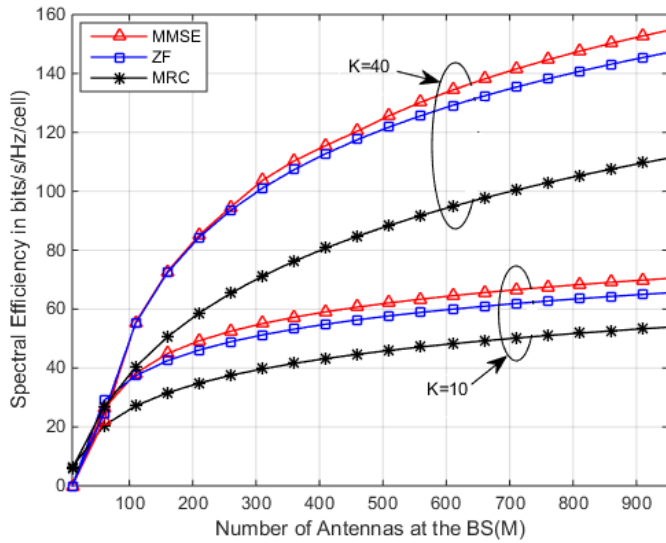


Figure 6.19 Impact of precoding techniques ZF and MRC on SE

two schemes and also the power penalty due to the interference suppression is smaller in MMSE than in ZF.

In Fig. 6.20 optimum value of UEs for different coherent block lengths (S) is plotted against varying number of BS antennas. Value of S depends mainly on the mobility of the user, frequency of operation and propagation environment. The CSI acquisition is limited by the channel coherence and how this impacts SEs is shown in the above graph. When the number of users is more, it needs more time to schedule all the users and a limited coherence block length limits the SE of the system. It is understood from this graph that the coherence block length limits the maximum number of active users in a single cell. Doubling the value of S from 200 to 400 gives an increase in K from 90 to 180.

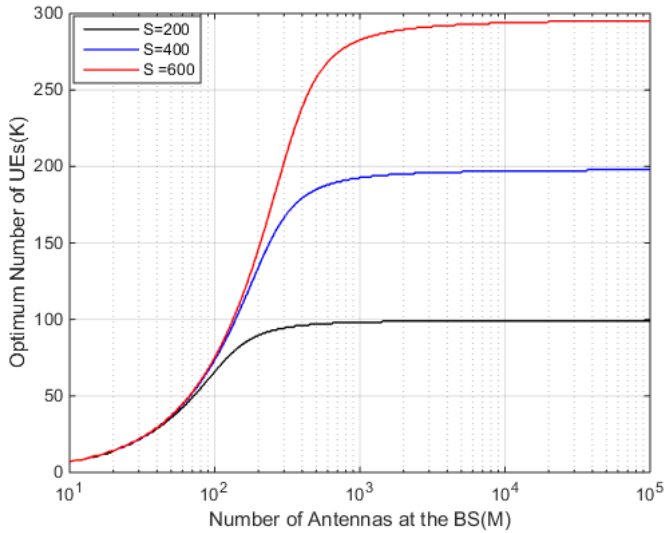


Figure 6.20 Optimum value of K versus M for different values of S

In Fig. 6.21 we have considered an interesting case where the number of BS antennas M is increasing proportionally to the number of UEs K . The curve is plotted for four different values of the antenna to UE ratio $M/K=[1,2,4,8]$. The spectral efficiency increases linearly with the number of UEs in all the four different M/K ratios where the gradient of the curve increases with the increase in M/K ratio. The reason for this sharp increase is that when $M \gg K$ it will become very easier for the system to cancel out the interferences. Corresponding to a value of $K=20$, the first doubling of M/K ratio provides an increase of 84% increase in SE whereas the 2nd doubling gives 50.8 % increase and the 3rd doubling gives 34.8 % increase in the SE. So, the relative increase in the improvement is decreasing as we increase the ration M/K . $M/K \geq 4$ can be considered as an optimum value for multi-user MIMO operations. Comparing this with Fig. 6.14 and also considering overhead incurred on channel estimation we can

conclude that for each value of M there is a particular value of K that maximizes the SE of the system.

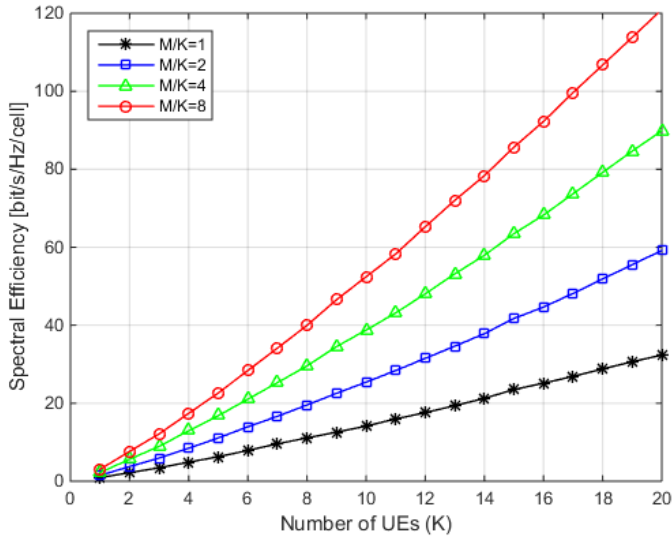


Figure 6.21 SE Vs. No. of UEs per cell with different BS antenna to UE ratios M/K .

To compare the SE performance of TDD and FDD systems in massive MIMO environment it is experimentally evaluated using simulation and the results are shown in Fig. 6.22. It clearly shows how pilot length restriction limits the spectral efficiency of the system in an FDD system under ZF and precoding scheme. TDD systems are highly scalable as they always get benefited by adding more number of antennas at the BS. Whereas in FDD the pilot sequence length limits the SE performance. When the pilot sequence length is kept as 10, the SE performance of FDD remains literally constant at the value of $M=10$ which illustrates the necessity of pilot sequence length of $(M+K)/2$ in FDD mode operation. FDD mode can take the benefit of

adding extra antennas to the BS only by correspondingly increasing the pilot sequence length which adds a lot of pilot overhead to the system.

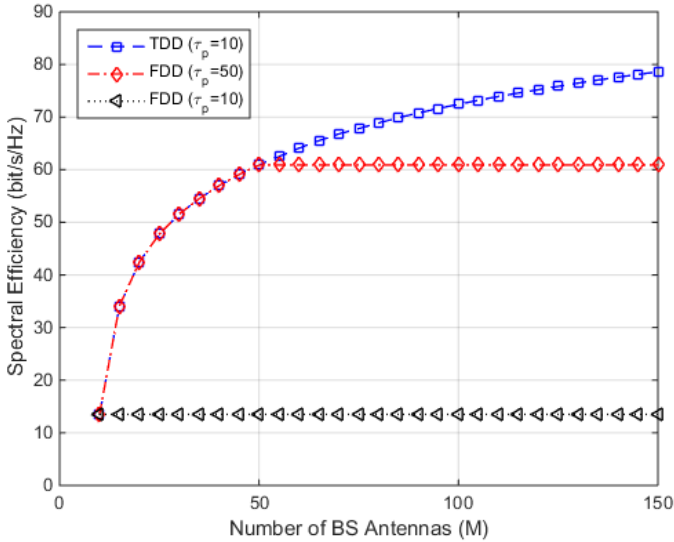


Figure 6.22 Effect of CSI and pilot sequence length under FDD and TDD mode

In Fig. 6.23 we study how the average SNR of the system affects the performance of the massive MIMO system. The SE reaches saturation at around and SNR value of 5dB SNR which is due to the array gain of massive mimo antenna system obtained through coherent processing. Because of this reason in all the previous simulations we have selected the average SNR value as equal to 5dB. As evident from the graph, the system can operate even at lower SNRs but at the expense of performance loss.

Fig. 6.24 shows the effect of SNR among different precoding schemes. The simulation is carried out for a fixed number of $M=500$ and it shows that MMSE and ZF are more sensitive to the average

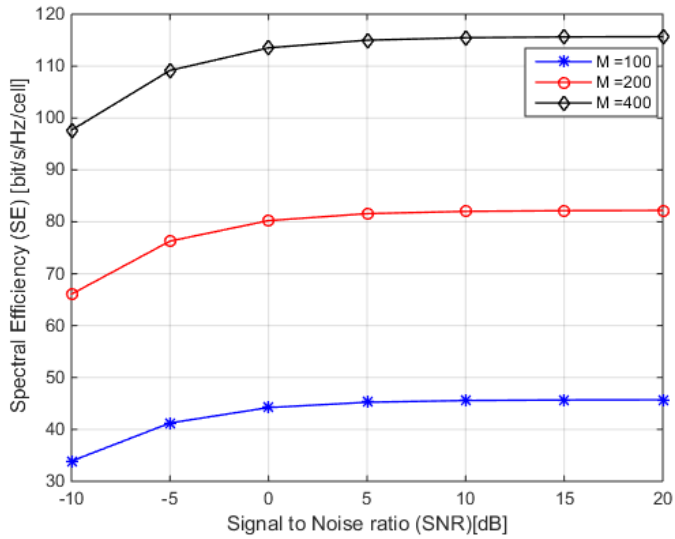


Figure 6.23 Effect of SNR variation on Spectral Efficiency

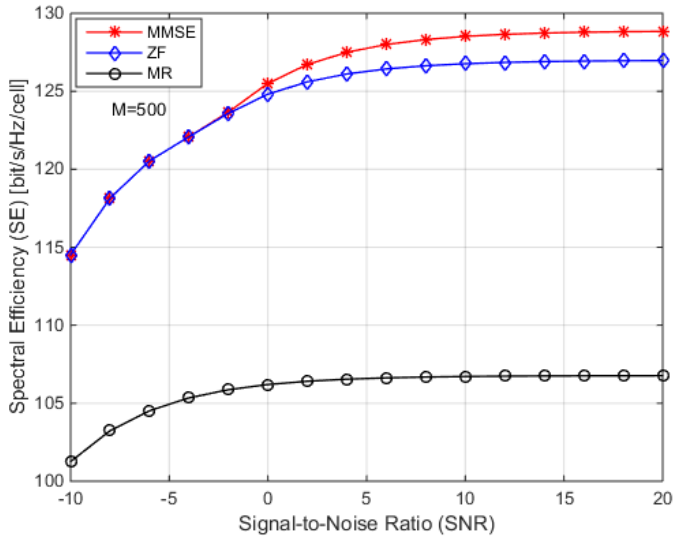


Figure 6.24 Effect of SNR variation and different precoding schemes on SE

SNR of the channel. This is due to the fact that the suppression of interference requires higher quality in CSI estimation than that required in MRC.

6.21 Practical Discussion

In massive MIMO communication system as the number of base station antennas are increased the random behaviour of channel properties starts to become more and more deterministic. The effect of intra cell interference in massive MIMO is greatly alleviated by spatially mitigating the interference. As the number of active UEs are increased keeping the number of BS antennas as constant, the SE will increase first and then reach a maximum value and finally start to decline to minimum. It means that as long as the multiplexing gain of the system balances the additional pilot overheads and added interferences the SE will increase and when it fails to do so the SE will start decaying. So, as shown in Fig. 6.25 three operating regions can be defined. First, the multiplexing region where the SE increases almost linearly with the number of UEs served by the BS. In this region, the large multiplexing gain of the system leads over the additional interferences and pilot overheads.

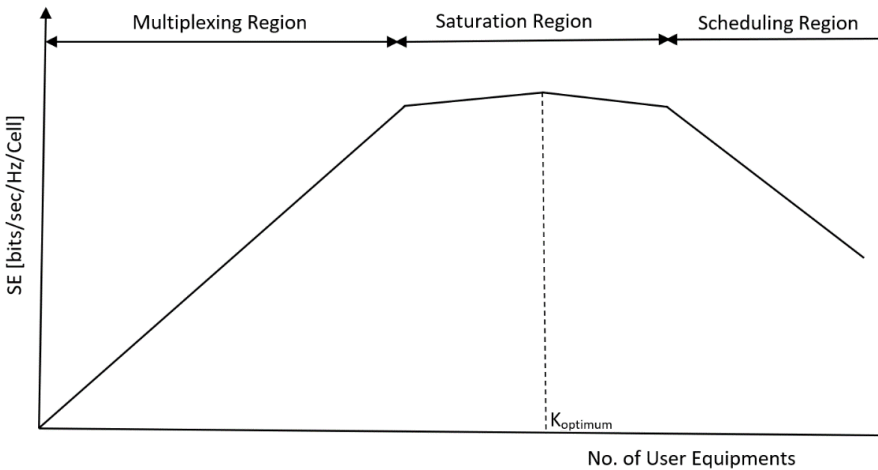


Figure 6.25 Massive MIMO operating regions

The second region can be called as saturation region where the increase in SE decelerates and ultimately reach the optimum number of UEs (K_{optimum}) that delivers the highest SE. Beyond this point for each extra UE that we add the SE deteriorates. A properly designed cellular network should work mostly in the saturation region and rarely in the multiplexing region when the data traffic goes low due to the lower number of UEs. Scheduling of the UE becomes trivial as all the frequency and time resources are already allotted to the presently served UEs. Finally, the third region can be called as scheduling region where the SE starts decreasing because all the active UEs cannot be served parallelly through spatial multiplexing. Proper scheduling of the time and frequency resources is to be used here to bring down the actual number of UEs to K_{optimum} when more than K users in a cell tries to access the network so that the system work near to the highest SE point.

6.22 Key Findings

The findings of the numerous analysis carried out on the SE performance of the massive MIMO system, with different parameters, methods and operating conditions, can be summarized as below.

- The most anticipated situation for massive MIMO for maximizing the SE is to ensure mutual orthogonality explained in favorable propagation.
- Massive MIMO with simple linear precoding techniques like ZF can achieve the same SE as that of complex nonlinear precoding techniques like DPC if the BS antenna size is greater than twice the number of UEs(K).

- Both the nonlinear and linear precoding schemes can provide approximately the ideal value (zero interference) of SE when the BS antenna size grows above 5K.
- TDD mode of operation is much superior to FDD mode in massive MIMO in term of SE performance. Only TDD can give the full benefits of adding extra antennas to BS while FDD needs to have increased pilot sequence length and pilot over head to achieve the same performance.
- With less number of UEs (<10), the SE saturates at around a BS antenna size of 25K but as the number of UEs grows larger, the saturation is delayed to much higher BS antenna sizes due to the increased ICI and pilot contamination effects.
- When the number of UEs are less, scheduling of all the UEs will be successful even with shorter coherence block lengths and the full benefits of adding extra BS antennas will be available as improvement in SE.
- MMSE and ZF are more sensitive to the average SNR of the channel. This is due to the fact that the suppression of interference requires higher quality in CSI estimation than that required in MRC.
- Owing to the maximization process of the received SNR at every user, MRC will be suitable for noise limited scenarios. In high SNR conditions the performance will be limited by inter user interference, and in that case, ZF is superior to MRC.

- The relative increase in the improvement of SE is decreasing as the ratio of M/K is increased. $M/K \geq 4$ can be considered as an optimum value for multi-user MIMO operations and for each value of M there is a value of K that maximizes the SE of the system.
- Compared to conventional communication systems the effect of channel SNR on system performance is very less in a massive MIMO system. Even with poor SNR and interference conditions, the SE can be considerably increased by increasing the number of BS antennas. An SNR value of 0dB itself can give even 95% of the saturated SE value.
- Practically each mobile user will have a separate coherence-time and coherence- bandwidth, it is very difficult for the network to adapt to these values because the same protocol will be applied to all the UEs. So it is preferred to select the coherence block size to the worst case condition that the communication network has to support.

6.23 Chapter Summary

In this chapter, the spectral efficiency and various aspects that affect the spectral efficiency performance of massive MIMO system has been investigated in detail. A Massive-MIMO system with TDD architecture is designed and different methods to maximize its SE are well examined. The effect of the number of active users in a cell, length of coherence block, number of base station antennas and

different linear precoding methods on the spectral efficiency are evaluated through simulation. The impact of SNR variation on the SE performance is also evaluated. From the results, it is inferred that high SE per cell is attained by simultaneously scheduling more number of UEs for transmission. Within the available spectrum, Massive MIMO can schedule more UEs with larger coherence block lengths and SE performance increases with increase in the number of BS antennas. MMSE precoding is the better option in terms of maximizing the SE and its implementation is very simple. We have also proved that for each value of the number of BS antennas there exist a particular value of the number of users that maximizes the SE of the system. Results also reveal that a massive MIMO with 100 BS antennas can easily achieve an SE much more than 10 times the International Mobile Telecommunications-Advanced (IMT-Advanced standard) requirement of 3 bit/s/Hz/cell [260] and BS with larger antenna arrays of 400 elements can go above 40 times the IMT requirement.

CHAPTER-7

PILOT DECONTAMINATION FOR MASSIVE MIMO USING SOCIAL SPIDER OPTIMIZATION ALGORITHM

7.1 Introduction

The promising capacity and data rate brought by massive MIMO communication systems lead to consider it as a very prominent fifth generation mobile technology. Pilot contamination is identified as the most significant impairment that limits the exploitation of its optimum capacity. It is caused by the re-use of the same, or at least non-orthogonal pilot sequences, among different cells that degrade the performance of channel estimation. In order to mitigate this issue, we propose a novel partial pilot re-use strategy among users in the adjacent cells, which are close to the base station and also possesses minimum movement velocity. The social spider optimization algorithm (SSOA), which imitates the cooperative behavior of social spiders, is used for selecting the eligible users for this pilot reuse in the neighboring cells. The algorithm tries to maximize the lowest SINR value for every user in the cell. The performance of the proposed method is evaluated through simulations, and it is confirmed that the proposed method gives a better bit error rate (BER), sum-rate, and normalized mean square error (NMSE), over the conventional pilot assignment schemes.

7.2 Pilot Contamination

In a massive MIMO system, the base stations are equipped with a large number of phase-coherently cooperating antennas. This enables spatial multiplexing of many user terminals using the same time-

frequency resources. This, in turn, gives a large coherent beam forming gain which is directly translated to increased spectral efficiency, reduced interference and better cell-edge coverage [261]. Although very promising, practical implementation of massive MIMO poses several challenges in its implementation, though the solutions for most of them are available at least in theory.

Collective research projects like Mobile and Wireless Communications Enablers for the 2020 Information Society (METIS) and 5G NOW, with other research organizations like 3rd Generation Partnership Project (3GPP), LTE-Advance and IEEE 802.16m cellular networks which are mainly drawn from industry, academia, and public-private partnership have taken up the challenges to make massive MIMO capable to meet the intense future demands in wireless data traffic [91].

Massive MIMO was originally proposed for time division duplex (TDD) operation but can effectively use also in frequency division duplex (FDD) operation. Even with TDD operation, channel reciprocity is a simplifying assumption that is not expected to hold in practice. However, calibration methods exist that can make the forward and reverse links approximately reciprocal and facilitate massive MIMO. The gains with MRT/MRC depend on the orthogonality of channel responses to different terminals, which set the conditions for favorable propagation. Recent studies point out that favorable propagation might be achievable even for moderate antenna sizes in practice [262]. The resources available for channel estimation are fundamentally limited by the coherence interval. In a multi-cell setup, these resources have to be reused across cells, leading to pilot

contamination. The capacity and other performances of Massive MIMO are upper bounded by pilot contamination. The impact of pilot contamination on real systems is hotly debated and is the topic of this chapter.

This work is aimed at examining the sources and the negative effects of pilot contamination in massive MIMO systems under TDD scheme. Analyzed most of the proposed methods to eliminate or to reduce the effects of pilot contamination in a multi-user multi-cell systems within the previous decade. It also suggested a simple and novel method and an algorithm to reduce the effects of pilot contamination. The algorithm has been implemented using MATLAB and results are analyzed to evaluate the performance.

In practice to attain the advantages of massive MIMO, an accurate estimate of the channel state information is to be acquired by every base station either by direct feedback or by reciprocity of channel. Compared to FDD, TDD has been considered as a better means to obtain precise and timely CSI in all modern wireless systems. In the case of TDD, estimation is performed in one direction and the estimates are used for both directions assuming channel reciprocity. Where as in FDD, both forward and reverse directions need to have estimation and feedback. [97,89]. However, due to the large antenna array and the aggressive spatial multiplexing channel estimation for massive MIMO is highly challenging [98].

Under TDD scheme, the pilot sequences (training signals) and the assumption of channel reciprocity are the important features for its successful application. Under reciprocity it is assumed that the channel

response in the reverse direction is equal to the transpose of the forward channel. The necessary estimates of CSI are calculated from the uplink pilots transmitted from the UEs to the BSs [253]. In order to successfully implement this in practice, an antenna calibration scheme must be implemented at the receiving and /or at the transmission side because the characteristics of the receive and transmit RF chains are different [263].

For calculating the minimum number of pilots required for CSI estimation, T. T. Marzetta [264] has suggested a number equal to the number of active users at any time of operation where as B. Hassibi et al. [9] shown that the number of pilot symbols has to be greater than the number of active users for making the data and pilot power to be equal. In most of the research works conducted in pilot contamination in massive MIMO, the number of pilot sequences is taken as same across all the cells irrespective of the differences in the number of active users. In contrary E. Bjornson et al. [265-266] have come up with successful performance with arbitrary pilot allocation in various cells of a multi-cell system.

Again, as discussed in the previous chapter spectral efficiency is the most important factor in a massive MIMO system and it requires the use of proper pilot reuse factor to maximize the system spectral efficiency [144]. Such pilots used for channel estimation in massive MIMO with TDD architecture may be contaminated due to the reuse of nonorthogonal pilot sequences among various cells of the multi-cell system [11,267]. This, in turn, produces ICI whose magnitude will be proportional to the number of base station antennas. This, in turn, puts a limit on the maximum number of BS antennas [268] that can be used

and hence limit the maximum achievable rate and spectral efficiency of the network [269].

Several methods have been suggested for the reduction of ICI with an importance on the elimination of pilot contamination during the channel estimation. Although reuse of the non-orthogonal pilot sequences is identified as the only source of pilot contamination by most of the authors, other sources of pilot contamination have been identified in recent literature. Under practical operating scenarios hardware impairments and the distortions produced, both in in-band and out of band, that interfere with training signals and non-reciprocal transceivers due to internal clock structures of the radio frequency chain [227, 270-271].

7.3 Pilot Based CSI Acquisition

Estimating the precise and timely CSI at the base station in a wireless communication scenario is very important, and it is the basic and core activity in a massive MIMO [272]. Precise CSI always helps the system to concentrate the transmitted power properly in the downlink to the required UEs and efficient reception of the UL power through the proper selection process and thereby it maximizes the network throughput. Therefore, effective and efficient methods for channel estimation are very essential in massive MIMO systems. The effects of unperfect channel estimation process on the performance of massive MIMO systems is mainly the ICI caused due to pilot contaminations [273-276]. Channel estimation can also be carried out with pilot sequences using blind [277-278] and semi-blind [279] based methods. Open-loop and Closed-loop methods are also being used

effectively for CSI estimation [280]. Channel reciprocity is used in open loop approach and is applicable only to TDD systems where as closed-loop approach is designed without the need for channel reciprocity requirements and hence it is suitable for FDD systems.

The different ways of using pilots for training and feedback discussed in the literature are summarized in Table 7.1. The Conventional Time Multiplexed (CTM) pilot scheme, CTM with blind pilots, CTM with Zadoff Chu sequence-based pilot and CTM with semi orthogonal pilots are the different schemes compared here.

Table 7.1 Comparison of different Pilot based training and feedback schemes

Pilot method used and Ref.	Channel Estimation schemes	Performance evaluation	Remarks
Conventional time multiplexed (CTM) pilot scheme. [282,282]	Coined Polynomial Expansion Channels, Bayesian channel with low complexity, diagonal Estimators and Weighed PEACH estimator.	Mean square error of different Estimators are evaluated. Varying order of Polynomials and computing complexity	Weighed PEACH estimator gives out best performance
CTM pilot scheme using semi-blind method. [283]	Maximum-a-posteriori using semi-blind and Least square estimate	Throughput (sum rate for DL) Channel estimation error.	Maximum-a-posteriori using semi-blind outperforms the Least square estimate based training
CTM pilot scheme, Zadoff Chu sequence based pilots [284]	Joint channel estimation method with Improved MMSE	Improved MMSE versus conventional MMSE in terms of Computational cost	Improved MMSE gave more than 60% savings in computational cost compared to conventional MMSE
CTM pilot scheme, Zadoff Chu sequence based pilots [285]	Chu-sequence for designing pilots of dissimilar phase shifts for UEs in every cell	Signal to interference ratio (SIR)	Proposed outperforms the normal method and reduces the partial interference

CTM pilot scheme, semi-orthogonal pilot Design. [286]	Successive interference cancellation (SIC) method	Uplink and downlink throughput	Throughput of proposed method is superior to the conventional one at low and high SNRs irrespective of the coherence interval
---	---	--------------------------------	---

7.4 Sources of Pilot Contamination and its Effects.

The various sources identified for pilot contamination in a massive MIMO environment are i) by the reuse of non-orthogonal pilot sequences among the cells in a multi-cell system due to restricted coherence time, ii) by the hardware impairments and iii) by non-reciprocal transceivers.

7.4.1 Contamination due to Non-orthogonal Pilot Sequences

The channel estimates obtained are useful only within the coherence interval, after which the channel must be estimated again. Moreover, the maximum number of mutually orthogonal pilot sequences is fundamentally limited by τ which must be smaller than the number of coherent time-frequency elements, $\tau \leq N_{coh}$. Within a cell, the K terminals always use orthogonal pilot sequences to eliminate intra-cell pilot interference ($\tau \geq K$). However, depending on the value of N_{coh} , these sequences may have to be reused in other cells, which leads to inter-cell interference. The effect of this interference on the received pilot signal is known as the pilot contamination (Fig. 7.1). In particular, it is found that the received pilot signal is contaminated with the transmissions from terminals from other cells reusing the same

sequence. The worst-case pilot contamination occurs when each cell reuses the same set of mutually orthogonal pilot sequences.

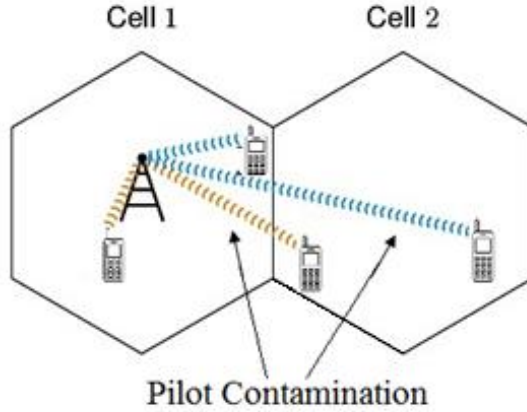


Figure 7.1 Contamination of uplink pilot signal due to reuse of same pilot sequences in other cells

The UL transmission when same pilots are used in all cells, at the l^{th} BS the received signal matrix, $\mathbf{Y}_l \in C^{M \times \tau}$ can be expressed as [261]

$$\mathbf{Y}_l = \sqrt{p_u} \sum_{j=1}^L \mathbf{G}_{l,j} \mathbf{S}_j^T + \mathbf{N}_l, \quad j = 1, 2, \dots, L. \quad (7.1)$$

where P_u is the average transmitted power from each user, $\mathbf{G}_{l,j} \in CM \times K$ is the channel matrix for all the K users in the j^{th} cell to the l^{th} BS. \mathbf{N}_l is the noise matrix at the l^{th} BS in the duration of the pilot transmission. At each base station, the pilot signal received are correlated with its own pilot signals where the pilot contamination caused is contributed by all the terminals in the nearby cells [88]. Hence for the l^{th} BS, the channel matrix estimated will be

$$\hat{\mathbf{G}}_{l,l} = \sqrt{p_u} \mathbf{G}_{l,l} + \sqrt{p_u} \sum_{j \neq l} \mathbf{G}_{l,j} \mathbf{S}_j^* + \mathbf{N}_l \quad (7.2)$$

7.4.2 Contamination due to Hardware Impairments

The significant merits of massive MIMO has been mainly judged and analyzed by theoretical studies. But working with experimental systems, [287-288], have shown that the hardware components in radio frequency are prone to hardware impairments such as quadrature imbalance (I/Q), quantization error, phase noise and amplifier non-linearity. Several studies had been done on the effect of hardware impairment on Massive MIMO includes [227], [271,289] which show how hardware impairment leads to a mismatch between the generated signal and the intended transmitted signal. Massive MIMO depends deeply on simple, low-cost power efficient base-band and RF hardware. However, the reduction in cost and increase in the power efficiency may result in substantial side effects. The most commonly identified impairments are quantization noise in digital to analog converter, phase noise, power amplifier distortion and mutual coupling between antennas. These impairments affect the accuracy of the channel estimation and thus leads to pilot contamination and performance degradation in massive MIMO systems.

7.4.3 Contamination due to Non-Reciprocal Transceivers

TDD systems operate on the same carrier frequency both on the upward and downward channel, and hence they are assumed to be reciprocal. The point-to-point reciprocity model in Fig. 7.2 was adopted from [290], where two scenarios may take place. If the system considered is ideal, then the low noise amplifiers (R_A and R_B), the effective electromagnetic channel $C(t)$ and the power amplifiers (T_A and T_B) are considered identical. In the case of a non-ideal system,

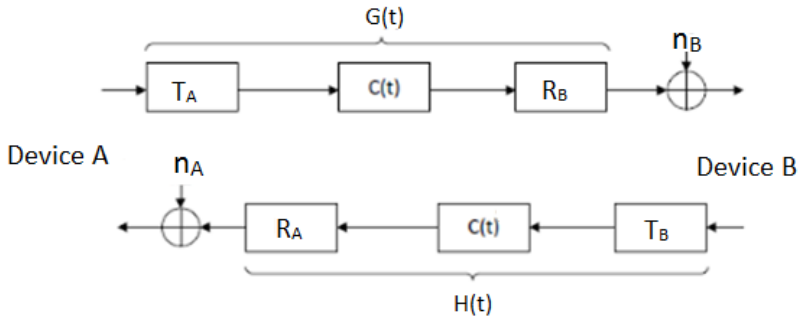


Figure 7.2 Point to point reciprocity model

the channel reciprocity will be affected by residual offset frequency [291].

The impulse response of the channel from A to B is modeled as $G(t, \tau) = R_B(\tau) * C(t, \tau) * T_A(\tau)$. Here convolutions are made over the delay domain τ . For information flow from B to A the response will be $H(t, \tau) = R_A(\tau) * C(t, \tau) * T_B(\tau)$. Both the $H(t)$ and $G(t)$ are considered as the functions of C . It is assumed that all the values R_A , R_B , T_A , and T_B remain fixed for the transmission interval.

Even a small offset of few Hz will cause the forward and the backward channels non-reciprocal. The imperfect CSI calibration, due to the presence of residual offset frequency, will play a major role in pilot contamination during channel estimation process.

7.5 Effect of Pilot Contamination on Massive MIMO Performance

In massive MIMO systems when the number of base station antennas is increased to a very high value, the effects of fast-fading, intra cell interference and additive noise at the receiver vanishes and the only problem persisting will be the inter-cell interference

developing through the reuse of the same pilot sequences or pilot contamination [88].

To analyze the effects of pilot contamination on massive MIMO, first we have to consider its effect on the signal to interference plus noise ratio (SINR), and then it is to be converted into throughput or achievable sum rates using various modeling parameters. It is showed that when the pilot contamination is not present the SINR increases linearly as the number of BS antennas grows larger and larger and it never saturates with the increase of the number of antennas to infinity. But the pilot contamination forces the SINR to saturate to a maximum limit due to the in accurate estimates of CSI [292].

Studies on the effect of path loss and shadow fading in the pilot contamination has shown that as the value of the ICI factor which accounts for the shadow fading and path loss components increases, it significantly degrades the energy efficiency as well as the spectral efficiency of the system.

Pilot reuse factor is another important parameter to be considered while designing pilots in massive MIMO networks. If the pilot reuse factor is selected as large, indicating fewer re-usage of pilots, then it gives a considerable improvement in the spectral efficiency. The clusters that will be repeated for reuse factors of 1, 2,3 and 4 are shown in Fig. 7.3.

The graph shown in Fig. 7.4 is plotted for the throughput variations corresponding to various pilot reuse factors along with the increasing number BS antennas. It clearly shows the degradation of

massive MIMO performance corresponding to the reuse factor of 1, which means that the same pilots are reused in all the cells of the

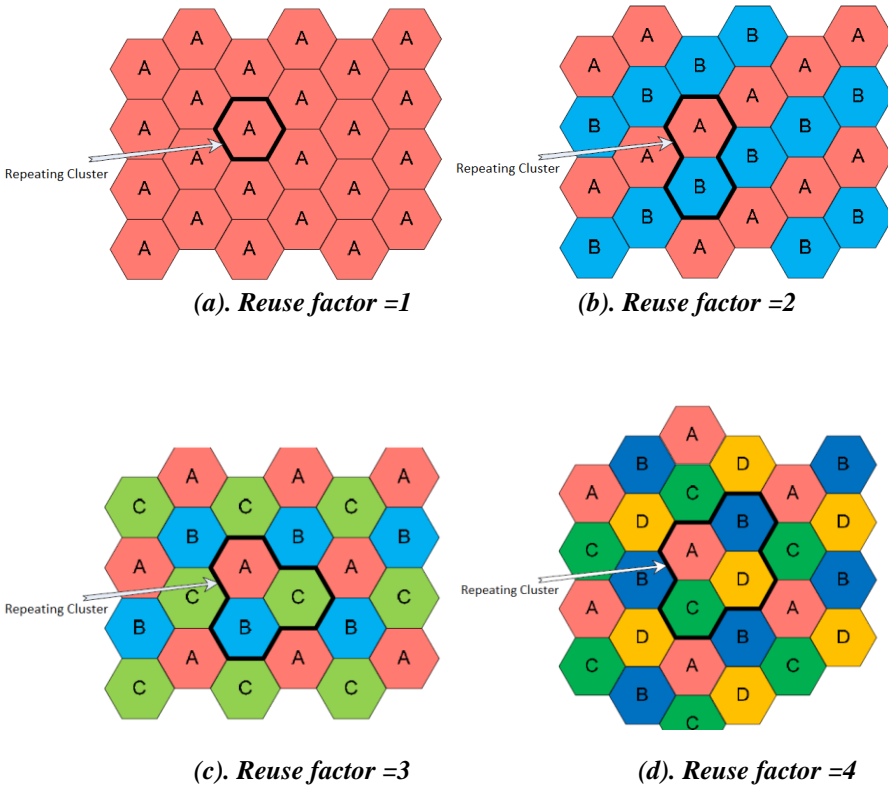


Figure 7.3 Cluster pattern that is repeated for pilot reuse factors of 1, 2, 3 and 4

network. The area throughput has been increased more than double when the reuse factor is increased from 1 to 4. Similarly, in Fig. 7.5 the energy efficiency of the system is shown for different pilot reuse factors, and there also we can find approximately a two-fold increase in energy efficiency corresponding to an increase of reuse factor from 1 to 4. This improvement in the performance is achieved due to the reduction in pilot contamination [293].

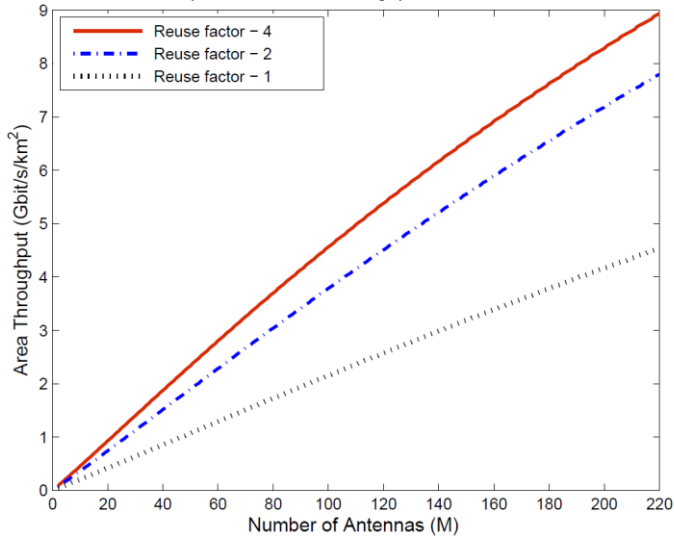


Figure 7.4 Effect of pilot contamination on area throughput

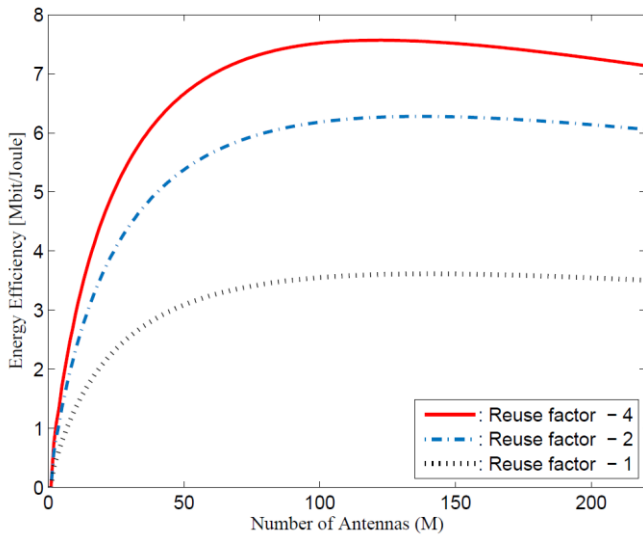


Figure 7.5 Effect of pilot contamination on energy efficiency

7.6 Pilot Contamination: Mitigation Methods

Right from the beginning of massive MIMO concept applied for cellular mobile communication to the present, researchers are working hard to trace out the adverse effects of pilot contamination and methods

to mitigate it. In this section, some of the important methods used for the mitigation of pilot contamination and its performance are discussed.

7.6.1 Time-Shifted Pilot Slot Allocation

Time-Shifted Pilot slots allocation strategy was first proposed by F. Fernandes et al. in [157] to mitigate the effects of pilot contamination. The widely used time division duplex architecture for massive MIMO systems contains four stages: (i) pilot sequence transmission in the uplink (ii) Processing and channel estimation at the base station (iii) data transmission in the uplink and (iv) transmission in the downlink. This technique allocates the transmission of non-orthogonal pilots between cross cells to different time-shifted slots. So non-overlapping time slots are allotted to pilot transmission by shifting the pilot locations as shown in Fig. 7.6.

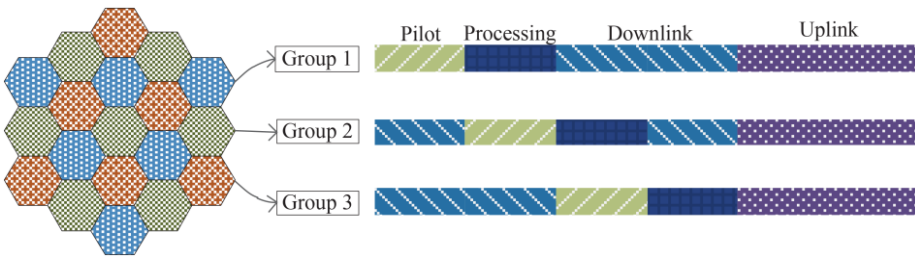


Figure 7.6 Pilot scheme based on time-shifted pilot slots.

Considering this scheme, if the time shift is efficiently controlled without having any overlap, pilot contamination was shown to be almost completely eliminated. But the draw back is the difficulty in practical implementation of the control mechanism to synchronously allocate the pilots across various cells without having any overlap. This issue will be more critical as we go with smaller cells with more cell density to increase the area throughput of massive MIMO networks.

Application of power allocation algorithms along with the time-shifted pilot allocation method discussed by F. Fernandes in [157] was initially suggested by H. Yin et al. in [294]. It improves the gain significantly across a wide range of active users and BS antennas, but managing and synchronizing the control mechanism is practically very challenging.

7.6.2 Covariance Aided Method

In this approach, a covariance aided channel estimation method by making use of the co-variance information available in the required channel as well as interfering channels is used. It was shown that the effect of pilot contamination, with huge antenna array system, vanishes when the interfering users and the desired users are located in separate sub-spaces [161,295]. It is also showed that users would not interfere and hence no pilot contamination will occur if the mutual Angle of Arrival (AoA) of each user is non-overlapping. The outcome of this method was promising where it gives a significant increase in DL and UL signal to interference noise ratio with a reduction in inter-cell interference. However, it is practically difficult to implement due to the second order statistics required for uplink channels.

7.6.3 Spatial Domain-Based Scheme

The spatial domain based scheme is working with the key idea that spatial or/and time-based characteristics of channel coefficients of different UEs are separately identifiable by the direction of arrival or the angle of arrival [296]. Again, the downlink beam former is selected from the strongest uplink path, and as discussed by Yin et al. in [295] the angle of arrivals of the UEs are made fully non-overlapping. The

important point is that the channel coherence interval should be taken into consideration when searching for the best steering vector for the DL precoding. The main drawback of this method is the high cost of training which may go to infinity as we increase the antenna size to a large value.

7.6.4 Multi-cell Cooperation

This method is originally proposed by Marzetta et al. in [297]. It is possible to completely get rid of pilot contamination by the cooperative working of the adjacent base stations. This is achieved by adding layer of precoding and decoding in all the BSs. This is called as pilot contamination precoding. All base stations used in the massive MIMO network needs a limited collaboration. Base stations exchange the estimates of the slow fading coefficients with the other base stations in the network. Based on this shared information among BSs, it computes the precoding matrix and is then forwarded to other base stations for computing the transmit signal vector for all the M antennas used by it. This method considerably reduces the intra cell interference and inter-cell interference thereby increasing the overall throughput in comparison with the conventional single cell precoding techniques. However, the success of this approach depends on the correctness of the information shared among the BSs and the computation of the precoding matrices.

7.6.5 EVD-based Method

It is a very attractive method of doing channel estimation as it requires no or very less number of pilot sequences for operation [298]. Many of the signal characteristics can be exploited for channel

estimation which includes fixed symbol rate, high order statistical properties, constant modulus, independence and finite alphabet structure. This method has been recommended for multi-cell massive MIMO TDD architecture for completely eliminating the pilot contamination. Eigen value decomposition(EVD) based subspace estimation scheme is used for the estimation of CSI.

This method is susceptible to errors because it is assumed that, when the number of BS antennas grows towards infinity, the channel vector between BS and user become pair wise orthogonal. But in the actual case, the number of antennas is finite and to reduce the errors, iterative least square along with projection algorithm is combined with the above EVD algorithm. Experimental studies showed that the EVD algorithm outperforms the conventional algorithms, but the precision depends on a large number of antennas as well as the number of sampling data present in the coherence-time interval [299].

7.6.6 Data-aided Approach

The traditional way of acquiring the CSI is solely dependent on the pilot training sequences and when two users use the same pilot sequence an interference is generated. In the data-aided method described by Junjie et al. in [300], both pilot and data signals are used for channel estimation. The advantage of using data signals for channel estimation is that the data signals sent by different users will always be independent and hence the inter-cell interference will be suppressed to the maximum extent.

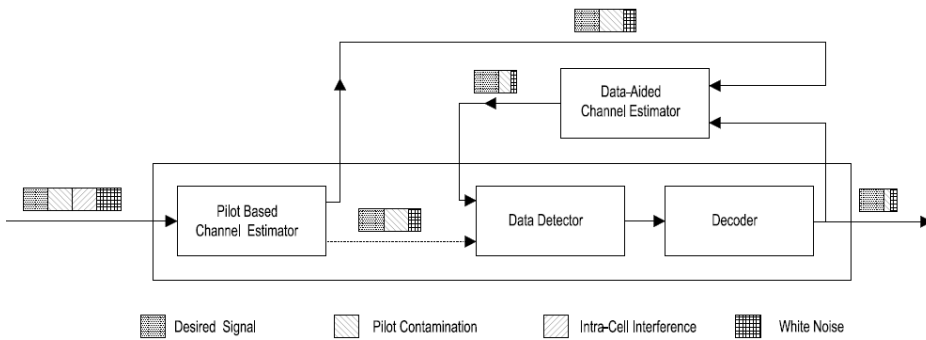


Figure 7.7 Data aided approach for pilot decontamination

Here as shown in Fig. 7.7, to the traditional receiver an additional data-aided channel estimator is also added. This additionally added module provides a feedback from the output of the decoder to the input of data detector. At the input of the detector both noise and inter-cell interference (pilot contamination) will be available, and with proper channel coding, the data can be easily detected even in the low SINR area. These data which are properly detected are untied to improve the quality of channel estimation. Since it is an iterative process, the continuous iteration creates positive feedback in between the decoder and the estimator which again supports the suppression of pilot contamination.

7.7 Related Works

In addition to the fundamental approaches for mitigating pilot contamination listed above tons of other proposals are found in the literature. Considering the importance of pilot contamination in massive MIMO for the 5th generation communication systems, in the following section, an extensive survey of the state of the art approaches and proposals, for completely eliminating or reducing the effects of pilot contamination has been provided.

The cells are divided into several clusters and an asynchronous time-shifted algorithm was proposed for reducing the effect of pilot contamination by F. Fernandes in [157] and K. Appaiah et al in [294]. When the user terminals in one cluster transmit pilots, BSs from other clusters transmit downlink data, which will eliminate the pilot contamination problem between users of different clusters. The drawback of this method is that since the transmitted power of downlink data is much higher than that of the pilot signals, precise channel estimation may not be possible.

A decontamination method based on multi-cell cooperation for Massive-MIMO systems, with a limited number of antennas, was suggested in [301] by Huh et al. and A. Ashikhmin et al. in [297]. The BS linearly combines the data meant for different users from different cells, which use identical pilot sequence, and an outer cellular precoding is performed on the combined data. It works satisfactorily only for BSs with less number of antennas.

H. Yin et al. in [295], Ngo et al in [302], and Cheng et al. in [303] have shown that by using covariance matrices a BS can have a better estimate on the CSI which in turn improves the system performance by mitigating the effect of pilot-contamination. Though the calculation of the covariance-matrices of all the channels is not so easy, the papers focus on different practical methods to do the same for a massive MIMO system.

Alqahtani et al. in [304] and Wu et al. in [305] designed and developed a new precoder/detector combination set up by using multiple cell linear preorders in the downlink path, and strong decoders

for the uplink channel of massive MIMO networks. Simulations demonstrated a good improvement in the negative effects of pilot contamination. In [306] Jiang et al. addressed the effects of pilot contamination by avoiding the simultaneous use of same pilot sequences in adjacent cells. Asymptotic orthogonality among different wanted channels and interference affected channels were effectively used by Ngo et al. in [307] and by Hu et al. in [308] for the pilot decontamination.

J. H. Sørensen et al. in [135] have analyzed the pilot decontamination methods in massive MIMO under crowded scenarios. Here a small set of pilot sequences were shared by users within a single cell causing intracellular pilot contamination. It is considered as a random-access problem and the solutions proposed were very efficient. The main drawback in this was higher error rate by building up of errors in the algorithm.

Two novel channel estimation schemes were proposed by Vu et al. in [309] for the effective removal of pilot contamination. The new scheme consists of repeated transmission stages of pilot symbols, where the BS stay idle in one stage and successively send pilots symbols in other stages. The performance gain of the suggested estimation schemes was demonstrated through simulation.

Pilot allocation based on graph coloring has been proposed by X. Zhu et al. in [152] for effective pilot decontamination. An interference graph is first prepared to show the possible inter-cell interference relationships of every user terminal. With the aid of this graph, the fully orthogonal pilot-sequences are allocated to the

potential users to avoid the interference and pilot contamination. The improvement in the spectral efficiency has been verified through simulations.

Björnson et al. in [310] have shown that the spectral efficiency can be increased without any limit even in the occurrence of pilot contamination by providing a simple condition of linear independence in the covariance matrices. Thus, they have derived the analytical proof for the same for a simple two user MIMO and then extended that to multi-cell scenarios.

Zhilin et al. in [311] reduced pilot contamination by exploiting channel sparsity considering the fact that a typical wideband massive MIMO channel is correlated in both frequency and space domains. The advantage of the proposed method is that it does not need channel statistics and pilot co-ordination and also does not introduce extra training overhead. Substantial sum rate gain is achieved by the proposed method over existing methods.

A novel algorithm for mitigating the pilot contamination problem was designed by Y. Han in [148]. The new pilot design with arbitrary length based on alternating minimization approach was used and tested using simulations. Thus, the main attraction of the approach was flexibility in designing the pilot sequences for maximizing the spectral efficiency.

Pilot contamination is identified as the most significant drawback of massive MIMO systems that limits the exploitation of its optimum capacity. Right from the beginning of massive MIMO concept for cellular mobile communication to till date researchers are working hard

to trace out the adverse effects and mitigation methods of pilot contamination. Though lot of proposals are available in the existing literature complete elimination of the same is still a bottle neck to be solved.

7.8 Problem Identification

From the detailed analysis of massive MIMO and the in-depth literature survey carried out, the main cause of performance deterioration of massive MIMO is identified as signal to interference plus noise ratio (SINR) saturation due to inter-cell interference, which is originated due to pilot contamination. So far, there has been no study towards the reduction of pilot contamination through proper pilot assignment strategy, according to the users' position related to the BS and users' mobility. Therefore, in this work we propose a novel partial pilot re-use strategy among users in the adjacent cells, which are close to the base station (BS) and possesses minimum movement velocity. The social spider optimization (SSO) algorithm, which makes use of the foraging behavior of community spiders, is used for solving the pilot assignment problem. It is to be noted that the existing SSO algorithm is working with single decision-making metric. Hence, in this paper, the existing algorithm is modified to make it suitable for multi-factors. Significantly, the considered multi-factors are time-varying metrics, which are optimized by the proposed SSO algorithm. These metrics are obtained from the CSI during the uplink training process. Using this modified SSO algorithm, one can easily assign the pilots based on the present position, and the mobility of the user.

7.9 The System Model

Consider a Massive-MIMO mobile cellular-network given in Fig. 7.8, which consists of multiple hexagonal-cells with a BS at the center, having an antenna array with M number of elements and K number of simultaneous users equipped with single transmit/receive antenna. All the users and the BSs are synchronized based on a time division duplex (TDD) protocol. In TDD, each frame consists of two phases, namely uplink training period and downlink data transmission. The channel reciprocity is assumed between the UL and DL. The BS needs to estimate the CSI of each user using pilot sequences, and then use the estimated CSI to detect uplink data and to establish the downlink transmissions. All the pilot signals used by the individual users in a cell are assumed to be mutually orthogonal.

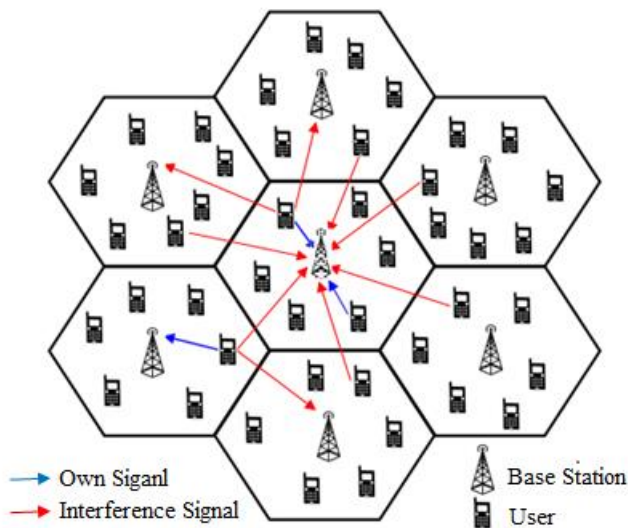


Figure 7.8 System Model

In the DL communication model shown in Fig. 7.9 the information symbols to different users are first multiplied by the conjugate of the

estimated channel, and then these products are added together and fed to the transmitting antenna. The process is repeated for every antenna in the BS and hence the signals intended for the n^{th} user from all the antennas will arrive in phase at user n and arrive out of phase at all the other users.

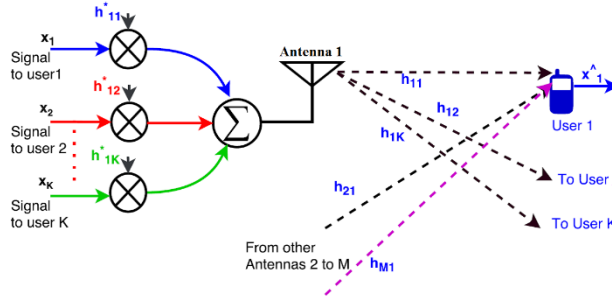


Figure 7.9. Downlink Communication

The precoding and beam forming technique used is zero forcing (ZF) which is considered as the simplest possible one and also very effective. Hence, for the downlink, the signal transmitted from the n^{th} antenna can be written as in Eqn. 7.3.

$$T_n = x_1 h_{n1}^* + x_2 h_{n2}^* + x_3 h_{n3}^* + \dots + x_k h_{nk}^* \quad (7.3)$$

where x_1 to x_k are the signals intended for k active users in the cell and h_{nk}^* his the conjugate of the channel estimate between the n^{th} antenna and k^{th} user.

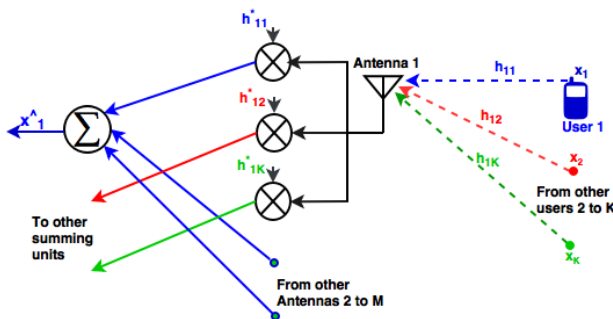


Figure 7.10 Uplink Communication

In the uplink communication model shown in Fig. 7.10, each of the antennas at the BS collects signals arriving from all the users and multiply that individually by the conjugate of the channel estimate. Therefore, in the UL the signal received by the n^{th} antenna from all the users can be expressed as

$$R_n = x_1 h_{n1} + x_2 h_{n2} + x_3 h_{n3} + \dots + x_k h_{nk} \quad (7.4)$$

To get good estimates of CSI, the number of orthogonal pilot sequences should be equal to the number of users. Moreover, in order to maintain orthogonality of each pilot sequence, the length of the sequence must increase and that, in turn, will increase the time required for transmitting the pilot sequences. However, in a practical wireless system, the coherence interval is limited, and only a fraction of this interval can be devoted to pilot symbols, the rest are reserved for the data. So, the length of the pilot sequence cannot be too long, which implies that the maximum number of orthogonal pilot sequences is limited. However, for massive MIMO networks, since the number of users in the system is very large and all users send pilot sequences to BSs simultaneously, the required number of orthogonal pilot sequences is also large. The practical number of available orthogonal pilot sequences is much less than the requirement, and therefore, the same or partially correlated pilot sequences are reused in different cells causing pilot contamination. The proposed SSO algorithm assigns these reused pilots in such a way that it will not create any inter-channel interference.

System model described in Fig. 7.8 also explains the pilot contamination effect. Consider the center BS as an example, where it

receives a combination of pilot sequences from all users. The blue color arrows represent the pilot sequences from own cell, and the red color arrows represent the pilot sequences from a neighboring cell. If the neighboring cells reuse the pilots used by the center cell, then the pilot sequences received by the center cell will interfere each other and cause contamination. The channel estimate of a user in the center cell is contaminated by those users sharing the same orthogonal pilot sequence located in adjacent cells.

Fig. 7.11 shows the standard pilot reuse pattern with a $\beta=3$, where the integer $\beta \geq 1$, represents the number of subsets of pilots used in the system and S_1 to S_3 represents the different subsets of orthogonal pilot sequences. The concept of pilot reuse advocates the use of orthogonal pilot subsets in nearby cells thereby minimizing the actual number of subsets of pilot sequences required [140]. This, in turn, maximizes the spectral efficiency for both downlink and uplink communication links.

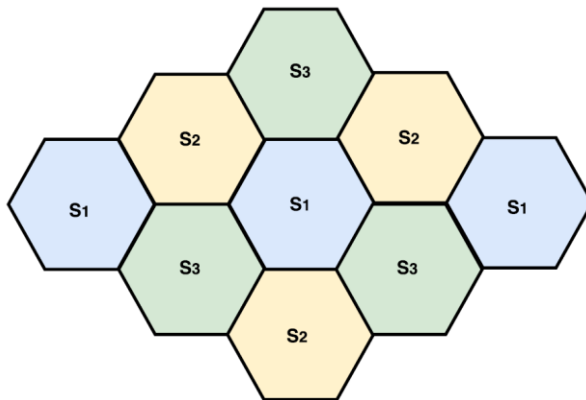


Figure 7.11 Pilot reuse

In the proposed model, the pilot sequences are partially reused in adjacent cells, and for that, the available set of orthogonal pilot sequences are divided into $\beta+1$ orthogonal subsets. Integer $\beta \geq 1$

represents the pilot reuse factor between the adjacent cells and an extra subset of pilots is reused in the center area of all the cells. This scenario with $3+1$ subsets of pilots is depicted in Fig. 12(a) (only 3 cells are shown for simplicity).

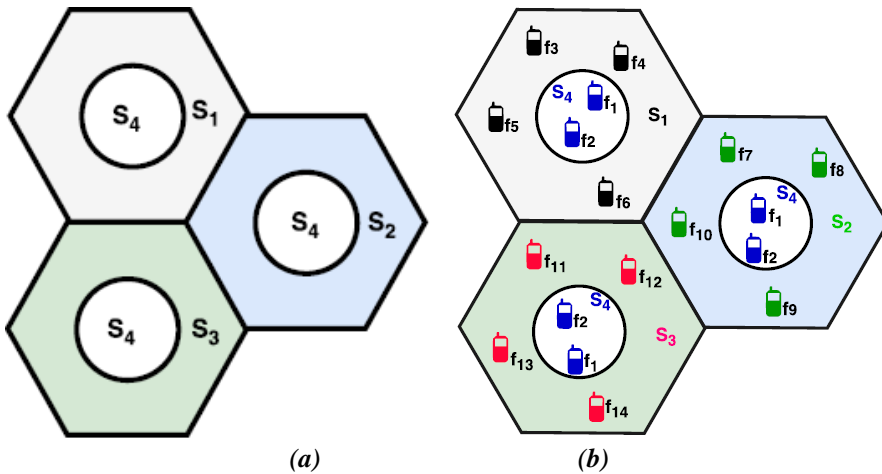
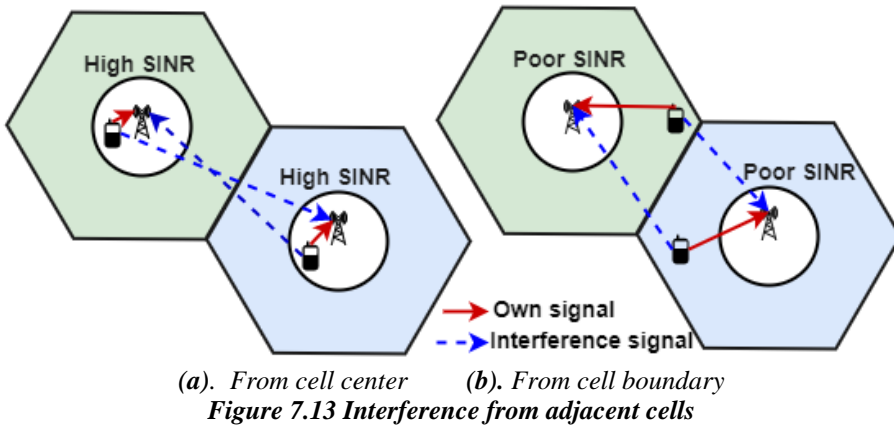


Figure 7.12 Partial pilot reuse

For the example shown in Fig 7.12(b), $\beta = 3+1$, i.e. four subsets of pilot sequences, $S_1=\{f_3, f_4, f_5, f_6\}$, $S_2=\{f_7, f_8, f_9, f_{10}\}$, $S_3=\{f_{11}, f_{12}, f_{13}, f_{14}\}$ and $S_4=\{f_1, f_2\}$ are used. The subset S_4 is reused in all the cell centers without causing any inter-cell interference and subsequent pilot contamination problem.

Fig. 7.13 describes how the proposed partial pilot assignment strategy benefits in eliminating the pilot contamination. The same set of pilots are re used only at the cell centers and hence as shown in Fig. 7.13(a) the interfering pilot signal from adjacent cell centers are very weak compared to the own pilot signals giving rise to high SINR. But if the same sequences are reused in the cell boundary area as shown in Fig. 7.13(b), the interfering pilot signals from adjacent cells will be



equally strong as the own pilot signal giving rise to a poor SINR and pilot contamination.

The proposed algorithm defines the radius of the cell center area according to the received signal strength(RSS) and SINR. Pilots are assigned to the users present in this area based on its distance from the BS and velocity of movement.

It is noteworthy that users with low mobility only are selected for assigning pilot sequences reserved for the cell center (S_4) because the probability of staying these user terminals (UT) within the cell center is much higher than the UTs with high mobility. Thus the algorithm tries to maximize the minimum SINR value for all the K users in the cell.

7.10 Social Spider Optimization Algorithm

Social spider optimization (SSO) algorithm is a swarm intelligence algorithm proposed by researchers for optimization. It imitates the natural food/mate hunting phenomenon of social spiders to the optimization of a process [312]. The hyper dimensional spider

web is considered as the search space in this problem of optimization and each point on this web is considered as a viable solution.

In addition to the space solution, the web acts as a communication media for the vibration produced by the spiders. Spiders are the primary functional agents in social spider algorithm. Every spider carries memory units which can store its present location on the web, fitness value corresponding to that position, and the vibration intensity experienced in the previous iteration. The algorithm uses the vibration intensity for determining the movement of the spider whereas the first two properties represent the features of the spider.

Biologically spiders are considered to be highly sensitive to vibrations. The position and intensity of the source of vibrations can be easily and accurately traced by spiders. They are also capable of differentiating separate simultaneous vibrations propagated through the web. These characteristics of social spiders are utilized in SSO algorithm [313-314]. Every time when a spider on a web makes a movement to a new location, it produces a new vibration which is communicated through the web to all the other spiders. The vibrations received by spider a_i from another spider or a prey a_j on the same web is given by

$$V_{a_i,j} = w_{a_j} e^{-d_{a_i,j}^2}, \quad d_{a_i,j} = \|x_{a_i} - x_{a_j}\| \quad (7.5)$$

w_{a_j} is the weight of the spider a_j given by Eqn. 7.6, $d_{a_i,j}$ represents the distance between the spiders and x gives the position of the spider with respect to the center of the web.

$$w_{a_j} = \frac{FF - W_x}{B_x - W_x} \quad (7.6)$$

where $FF(a_j)$ represents the fitness function of the spider a_j , B_x and W_x are the best and worst cases of x and these are defined by the following equations.

$$B_x = \max_{k=1, \dots, k} FF(x_k) \quad (7.7)$$

$$W_x = \min_{k=1, \dots, k} FF(x_k) \quad (7.8)$$

Two methods are followed to learn the updated position of the spider which depends on the gender of the spider. Following equation gives the updated position for female spiders.

$$X_{FM_{a_i}}^{k+1} = \begin{cases} X_{FF_{a_i}}^k + r_1 \times V_{a_i} \times (a_1 - X_{FF_{a_i}}^k) + r_2 \times V_{a_2} \times \\ (a_2 - X_{FF_{a_i}}^k) + r_3 \times (\xi - 0.5), \text{Random} \geq M \\ X_{FF_{a_i}}^k - r_1 \times V_{a_i} \times (a_1 - X_{FF_{a_i}}^k) - r_2 \times V_{a_2} \times \\ (a_2 - X_{FF_{a_i}}^k) - r_3 \times (\xi - 0.5), \text{Otherwise} \end{cases} \quad (7.9)$$

where r_1 , r_2 , r_3 , and ξ are random integers between 0 and 1, k is the number iterations made and M is the threshold value that makes the spider move either towards or away from the origin of vibration. a_1 is the spider with maximum weight and nearest to the spider a_i and a_2 is the best spider. V_a is the vibration intensity of the spider which is calculated by Eqn. 7.3 and its weight is given by

$$W_{a_2} = \max_{k=1..k} W(a_k) \quad (7.10)$$

When the female spider decides to travel to the origin of vibration, the first condition of Eqn. 7.9 is used or else the second condition is used. The male spiders, on the other hand, update their current location according to the following equation.

$$X_{M_{a_i}}^{k+1} = \begin{cases} X_{M_{a_i}}^k + r_1 \times V_{a_3} \times (a_3 - X_{M_{a_i}}^k) + r_3 \times (\xi - 0.5); & W_{M_{a_i}} \geq W_{median} \\ X_{M_{a_i}}^k + r_1 \left(\left(\frac{\sum_{a_j=1}^{M_n} X_{M_{a_j}}^k \cdot \frac{W_{a_3+j}}{\sum_{a_j=1}^{M_n} W_{a_3+j}} \right) - X_{M_{a_i}}^k \right); & \textit{Otherwise} \end{cases} \quad (7.11)$$

here W_{median} is the median weight calculated from all the male spiders and M_n gives the total number of male spiders. For dominant spiders, the weight value will be greater than the median weight or else it is considered as non-dominant. a_3 is the female spider nearest to the fa_i^{th} male spider and V_{a_3} is given by

$$V_{a_3} = W_{a_3} \cdot e^{-d_{ai,a_3}^2} \quad (7.12)$$

The SSO algorithm is executed in an iterative manner and the vibration intensity of the next iteration is calculated by the equation

$$V_{(i+1)} = V_{(i)} \times \alpha_a \quad (7.13)$$

where i and $i+1$ are the two successive iterations and α_a is the attenuation coefficient. The following equation gives the attenuation in intensity of vibration as it propagates over a distance of X .

$$V_{(D)} = V_o \times \exp\left(\frac{-X_{(O,D)}}{X_{max} \alpha_a}\right) \quad (7.14)$$

O and D are the originating and terminating positions, X_{OD} is the distance between them and X_{max} is the maximum distance between any two points on the web.

In SSO algorithm, three separate steps are involved; the first stage is the initialization phase which is then followed by the iteration stage, and then the final stage. All the optimization parameters search space and objective functions are initialized first and then, a number of spiders are generated and randomly placed on the search space. Then

these positions are initialized as the current position with an intensity of zero; this completes the initial setup of the social spider algorithm and then it moves to the iteration stage where the optimization process is performed in an iterative manner. The fitness value of every spider in the web is calculated first and then the vibrations obtained in the previous phase are attenuated. Then according to Eqn. 7.5, these spiders will generate vibrations in the present locations. These vibrations are transmitted using Eqn. 7.14 to the entire web. Then each spider receives all the vibrations from other spiders from all sides of the web. Out of all these received vibrations, each spider selects one vibration with maximum intensity (V_{max}) which is then compared with the value used in the previous iteration. Location of the spider is then calculated by the equation

$$X_{a(i+1)} = X_{a(i)} + (X_{max(i)} - X_{a(i)}) \cdot (1 - R) \cdot R \quad (7.15)$$

where $X_{a(i)}$ and $X_{a(i+1)}$ represents the location of the spider at iterations i and $i+1$ respectively, (\cdot) is the elements wise multiplication. X_{max} is the source location of the spider with a maximum intensity of vibration V_{max} . R is a uniformly generated vector of random numbers from 0 to 1.

Finally, when a dominant male spider locates one or more female spiders within the specific range called as mating radius, it mates with all the females. The mating radius is given by

$$r = \frac{\sum_{j=1}^n (X_j^{max} - X_j^{min})}{2n} \quad (7.16)$$

where $J= 1, 2, \dots, n$. and X^{max} and X^{min} are the boundary values of X .

In the proposed SSO algorithm, it first assigns random locations to each mobile user (spider), for that a population of users is created and then its assigned locations are transformed to binary vectors of size M by the following equation.

$$TP(X_{a_i}^{a_j}(t)) = \frac{1}{1 + e^{-X_{a_i}^{a_j}(t)}} \quad (7.17)$$

$$X_{a_i}^{a_j}(t+1) = \begin{cases} 1; & \text{if } TP(X_{a_i}^{a_j}(t)) > [0,1]_c \\ 0; & \text{Otherwise} \end{cases} \quad (7.18)$$

where $X_{a_i}^{a_j}(t)$ is the user's value at iteration t . For each user a_i , the features selected correspond to 1s and the rests which are not selected correspond to 0s. The multiple UL data metrics are used to compute the fitness function for the proposed optimization algorithm. The multi-factors obtained from the UL pilot sequences are $SINR$, received signal strength (RSS), the position of the user as a distance from the BS (X_n) and the velocity of user movement (v). The multi-factor metrics gathered from every user is considered as input and the proposed SSO algorithm serves the pilot sequence request from multiple users according to its fitness function.

The suitability of the SSOA for a cellular network is demonstrated through the comparison shown in table 7.2

Table 7.2 Comparison between social spider colony and cellular network

	Social spider colony	Cellular network
1	The web of social spiders is taken as the search space for the optimization problem and each point on this web is considered as a possible solution.	The entire area under a single hexagonal cell of a cellular network is considered as the search space and each point inside this cell can be a viable position for the UTs.

2	In the social spider colony, dominant male spider usually resides at the center of the web(hub) and female spiders are distributed over the entire web.	BS (equivalent to the dominant male spider) is located in the center of the cell and the UTs (equivalent to female spiders) are distributed in the entire cell area.
3	Male spider at the center receives vibrations from the female spiders through radial threads of the web and from those vibrations it identifies the weight and location of the female spider.	BS receives CSI and other information from the mobile nodes through direct wireless links. Position and velocity of the mobile nodes are determined from the received information.
4	Male spider is capable of receiving and identifying simultaneous vibrations from multiple female spiders.	BS with massive MIMO antenna is capable of communicating simultaneously with the number of UTs through spatial diversity.
5	Male spider moves towards the female spider and mates with it when it comes inside the mating radius.	BS assigns a reusable pilot sequence to the UT if it is located in the center cell area and satisfies the speed condition.

SSO algorithm is based on swarm intelligence. Due to the use of mobile agents and stigmergy, it has got the following advantages over the existing solutions available in the literature, when it is used for pilot assignment.

1. Scalability: The population of the mobile agents (UTs) can be changed to any value according to the cellular network requirement.
2. Adaptation: UTs can change its communication characteristics according to the change in communication environments.
3. Speed: System adapts to the network changes very fast and is very useful in a dynamic wireless environment.

4. **Autonomy:** The system automatically accepts all the changes and acts accordingly to get the best performance.
5. **Parallelism:** Mobile agent's function is essentially parallel which again increases the speed.
6. **Fault tolerance:** Failure of few nodes or links does not result in any disastrous failures.
7. **Modularity:** The mobile agents act independently of the other layers of the network.

All the above benefits are attained in a very simple and expeditious way. It requires only RSS and velocity of UTs to effectively assign pilot sequences in order to mitigate the effects of pilot contamination. These values will not change with the number of antennas used at the BS and also will remain constant within a considerable frequency and time interval. Hence implementation of the proposed pilot assignment scheme using SSO algorithm for massive MIMO system is a definite possibility.

7.10.1 Fitness Calculation using Multi-factors

The SSO algorithm performs the optimization on the basis of the time-varying metrics calculated in each iteration. The fitness function (FF) for each user is calculated as per the following rule

$$FF = \text{Min} \left\{ \frac{1}{RSS}, \frac{1}{SINR}, X_n, v \right\} \quad (7.19)$$

The steps for the proposed algorithm for pilot assignment are given in Table 7.3. The FF is calculated individually for every user in the cell and is compared with the total best fitness value FF_{best} . If the present value of fitness function FF_i is better, then the FF_{best} is replaced with

FF_i . This process is repeated until all the users are iterated. Finally, the pilot assignment is done for the user with FF_{best} .

7.10.2 Mobility Calculation with Received Signal Strength (RSS)

The energy consumption depends on both transmitter and receiver energy requirements. The energy consumed by any UT is directly proportional to the square of the distance (D^2) when the transmission distance is lesser compared to the threshold value (D_0) or else proportional to D^4 . When a data packet carrying b number of bits is transmitted by the network and received by a UT the total energy consumed will be

$$E_T = E_{tx}(b, d) + E_{rx}(b) \quad (7.20)$$

where $E_{tx}(b, d)$ and $E_{rx}(b)$ are energy consumed by the transmitter and receiver.

$$E_{tx}(b, d) = \begin{cases} b \times E_d + b \times \varepsilon_{fs} \times D^2; & \text{if } D < D_0 \\ b \times E_d + b \times \varepsilon_{mp} \times D^4; & \text{if } D \geq D_0 \end{cases} \quad (7.21)$$

where E_d is the energy dissipated per bit to run the transmitter or receiver circuit. ε_{mp} and ε_{fs} are the energy consumed by the amplifier circuit under the multipath model and free space model respectively which depends on the amplifier model and threshold distance.

RSS is calculated from the linear average of the energy consumed considering the adjacent channel interference and thermal noise. RSS can be calculated from the transmitted energy and the distance between the source and destination. If a packet with b number of bits and energy $E_{tx}(b, d)$ is transmitted by a user the received signal strength at a distance D from the source is given by [315]

$$RSS = \frac{E_{tx}(b, d)}{4\pi D^2} + T_{x,y/z} \quad (7.22)$$

$$D = \sqrt{\frac{E_{rx}(b,d)}{4\pi RSS}} \quad (7.23)$$

where $T_{x,y/z}$ is the time taken by the UT to move to the new location x or y . The differential speeds of the transmitter and receiver and distance between them determine the actual speed of the node. Sample points are chosen in such way as to meet the condition $\Delta t_y = \Delta t_z = \Delta t$. In practice, a number of different sample points are selected for calculation of the actual signal strength of the user. Differential speed calculation is shown in Fig. 7.14. Assume x as the current location of the node and it can move to location y

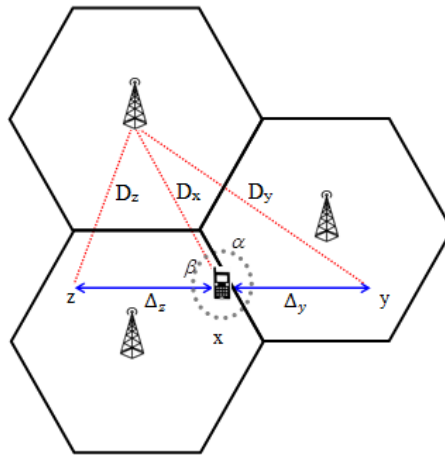


Figure 7.14 Mobile nodes movement computation

and z . D_x is the distance from the BS to the current location, D_y and D_z are the updated distances calculated by the cosine laws as given in equation (7.24) and (7.25).

$$D_y^2 = D_x^2 + \Delta_y^2 - 2D_x\Delta_y\cos(\alpha) \quad (7.24)$$

$$D_z^2 = D_x^2 + \Delta_z^2 - 2D_x\Delta_z\cos(\beta) \quad (7.25)$$

since $\cos(\pi-\theta) = -\cos(\theta)$, $\cos(\alpha)$ can be considered as $-\cos(\beta)$, hence by adding equations (7.24) and (7.25) and assuming $\Delta_y = \Delta_z$ we get

$$2\Delta_y^2 = D_y^2 + D_z^2 - 2D_x^2 \quad (7.26)$$

Then the velocity of the node movement is given by

$$v = \frac{\sqrt{(D_y^2 + D_z^2 - 2D_x^2)/2}}{\Delta_t} \quad (7.27)$$

where Δ_t is the time taken by the node to move from the present location to the new location y or z .

The proposed pilot allocation scheme is implemented as follows.

1. The BS is initialized in each cell and a fixed number of UTs are randomly placed across each cell.
2. A pilot reuse pattern with a β of 4 as explained in Fig. 7.12 is selected and the users from all the cells transmit the pilot signals to their corresponding BSs.
3. The BS calculates the position and velocity of UT movement
4. SINR corresponding to each UT is also calculated by the BS from the received CSI.
5. Based on the above information the SSO algorithm determines the best UT to assign a reusable pilot sequence.
6. The process is repeated until all the pilot sequences in set S4 are assigned to the best possible UTs which are selected by considering the $\max(\text{SINR})$, $\min(Xn)$, $\max(\text{RSS})$ and $\min(v)$ values.

Table 7.3 describes the proposed SSO algorithm.

Table 7.3-Social spider optimization algorithm for pilot assignment

1	Initialize the number of users, number of cells, number of iteration(I_{max}) and best fitness function (FF_{best})
2	Initialize a population of n users a_{x_i}
3	$I=0$ Repeat for all a_{x_i} do Calculate D from Eqn. (7.23) Calculate v from Eqn. (7.27) $FF = Min \left\{ \frac{1}{RSS}, \frac{1}{SINR}, X_n, v \right\}$ If ($FF_i < FF_{best}$) then $a_{x_{best}} = a_{x_i}, FF_{best} = FF_i$ end if end for
4	Perform the pilot assignment to $a_{x_{best}}$ based on FF_{best}
5	$I=I+1$
6	Repeat until $I < I_{max}$

7.11 Normalized Mean Square ERROR (NMSE)

NMSE is the estimator used for calculating the overall deviations between the predicted value and the actual measured value. In NMSE the variations (absolute values) are added instead of taking the differences and hence NMSE always indicates the predominant differences in the simulation models. A simulation model having very less NMSE can be considered as well performing.

The performance of channel estimation in wireless communication networks are measured using NMSE and it is given by the following equation.

$$NMSE = \frac{E\{\hat{H}_{i,i} - H_{i,i}\}^2}{E\{H_{i,i}^2\}} \quad (7.28)$$

where $\hat{H}_{i,i}$ represents the estimate of the wireless channel from the i^{th} transmitter to the i^{th} receiver and $H_{i,i}$, is the corresponding measured value.

7.12 Sum-rate

If the CSI obtained is assumed as perfect, then the BS correctly estimates the channel matrix and SNR of the n^{th} user in the l^{th} cell can be represented as [12]

$$SNR_{nl} = \frac{M P_{dn} \beta_n^2}{\sigma^2} \quad (7.29)$$

where σ^2 is the noise variance at the receiver, M is the number of BS antennas, β is the attenuation coefficient P_{dn} is the downlink power from the BS to the n^{th} user in the l^{th} cell. Then the total achievable sum-rate of the n^{th} user in the l^{th} cell is given by

$$R_n = (1 + SNR_{nl}) \quad (7.30)$$

The total sum-rate of the l^{th} cell is given by

$$R_l = \sum_{n=1}^N R_n \quad (7.31)$$

where N is the total number of active users in the l^{th} cell.

7.13 Results and Discussions

The performance of the SSO algorithm for the effective pilot assignment in massive MIMO cellular communication system was investigated through simulation. The proposed pilot decontamination

in a time-varying channel was implemented using MATLAB. The evaluation metrics used were NMSE, bit error rate, and sum-rate. Simulations were carried out for two different modulation techniques, BPSK and 16-QAM, and the performance was analyzed under varying number of BS antennas as well as for varying number of mobile users.

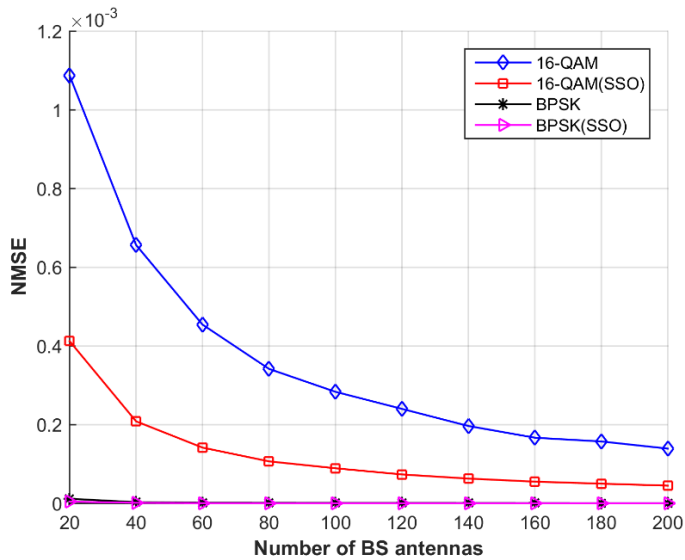


Figure 7.15 NMSE Vs No. of BS antennas (linear scale)

Fig. 7.15 shows the variation NMSE with increasing number of BS antennas. As we increase the number of BS antennas it provides more spatial diversity and increased beam forming to make the communication more error free. Due to the increased beam forming the ICI decreases and that in turn increases the SINR. The NMSE performance is improved more rapidly at the initial stage, and later, it becomes more or less saturated because the number of receiving nodes is kept constant at 20 and as the number of BS antennas increases and reaches about 150 it becomes sufficient to form the necessary spatial diversity and beam-forming for 20 UTs. The proposed method

QAM(SSO) and BPSK(SSO) gives improved performance compared to standard QAM and BPSK irrespective of the number of antennas and is clearly due to the mitigation of pilot contamination by proper pilot assignment.

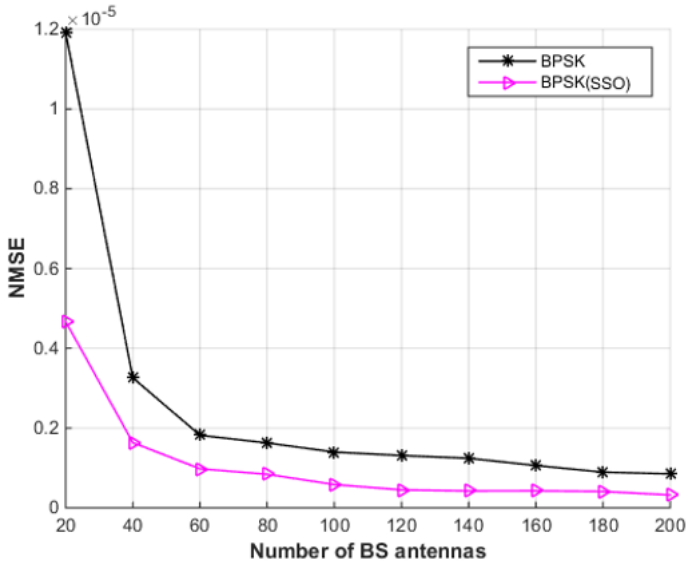


Figure 7.16 NMSE Vs No. of BS antennas for BPSK (linear scale)

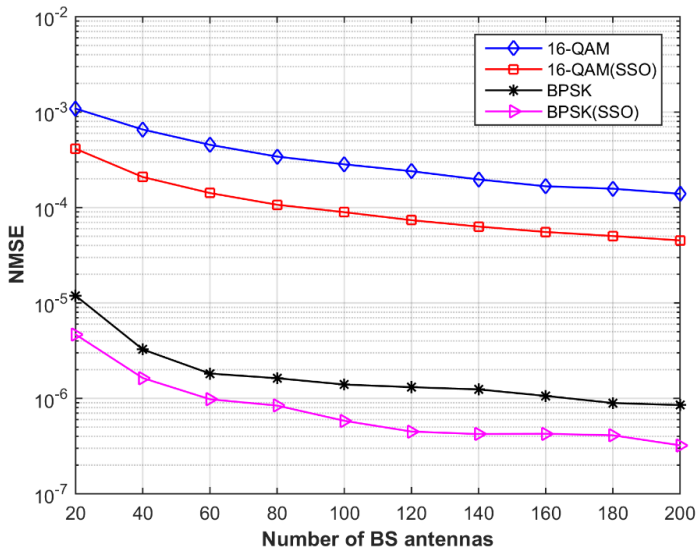


Figure 7.17 NMSE Vs No. of BS antennas (log scale)

The comparison of NMSE under BPSK modulation is not distinguishable in Fig. 7.15 as the value of NMSE becomes very small compared to that in the 16-QAM scheme, Hence in Fig 7.16 the NMSE plot is given only for BPSK and in Fig 7.17 the comparison is redrawn in logarithmic scale . It shows that in BPSK also the proposed pilot assignment scheme gives considerable performance improvement in NMSE.

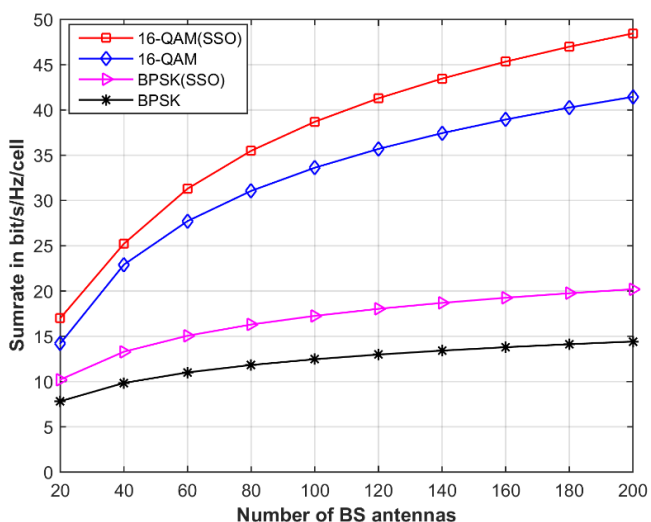


Figure 7.18 Sum-rate Vs. no. of BS antennas

Fig. 7.18 shows the total sum-rate variation in a cell with increasing number of BS antennas. It gives the improvement in the sum-rate performance of the proposed scheme under two modulation schemes. The sum-rate degradation due to inter-cell interference from nearby cells is minimized by using the SSO algorithm for pilot assignment. The SSO algorithm considers both mobility and position of the user node for selecting the pilot sequence and hence the

contamination effect due to the high mobility of users is also reduced giving rise to better performance.

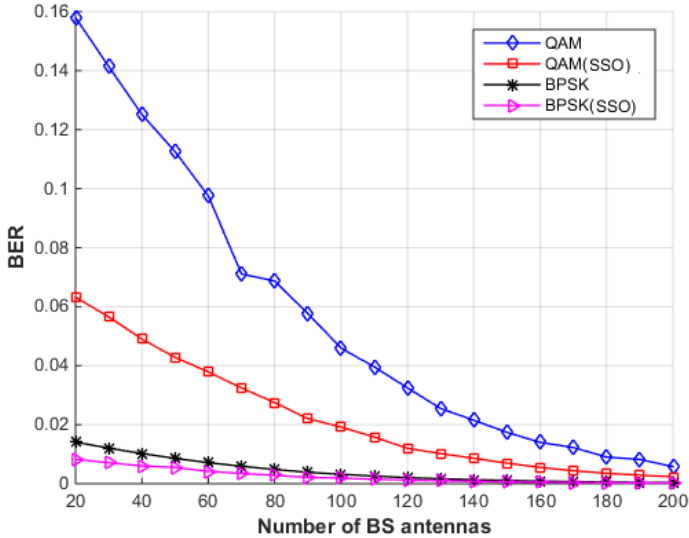


Figure 7.19 BER Vs No. of BS antennas (linear scale)

Fig. 7.19 compares the BER of the system under the four different scenarios. We considered a fixed number of users, $K=20$ and number of BS antennas M is varied from 20 to 200. The BER performance of the system is improved using SSO algorithm for pilot assignment both in 16-QAM and BPSK type of modulation. As the number of base station antennas are increased the random behavior of channel properties starts to become more and more deterministic and the effect of intra cell interference is greatly alleviated by spatially mitigating the interference. Also, it is assumed that the UEs are separated by multiple wavelengths and their channels are uncorrelated. Hence the BER performance of the system improves as we increase the number of BS antennas. Fig 7.20 shows the BER performance for BPSK system alone and Fig 7.21 shows the BER variation in log scale.

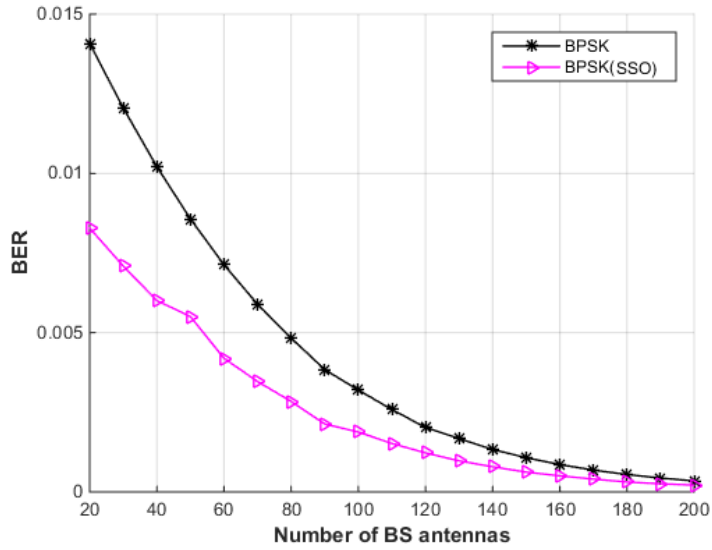


Figure 7.20 BER Vs No. of BS antennas BPSK (linear scale)

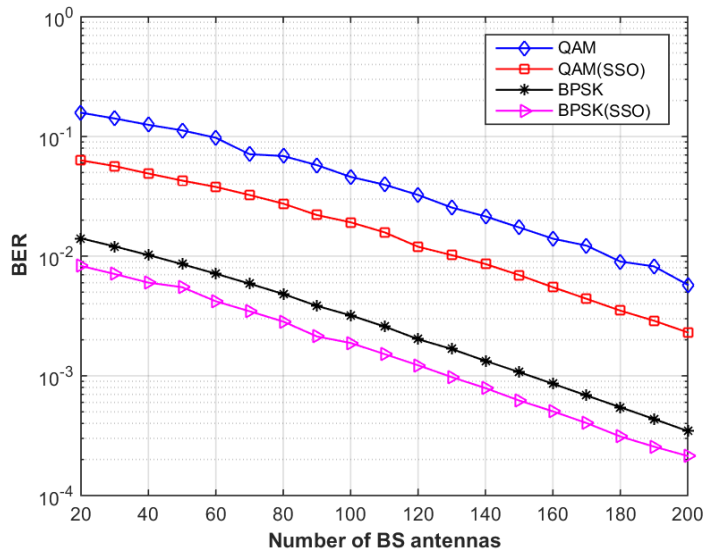


Figure 7.21 BER Vs No. of BS antennas (log scale)

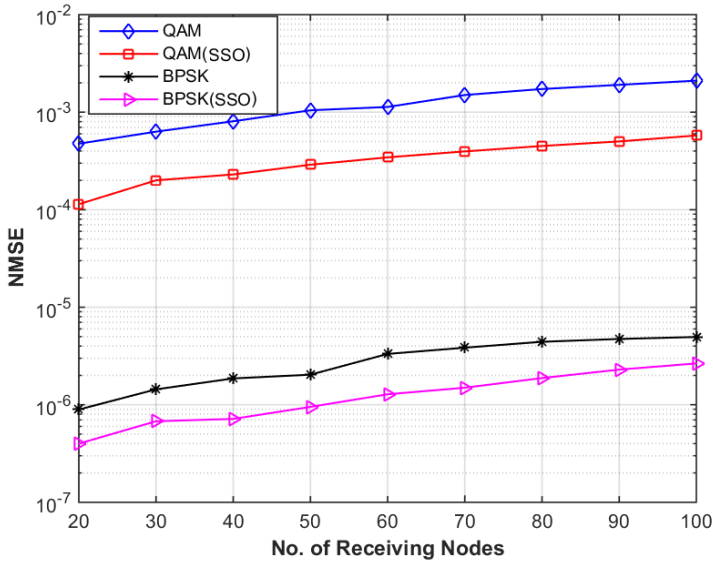


Figure 7.22 NMSE Vs Number of receiving nodes

Fig. 7.22 shows the variation of NMSE with increasing number of UTs keeping the number of BS antennas as constant at 200. The spatial diversity and beam forming requirements of the system increase with the increase in the number of UTs. The SINR goes down with the increase in number of nodes because of ICI as well as pilot contamination. But since the number of transmitting antennas is kept as constant, the system performance starts deteriorating and gives an increased error.

7.14 Key Findings

The pilot contamination problem, which is identified as the most significant impairment of massive MIMO networks, has been investigated in detail and key findings are listed below.

- Non-orthogonal pilots from adjacent cells are the main cause for pilot contamination.

- Interfering pilot signals from adjacent cell centers are very weak compared to the own pilot signals which results in good SINR and will not create severe pilot contamination problem.
- Interfering pilot signals from adjacent cell boundaries will be equally strong as the own pilot signal and results poor SINR and causes pilot contamination.
- A partial pilot reuse strategy which differentiates the users in the cell center and cell boundaries for pilot reuse can reduce the pilot contamination effect.
- SSO algorithm, which makes use of the foraging behavior of social spiders, can be effectively used for optimum pilot allocation in massive MIMO cellular networks to reduce the interference causing pilot contamination.

7.15 Chapter Summary

In this work, we proposed a novel method for pilot decontamination in massive MIMO cellular communication system. In this method, each cell is divided into two sectors, and the users near to their respective BSs in all cells, get the same subset of pilot sequences based on their speed and distance from the BS. This is made possible by using the SSO algorithm, which imitates the cooperative behavior of social spiders, for coordinating the pilot assignment for these mobile users. The algorithm was implemented using MATLAB and tested over a massive MIMO system employing ZF precoding and TDD architecture with two types of modulation techniques 16-QAM and BPSK. Further, the performance gain was measured by comparing BER, NMSE and system sum-rate under different scenarios. The

yielded results proved that the effect of pilot contamination can be reduced by the proposed pilot assignment strategy. The proposed SSO algorithm outperforms the regular pilot assignment method in terms of BER, NMSE, and sum-rate.

CHAPTER-8

CONCLUSION AND FUTURE WORKS

8.1 Introduction

Famous studies carried out, by many research and development organizations, in the area of wireless communications have predicted that the global demand for wireless data would grow by a factor more than 100 by the year 2020. Increasing the capacity of cellular networks by more than 100-fold is not an easy problem. Consequently, a lot of research works are under way in the industry and academia to solve this problem. The answer is not yet clear, but we do know some of the enabling technologies that would give us the predicted 100x or more increase in the capacity. Massive MIMO is the first in that list along with multiuser MIMO, dense user deployed small cells and cooperative communications as other options. In all these technological innovations there are so many research problems that are to be solved before they can be used in the industry on a wide scale.

8.2 Summary and Major Findings

This thesis has provided an overview of LTE, the standard for 4G wireless broadband technology developed by the Third Generation Partnership Project (3GPP). The basic building blocks of LTE, MIMO, and OFDM, along with its merits and challenges when used for highspeed wireless communication are also discussed in detail. In a practical scenario, the quality of a wireless channel is

continuously being modified by many factors, and its best throughput cannot be achieved by employing a fixed modulation scheme tailored for a particular (generally worst case) channel state condition. To cope up with this situation link adaptation techniques are used in LTE. We have analyzed the link adaptation methods used in LTE and developed a simple and comprehensive algorithm for adaptive modulation in MIMO-OFDM wireless networks. In sub-frames with higher channel quality, higher modulation rates are selected, and when the channel quality is low, modulation with lower constellation is used so as to maintain acceptable BER with minimum expense of data rate. As demonstrated through simulations, the adaptive modulation which dynamically acts in response to the channel quality performs at its best.

The combination of MIMO and OFDM system is the most attractive air-interface technology for the next generation wireless communication systems because of its improved spectral efficiency and robustness against inter symbol interference. However, the Doppler shift and RF impairments like phase noise and I/Q imbalance may result in inter-carrier interference which severely limits the performance of wireless communication system. In this thesis, the different sources of interference in MIMO-OFDM communication network and methods to mitigate the same have been studied. To overcome the effect of interferences, an interference cancellation technique combined with adaptive modulation for the MIMO-OFDM wireless network is proposed. Doppler assisted channel estimation method is used to estimate the channel. Also, inter-channel/carrier interference (ICI) cancellation scheme is used to

integrate the parallel interference cancellation together with the decision statistical combining module to detect the data and transmit it to the estimator to iteratively refine the channel and give interference free channel. Simulation results showed that the proposed method improves the BER performance of the system for a wide range of SNR and Doppler spreads.

Massive MIMO, a candidate for 5G technology, promises significant gains in wireless data rates and link reliability by using significantly more antennas at the base transceiver station than in current wireless technologies. A detailed review of previous research works done in the field of Massive MIMO technology, and its different aspects are presented in this work. Since wireless spectrum is a limited resource, maximizing the spectral efficiency of the available spectrum is identified as the best option to meet the growing demand for wireless data traffic. We modeled a massive MIMO system with TDD architecture and analyzed the different ways to optimize its spectral efficiency. The system performance under various practical constraints such as limited coherence block length, number of base station antennas, number of active users, varying range of SNR, etc. are evaluated through simulation. The SE performance is also evaluated under different linear precoding techniques namely, ZF, MRC, and MMSE. The limitation of massive MIMO while operating in FDD mode is also demonstrated through simulation.

From the results, it is inferred that high SE per cell is attained by simultaneously scheduling more number of UEs for transmission. Within the available spectrum, Massive MIMO can schedule more

UEs with larger coherence block lengths and SE performance increases with increase in the number of BS antennas. MMSE precoding is the better option in terms of maximizing the SE, and its implementation is very simple. Results also revealed that a massive MIMO with 100 BS antennas can easily achieve an SE much more than ten times the International Mobile Telecommunications-Advanced (IMT-Advanced standard) requirement of 3 bit/s/Hz/cell and BS with larger antenna arrays of 400 elements can go above 40 times the IMT requirement.

Pilot contamination is identified as the most significant impairment that limits the exploitation of the optimum capacity of massive MIMO systems. It is caused by the re-use of the same, or at least non-orthogonal pilot sequences, among different cells that degrade the performance of channel estimation. In order to mitigate this issue, we proposed a novel partial pilot re-use strategy among users in the adjacent cells, which are close to the base station and also possesses minimum movement velocity. The social spider optimization algorithm that imitates the cooperative behavior of social spiders is used for selecting the eligible users for this pilot reuse in the neighboring cells. The algorithm was implemented using MATLAB and tested over a massive MIMO system employing ZF precoding and TDD architecture with two types of modulation techniques 16-QAM and BPSK. Further, the performance gain was measured by comparing BER, NMSE and system sum-rate under different scenarios. The yielded results proved that the effect of pilot contamination can be reduced by the proposed pilot assignment

strategy. The proposed SSO algorithm outperforms the regular pilot assignment method in terms of BER, NMSE, and sum-rate.

8.3 Limitations of the Research.

Most of the works so far carried out in massive MIMO are based on theoretical assumptions and simulation experiments. So when the findings from the theoretical research are linked with the prototype or actual hardware implementations, many new issues may come into the picture. Massive MIMO is involved with 100s of antennas at the base station, and all of them are not used at all the times for transmission. Only a subset of those antennas are used at any given time and formation of such subsets and individual antenna elements to be added in each subsets are all solved theoretically and may find many issues on practical implementations.

Similarly, user deployed small cells, also called as HetNets or heterogeneous networks are expected to be a major part of future cellular networks. Such HetNets are formed by variety of users and are purely unplanned. The interferences formed by such networks are absolutely indeterministic and all the models and algorithms used may not be suitable to manage it.

All individual antenna elements in the massive mimo base station need low-cost RF chains consisting of up/down converters and amplifiers. Manufacturing of 100s of such RF chains at an affordable cost may associate a lot of hardware impairments and result in hardware imperfections such as I/Q imbalance and phase noise. The research is carried out with an assumption that all these effects will be negligible but in practice that may not be the case.

8.4 Future works

Some potential directions for future work are given below.

In this work, it is assumed that the cells are symmetric as well as the users in the cell are uniformly distributed which is not the case in any practical system. Also, the number of users in each cell is assumed as the same which is not true in a real scenario. Considering these issues in the study is an interesting possibility for future work.

In all our simulations UEs with a single antenna are considered. The analysis of SE by utilizing UEs with multiple antennas (because of the size limit many are not possible, but 2 to 4 are practically feasible) can be carried out as a future work. The main advantage of using more number of antennas at the UE is that it can spatially multiplex number of data streams simultaneously from and to a UE.

All work in this thesis assumed TDD operation for massive MIMO to acquire CSI at the BS for DL transmission. However, it is still unknown whether massive MIMO will operate at TDD or frequency-division-duplexing (FDD) when deployed, since both have their own advantages and disadvantages in acquiring the CSI. This motivates the investigation of the fundamental limits of various channel estimation techniques, as well as how they perform for both TDD and FDD mode of operation as a future work.

REFERENCES

- [1]. QUALCOMM, “*The 1000x data challenge*”, Available at: <https://www.qualcomm.com/invention/1000x>.
- [2]. ERICSSON, “*5G radio access - capabilities and technologies*”, Available at: <https://www.ericsson.com/en/publications/white-papers/5g-radio-access--capabilities-and-technologies/white-paper-5g-radio-access>
- [3]. CISCO, “*Cisco Visual Networking Index: Global Mobile Data Traffic Forecast Update, 2016–2021 White Paper*” Available at: <https://www.cisco.com/c/en/us/solutions/collateral/service-provider/visual-networking-index-vni/mobile-white-paper-c11-520862.html>
- [4]. Ericsson. “*Ericsson Mobility Report: MWC 2015 Edition.*” [Online]. Available at: <http://www.ericsson.com/mobility-report>
- [5]. H. Shariatmadari et al., “*Machine-type communications: Current status and future perspectives toward 5G systems*”, *IEEE Communications Magazine*, vol. 53, no. 9, pp. 10-17, Sep. 2015.
- [6]. G. Americas, *Meeting the 1000x Challenge: The Need for Spectrum, Technology and Policy Innovation*, 4G Americas, Oct 2015
- [7]. The Guardian.com, “*Tsunami of data*”, Available at: <https://www.theguardian.com/environment/2017/dec/11/tsunami-of-data-could-consume-fifth-global-electricity-by-2025>
- [8]. Zhang, Shan, et al. “*Wireless Traffic Steering For Green Cellular Networks*”, Springer, 2016.
- [9]. Nokia Siemens Networks, “*2020: Beyond 4G - Radio Evolution for the Gigabit Experience*,” NSN, White Paper, 2011. [Online]. Available at: http://nsn.com/sites/default/files/document/nokia_siemens_networks_beyond_4g_white_paper_online_20082011_0.pdf
- [10]. Baldemair, Robert, et al. “*Evolving wireless communications: Addressing the challenges and expectations of the future.*” *IEEE Vehicular Technology Magazine* (2013): 24-30.
- [11]. Boccardi, Federico, et al. “*Five disruptive technology directions for 5G.*” *IEEE Communications Magazine* 52.2 (2014): 74-80.
- [12]. C. Shannon, “*A Mathematical Theory of Communication*,” *Bell System Technical Journal*, vol. 27, pp. 379–423, 1948
- [13]. S. Haykin, “*Cognitive Radio: Brain-Empowered Wireless Communications*,” *IEEE Journal on Selected Areas in Communications*, vol. 23, no. 2, pp. 201–219, 2005.
- [14]. Tandra, Rahul, Shridhar Mubaraq Mishra, and Anant Sahai. “*What is a spectrum hole and what does it take to recognize one?*.” *Proceedings of the IEEE* 97.5 (2009): 824-848.
- [15]. C.-C. Chong, K. Hamaguchi, P. F. Smulders, and S.-K. Yong, “*Millimeter wave Wireless Communication Systems: Theory and Applications*,” *EURASIP Journal on Wireless Communications and Networking*, 2007.
- [16]. Z. Pi and F. Khan, “*An Introduction to Millimeter-wave Mobile Broadband Systems*,” *IEEE Communications Magazine*, vol. 49, no. 6, pp. 101–107, 2011.
- [17]. S. Cripps, “*RF Power Amplifiers for Wireless Communications*”, Artech House, 2006.
- [18]. W. Webb, “*Wireless Communications: The Future*”, John Wiley & Sons, 2007.

- [19]. D. C. Cox, "Cochannel Interference Considerations in Frequency Reuse Small-coverage-area Radio Systems," IEEE Transactions on Communications, vol. 30, no. 1, pp. 135–142, 1982.
- [20]. V. Mac Donald, "Advanced Mobile Phone Service: The Cellular Concept," Bell System Technical Journal, The, vol. 58, no. 1, pp. 15–41, 1979.
- [21]. E. Björnson, E. G. Larsson, and M. Debbah, "Optimizing Multi-Cell Massive MIMO for Spectral Efficiency: How Many Users Should Be Scheduled?" in IEEE Global Conference on Signal and Information Processing (GlobalSIP), Atlanta, USA, December 2014.
- [22]. Alouini and Goldsmith, "Area Spectral Efficiency of Cellular Mobile Radio Systems," IEEE Transactions on Vehicular Technology, vol. 48, no. 4, pp. 1047–1066, 1999. 3, 23
- [23]. ERICSON, "LTE Release 12 - taking another step toward the Networked Society", Available at: <http://4g5gworld.com/whitepaper/lte-release-12-taking-another-step-toward-networked-society>'.
- [24]. Analysis Mason. MWC 2015: "LTE-A Carrier Aggregation Enables Macro cells to Reduce the Need for Small Cells". [Online]. Available at: <http://www.analysismason.com/Research/Content/Comments/LTE-A-CA-small-cells-MWC-Mar2015-RDTN0/>
- [25]. Holma, H. & Toskala, "A. LTE-Advanced: 3GPP Solution for IMT-Advanced". John Wiley & Sons, 1st edition, 2012.
- [26]. Yi, S., et al. Y. "Radio Protocols for LTE and LTE-Advanced". John Wiley & Sons, 2012.
- [27]. Shen, Z., et al. "Overview of 3GPP LTE-Advanced Carrier Aggregation for 4G wireless Communications". IEEE Communications Magazine, 2012.
- [28]. Scheit, Oliver. "Self-Healing in Self-Organizing Networks." Seminar Innovative Internettechnologien und Mobilkommunikation SS2014. 2014.
- [29]. Tran, Thien-Toan, Yoan Shin, and Oh-Soon Shin. "Overview of enabling technologies for 3GPP LTE-advanced." EURASIP Journal on Wireless Communications and Networking 2012.1 (2012): 54.
- [30]. Liu, Lingjia, et al. "Downlink mimo in lte-advanced: Su-mimo vs. mu-mimo." IEEE Communications Magazine 50.2 (2012).
- [31]. Weinstein, S., and Paul Ebert. "Data transmission by frequency-division multiplexing using the discrete Fourier transform." IEEE transactions on Communication Technology 19.5 (1971): 628-634.
- [32]. Jha, Uma Shanker, and Ramjee Prasad. "OFDM towards fixed and mobile broadband wireless access" Artech House. (2007).
- [33]. Bhardwaj, Manushree, Arun Gangwar, and Devendra Soni. "A review on OFDM: concept, scope & its applications." IOSR Journal of Mechanical and Civil Engineering (IOSRJMCE) 1.1 (2012): 07-11.
- [34]. Biglieri, Ezio, et al. "MIMO wireless communications", Cambridge unty. press, 2007.
- [35]. Clerckx, Bruno, et al. "MIMO wireless networks: channels, techniques and standards for multi-antenna, multi-user and multi-cell systems", Academic Press, 2013.
- [36]. Jagannatham, Aditya K. "NOC: Principles of Modern CDMA/MIMO/OFDM Wireless Communications." (2015).
- [37]. Alumona, T. L., et al. "Adaptive modulation techniques for capacity improvement of BER in WCDMA."
- [38]. Raut, Rajeshree, Priti Subramaniam, and Kavita Bramahankar. "Adaptive Coding Techniques to Improve BER in OFDM System." International Journal of Image Processing and Vision Sciences (IJIPVS) ISSN (Print) 2278 1110 (2012).

- [39]. Barnela, Manoj, and Dr Suresh Kumar. "Digital modulation schemes employed in wireless communication: A literature review." *International Journal of Wired and Wireless Communications* 2.2 (2014): 15-21.
- [40]. Achra, Nisha, Garima Mathur, and R. P. Yadav. "Performance analysis of MIMO OFDM system for different modulation schemes under various fading channels." *International Journal of Advanced Research in Computer and Communication Engineering* 2.5 (2013): 2098-2103.
- [41]. Mohammadi, Abbas, and Fadhel M. Ghannouchi. "RF transceiver design for MIMO wireless communications." Vol. 145. Springer Science & Business Media, 2012.
- [42]. Saad, W. K., Ismail, M., & Nordin, R. "Survey of adaptive modulation scheme in MIMO transmission". *Journal of Communications*, 7(12), 873-884 (2012).
- [43]. Kanchi, Sravanthi, et al. "Overview of LTE-A technology." *Global High Tech Congress on Electronics (GHTCE)*, 2013 IEEE. IEEE, 2013.
- [44]. Hadi, S. S., and T. C. Tiong. "Adaptive Modulation and Coding for LTE Wireless Communication." *IOP Conference Series: Materials Science and Engineering*. Vol. 78. No. 1. IOP Publishing, 2015.
- [45]. Bertrand, Pierre, Jing Jiang, and Anthony Ekpenyong. "Link adaptation control in LTE uplink." *Vehicular Technology Conference (VTC Fall)*, 2012 IEEE. IEEE, 2012.
- [46]. Z. Zhendong, V. Branka, D. Mischa, and L. Yonghui, "MIMO Systems with Adaptive Modulation", *IEEE Trans. Veh. Technol.*, vol. 54, no. 5, pp. 1828–1842, 2005.
- [47]. H. Jinliang, et al., "On Performance of Adaptive Modulation in MIMO Systems Using Orthogonal Space–Time Block Codes", *IEEE Trans. Veh. Technol.*, vol. 58, no. 8, 2009.
- [48]. Z. Zhou, and B. Vucetic, "Design of adaptive modulation using imperfect CSI in MIMO systems", *IET Journals, Electronics Letters*, vol. 40, Issue 17, pp. 1073-1075, 2004.
- [49]. D. M. Jimenez, G. Gomez, and J. T. Entrambasaguas, "Joint Adaptive Modulation and MIMO Transmission for Non-Ideal OFDMA Cellular Systems," conference IEEE, 2009.
- [50]. Y. Xiangbin, L. Shu-Hung, H. M. Wai, and W. Wai-Ki, "Performance of Variable-Power Adaptive Modulation With Space–Time Coding and Imperfect CSI in MIMO Systems" *IEEE Trans. Veh. Technol.*, vol. 58, no. 4, 2009.
- [51]. X. B. Yu, S. H. Leung, and W. K. Wong, "Performance analysis of variable-power adaptive modulation with antenna selection over Rayleigh fading channels", *IET Commun.*, vol. 5, Iss. 10, pp. 1394–1404, 2011.
- [52]. Isam, et al. "Characterizing the intercarrier interference of non-orthogonal spectrally efficient FDM system." *Communication Systems, Networks & Digital Signal Processing (CSNDSP)*, 2012 8th International Symposium on. IEEE, 2012.
- [53]. Master, S., "Fundamentals of Interference in Wireless Networks".
- [54]. Zheng, Gan, et al. "Rethinking the role of interference in wireless networks." *IEEE Communications Magazine* 52.11 (2014): 152-158.
- [55]. Shamsan, et al. "Co-channel and adjacent channel interference evaluation for IMT-Advanced coexistence with existing fixed systems." *RF and microwave conference, 2008. RFM 2008. IEEE international. IEEE, 2008.*
- [56]. Tailor, K.H. and Shah, S.N., "A Review On Various Interference Effects In A MIMO-OFDM System." *International Journal of Engineering*, 2(1) 2013.
- [57]. Avestimehr, A. S., et al. "Introduction to the special issue on interference networks." *IEEE Transactions on Information Theory* 57.5 (2011): 2545-2547.
- [58]. Syrjala et al. "Phase noise modelling and mitigation techniques in OFDM communications systems." *Wireless Telecommunications Symposium, IEEE, 2009.*

- [59]. Robertson, Patrick, and Stefan Kaiser. "Analysis of the effects of phase-noise in orthogonal frequency division multiplex systems." Communications, 1995. ICC'95 Seattle, 'Gateway to Globalization', 1995 IEEE International Conference on. Vol. 3.
- [60]. Armada, A. Garcia. "Understanding the effects of phase noise in orthogonal frequency division multiplexing (OFDM)." IEEE Transactions on Broadcasting (2001): 153-159.
- [61]. Chung, Wonzoo. "A matched filtering approach for phase noise suppression in CO-OFDM systems." IEEE Photonics technology letters 22.24 (2010): 1802-1804.
- [62]. Raghu Mysore Rao, Babak Daneshrad, "V/Q Mismatch Cancellation for MIMO-OFDM Systems", Proceedings of the IEEE 15th International Symposium on Personal, Indoor and Mobile Radio Communications, PIMRC, (2004):2710-2714.
- [63]. Raghu Mysore Rao and Babak Daneshrad, "Analog Impairments in MIMO-OFDM Systems", IEEE Transactions on Wireless Communications 2006, 5(12): 3382-3387.
- [64]. Kumbhani, Brijesh, et al. "Narrow Band Interference (NBI) mitigation technique for TH-PPM UWB systems in IEEE 802.15. 3a channel using wavelet packet transform." Emerging Trends and Applications in Computer Science (ICETACS), 2013 1st International Conference on. IEEE, 2013.
- [65]. Batra, Arun, and J R. Zeidler. "Narrowband interference mitigation in OFDM systems." Military Communications Conference, 2008. MILCOM 2008. IEEE. IEEE, 2008.
- [66]. Poulkov, Vladimir, et al. "Narrowband interference suppression in MIMO systems." MIMO Systems, Theory and Applications. InTech, 2011.
- [67]. Coleri, Sinem, et al. "Channel estimation techniques based on pilot arrangement in OFDM systems." IEEE Transactions on broadcasting 48.3 (2002): 223-229.
- [68]. Kharel, Manita Baral, and Sarbagy Ratna Shakya. "Simulation on Effect of Doppler shift in Fading channel and Imperfect Channel Estimation for OFDM in Wireless Communication." Proceedings of IOE Graduate Conference. Vol. 537. 2014.
- [69]. Chiueh, T.D., Tsai, P.Y. and Lai, I.W. "Baseband receiver design for wireless MIMO-OFDM communications." John Wiley & Sons. 2012
- [70]. Corvaja, Roberto, and Ana García Armada. "SINR degradation in MIMO-OFDM systems with channel estimation errors and partial phase noise compensation." IEEE Transactions on Communications 58.8 (2010): 2199-2203.
- [71]. Sen, Souvik, et al. "Successive interference cancellation: A back-of-the-envelope perspective." Proceedings of the 9th ACM SIGCOMM Workshop on Hot Topics in Networks. ACM, 2010.
- [72]. Miridakis, N.I. and Vergados, D.D., "A survey on the successive interference cancellation performance for single-antenna and multiple-antenna OFDM systems." IEEE Communications Surveys & Tutorials, 15(1), (2013):312-335.
- [73]. Kohno, R., Imai, H., Hatori, M. and Pasupathy, S., "Combinations of an adaptive array antenna and a canceller of interference for direct-sequence spread-spectrum multiple-access system." IEEE journal on Selected Areas in Communications, (1990):675-682.
- [74]. Foschini, G. J., and R. A. Valenzuela. "Vblast: An architecture for realizing very high data rates over the rich-scattering wireless channel." Proc. 1998 Int. Symp. on Advanced Radio Technologies. 1998.
- [75]. Baro, Stephan, et al. "Improving BLAST performance using space-time block codes and turbo decoding." Global Telecommunications Conference, 2000. GLOBECOM'00. IEEE. Vol. 2. IEEE, 2000.
- [76]. Zhu, Hufei, Zhongding Lei, and Francois Chin. "On interference cancellation ordering of V-BLAST detectors." Information, Communications and Signal Processing, 2003 and Fourth Pacific Rim Conference on Multimedia. Proceedings of the 2003 Joint Conference of the Fourth International Conference on. Vol. 2. IEEE, 2003.

- [77]. Kim, Young-Doo, et al. "Adaptive modulation for MIMO systems with V-BLAST detection." Vehicular Technology Conference, 2003. VTC 2003-Spring. The 57th IEEE Semiannual. Vol. 2. IEEE, 2003.
- [78]. Halperin, Daniel, et al. "Interference Cancellation: Better Receivers for a New Wireless MAC." HotNets. 2007.
- [79]. Andrews, Jeffrey G. "Interference cancellation for cellular systems: a contemporary overview." IEEE Wireless Communications 12.2 (2005): 19-29.
- [80]. Aboutorab, Neda, Wibowo Hardjawana, and Branka Vucetic. "A new iterative Doppler-assisted channel estimation joint with parallel ICI cancellation for high-mobility MIMO-OFDM systems." IEEE Transactions on Vehicular Technology 61.4 (2012): 1577-1589.
- [81]. Shaverdian, Ararat, and Mohammad Reza Nakhai. "Robust distributed beamforming with interference coordination in downlink cellular networks." IEEE Transactions on Communications 62.7 (2014): 2411-2421.
- [82]. Septimus, et al. "A spectral approach to inter-carrier interference mitigation in OFDM systems." IEEE Transactions on Communications 62.8 (2014): 2802-2811.
- [83]. Lu, Yi, et al. "Blind interference alignment with diversity in K -user interference channels." IEEE Transactions on Communications 62.8 (2014): 2850-2859.
- [84]. Sagias, Nikos C. "On the ASEP of decode-and-forward dual-hop networks with pilot-symbol assisted M-PSK." IEEE Transactions on Communications 62.2 (2014): 510-521.
- [85]. Wilson, Craig, and Venugopal V. Veeravalli. "Degrees of freedom for the constant MIMO interference channel with CoMP transmission." IEEE Transactions on Communications 62.8 (2014): 2894-2904.
- [86]. Phan-Huy, Dinh-Thuy, Pierre Siohan, and Maryline Helard. "Make-It-Real precoders for MIMO OFDM/OQAM without inter carrier interference." Global Communications Conference (GLOBECOM), 2013 IEEE. IEEE, 2013.
- [87]. Borkar, Nita J., et al. "BER performance of OFDM system with adaptive modulation." Complex Systems (ICCS), 2012 International Conference on. IEEE, 2012.
- [88]. T L. Marzetta, "Non cooperative cellular wireless with unlimited numbers of base station antennas," IEEE Transactions on wireless Communications, vol. 9, no. 11, pp. 3590–3600, 2010
- [89]. Rusek, Fredrik, et al. "Scaling up MIMO: Opportunities and challenges with very large arrays." IEEE signal processing magazine 30.1 (2013): 40-60.
- [90]. Han, Shuangfeng, et al. "Reference signals design for hybrid analog and digital beamforming." IEEE communications letters 18.7 (2014): 1191-1193.
- [91]. Andrews, Jeffrey G., et al. "What will 5G be?." IEEE Journal on selected areas in communications 32.6 (2014): 1065-1082.
- [92]. Bhushan, N., Li, J., et al. "Network densification: the dominant theme for wireless evolution into 5G." IEEE Communications Magazine, 52.2(2014):82-89.
- [93]. Bjornson, Emil, Marios Kountouris, and Mérouane Debbah. "Massive MIMO and small cells: Improving energy efficiency by optimal soft-cell coordination." Telecommunications (ICT), 2013 20th International Conference on. IEEE, 2013.
- [94]. Ngo, Hien Quoc, Erik G. Larsson, and Thomas L. Marzetta. "Energy and spectral efficiency of very large multiuser MIMO systems." IEEE Transactions on Communications 61.4 (2013): 1436-1449.
- [95]. Long Zhao, Hui Zhao, and Kan Zheng. "Energy efficient power allocation strategy for downlink MU-MIMO with massive antennas." The Journal of China Universities of Posts and telecommunications, 20(3) :1–7, June 2013.
- [96]. Jungnickel, Volker, et al. "The role of small cells, coordinated multipoint, and massive MIMO in 5G." IEEE Communications Magazine 52.5 (2014): 44-51.

- [97]. E. G. Larsson et al. "Massive MIMO for next generation wireless systems," in IEEE Communications Magazine, vol. 52, no. 2, pp. 186-195, February 2014.
- [98]. L. Lu, et al. "An Overview of Massive MIMO: Benefits and Challenges", IEEE Journal of Selected Topics in Signal Processing, 2013.
- [99]. Shen, et al. "Downlink user capacity of massive MIMO under pilot contamination." IEEE Transactions on Wireless Communications 14.6 (2015): 3183-3193.
- [100]. Arash, et al. "Employing antenna selection to improve energy efficiency in massive MIMO systems." Transactions on Emerging Telecomm. Technologies 28.12 (2017).
- [101]. Jabbar, S.Q. and Li, Y. "Analysis and Evaluation of Performance Gains and Tradeoffs for Massive MIMO Systems". Applied Sciences, 6.10 (2016): 268.
- [102]. Kapetanovic, et al. "Physical layer security for massive MIMO: An overview on passive eavesdropping and active attacks." IEEE Communications Magazine, 53.6 (2015):21-27.
- [103]. Ngo, Hien Quoc, Erik G. Larsson, and Thomas L. Marzetta. "Massive MU-MIMO downlink TDD systems with linear precoding and downlink pilots." Communication, Control, and Computing, 2013 51st Annual Allerton Conference on. IEEE, 2013.
- [104]. Chen, et al., "Channel Hardening and Favorable Propagation in Cell-Free Massive MIMO with Stochastic Geometry." arXiv preprint arXiv:1710.00395 (2017).
- [105]. C. Xu, et al., "Massive MIMO, Non-Orthogonal Multiple Access and Interleave Division Multiple Access," in IEEE Access, vol. 5, pp. 14728-14748, 2017.
- [106]. Luo, F.L. and Zhang, C. eds. "Signal processing for 5G: algorithms and implementations. John Wiley & Sons." 2016
- [107]. Haartsen, Jaap C. "Impact of non-reciprocal channel conditions in broadband TDD systems." Personal, Indoor and Mobile Radio Communications, 2008. PIMRC 2008. IEEE 19th International Symposium on. IEEE, 2008.
- [108]. Neumann, David, Michael Joham, and Wolfgang Utschick. "Channel estimation in massive MIMO systems." arXiv preprint arXiv:1503.08691 (2015).
- [109]. Yuan, H., Wang, C., Li, Y., Liu, N. and Cui, G., 2016, October. "The design of array antennas used for Massive MIMO system in the fifth generation mobile communication". In Antennas, Propagation and EM Theory (ISAPE), 2016 11th International Symposium on (pp. 75-78). IEEE.
- [110]. Harris, P., Vieira, J., Hasan, W.B., Liu, L., Malkowsky, S., Beach, M., Armour, S., Tufvesson, F. and Edfors, O., 2018. "Achievable Rates and Training Overheads for a Measured LOS Massive MIMO Channel". IEEE Wireless Communications Letters.
- [111]. E. Björnson, E. G. Larsson, T. L. Marzetta, "Massive MIMO: Ten Myths and One Critical Question", IEEE Commun. Mag., Mar. 2015.
- [112]. S. Yang, L. Hanzo, "Fifty Years of MIMO Detection: The Road to Large-Scale MIMOs", IEEE Communications Surveys & Tutorials, Vol.17, no. 4, pp. 1941 - 1988, Sep. 2015
- [113]. K. Li, R. Sharan, Y. Chen, J. R. Cavallaro, T. Goldstein, and C. Studer, "Decentralized Beamforming for Massive MU-MIMO on a GPU Cluster", IEEE Global Conference on Signal and Information Processing (GlobalSIP), Dec. 2016.
- [114]. S. Chaudhari and D. Cabric, "Downlink transceiver beamforming and admission control for massive MIMO cognitive radio networks", 2015 49th Asilomar Conference on Signals, Systems and Computers, Pacific Grove, CA, 2015, pp. 1257-1261.
- [115]. B. Chen, C. Zhu, W. Li, J. Wei, V. C. M. Leung, and L. T. Yang, "Original Symbol Phase Rotated Secure Transmission Against Powerful Massive MIMO Eavesdropper", IEEE Access, vol. 4, pp. 3016-3025, 2016
- [116]. T. Bogale, L. B. Le, X. Wang, and L. Vandendorpe, "Orthogonal Faster Than Nyquist Transmission for SIMO Wireless Systems", IEEE GLOBECOM 2016.

- [117]. J. Wang, et al., “*Jamming-Aided Secure Communication in Massive MIMO Rician Channels*”, IEEE Transactions on Wireless Communications, July 2015.
- [118]. H. Pirzadeh, S. M. Razavizadeh, E. Björnson, “*Subverting Massive MIMO by Smart Jamming*”, IEEE Wireless Communications Letters, Sept. 2015.
- [119]. H. Q. Ngo, H. A. Suraweera, M. Matthaiou, and E. G. Larsson, “*Multipair full-duplex relaying with massive arrays and linear processing*”, IEEE Journal on Selected Areas in Communications, May 2014.
- [120]. K. T. Truong and R. W. Heath, Jr., “*The Viability of Distributed Antennas for Massive MIMO Systems*”, Proc. of the Asilomar Conf. on Signals, Systems, and Computers, Pacific Grove, CA, November 3-6, 2013.
- [121]. K. Hosseini, J. Hoydis, S. ten Brink, and M. Debbah, “*Massive MIMO and Small-Cells: How to Densify Heterogeneous Networks*”, in Proc. IEEE International Conference Communications (ICC), June 2013.
- [122]. Z. Xiang, Me. Tao and X. Wang, “*Massive MIMO multicasting in noncooperative cellular networks*”, IEEE JSAC Special Issue on 5G Wireless Communication Systems, vol. 32, no. 6, pp. 1180-1193, June 2014.
- [123]. Zhu J., et al., “*Secure Transmission in Multicell Massive MIMO Systems*”, IEEE Transactions on Wireless Communications, vol. 13, no. 9, September 2014.
- [124]. Qiang He, Limin Xiao, Xiaofeng Zhong, and Shidong Zhou, “*Increasing the Sum-Throughput of Cells With a Sectorization Method for Massive MIMO*”, IEEE Communications Letters, vol. 18, no. 10, pp. 1827-1830, Oct. 2014.
- [125]. Neil, Callum T., et al. “*Deployment issues for massive MIMO systems.*” Communication Workshop (ICCW), 2015 IEEE International Conference on. IEEE, 2015.
- [126]. Zhang, Chao. “*Fractional Pilot Reuse in Massive MIMO System.*” IEICE Transactions on Fundamentals of Electronics, Commns. and Computer Sciences 98.11 (2015).
- [127]. F. Jiang, J. Chen, A. L. Swindlehurst and J. A. Lopez-Salcedo, “*Massive MIMO for Wireless Sensing with a Coherent Multiple Access Channel*”, March 2015, submitted.
- [128]. Smith, et al., “*On the Convergence and Performance of MF Precoding in Distributed Massive MU-MIMO Systems*”. arXiv preprint arXiv:1503.00796. 2015
- [129]. Xu, Y. and Mao, S., 2017. “*User association in massive MIMO HetNets*”. IEEE Systems Journal, 11(1), pp.7-19.
- [130]. J. S. Lemos, F. Rosário, F. A. Monteiro, J. Xavier, A. Rodrigues, “*Massive MIMO Full-Duplex Relaying with Optimal Power Allocation for Independent Multipairs*”, in Proc. IEEE International Workshop on Signal Processing Advances in Wireless Communications (SPAWC), Stockholm, Sweden, June 2015.
- [131]. Lakshminarayana, S., Assaad, M. and Debbah, M., 2015. “*Coordinated multicell beamforming for massive MIMO: A random matrix approach*”. IEEE Transactions on Information Theory, 61(6), pp.3387-3412.
- [132]. J. Choi, “*Distributed Beamforming for Macro Diversity and Power Control With Large Arrays in Spatial Correlated Channels*”, IEEE Transactions on Wireless Communications, vol. 14, no. 4, pp. 1871-1881, April 2015
- [133]. Basciftci, Y. Ozan, C. Emre Koksal, and Alexei Ashikhmin. “*Securing massive MIMO at the physical layer.*” Communications and Network Security (CNS), 2015 IEEE Conference on. IEEE, 2015.
- [134]. D. Kapetanovic, G. Zheng and F. Rusek, “*Physical Layer Security for Massive MIMO: An Overview on Passive Eavesdropping and Active Attacks,*” April 2015, submitted.
- [135]. J. H. Sørensen, E. de Carvalho, and P. Popovski, “*Massive MIMO for Crowd Scenarios: A Solution Based on Random Access,*” in Proc. IEEE Global Communications Conf. (GLOBECOM), MassMIMO Workshop, Austin, TX, USA, December 2014.

- [136]. H. Q. Ngo, A. Ashikhmin, H. Yang, E. G. Larsson, and T. L. Marzetta, "Cell-Free Massive MIMO: Uniformly great service for everyone," in Proc. IEEE International Workshop on Signal Processing Advances in Wireless Communications (SPAWC), Stockholm, Sweden, 2015.
- [137]. Z. Gao, et al., "Asymptotic Orthogonality Analysis of Time-Domain Sparse Massive MIMO Channels," IEEE Communications Letters, Volume:19 Issue:10, Oct. 2015.
- [138]. T. L. Marzetta, "Noncooperative Cellular Wireless with Unlimited Numbers of Base Station Antennas.," IEEE Trans. Wireless Communications, vol. 9, no. 11, pp. 3590-3600, Nov. 2010.
- [139]. Pitarokoilis, et al., "On the Optimality of Single-Carrier Transmission in Large-Scale Antenna Systems.," IEEE Wireless Commun. Lett., vol. 1, no. 4, pp. 276-279, Aug. 2012.
- [140]. Müller, et al., "Blind pilot decontamination." IEEE Journal of Selected Topics in Signal Processing 8.5 (2014): 773-786.
- [141]. H. Huh, et al., "Achieving "Massive MIMO" Spectral Efficiency with a Not-so-Large Number of Antennas." IEEE Trans. Wireless Communications, vol. 11, no. 9, pp. 3226-3239, Sept. 2012.
- [142]. H. Yang and T. L. Marzetta, "Performance of Conjugate and Zero-Forcing Beamforming in Large-Scale Antenna Systems.," IEEE J. Sel. Areas Commun, vol. 31, no. 2, pp. 172-179, Feb. 2013.
- [143]. Ozgur, O. Leveque, and D. Tse, "Spatial Degrees of Freedom of Large Distributed MIMO Systems and Wireless Ad Hoc Networks.," IEEE J. Sel. Areas Commun, vol. 31, no. 2, pp. 202-214, Feb. 2013.
- [144]. Jose, Jubin, et al. "Pilot contamination and precoding in multi-cell TDD systems." IEEE Transactions on Wireless Communications 10.8 (2011): 2640-2651.
- [145]. Farhang, Arman, et al. "Filter bank multicarrier for massive MIMO." Vehicular Technology Conference (VTC Fall), 2014 IEEE 80th. IEEE, 2014.
- [146]. Masouros, et al., "Space-constrained massive MIMO: Hitting the wall of favorable propagation." IEEE Communications Letters 19.5 (2015): 771-774.
- [147]. Ngo, Hien Quoc, and Erik G. Larsson. "No downlink pilots are needed in TDD massive MIMO." IEEE Transactions on Wireless Communications 16.5 (2017): 2921-2935.
- [148]. Han, Yonghee, and Jungwoo Lee. "Uplink pilot design for multi-cell massive MIMO networks." IEEE Communications Letters 20.8 (2016): 1619-1622.
- [149]. Han, et al., "Projection-based differential feedback for FDD massive MIMO systems." IEEE Transactions on Vehicular Technology 66.1 (2017): 202-212.
- [150]. Zaib, Alam, et al. "Distributed channel estimation and pilot contamination analysis for massive MIMO-OFDM systems." IEEE Transactions on Commns. (2016): 4607-4621.
- [151]. De Carvalho, Elisabeth, et al. "Random access for massive MIMO systems with intra-cell pilot contamination." Acoustics, Speech and Signal Processing (ICASSP), 2016 IEEE International Conference on. IEEE, 2016.
- [152]. X, Zhu, L. Dai, Z. Wang, "Graph Coloring Based Pilot Allocation to Mitigate Pilot Contamination for Multi-Cell Massive MIMO Systems.," IEEE Communications Letters, Volume:19 Issue:10, Oct. 2015.
- [153]. L. Byungju, J. Choi ; J. Seol ; D. J. Love, "Antenna Grouping Based Feedback Compression for FDD-Based Massive MIMO Systems.," IEEE Transaction on Communications, Volume:63 Issue:9, Sept. 2015.
- [154]. J.K. Tugnait, "Self-Contamination for Detection of Pilot Contamination Attack in Multiple Antenna Systems.," IEEE Wireless Communications Letters, Oct. 2015.
- [155]. Choi, Junil, et al. "Noncoherent trellis coded quantization: A practical limited feedback technique for massive MIMO systems." IEEE Transactions on Communications 61.12 (2013): 5016-5029.

- [156]. Choi, Junil, David J. Love, and Patrick Bidigare. "Downlink training techniques for FDD massive MIMO systems: Open-loop and closed-loop training with memory." *IEEE Journal of Selected Topics in Signal Processing* 8.5 (2014): 802-814.
- [157]. Fernandes, Fabio, Alexei Ashikhmin, and Thomas L. Marzetta. "Inter-cell interference in noncooperative TDD large scale antenna systems." *IEEE Journal on Selected Areas in Communications* 31.2 (2013): 192-201.
- [158]. K. T. Truong and R. W. Heath, Jr., "Effects of Channel Aging in Massive MIMO Systems, *Journal of Communications and Networks*," Special Issue on Massive MIMO, vol. 15, no. 4, pp. 338-351, Aug. 2013.
- [159]. C. Knievel and P. A. Hoeher, "On Particle Swarm Optimization for MIMO Channel Estimation, *Journal of Electrical and Computer Engineering*," vol. 2012, Article ID 614384, 10 pages, 2012.
- [160]. C. Knievel, M. Noemm, and P. A. Hoeher, "Low Complexity Receiver for Large-MIMO Space Time Coded Systems," in Proc. IEEE VTC-Fall'2011, Sept. 2011.
- [161]. H. Yin, D. Gesbert, M. Filippou, and Y. Liu, "A Coordinated Approach to Channel Estimation in Large-scale Multiple-antenna Systems," *IEEE J. Sel. Areas Commun*, vol. 31, no. 2, pp. 264-273, Feb. 2013.
- [162]. T. E. Bogale and L. B. Le, "Pilot Optimization and Channel Estimation for Multiuser Massive MIMO Systems," in Proc. CISS 2014.
- [163]. Ch. Jeon, R. Ghods, A. Maleki, Ch. Studer, "Optimality of Large MIMO Detection via Approximate Message Passing," Proc. IEEE International Symposium on Information Theory, pp 1227-1231, Jun. 2015.
- [164]. Al-Askery, Ali J., Charalampos C. Tsimenidis, and Said Boussakta. "Fixed-point arithmetic detectors for massive MIMO-OFDM systems." *Signal Processing Conference (EUSIPCO), 2015 23rd European. IEEE*, 2015.
- [165]. A. Chockalingam, "Low-Complexity Algorithms for Large-MIMO Detection," in Proc. Communications., Control and Signal Processing (ISCCSP), 2010.
- [166]. Q. Zhou and X. Ma, "Element-Based Lattice Reduction Algorithms for Large MIMO Detection," *IEEE J. Sel. Areas Commun*, vol. 31, no. 2, pp. 274-286, Feb. 2013.
- [167]. Wu, Sheng, et al. "Low-complexity iterative detection for large-scale multiuser MIMO-OFDM systems using approximate message passing." *IEEE Journal of Selected Topics in Signal Processing* 8.5 (2014): 902-915.
- [168]. Wu, Michael, et al. "Large-scale MIMO detection for 3GPP LTE: Algorithms and FPGA implementations." *IEEE Journal of Selected Topics in Signal Processing* 8.5 (2014)
- [169]. Torres, Paulo, Luis Charrua, and Antonio Gusmao. "On Detection Issues in the SC-based Uplink of a MU-MIMO System with a Large Number of BS Antennas." *Vehicular Technology Conference (VTC Fall), 2015 IEEE 82nd. IEEE*, 2015.
- [170]. Alkhateeb, Ahmed, Geert Leus, and Robert W. Heath. "Multi-layer precoding: A potential solution for full-dimensional massive MIMO systems." *IEEE Transactions on Wireless Communications* 16.9 (2017): 5810-5824.
- [171]. S. K. Mohammed and E. G. Larsson, "Constant-Envelope Multi-User Precoding for Frequency-Selective Massive MIMO Systems," *IEEE Wireless Commun. Lett.*, vol. 2, no. 5, pp. 547-550, Oct. 2013.
- [172]. C. Artigue, P. Loubaton, "On the Precoder Design of Flat Fading MIMO Systems Equipped with MMSE Receivers: A Large System Approach," *IEEE Trans. Inform. Theory*, vol. 57, no. 7, pp. 4138-4155, July 2011.
- [173]. Zaidel, Benjamin M., et al. "Vector precoding for Gaussian MIMO broadcast channels: Impact of replica symmetry breaking." *IEEE Transactions on Information Theory* 58.3 (2012): 1413-1440.

- [174]. J. Zhang, X. Yuan, and L. Ping, "Hermitian Precoding for Distributed MIMO Systems with Individual Channel State Information.", IEEE J. Sel. Areas Commun, vol. 31, no. 2, pp. 241-251, Feb. 2013.
- [175]. Park, Jaehyun, and Bruno Clerckx. "Multi-user linear precoding for multi-polarized massive MIMO system under imperfect CSIT." IEEE Transactions on Wireless Communications 14.5 (2015): 2532-2547.
- [176]. Müller, Axel, et al. "Linear precoding based on truncated polynomial expansion—Part I: Large-scale single-cell systems." IEEE J. Sel. Topics Signal Process (2013).
- [177]. A. Kammoun, A. Muller, E. Bjornson, and M. Debbah, "Linear Precoding Based on Truncated Polynomial Expansion—Part II: Large-Scale Multi-Cell Systems, IEEE Journal of Selected Topics in Signal Processing, submitted, 2014.
- [178]. Gao, Xiang, et al. "Massive MIMO performance evaluation based on measured propagation data." IEEE Transactions on Wireless Communications 14.7 (2015)
- [179]. Gao, Xiang, et al. "Massive MIMO in real propagation environments: Do all antennas contribute equally?." IEEE Transactions on Communications 63.11 (2015): 3917-3928.
- [180]. Hoydis, Jakob, et al. "Channel measurements for large antenna arrays." Wireless Communication Systems (ISWCS), 2012 International Symposium on. IEEE, 2012.
- [181]. Payami, Sohail, and Fredrik Tufvesson. "Channel measurements and analysis for very large array systems at 2.6 GHz." Antennas and Propagation (EUCAP), 2012 6th European Conference on. IEEE, 2012.
- [182]. Wu, Shangbin, et al. "A non-stationary wideband channel model for massive MIMO communication systems." IEEE transactions on wireless communications 14.3 (2015)
- [183]. Hamdi, Rami, Elmahdi Driouch, and Wessam Ajib. "Resource Allocation in Downlink Large-Scale MIMO Systems." IEEE Access 4 (2016): 8303-8316.
- [184]. Liu, Pei, et al. "Pilot power allocation through user grouping in multi-cell Massive MIMO systems." IEEE Transactions on Communications 65.4 (2017): 1561-1574.
- [185]. Naghsh, Mohammad Mahdi, et al. "Rate optimization for massive MIMO relay networks: A minorization-maximization approach." Acoustics, Speech and Signal Processing (ICASSP), 2016 IEEE International Conference on. IEEE, 2016.
- [186]. H. V. Cheng, E. Björnson, E. G. Larsson, "Uplink Pilot and Data Power Control for Single Cell Massive MIMO Systems with MRC.", ISWCS 2015, Sept. 2015.
- [187]. Nguyen, Tri Minh, Vu Nguyen Ha, and Long Bao Le. "Resource allocation optimization in multi-user multi-cell massive MIMO networks considering pilot contamination." IEEE Access 3 (2015): 1272-1287.
- [188]. Ghods, Ramina, et al. "Optimal large-mimo data detection with transmit impairments." Communication, Control, and Computing (Allerton), 2015 53rd Annual Allerton Conference on. IEEE, 2015.
- [189]. Yin, Bei, et al. "Full-duplex in large-scale wireless systems." Signals, Systems and Computers, 2013 Asilomar Conference on. IEEE, 2013.
- [190]. Li, Kaipeng, et al. "Decentralized baseband processing for massive MU-MIMO systems." IEEE Journal on Emerging and Selected Topics in Circuits 4 (2017): 491-507.
- [191]. Li, Kaipeng, et al. "Decentralized data detection for massive MU-MIMO on a Xeon Phi cluster." Signals, Systems and Computers, 2016 50th Asilomar Conference on. IEEE,
- [192]. Li, Kaipeng, et al. "Decentralized beamforming for massive MU-MIMO on a GPU cluster." Signal and Information Processing (GlobalSIP), 2016 IEEE Global Conference on. IEEE, 2016.
- [193]. Qiao, Deli, Haifeng Qian, and Geoffrey Ye Li. "On the design of broadbeam for massive MIMO systems." Computing, Networking and Communications (ICNC), 2016 International Conference on. IEEE, 2016.

- [194]. Flordelis, Jose, et al. "*Spatial separation of closely-spaced users in measured massive multi-user MIMO channels.*" Communications (ICC), 2015 IEEE International Conference on. IEEE, 2015.
- [195]. Glazunov, Andrés Alayón, Sathyaveer Prasad, and Peter Handel. "*Experimental characterization of the propagation channel along a very large virtual array in a reverberation chamber.*" Progress In Electromagnetics Research 59 (2014): 205-217.
- [196]. Y. Liu, G. Y. Li, Z. Tan, D. Qiao, "*Single-Carrier Modulation for Large-Scale Antenna Systems.*", IEEE Transactions on Vehicular Technologies, LSA-SC, Aug. 2015.
- [197]. Yang, Ang, et al. "*Performance analysis and location optimization for massive MIMO systems with circularly distributed antennas.*" IEEE Transactions on Wireless Communications 14.10 (2015): 5659-5671.
- [198]. Geraci, et al. "*Operating massive MIMO in unlicensed bands for enhanced coexistence and spatial reuse.*" IEEE Journal on Selected Areas in Communications 35.6 (2017):
- [199]. Ngo, Hien Quoc, et al. "*Cell-free massive MIMO versus small cells.*" IEEE Transactions on Wireless Communications 16.3 (2017): 1834-1850.
- [200]. Li, Kaipeng, et al. "*Decentralized beamforming for massive MU-MIMO on a GPU cluster.*" Signal and Information Processing (GlobalSIP), 2016 IEEE Global Conference
- [201]. Li, Boyu, Dengkui Zhu, and Ping Liang. "*Small cell in-band wireless backhaul in massive MIMO systems: A cooperation of next-generation techniques.*" IEEE Transactions on Wireless Communications 14.12 (2015): 7057-7069.
- [202]. J. Hoydis, et al., "*Making Smart Use of Excess Antennas: Massive MIMO, Small Cells, and TDD.*", Bell Labs Technical Journal, vol. 18, no. 2, pp. 5-21, Sep. 2013.
- [203]. Bogale, Tadilo Endeshaw, and Long Bao Le. "*Beamforming for multiuser massive MIMO systems: Digital versus hybrid analog-digital.*" Global Communications Conference (GLOBECOM), 2014 IEEE. IEEE, 2014.
- [204]. Gao, Xiang, et al. "*Massive MIMO in real propagation environments: Do all antennas contribute equally?.*" IEEE Transactions on Communications 63.11 (2015): 3917-3928.
- [205]. Ye, Qiaoyang, Ozgun Y. Bursalioglu, and Haralabos C. Papadopoulos. "*Harmonized cellular and distributed massive MIMO: Load balancing and scheduling.*" Global Communications Conference (GLOBECOM), 2015 IEEE. IEEE, 2015.
- [206]. J. Hoydis, et al., "*Massive MIMO in the UL/DL of Cellular Networks: How Many Antennas Do We Need?.*", IEEE J. Sel. Areas Commun, vol. 31, no. 2, Feb. 2013.
- [207]. Joung J., Chia Y.K., and Sun S., "*Energy-Efficient, Large-Scale Distributed-Antenna System (L-DAS) for Multiple Users.*", IEEE Journal of Selected Topics in Signal Processing, vol. 8, no. 5, October 2014.
- [208]. Agyapong, Patrick Kwadwo, et al. "*Design considerations for a 5G network architecture.*" IEEE Communications Magazine 52.11 (2014): 65-75.
- [209]. "*Mobile Broadband Transformation: LTE to 5G - 5G Americas.*", white paper, Available at: http://www.5gamericas.org/files/2214/7257/3276/Final_Mobile_Broadband_Transformation_Rsavy_whitepaper.pdf
- [210]. Wu, Qingqing, et al. "*An overview of sustainable green 5G networks.*" IEEE Wireless Communications 24.4 (2017): 72-80.
- [211]. Zheng, Kan, Suling Ou, and Xuefeng Yin. "*Massive MIMO channel models: A survey.*" International Journal of Antennas and Propagation 2014 (2014). Xie, Xiufeng, and Xinyu Zhang. "Scalable user selection for MU-MIMO networks." INFOCOM, 2014 Proceedings IEEE. IEEE, 2014.
- [212]. Michaloliakos, Antonios, et al. "*Efficient MAC for distributed multiuser MIMO systems.*" Wireless On-demand Network Systems and Services (WONS), 2013 10th Annual Conference on. IEEE, 2013.

- [213]. Ngo, Hien Quoc. “*Massive MIMO: Fundamentals and system designs.*”, Vol. 1642. Linköping University Electronic Press, 2015.
- [214]. Marzetta, Thomas L., et al. “*Fundamentals of Massive MIMO.*”, Cambridge University Press, 2016. Ipsen, Jesper R. "Products of independent Gaussian random matrices." arXiv preprint arXiv:1510.06128 (2015).
- [215]. Couillet, Romain, and Merouane Debbah. “*Random matrix methods for wireless communications.*”, Cambridge University Press, 2011.
- [216]. NATIONAL INSTRUMENTS, “*Doppler Spread and Coherence Time*”, white paper, Available at: <http://www.ni.com/white-paper/14911/en/>
- [217]. Martínez, et al., “*Massive MIMO properties based on measured channels: Channel hardening, user decorrelation and channel sparsity.*” Signals, Systems and Computers, 2016 50th Asilomar Conference on. IEEE, 2016.
- [218]. Lee, Juyul, and Nihar Jindal. “*Dirty paper coding vs. linear precoding for MIMO broadcast channels.*” Signals, Systems and Computers, 2006. ACSSC'06. Fortieth Asilomar Conference on. IEEE, 2006.
- [219]. H. Weingarten, et al., “*The capacity region of the Gaussian MIMO broadcast channel,*” in Proc. International Symposium on Information Theory (ISIT), June 2004.
- [220]. M. Costa, “*Writing on dirty paper,*” IEEE Transactions on Information Theory, vol. 29, no. 3, pp. 439-441, 1983.
- [221]. G. Caire et al., “*On the achievable throughput of a multiantenna Gaussian broadcast channel,*” IEEE Transactions on Information Theory, vol. 49, no. 7, July 2003.
- [222]. M. Sadek, A. Tarighat, and A. H. Sayed, “*Active antenna selection in multiuser MIMO communications,*” IEEE Transactions on Signal Processing, vol. 55, no. 4, pp. 1498{1510, Apr. 2007.
- [223]. C. B. Peel, B. M. Hochwald, and A. L. Swindlehurst, “*A vector-perturbation technique for near-capacity multiantenna multiuser communication-part I: channel inversion and regularization,*” IEEE Transactions on Comms, vol. 53, no. 1, pp. 195{202, Jan. 2005.
- [224]. M. Joham, et al., “*Linear transmit processing in MIMO communications systems,*” IEEE Transactions on Signal Processing, vol. 53, no. 8, pp. 2700-2712, Aug. 2005.
- [225]. Liang, Ning, Wenyi Zhang, and Cong Shen. “*An uplink interference analysis for massive MIMO systems with MRC and ZF receivers.*” Wireless Communications and Networking Conference (WCNC), 2015 IEEE. IEEE, 2015.
- [226]. Li, Xueru, et al. “*A multi-cell MMSE precoder for massive MIMO systems and new large system analysis.*” Global Communications Conference (GLOBECOM), 2015 IEEE.
- [227]. Björnson, E., Hoydis, J., Kountouris, M. and Debbah, M., 2014. “*Massive MIMO systems with non-ideal hardware: Energy efficiency, estimation, and capacity limits.*” IEEE Transactions on Information Theory, 60(11), pp.7112-7139.
- [228]. Zheng, K., Ou, S. and Yin, X., 2014. “*Massive MIMO channel models: A survey.*” International Journal of Antennas and Propagation, 2014.
- [229]. Mohanan, et al. “*Dirty paper coding versus beamforming in multi-user MIMO under OFDM.*” Signals, Systems and Computers, 50th Asilomar Conference on. IEEE, 2016.
- [230]. B. M. Hochwald, T. L. Marzetta, and V. Tarokh, “*Multiple-antenna channel hardening and its implications for rate feedback and scheduling,*” IEEE Transactions on Information Theory, vol. 50, no. 9, pp. 1893-1909, Sept. 2004.
- [231]. T. L. Narasimhan and A. Chockalingam, “*Channel hardening-exploiting message passing (CHEMP) receiver in large-scale MIMO systems,*” IEEE Journal of Selected Topics in Signal Processing, vol. 8, no. 5, pp. 847-860, Oct. 2014.

- [232]. Y.-H. Nam, B. L. Ng, K. Sayana, Y. Li, J. Zhang, Y. Kim, and J. Lee, "Full-dimension MIMO (FD-MIMO) for next generation cellular technology," IEEE Communications Magazine, vol. 51, no. 6, pp. 172-179, June 2013.
- [233]. J. A. Rice, "Mathematical Statistics and Data Analysis." Duxbury Press, 2006.
- [234]. Y. Kim, H. Ji, J. Lee, Y.-H. Nam, B. L. Ng, I. Tzanidis, Y. Li, and J. Zhang, "Full dimension MIMO (FD-MIMO): The next evolution of MIMO in LTE systems," IEEE Wireless Communications, vol. 21, no. 3, pp. 92-100, June 2014.
- [235]. Y. Xin, D. Wang, J. Li, H. Zhu, J. Wang, and X. You, "Area spectral efficiency and area energy efficiency of massive mimo cellular systems," IEEE Transactions on Vehicular Technology, vol. 65, no. 5, pp. 3243– 3254, 2016.
- [236]. Wang, Dongming, et al. "Uplink sum-rate analysis of multi-cell multi-user massive MIMO system." Communications (ICC), IEEE International Conference on. IEEE, 2013.
- [237]. Guey, Jiann-Ching, and L. Daniel Larsson. "Modeling and evaluation of MIMO systems exploiting channel reciprocity in TDD mode." Vehicular Technology Conference, 2004. VTC2004-Fall. 2004 IEEE 60th. Vol. 6. IEEE, 2004.
- [238]. H. Cui, L. Song, and B. Jiao, "Multi-pair two-way amplify-and-forward relaying with very large number of relay antennas," IEEE Transactions on Wireless Communications, vol. 13, no. 5, pp. 2636–2645, 2014.
- [239]. S. Jin, X. Liang, K.-K. Wong, X. Gao, and Q. Zhu, "Ergodic rate analysis for multipair massive mimo two-way relay networks," IEEE Transactions on Wireless Communications, vol. 14, no. 3, pp. 1480–1491, 2015.
- [240]. H. D. Nguyen and S. Sun, "Massive mimo versus small-cell systems: spectral and energy efficiency comparison," arXiv preprint arXiv:1509.03998, 2015.
- [241]. T. Van Chien, E. Björnson, and E. G. Larsson, "Joint power allocation and user association optimization for massive mimo systems," arXiv preprint arXiv:1601.02436, 2016.
- [242]. Z. Zhang, Z. Chen, M. Shen, and B. Xia, "Spectral and energy efficiency of multipair two-way full-duplex relay systems with massive mimo," IEEE Journal on Selected Areas in Communications, vol. 34, no. 4, pp.848–863, 2016.
- [243]. Selvan, V. P., M. S. Iqbal, and H. S. Al-Raweshidy. "Performance analysis of linear precoding schemes for very large Multi-user MIMO downlink system." Innovative Computing Technology (INTECH), Fourth International Conference on. IEEE, 2014.
- [244]. Lin, Yingchao, et al. "Spectral efficiency analysis for downlink massive MIMO systems with MRT precoding." China Communications 12.Supplement (2015): 67-73.
- [245]. Björnson, Emil, Erik G. Larsson, and Mérouane Debbah. "Massive MIMO for maximal spectral efficiency: How many users and pilots should be allocated?." IEEE Transactions on Wireless Communications 15.2 (2016): 1293-1308.
- [246]. Risi, Chiara, Daniel Persson, and Erik G. Larsson. "Massive MIMO with 1-bit ADC." arXiv preprint arXiv:1404.7736 (2014).
- [247]. Liang, Ning, and Wenyi Zhang. "Mixed-ADC Massive MIMO." IEEE Journal on Selected Areas in Communications 34.4 (2016): 983-997.
- [248]. Zhang, Jiayi, et al. "On the spectral efficiency of massive MIMO systems with low-resolution ADCs." IEEE Communications Letters 20.5 (2016): 842-845.
- [249]. Xia, et al. "A CDMA-distributed antenna system for in-building personal commns services." IEEE Journal on Selected Areas in Communications 14.4 (1996): 644-650.
- [250]. Schuh, Ralf E., and Magnus Sommer. "W-CDMA coverage and capacity analysis for active and passive distributed antenna systems." Vehicular Technology Conference, 2002. VTC Spring 2002. IEEE 55th. Vol. 1. IEEE, 2002.

- [251]. G. N. Kamga, M. Xia, and S. A'issa, "Spectral-efficiency analysis of massive mimo systems in centralized and distributed schemes," IEEE Transactions on Communications, vol. 64, no. 5, pp. 1930–1941, 2016.
- [252]. Ramprasad, Sean A., Giuseppe Caire, and Haralabos C. Papadopoulos. "Cellular and network MIMO architectures: MU-MIMO spectral efficiency and costs of channel state information." Signals, Systems and Computers, 2009 Conference Record of the Forty-Third Asilomar Conference on. IEEE, 2009.
- [253]. Marzetta, Thomas L. "How much training is required for multiuser MIMO?." Signals, Systems and Computers, ACSSC'06. Fortieth Asilomar Conference on. IEEE, 2006.
- [254]. Forenza, Antonio, et al. "Performance of the MIMO downlink channel with multi-mode adaptation and scheduling." Signal Processing Advances in Wireless Communications, 2005 IEEE 6th Workshop on. IEEE, 2005.
- [255]. Papadogiannis, Agisilaos, David Gesbert, and Eric Hardouin. "A dynamic clustering approach in wireless networks with multi-cell cooperative processing." Communications, 2008. ICC'08. IEEE International Conference on. IEEE, 2008.
- [256]. Chen, Runhua, et al. "Multimode transmission for multiuser MIMO systems with block diagonalization." IEEE Transactions on Signal Processing 56.7 (2008): 3294-3302.
- [257]. Shirani-Mehr, Hooman, Giuseppe Caire, and Michael J. Neely. "MIMO downlink scheduling with non-perfect channel state knowledge." IEEE Transactions on Communications 58.7 (2010): 2055-2066.
- [258]. Papadopoulos, et al., "Achieving large spectral efficiencies from MU-MIMO with tens of antennas: Location-adaptive TDD MU-MIMO design and user scheduling." Signals, Systems and Computers (ASILOMAR), 2010 Conference Record of the Forty Fourth Asilomar Conference on. IEEE, 2010.
- [259]. Huh, Hoon, et al., "Network MIMO with linear zero-forcing beamforming: Large system analysis, impact of channel estimation, and reduced-complexity scheduling." IEEE Transactions on Information Theory 58.5 (2012): 2911-2934.
- [260]. Bai, Dongwoon, et al. "LTE-advanced modem design: challenges and perspectives." IEEE Communications Magazine 50.2 (2012).
- [261]. Hossain, Ekram, and Monowar Hasan. "5G cellular: key enabling technologies and research challenges." IEEE Instrumentation & Measurement Magazine (2015): 11-21.
- [262]. R. Chávez-Santiago et al., "5G: The convergence of wireless communications," *Wireless Personal Communications*, pp. 1–26.
- [263]. X. Hou, A. Harada, and H. Suda, "Experimental study of advanced MU-MIMO scheme with antenna calibration for the evolving LTE TDD system," in *Personal Indoor and Mobile Radio Communications*, 2012 IEEE 23rd International Symposium on, Sept 2012, pp. 2443–2448.
- [264]. B. Hassibi and B. Hochwald, "How much training is needed in multiple-antenna wireless links?" *Information Theory, IEEE Trans. on*, vol. 49, no. 4, pp. 951–963, April 2003.
- [265]. E. Bjornson and B. Ottersten, "A framework for training-based estimation in arbitrarily correlated rician MIMO channels with rician disturbance," *Signal Processing, IEEE Transactions on*, vol. 58, no. 3, pp. 1807–1820, 2010.
- [266]. E. Bjornson, L. Sanguinetti, J. Hoydis, and M. Debbah, "Optimal design of energy-efficient multi-user MIMO systems: Is massive MIMO the answer?" *Wireless Communications, IEEE Transactions on*, vol. 14, no. 6, pp. 3059–3075, June 2015.
- [267]. C. ZHANG and G. ZENG, "Pilot contamination reduction scheme in massive MIMO multi-cell TDD systems," *Journal of Computational Information Systems*, vol. 10, no. 15, pp. 6721–6729, 2014.

- [268]. A. Ashikhmin, T. L. Marzetta, and L. Li, "Interference reduction in multi-cell massive mimo systems i: Large-scale fading precoding and decoding," *arXiv preprint arXiv:1411.4182*, 2014.
- [269]. Jose, Jubin, et al. "*Pilot contamination problem in multi-cell TDD systems.*" Information Theory, 2009. ISIT 2009. IEEE International Symposium on. IEEE, 2009.
- [270]. Maham, et al., "*Transmit antenna selection OFDM systems with transceiver I/Q imbalance.*" IEEE Transactions on Vehicular Technology 61.2 (2012): 865-871.
- [271]. Björnson, Emil, Per Zetterberg, and Mats Bengtsson. "*Optimal coordinated beamforming in the multicell downlink with transceiver impairments.*" Global Communications Conference (GLOBECOM), 2012 IEEE. IEEE, 2012.
- [272]. Marzetta, Thomas L., et al. "*Special issue on massive MIMO.*" Journal of Communications and Networks 15.4 (2013): 333-337.
- [273]. L. Berriche, et al., "*Investigation of the channel estimation error on MIMO system performance,*" Third European Signal Processing (EUSIPCO2005), Antalya, 2005.
- [274]. Medard, Muriel. "*The effect upon channel capacity in wireless communications of perfect and imperfect knowledge of the channel.*" IEEE Transactions on Information theory 46.3 (2000): 933-946.
- [275]. Yoo, Taesang, et al., "*Capacity of fading MIMO channels with channel estimation error.*" Communications, 2004 IEEE International Conference on. Vol. 2. IEEE, 2004.
- [276]. Dong, Min, and Lang Tong. "*Optimal design and placement of pilot symbols for channel estimation.*" IEEE Transactions on Signal Processing 50.12 (2002): 3055-3069.
- [277]. Bolcskei, Helmut, Robert W. Heath, and Arogyaswami J. Paulraj. "*Blind channel identification and equalization in OFDM-based multiantenna systems.*" IEEE Transactions on signal Processing 50.1 (2002): 96-109.
- [278]. Muquet, et al., "*Subspace-based blind and semi-blind channel estimation for OFDM systems.*" IEEE Transactions on signal processing 50.7 (2002): 1699-1712.
- [279]. Wo, Tianbin, and Peter Adam Hoehner. "*Semi-blind channel estimation for frequency-selective MIMO systems.*" Proc. 14-th IST Mobile & Wireless Communications Summit, Dresden, Germany (2005).
- [280]. Kudo, Riichi, et al. "*A channel state information feedback method for massive MIMO-OFDM.*" Journal of Communications and Networks 15.4 (2013): 352-361.
- [281]. Shariati, et al. "*Low-complexity polynomial channel estimation in large-scale MIMO with arbitrary statistics.*" IEEE Journal of Selected Topics in Signal Processing (2014)
- [282]. Shariati, Nafiseh, et al. "*Low-complexity channel estimation in large-scale MIMO using polynomial expansion.*" Personal Indoor and Mobile Radio Communications (PIMRC), 2013 IEEE 24th International Symposium on. IEEE, 2013.
- [283]. D. Neumann, M. Joham, and W. Utschick, "*Channel estimation in massive MIMO systems,*" arXiv preprint arXiv:1503.08691, 2015.
- [284]. Li, Ke, et al. "*An improved multicell MMSE channel estimation in a massive MIMO system.*" International Journal of Antennas and Propagation 2014 (2014).
- [285]. Hu, Anzhong, et al. "*Pilot design for large-scale multi-cell multiuser MIMO systems.*" Communications (ICC), 2013 IEEE International Conference on. IEEE, 2013.
- [286]. Zhang, Hua, et al. "On massive MIMO performance with semi-orthogonal pilot-assisted channel estimation." EURASIP Journal on Wireless Commns and Networking 2014.
- [287]. Zetterberg, Per. "*Experimental investigation of TDD reciprocity-based zero-forcing transmit precoding.*" EURASIP Journal on Advances in Signal Processing 2011.1

- [288]. Goransson, Bo, et al. "*Effect of transmitter and receiver impairments on the performance of MIMO in HSDPA.*" Signal Processing Advances in Wireless Communications, 2008. SPAWC 2008. IEEE 9th Workshop on. IEEE, 2008.
- [289]. Pitarokoilis, Antonios, Saif Khan Mohammed, and Erik G. Larsson. "*Uplink performance of time-reversal MRC in massive MIMO systems subject to phase noise.*" IEEE Transactions on Wireless Communications 14.2 (2015): 711-723.
- [290]. Guillaud, Maxime, and Florian Kaltenberger. "*Towards practical channel reciprocity exploitation: Relative calibration in the presence of frequency offset.*" Wireless Communications and Networking Conference (WCNC), 2013 IEEE. IEEE, 2013.
- [291]. Björnson, et al., "*Optimal resource allocation in coordinated multi-cell systems.*" Foundations and Trends® in Communications and Information Theory 9.2–3 (2013): 113-381.
- [292]. Gopalakrishnan, Balasubramanian, and Nihar Jindal. "*An analysis of pilot contamination on multi-user MIMO cellular systems with many antennas.*" Signal Processing Advances in Wireless Communications (SPAWC), 2011 IEEE 12th International Workshop on. IEEE, 2011.
- [293]. Elijah, Olakunle, et al. "*A comprehensive survey of pilot contamination in massive MIMO—5G system.*" IEEE Communications Surveys & Tutorials 18.2 (2016): 905-923.
- [294]. Appaiah, et al., "*Pilot contamination reduction in multi-user TDD systems.*" Communications (ICC), 2010 IEEE International Conference on. IEEE, 2010.
- [295]. Yin, Haifan, et al. "*Decontaminating pilots in massive MIMO systems.*" Communications (ICC), 2013 IEEE International Conference on. IEEE, 2013.
- [296]. Wang, Hualei, et al. "*A spatial domain based method against pilot contamination for multi-cell massive MIMO systems.*" Communications and Networking in China (CHINACOM), 2013 8th International ICST Conference on. IEEE, 2013.
- [297]. Ashikhmin, Alexei, and Thomas Marzetta. "*Pilot contamination precoding in multi-cell large scale antenna systems.*" Information Theory Proceedings (ISIT), 2012 IEEE International Symposium on. IEEE, 2012.
- [298]. Van Der Veen, A-J., Shilpa Talwar, and Arogyaswami Paulraj. "*A subspace approach to blind space-time signal processing for wireless communication systems.*" IEEE Transactions on Signal Processing 45.1 (1997): 173-190.
- [299]. Talwar, Shilpa, Mats Viberg, and Arogyaswami Paulraj. "*Blind separation of synchronous co-channel digital signals using an antenna array. I. Algorithms.*" IEEE Transactions on Signal Processing 44.5 (1996): 1184-1197.
- [300]. Ma, Junjie, and Li Ping. "*Data-aided channel estimation in large antenna systems.*" Communications (ICC), 2014 IEEE International Conference on. IEEE, 2014.
- [301]. Huh, Hoon, et al. "*Multi-cell MIMO downlink with cell cooperation and fair scheduling: A large-system limit analysis.*" IEEE Transactions on Information Theory 57.12 (2011)
- [302]. Ngo, Hien Quoc, Erik G. Larsson, and Thomas L. Marzetta. "*The multicell multiuser MIMO uplink with very large antenna arrays and a finite-dimensional channel.*" IEEE Transactions on Communications 61.6 (2013): 2350-2361.
- [303]. Cheng, Qingqing, et al. "*Novel pilot decontamination methods for Massive MIMO systems under practical scenarios.*" Communications and Information Technologies (ISCIT), 2016 16th International Symposium on. IEEE, 2016.
- [304]. Alqahtani, Ali H., Ahmed Iyanda Sulyman, and Abdulhameed Alsanie. "*Rateless space-time block code for mitigating pilot contamination effects in multi-cell massive MIMO system with lossy links.*" IET Communications 10.16 (2016): 2252-2259.
- [305]. Wu, et al., . "*Robust Equalizer for Multicell Massive MIMO Uplink With Channel Model Uncertainty.*" IEEE Transactions on Vehicular Technology 65.5 (2016): 3231-3242.

- [306]. JIANG, Jing, et al. "*Interference alignment scheme for massive MIMO system.*" The Journal of China Universities of Posts and Telecommunications 21.4 (2014): 19-24.
- [307]. Ngo, Hien Quoc, and Erik G. Larsson. "*EVD-based channel estimation in multicell multiuser MIMO systems with very large antenna arrays.*" Acoustics, Speech and Signal Processing (ICASSP), 2012 IEEE International Conference on. IEEE, 2012.
- [308]. Hu, Die, Lianghua He, and Xiaodong Wang. "*Semi-blind pilot decontamination for massive MIMO systems.*" IEEE Transactions on Wireless Communications (2016).
- [309]. Vu, Thang X., et al., "*Successive pilot contamination elimination in multiantenna multicell networks.*" IEEE Wireless Communications Letters 3.6 (2014): 617-620.
- [310]. Björnson, Emil, Jakob Hoydis, and Luca Sanguinetti. "*Pilot contamination is not a fundamental asymptotic limitation in massive MIMO.*" Communications (ICC), 2017 IEEE International Conference on. IEEE, 2017.
- [311]. Chen, Zhilin, and Chenyang Yang. "*Pilot decontamination in wideband massive MIMO systems by exploiting channel sparsity.*" IEEE Transactions on Wireless Communications 15.7 (2016): 5087-5100.
- [312]. Cuevas, Erik, et al. "*A swarm optimization algorithm inspired in the behavior of the social-spider.*" Expert Systems with Applications 40.16 (2013): 6374-6384.
- [313]. James, J. Q., and Victor OK Li. "*A social spider algorithm for global optimization.*" Applied Soft Computing 30 (2015): 614-627.
- [314]. El Aziz, Mohamed Abd, and Aboul Ella Hassanien. "*An improved social spider optimization algorithm based on rough sets for solving minimum number attribute reduction problem.*" Neural Computing and Applications (2017): 1-12.
- [315]. Paul, L. Yu, and Brian M. Sadler. "*Received signal strength gradient estimation for mobile networks.*" Military Communications Conference, 2010-MILCOM IEEE, 2010

LIST OF PUBLICATIONS

Journal Publications:

1. Ali M A and Jasmin E A “Adaptive modulation and interference cancellation techniques for MIMO-OFDM wireless networks”. International Journal of Networking and Virtual Organisations, 18(3), 2018, pp.246-264.
2. Ali M A and Jasmin E A, "A Novel Pilot Decontamination Method for Massive MIMO Systems Using Social Spider Optimization Algorithm," Journal of Communications, vol. 13, no. 4, pp. 145-154, 2018. Doi: 10.12720/jcm.13.4.145-154.
3. Ali M A and Jasmin E A, “Optimization of Spectral Efficiency in Massive-MIMO TDD Systems with Linear Precoding” International Journal of Advances in Computational Sciences and Technology, Research India Publications, ISSN 0973-6107 Volume 10, Number 4 (2017) pp. 501-517

Conference Publication:

1. Ali M A and Jasmin E A, "Physical layer improvements in 4G/5G wireless communication networks through link adaptation techniques," 2015 IEEE International Conference on Power, Instrumentation, Control and Computing (PICC), Thrissur, 2015, pp. 1-5. doi: 10.1109/PICC.2015.7455803

ABOUT THE AUTHOR

Ali M A was born on 12th January 1965 in Ernakulam district of Kerala. He obtained his bachelor's degree in Electronics & Communication Engineering from TKM College of Engineering, Kollam, Kerala in the year 1988. He received his master's degree in Fiber Optics and Light Wave Engineering from Indian Institute of Technology, Kharagpur in 1995.

He joined as a faculty under the Department of Technical Education, Government of Kerala in the year 1989 and he has got 29 years of teaching experience in various institutes both in India and abroad. Currently he is working as Associate Professor in the department of Computer Applications at Government Engineering College, Thrissur, Kerala.

He joined as a part-time research scholar in the Dept. of Electrical Engineering, Govt. Engineering College, Thrissur in August 2013. His areas of interest include wireless communications, physical layer techniques, diversity techniques and massive MIMO.

Permanent Address:
Bait al Ahlam
Mekalady,
Kalady P. O,
Ernakulam District,
Kerala, India-683574
Email: alima123@gmail.com